

**UFRRJ**  
**INSTITUTO DE TECNOLOGIA**  
**PROGRAMA DE PÓS GRADUAÇÃO EM CIÊNCIA E**  
**TECNOLOGIA DE ALIMENTOS**

**TESE**

**Encapsulação do óleo essencial de pimenta preta (*Piper nigrum L.*) por  
coacervação complexa, utilizando proteínas e alginato de sódio como  
materiais de parede**

**Livia Pinto Heckert Bastos**

**2019**



**UNIVERSIDADE FEDERAL RURAL DO RIO DE JANEIRO  
INSTITUTO DE TECNOLOGIA  
PROGRAMA DE PÓS-GRADUAÇÃO EM CIÊNCIA E  
TECNOLOGIA  
DE ALIMENTOS**

**ENCAPSULAÇÃO DO ÓLEO ESSENCIAL DE PIMENTA PRETA  
(*PIPER NIGRUM L.*) POR COACERVAÇÃO COMPLEXA,  
UTILIZANDO PROTEÍNAS E ALGINATO DE SÓDIO COMO  
MATERIAIS DE PAREDE**

**LÍVIA PINTO HECKERT BASTOS**

*Sob a orientação do professor*

**Dr. Edwin Elard Garcia Rojas**

Tese submetida como requisito parcial para obtenção do grau de **Doutora em Ciências**, no Programa de Pós-Graduação em Ciências e Tecnologia de Alimentos.

Seropédica-RJ

Agosto de 2019

Universidade Federal Rural do Rio de Janeiro  
Biblioteca Central / Seção de Processamento Técnico

Ficha catalográfica elaborada  
com os dados fornecidos pelo(a) autor(a)

B327e Bastos, Livia Pinto Heckert , 1987-  
ENCAPSULAÇÃO DO ÓLEO ESSENCIAL DE PIMENTA PRETA  
(PIPER NIGER L.) POR COACERVAÇÃO COMPLEXA, UTILIZANDO  
PROTEÍNAS E ALGINATO DE SÓDIO COMO MATERIAIS DE PAREDE  
/ Livia Pinto Heckert Bastos. - Seropédica, 2019.  
178 f.: il.

Orientador: Edwin Elard Garcia Rojas.  
Tese(Doutorado). -- Universidade Federal Rural do Rio  
de Janeiro, Programa de Pós-Graduação em Ciência e  
Tecnologia de Alimentos, 2019.

1. óleo essencial de pimenta preta. 2. proteínas do  
soro de leite. 3. gelatina. 4. alginato de sódio. 5.  
complexo coacervado. I. Rojas, Edwin Elard Garcia ,  
1972-, orient. II Universidade Federal Rural do Rio  
de Janeiro. Programa de Pós-Graduação em Ciência e  
Tecnologia de Alimentos III. Título.

**O presente trabalho foi realizado com apoio da Coordenação de Aperfeiçoamento  
de Pessoal de Nível Superior-Brasil (CAPES)- Código de Financiamento 001**

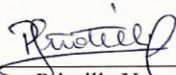
UNIVERSIDADE FEDERAL RURAL DO RIO DE JANEIRO  
INSTITUTO DE TECNOLOGIA  
PROGRAMA DE PÓS-GRADUAÇÃO EM CIÊNCIA E  
TECNOLOGIA  
DE ALIMENTOS

LÍVIA PINTO HECKERT BASTOS

Tese submetida como requisito parcial para obtenção do grau de **Doutor em Ciências**,  
no Programa de Pós-Graduação em Ciência e Tecnologia de Alimentos, área de  
concentração em Ciência de Alimentos.



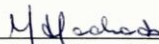
Edwin Elard García Rojas (Dr). EEIMVR/UFF  
(Orientador)



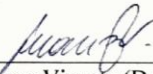
Priscilla Vanessa Finotelli (Dr<sup>a</sup>) UFRJ



Silvio José Sabino (Dr) UFF



Mariana Teixeira da Costa Machado (Dr<sup>a</sup>) UFRRJ



Juárez Vicente (Dr) UFRRJ

## **DEDICATÓRIA**

Dedico esta tese aos meus pais Lucia e Eber, ao meu irmão Lucas, e à tia Ângela.

## AGRADECIMENTOS

À Deus, pela minha vida, por iluminar meu caminho.

À minha família, principalmente à minha mãe, minha grande incentivadora, meu grande amor.

Ao meu pai e irmão, pelo companheirismo, incentivo e carinho.

À minha tia madrinha Ângela Esméria, pelo acolhimento, e sempre disposta a ajudar.

Aos meus primos, Diana Costa, Miguel Ataide, e Simone Costa, por estarem presentes em minha vida, e contribuírem com minha vida acadêmica desde o seu início.

A colaboradora Cristiane dos Santos, pelo apoio, e por preparar minhas refeições.

Ao meu orientador Prof. Dr. Edwin Elard Garcia Rojas, pelos ensinamentos e atenção que sempre teve comigo, e pelo carinho.

Ao Dr. Carlos Henrique e aos professores Dr. Bernardo de Sá, Dr. Carlos Piler, Dr. Mario Geraldo, e Dr. Rodrigo Siqueira que colaboraram na realização das minhas análises e nas suas respectivas discussões.

Aos amigos da UFRRJ, André, Ediná Rodrigues, Edlene, Gabriela Viana, Ivan Bianco, Roberto Laureano, pela amizade, carinho e sempre dispostos a ajudar.

Aos secretários, professores, alunos e coordenação do programa de Ciência e tecnologia em alimentos da UFRRJ, em especial a professora Dra. Maria Ivone pelo carinho.

Aos amigos do Laboratório de Engenharia e Tecnologia Agroindustrial (LETA) da UFF, Ahmad, Aline, Angélica, Augusto, Clitor, Clyselen, Eliana, Juarez, Letícia, Mariane, Mayara, Monique, Renata, em especial a amiga Bárbara por todo carinho, bondade e atenção.

As amigas Anália Barbosa, Camila Marques, Débora Gomes, e Vanessa Bosi pela torcida para que esse trabalho fosse concluído com êxito.

Ao meu namorado, Rômulo Pacheco pela compreensão e amor, e a sua família pelo carinho.

A Coordenação de Aperfeiçoamento de Pessoal de Nível Superior (CAPES) pela concessão da bolsa de estudos.

A todos que contribuíram para a realização deste trabalho, muito obrigada!

## RESUMO GERAL

BASTOS, Livia Pinto Heckert. **Encapsulação do óleo essencial de pimenta preta (*Piper nigrum L.*) por coacervação complexa, utilizando proteínas e alginato de sódio como materiais de parede.** 2019.p. Tese (Doutorado em Ciência e Tecnologia de Alimentos). Instituto de Tecnologia, Universidade Federal Rural do Rio de Janeiro, Seropédica, RJ. 2019.

O óleo essencial (OE) de pimenta preta (*Piper nigrum L.*) é rico em compostos ativos como os terpenos, sendo sua aplicação como aditivo alimentar alvo de pesquisas, devido as suas atividades antimicrobianas e antioxidantes. Os terpenos, entretanto, são voláteis e quando expostos a certas condições (oxigênio, altas temperaturas, luz, baixos pHs, fluidos gastrointestinais) podem ter o seu potencial biológico reduzido e, nesse sentido, a microencapsulação é uma alternativa na proteção dos OE e seus componentes. Dentre os métodos de microencapsulação, a coacervação complexa apresenta vantagens como baixa concentração de materiais de parede, elevada eficiência de encapsulação, e uma variedade de biopolímeros que podem ser utilizados como materiais de parede. O objetivo deste trabalho foi caracterizar e avaliar a estabilidade do OE de pimenta preta (*Piper nigrum L.*) e de suas cápsulas formadas por diferentes biopolímeros pela técnica de coacervação complexa. Os biopolímeros e agentes reticulantes utilizados foram eficazes na proteção do OE apresentando elevada eficiência de encapsulação, preservando os principais terpenos no OE encapsulado. Adicionalmente, as cápsulas fabricadas com lactoferrina/alginato de sódio e  $\beta$ -lactoglobulina/alginato de sódio preservaram o OE quando expostos a condição oral e gástrica simuladas *in vitro*. Nas cápsulas produzidas pelo sistema  $\beta$ -lactoglobulina/alginato de sódio foi avaliada a liberação do óleo essencial em diferentes matrizes alimentícias simuladas, em matrizes alimentícias aquosas, ocorreu baixa liberação do OE, e sua liberação foi por difusão *Fickian* de acordo com modelo *Rigger-Peppas*. Os resultados obtidos sugerem que os materiais de parede utilizados foram eficientes e podem ser utilizados para encapsular novos ingredientes ativos.

**Palavras-chave:** biopolímeros, proteínas do soro do leite, interação eletrostática, terpenos, eficiência de encapsulação, estabilidade térmica.

## ABSTRACT

BASTOS, Livia Pinto Heckert. **Encapsulation of the black pepper (*Piper nigrum L.*) essential oil by complex coacervation using proteins and sodium alginate as wall materials.** 2019. p. Thesis (PhD in Food Science and Technology). Technology Institute. Federal Rural University of Rio de Janeiro, Seropédica, RJ. 2019.

The black pepper (*Piper nigrum L.*) essential oil (EO) is a rich source of biologically active compounds (e.g. terpenes) and your applicability as a food additive has been the subject of several studies due to the antimicrobial and antioxidant activity of these compounds. Terpenes, however, are volatile and when exposed to certain conditions (high temperatures, light, low pH and gastrointestinal fluids) can reduce their biological potential and, in this sense, microencapsulation is an alternative way to the conserve EOs properties and their components. Among the microencapsulation methods, the complex coacervation method has advantages such as low concentrations of the wall materials, high encapsulation efficiency, and a variety of biopolymers that can be applied as wall materials. The aim of the present study was to characterize and evaluate the stability of black pepper EO encapsulated by complex coacervation using different biopolymers wall materials. The biopolymers and cross-linking agents used were effective in the protection of the EO, presented high encapsulation efficiency and preserved their main terpenes. Capsules formed by lactoferrin/sodium alginate and  $\beta$ -lactoglobulin/sodium alginate preserved the EO when exposed to simulated oral and gastric conditions *in vitro*. In simulated aqueous foods, the EO release was lower from  $\beta$ -lactoglobulin/sodium alginate microcapsules, and the EO release was by Fickian diffusion according to the Rigger-Peppas model. The obtained results suggest that the wall materials used were efficient and could be applied to encapsulate new active ingredients.

**Keywords:** biopolymers, whey proteins, electrostatic interaction, terpenes, encapsulation efficiency, thermal stability.



## LISTA DE FIGURAS

### CAPITULO I - REVISÃO DE LITERATURA

**Figura 1.** Modelos de microcápsulas.....7

**Figura 2.** Representação esquemática das etapas de encapsulação de um óleo por coacervação complexa.....9

**Figura 3.** (A) Estrutura da reticulação do cloreto de cálcio no alginato de sódio, (b) modelo do “*egg box*” representado por proções de zig-zag e estrutura polimérica do alginato de sódio representada por partes lineares.....10

**Figura 4.**(A) e (B): Apresenta as características estruturais do alginato de sódio.....15

### CAPÍTULO II- FORMATION AND CHARACTERIZATION OF THE COMPLEX COACERVATES OBTAINED BETWEEN LACTOFERRIN AND SODIUM ALGINATE

**Figure 1.** (A)  $\zeta$  potential of the isolated biopolymers (Lf and NaAlg) and the Lf/NaAlg complex at different ratios. (B) Turbidity ( $\text{cm}^{-1}$ ) as a function of pH in the system containing Lf/NaAlg complexes with different ratios. (C)  $\text{pH}_{\phi 1}$ ,  $\text{pH}_{\text{máx}}$  and  $\text{pH}_{\phi 2}$  of the Lf/NaAlg complex at a ratio of 8:1.....49

**Figure 2.**Turbidity ( $\text{cm}^{-1}$ ) as a function of pH in the system containing complex Lf/NaAlg ratio  $r=8:1$  at different concentrations of NaCl.....50

**Figure 3.** (A) Heat flow thermogram ( $\mu\text{cal/s}$ ) as a function of time (s), obtained during the titration of 0.15mM Lf in 0.0015mM NaAlg in a 10mM citrate buffer (pH 4.0) at 25°C. (B) Graphical representation of the integral of the area under each peak (kcal/mol) as a function of the molar ratio ( $r_m$ ) of Lf/NaAlg, ( $p<0.1$ ).....50

**Figure 4.** FT-IR spectra of NaAlg, Lf and the Lf/NaAlg complex at a ratio of 8:1 at pH 4.0.....51

**Figure 5.** SEM of the (A) NaAlg, (B) Lf, and (C) complex of Lf/NaAlg at a ratio of 8:1 at pH 4.0.....51

**Figure 6.** (A) Thermogram generated by DSC analysis of Lf, NaAlg and samples from the Lf/NaAlg complex at a ratio of 8:1 at pH 4.0. (B) Thermogram generated by DSC analysis of Lf.....52

**CAPÍTULO III- ENCAPSULATION OF THE BLACK PEPPER (*PIPER NIGRUM L.*) ESSENTIAL OIL BY LACTOFERRIN-SODIUM ALGINATE COMPLEX COACERVATES: STRUCTURAL CHARACTERIZATION AND SIMULATED GASTROINTESTINAL CONDITIONS**

**Figure 1.** FT-IR spectra of NaAlg, Lf, black pepper EO and black pepper EO capsule (Lf/NaAlg ratio r= 8:1) at pH 4.0.....77

**Figure 2.** <sup>1</sup>H NMR spectrum of the black pepper (BP) EO unencapsulated and encapsulated (500 MHz, CDCl<sub>3</sub>).....77

**Figure 3.**(A) Optical microscopy image at 100x of black pepper EO capsules at ratio 1:2 (core/ wall material), and (B) SEM of the black pepper EO capsule.....78

**Figure 4.** Release of the black pepper EO from the capsule during *in-vitro* digestion..78

**CAPÍTULO IV- ENCAPSULATION OF BLACK PEPPER (*PIPER NIGRUM L.*) ESSENTIAL OIL WITH GELATIN AND SODIUM ALGINATE BY COMPLEX COACERVATION.**

**Figure 1.** Effect of the ratio on the formation of the GE/NaAlg complex. Figure 1 (A) shows the turbidity variation of the biopolymers individually and as a function of the GE/NaAlg ratios at 600 nm. Figure 1 (B) shows the zeta potential variation of the biopolymers individually and as a function of the GE/NaAlg ratios, both at pH 4.0. Data represent the mean ± one standard deviation (n = 3).....106

**Figure 2.** Effect of the pH on the formation of the GE/NaAlg complex. Figure 2 (A) shows the turbidity at 600 nm. Figure 2 (B) shows the zeta potential. The GE/NaAlg concentration ratio was 6:1 and the pH values were 2.0, 3.0, 4.0, 5.0, 6.0 and 7.0. Data represent the mean ± one standard deviation (n = 3).....107

**Figure 3.** FT-IR spectra of NaAlg, GE, EO and microcapsule (S3) (GE/NaAlg ratio r= 6:1) at pH 4.0.....108

## CAPÍTULO V- INFLUENCE OF THE HEAT TREATMENT OF $\beta$ -LACTOGLOBULIN ON THE FORMATION OF INTERPOLYMERIC COMPLEXES WITH SODIUM ALGINATE

- Figure 1.** Particle size of the  $\beta$ -LG and  $\beta$ -LG<sub>n</sub> (0.1% w/w) in fixed pHs 4.5 and 4.0, respectively.....132
- Figure 2.**  $\zeta$ -Potential and SEI of the  $\beta$ -LG, NaAlg and their  $\beta$ -LG/NaAlg complexes133
- Figure 3.**(A) Heat flow thermogram ( $\mu$ cal/s) as a function of time (s), obtained during the titration of 0.25mM  $\beta$ -LG in  $9.37 \times 10^{-5}$  mM (pH 4.5) at 25°C and graphical representation of the integral of the area under each peak (kcal/mol) as a function of the molar ratio ( $r_m$ ) of  $\beta$ -LG/NaAlg, ( $p < 0.1$ ). (B) Heat flow thermogram ( $\mu$ cal/s) as a function of time (s), obtained during the titration of 0.25mM  $\beta$ -LG<sub>n</sub> in  $3.75 \times 10^{-4}$  mM (pH 4.0) and graphical representation of the integral of the area under each peak (kcal/mol) as a function of the molar ratio ( $r_m$ ) of  $\beta$ -LG<sub>n</sub>/NaAlg, ( $p < 0.1$ ).....134
- Figure 4.** FT-IR spectra of NaAlg,  $\beta$ -LG,  $\beta$ -LG/NaAlg (pH 4.5) and  $\beta$ -LG<sub>n</sub>/NaAlg (pH 4.0).....135
- Figure 5.** (A)Thermogram generated by DSC analysis of  $\beta$ -LG, NaAlg and  $\beta$ -LG/NaAlg complex at pH 4.5. (B) Thermogram generated by DSC analysis of  $\beta$ -LG.....135

## CAPÍTULO VI- MICROENCAPSULATION OF BLACK PEPPER (*PIPER NIGRUM L.*) ESSENTIAL OIL WITH $\beta$ -LACTOGLOBULIN AND SODIUM ALGINATE BY COMPLEX COACERVATION: SIMULATED GASTROINTESTINAL CONDITIONS AND MODELING THE KINETICS OF RELEASE

- Figure 1.** FT-IR spectra of NaAlg,  $\beta$ -LG, black pepper EO and black pepper microcapsule (pH 4.5).....161
- Figure 2.** Particle size of the  $\beta$ -LG, NaAlg and black pepper microcapsule (ME) at pH 4.5.....161
- Figure 3.**The cumulative release profile of the black pepper EO in different food stimulants.....162

**Figure 4.** Release of the black pepper EO from the capsule during *in vitro* digestion.....162

**Figure 5.**Optical microscopy image at 100x of black pepper EO microcapsules.....163

**Figure 6.** (A) SEM of the black pepper EO microcapsule, (B) after oral digestion, (C) after gastric digestion, (D) after intestinal digestion. All the micrographs were obtained at 500x.....164

## LISTA DE TABELAS

### CAPITULO I – REVISÃO DE LITERATURA

**Tabela 1.** Biopolímeros utilizados como materiais de parede na microencapsulação por coacervação complexa.....12

**Tabela 2.** Óleos essenciais microencapsulados pela técnica de coacervação complexa utilizando diferentes biopolímeros.....16

### CAPÍTULO III- ENCAPSULATION OF THE BLACK PEPPER (*PIPER NIGRUM L.*) ESSENTIAL OIL BY LACTOFERRIN-SODIUM ALGINATE COMPLEX COACERVATES: STRUCTURAL CHARACTERIZATION AND SIMULATED GASTROINTESTINAL CONDITIONS

**Table 1.**Chemical composition of the original black pepper EO and content in capsule by GC.<sup>a</sup>KI= Kovats indices to n-alkanes (C<sub>8</sub>–C<sub>20</sub>) on an HP- 5MS column, <sup>b</sup>KI=identification based on comparison of retention index with those of published data (Adams, 2007), <sup>c</sup>RT= Retention time, <sup>d</sup>Relative content obtained by GC-FID.....79

**Table 2.**<sup>13</sup>C and <sup>1</sup>H NMR data of identified major compounds in the black pepper EO ( $\delta_C$  and  $\delta_H$  in ppm).....80

**Table 3.** Composition of the formulations and encapsulation efficiency of the microcapsules produced by complex coacervation.....81

### CAPÍTULO IV- ENCAPSULATION OF BLACK PEPPER (*PIPER NIGRUM L.*) ESSENTIAL OIL WITH GELATIN AND SODIUM ALGINATE BY COMPLEX COACERVATION.

**Table 1.**Chemical composition of the original black pepper EO and content in microcapsule by GC.<sup>a</sup>KI= Kovats indices to n-alkanes (C<sub>8</sub>–C<sub>20</sub>) on an HP- 5MS column, <sup>b</sup>KI=identification based on comparison of retention index with those of published data (Adams, 2007), <sup>c</sup>RT= Retention time, <sup>d</sup>Relative content obtained by GC-FID.....109

**Table 2.**<sup>13</sup>C and <sup>1</sup>H NMR data of identified major compounds in the black pepper EO ( $\delta_C$  and  $\delta_H$  in ppm).....110

**Table 3.** Composition of the formulations and encapsulation efficiency of the microcapsules produced by complex coacervation.....111

**CAPÍTULO V- INFLUENCE OF THE HEAT TREATMENT OF  $\beta$ -LACTOGLOBULIN ON THE FORMATION OF INTERPOLYMERIC COMPLEXES WITH SODIUM ALGINATE**

**Table 1.** Thermodynamic parameters of  $\beta$ -LG/NaAlg complex and  $\beta$ -LG<sub>n</sub>/NaAlg complex in 10 mM citrate buffer were determined with the TA NanoAnalyze® software.....136

**CAPÍTULO VI- MICROENCAPSULATION OF BLACK PEPPER (*PIPER NIGRUM L.*) ESSENTIAL OIL WITH  $\beta$ -LACTOGLOBULIN AND SODIUM ALGINATE BY COMPLEX COACERVATION: SIMULATED GASTROINTESTINAL CONDITIONS AND MODELING THE KINETICS OF RELEASE**

**Table 1.** Composition of the formulations and EE of the microcapsules produced by complex coacervation.....165

**Table 2.** Kinetics constant of the black pepper EO release profile in different food simulants.....166

## LISTA DE ABREVIACOES E SMBOLOS

NaCl – Sodium Chloride

kDa - Kilodaltons

pI - Isoelectric Point

pH<sub>c</sub>– Critical pH

pH<sub>φ1</sub>– Abrupt Turbidity Increased Region

pH<sub>max</sub> - Maximum pH

pH<sub>φ2</sub>– Complex Dissociation Region

Lf- Lactoferrin

NaAlg- Sodium Alginate

ITC- Isothermal Titration Calorimetry

FT-IR- Fourier Transform Infrared Spectroscopy

DSC- Differential Scanning Calorimetry

SEM- Scanning Electron Microscopy

IUPAC - International Union of Pure and Applied Chemistry

EO- Essential Oil

GC- Gas Chromatography

NMR - Nuclear Magnetic Resonance

GE- Gelatin

CaCl<sub>2</sub> – Calcium Chloride

EE- Encapsulation Efficiency

TG- Transglutaminase

SSF- Simulated Salivary Fluid

SGF- Simulated Gastric Fluid

SIF- Simulated Intestinal Fluid

β-LG - β-Lactoglobulin

β-LG<sub>n</sub> - β-Lactoglobulin Nanoparticle

DLS - Dynamic Light Scattering

SEI - Strength of the Electrostatic Interaction

T<sub>g</sub>- Glass Transition

ΔH<sub>d</sub>- Enthalpy of Denaturation

## SUMÁRIO

INTRODUÇÃO GERAL .....	1
OBJETIVO GERAL.....	4
OBJETIVOS ESPECÍFICOS .....	4
CAPÍTULO I- REVISÃO DE LITERATURA .....	5
1. Microencapsulação .....	6
1.1. Técnicas de microencapsulação.....	7
1.1.1. Coacervação.....	8
1.1.1.1. Cloreto de Cálcio .....	10
1.1.1.2. Transglutaminase.....	11
1.2. Materiais de Parede .....	11
1.2.1. Gelatina.....	12
1.2.2. Lactoferrina .....	13
1.2.3. $\beta$ -lactoglobulina .....	14
1.2.4. Alginato de sódio.....	14
1.3. Óleos essenciais (OEs) .....	15
1.3.1. Estabilidade dos óleos essenciais microencapsulados após simulação gastrointestinal.....	17
1.3.2. Estudo da liberação dos OEs em diferentes matrizes alimentícias simuladas.....	17
1.4. Pimenta preta ( <i>Piper nigrum L.</i> ).....	18
2. Referências .....	19
CAPÍTULO II- FORMATION AND CHARACTERIZATION OF THE COMPLEX COACERVATES OBTAINED BETWEEN LACTOFERRIN AND SODIUM ALGINATE.....	28
Abstract.....	29
1. Introduction .....	30
2. Materials and Methods .....	31
2.1 Materials.....	31
2.2. Determination of the molecular weight of NaAlg .....	31
2.3. Formation of the Lf/NaAlg complex .....	32
2.3.1. Preparation of the solutions of Lf and NaAlg.....	32
2.3.2. Turbidimetric measurements .....	32
2.3.3. $\zeta$ -Potential .....	33



2.3.4. Isothermal titration calorimetry (ITC).....	33
2.4. Characterization of the complex coacervate formed by Lf-NaAlg .....	34
2.4.1 Fourier transform infrared spectroscopy (FT-IR).....	34
2.4.2. Differential Scanning Calorimetry (DSC).....	34
2.4.3. Scanning electron microscopy (SEM).....	35
3. Results and discussion .....	35
3.1. Intrinsic viscosity and molecular weight of NaAlg .....	35
3.2. Effect of the pH and ratio on the formation of the Lf/NaAlg complex .....	35
3.3.Effect of NaCl concentration on the formation of the coacervate complex of Lf/NaAlg.....	35
3.4. Isothermal Titration Calorimetry .....	39
3.5.Chemical and morphological characterization of the Lf/NaAlg complex.....	40
3.6. Differential scanning calorimetry .....	41
4.Conclusion.....	42
5. References .....	44
<b>CAPÍTULO III- ENCAPSULATION OF THE BLACK PEPPER (PIPER NIGRUM L.) ESSENTIAL OIL BY LACTOFERRIN-SODIUM ALGINATE COMPLEX COACERVATES: STRUCTURAL CHARACTERIZATION AND SIMULATED GASTROINTESTINAL CONDITIONS.....</b>	
Abstract.....	54
1. Introduction .....	55
2. Materials and Methods .....	56
2.1.Materials .....	56
2.2.Methods .....	57
2.2.1. Chemical composition of black pepper EO .....	57
2.2.1.1. Gas Chromatography (GC).....	57
2.2.1.2. Nuclear Magnetic Resonance (NMR) .....	57
2.2.2. Preparation of the black pepper EO capsules .....	58
2.3. Characterization of the microcapsules.....	58
2.3.1. Determination of standard curve and encapsulation efficiency.....	58
2.3.2. Fourier transform infrared spectroscopy (FT-IR).....	60
2.3.3. Chemical composition of the black pepper EO after encapsulation.....	60
2.3.4. Morphology .....	60
2.3.4.1 Optical microscopy.....	60

2.3.4.2. Scanning Electron Microscopy (SEM).....	60
2.4. <i>In vitro</i> digestion.....	60
2.4.1. Simulated oral digestion .....	60
2.4.2. Simulated gastric digestion.....	61
2.4.3. Simulated intestinal digestion.....	61
2.5. Statistical analysis.....	61
3. Results and Discussion .....	62
3.1. Composition of black pepper EO .....	62
3.1.1. Gas Chromatography analysis .....	62
3.1.2. Nuclear Magnetic Resonance analysis .....	62
3.2. Characterization of the microcapsules.....	63
3.2.1. Encapsulation Efficiency (EE). .....	64
3.2.2. Chemical characterization of the black pepper EO microcapsule.....	65
3.2.3. Composition of the black pepper EO after encapsulation .....	66
3.2.3.1. Gas Chromatography .....	66
3.2.3.2. Nuclear Magnetic Resonance .....	67
3.2.4. Morphology .....	67
3.3. <i>In vitro</i> digestion.....	68
4. Conclusion.....	70
5. References.....	71
<b>CAPÍTULO IV- ENCAPSULATION OF BLACK PEPPER (<i>PIPER NIGRUM L.</i>) ESSENTIAL OIL WITH GELATIN AND SODIUM ALGINATE BY COMPLEX COACERVATION.....</b>	<b>82</b>
Abstract.....	83
1. Introduction.....	84
2. Materials and Methods .....	86
2.1. Materials .....	86
2.2 Methods... ..	86
2.2.1. Chemical composition of black pepper ( <i>Piper nigrum L.</i> ) EO.....	86
2.2.1.1. Gas Chromatography (GC).....	86
2.2.1.2. Nuclear Magnetic Resonance (NMR) .....	87
2.2.2. Determination of the molecular weights of the biopolymers .....	87
2.2.3. Formation of the complex GE/NaAlg .....	88
2.2.3.1. Preparations of the solutions of GE and NaAlg.....	88

2.2.3.2. Effect of protein ratio on the formation of the GE/NaAlg .....	88
2.2.3.3. Effect of pH on the formation of the GE/NaAlg complex .....	89
2.2.4. Preparation of the microcapsules .....	89
2.2.5. Characterization of the microcapsules .....	89
2.2.5.1. Loaded oil content and Encapsulation Efficiency (EE).....	90
2.2.5.2. Fourier transform infrared spectroscopy (FT-IR).....	90
2.2.5.3. Chemical composition of the black pepper EO microencapsulated .....	91
2.2.6. Statistical analysis.....	91
3. Results and Discussion .....	91
3.1. Composition of black pepper EO .....	91
3.1.1. Gas Chromatography analysis .....	91
3.1.2. Nuclear Magnetic Resonance analysis .....	92
3.2. Intrinsic viscosity and molecular weights of the biopolymers .....	93
3.3. Effect of the ratio on the formation of the GE/NaAlg complex .....	93
3.4. Effect of the pH on the formation of the GE/NaAlg complex.....	95
3.5. Formation and characterization of microcapsules .....	96
3.5.1. Encapsulation Efficiency (EE) .....	96
3.5.2. Fourier transform infrared spectroscopy (FT-IR).....	97
3.5.3. Composition of the EO after microencapsulation .....	98
4. Conclusion .....	99
5. References.....	101
CAPÍTULO V- INFLUENCE OF THE HEAT TREATMENT OF $\beta$ -LACTOGLOBULIN ON THE FORMATION OF INTERPOLYMERIC COMPLEXES WITH SODIUM ALGINATE.....	
	112
Abstract.....	113
1. Introduction.....	114
2. Material and Methods .....	115
2.1. Materials. ....	115
2.2. Methods.. ....	115
2.2.1. Preparation of the solutions of $\beta$ -LG and NaAlg.....	115
2.2.2. Determination of the molecular weight of the NaAlg.....	116
2.2.3. Particle size analysis of native $\beta$ -LG and $\beta$ -LG <sub>n</sub> .....	116
2.2.4. Formation of the $\beta$ -LG/NaAlg complexes.....	116
2.2.4.1. $\zeta$ -Potential .....	116

2.2.4.2. Isothermal titration calorimetry (ITC) .....	117
2.2.5. Characterization of the $\beta$ -LG/NaAlg complexes .....	117
2.2.5.1. Fourier transform infrared spectroscopy (FT-IR).....	118
2.2.5.2. Differential Scanning Calorimetry (DSC) .....	118
3. Results and discussion .....	118
3.1. Molecular weight of NaAlg.....	118
3.2. Characterization of native $\beta$ -LG and $\beta$ -LG <sub>n</sub> .....	118
3.2.1. Particle size.....	118
3.3. Complex between $\beta$ -LG and NaAlg .....	119
3.3.1. Optimal pH for $\beta$ -LG/NaAlg complexes .....	119
3.3.2. Isothermal Titration Calorimetry (ITC).....	120
3.4. Chemical and thermal characterization of the $\beta$ -LG/NaAlg complexes.....	122
3.4.1. Fourier transform infrared spectroscopy (FT-IR).....	122
3.4.2. Differential Scanning Calorimetry (DSC).....	123
4. Conclusion .....	124
5. References.....	126
CAPÍTULO VI- MICROENCAPSULATION OF BLACK PEPPER ( <i>PIPER NIGRUM L.</i> ) ESSENTIAL OIL WITH $\beta$ -LACTOGLOBULIN AND SODIUM ALGINATE BY COMPLEX COACERVATION: SIMULATED GASTROINTESTINAL CONDITIONS AND MODELING THE KINETICS OF RELEASE.....	
Abstract.....	138
1. Introduction .....	139
2. Material and Methods .....	140
2.1. Materials .....	140
2.2. Methods.. .....	141
2.2.1. Preparation of the black pepper EO microcapsules .....	141
2.2.2. Characterization of the black pepper EO microcapsules.....	141
2.2.2.1. Determination of standard curve and encapsulation efficiency (EE).....	141
2.2.2.2. Fourier transform infrared spectroscopy (FT-IR).....	142
2.2.2.3. Particle size .....	142
2.2.2.4. Release kinetics of the black pepper EO in food stimulants.....	143

2.2.2.5. Optical microscopy .....	143
2.2.2.6. Scanning Electron Microscopy (SEM) .....	143
2.2.3. <i>In vitro</i> digestion .....	143
2.2.3.1. Simulated oral digestion .....	144
2.2.3.2. Simulated gastric digestion .....	144
2.2.3.3. Simulated intestinal digestion .....	144
2.2.4. Stability and bioaccessibility of the black pepper EO .....	145
2.2.5. Statistical analysis .....	146
3. Results and Discussion .....	146
3.1. Characterization of the microcapsules .....	146
3.1.1. Encapsulation Efficiency (EE) .....	146
3.1.2. Chemical characteristics .....	147
3.1.3. Particle size .....	148
3.1.4. Release of the EO in foods stimulants .....	149
3.2. Gastrointestinal <i>in vitro</i> simulated .....	150
3.3. Stability and bioaccessibility of the black pepper EO .....	152
3.4. Morphology .....	152
4. Conclusion .....	153
5. References .....	154
CONCLUSÃO GERAL .....	168
ANEXOS .....	171
ANEXO A: .....	171
ANEXO A1: Chromatogram of volatile compounds from black pepper EO identified by GC-MS. Peak numbers correspond to that in Table 1 .....	171
ANEXO B: .....	172
ANEXO B1: <sup>1</sup> H NMR spectrum of black pepper EO at 500.13MHz. Peak numbers correspond to that in Table 2. ....	172
ANEXO C: .....	173
ANEXO C1: NMR data of limonene (CDCl <sub>3</sub> , 500MHz) .....	173
ANEXO C2: NMR data of sabinene (CDCl <sub>3</sub> , 500MHz) .....	174
ANEXO C3: NMR data of β-cariophyllene (CDCl <sub>3</sub> , 500MHz) .....	175
ANEXO C4: NMR data of α-pinene (CDCl <sub>3</sub> , 500MHz) .....	176
ANEXO C5: NMR data of β -pinene (CDCl <sub>3</sub> , 500MHz) .....	177

## INTRODUÇÃO GERAL

O óleo essencial de pimenta preta (*Piper nigrum L.*) destaca-se por possuir propriedades antimicrobianas e antioxidantes, devido as seus terpenos, no entanto tais benefícios podem ser reduzidos quando este é exposto ao oxigênio, altas temperaturas, baixo pH, e fluidos gastrointestinais. A microencapsulação torna-se uma alternativa viável para proteção dos componentes presentes no óleo essencial. Dentre as técnicas de microencapsulação, a coacervação complexa apresenta diversas vantagens como: alta eficiência de encapsulação, baixa concentração de materiais de parede, integridade do material de parede, variedade de biopolímeros que podem ser utilizados como materiais de parede, entre outras. Os biopolímeros como proteínas e polissacarídeos são os mais utilizados como materiais de parede na microencapsulação por coacervação complexa, estes são naturais e apresentam propriedades funcionais. Na técnica de coacervação complexa podem ser utilizados agentes reticulantes com a finalidade de enrijecer a camada das microcápsulas. No presente estudo o cloreto de cálcio e a transglutaminase foram selecionados por serem de origem natural e não tóxicos à saúde. Como já mencionado, o óleo essencial de pimenta preta é importante devido à presença de seus componentes (terpenos), no entanto, há escassez de estudos que utilizaram a técnica de coacervação complexa para encapsulá-lo e obter melhor aproveitamento da sua composição e funcionalidade.

Sendo assim, nesta tese de doutorado foi estudado o encapsulamento do óleo essencial de pimenta preta (*Piper nigrum L.*) por coacervação complexa, utilizando diferentes sistemas contendo biopolímeros (gelatina, lactoferina ou  $\beta$ -lactoglobulina-alginato de sódio) como materiais de parede. Os capítulos que compõem o presente trabalho são artigos publicados, submetidos e a serem submetidos à publicação em revistas científicas. Os assuntos abordados em cada capítulo são resumidos a seguir:

Capítulo I foi realizado uma breve revisão de literatura na qual foram abordados os seguintes tópicos: microencapsulação, técnicas de microencapsulação, coacervação complexa, agentes reticulantes, materiais de parede, óleos essenciais, estabilidade dos óleos essenciais microencapsulados após simulação gastrointestinal, estudo da liberação dos óleos essenciais em diferentes matrizes alimentícias simuladas, e pimenta preta (*Piper nigrum L.*).

Capítulo II foi determinada a massa molar do alginato de sódio pelo método viscosimétrico e estudado o processo de formação dos complexos coacervados entre a

lactoferrina e o alginato de sódio em função da razão dos biopolímeros, do pH e da concentração de NaCl. Para isso, foram realizadas as análises de turbidimetria e de potencial- $\zeta$ . Parâmetros termodinâmicos foram obtidos pela análise de calorimetria de titulação isotérmica (ITC). Para caracterizar o complexo coacervado foram realizadas análises de espectroscopia de infravermelho por transformada de Fourier (FT-IR), calorimetria de varredura diferencial (DSC) e microscopia eletrônica de varredura (MEV).

Capítulo III o óleo essencial de pimenta preta (*Pipiper nigrum L.*) foi encapsulado utilizando a lactoferrina e o alginato de sódio como materiais de parede, suas cápsulas foram caracterizadas pelas análises de EE, FT-IR, microscopia ótica, MEV e a composição do óleo essencial encapsulado foi realizada por CG e RMN. A estabilidade das cápsulas de óleo essencial de pimenta preta durante simulação gastrointestinal *in vitro* também foram avaliadas.

Capítulo IV foram identificados os principais componentes do óleo essencial de pimenta preta (*Pipiper nigrum L.*) por cromatografia gasosa (CG) e ressonância magnética nuclear (RMN). Foi determinada a massa molar da gelatina pelo método viscosimétrico, e estudado o processo de formação dos complexos coacervados entre a gelatina e o alginato de sódio em função da razão dos biopolímeros e do pH. Para isso, foram feitas análises de turbidimetria e de potencial- $\zeta$ . Em seguida, o óleo essencial de pimenta preta foi encapsulado e suas cápsulas foram caracterizadas utilizando as análises de eficiência de encapsulação (EE), FT-IR e a composição do óleo essencial encapsulado foi realizada por CG.

Capítulo V foi realizada a caracterização da  $\beta$ -lactoglobulina ( $\beta$ -LG) nativa e após tratamento térmico, onde se obteve sua nanopartícula ( $\beta$ -LG<sub>n</sub>), foram obtidos os tamanhos de partícula das proteínas. Foi estudado o processo de formação dos complexos interpoliméricos entre a  $\beta$ -LG e o alginato de sódio em função da razão dos biopolímeros, do pH e do tratamento térmico da proteína. Para isso foram realizadas as análises de potencial- $\zeta$  e ITC. As cápsulas foram caracterizadas pelas análises de FT-IR e DSC.

Capítulo VI o óleo essencial de pimenta preta (*Pipiper nigrum L.*) foi encapsulado utilizando a  $\beta$ -LG e o alginato de sódio como materiais de parede, as cápsulas foram caracterizadas pelas análises de EE, FT-IR, tamanho de partícula, microscopia ótica e MEV. A estabilidade do óleo essencial de pimenta preta durante a

simulação gastrointestinal *in vitro* e sua liberação em diferentes matrizes alimentícias simuladas foram avaliadas.



## OBJETIVO GERAL

Caracterizar e avaliar a estabilidade do óleo essencial de pimenta preta (*Piper nigrum L.*) e de suas cápsulas formadas por biopolímeros pela técnica de coacervação complexa.

## OBJETIVOS ESPECÍFICOS

- Determinar a influência do pH, razão dos biopolímeros e concentração de NaCl na formação do complexo coacervado obtido a partir de lactoferrina e alginato de sódio, e caracterizar o complexo quanto as suas propriedades térmicas, químicas e morfológicas.
- Encapsular o óleo essencial de pimenta preta (*Piper nigrum L.*) por coacervação complexa utilizando a lactoferrina e o alginato de sódio como materiais de parede, caracterizar a eficiência de encapsulação, estrutura química, composição e estabilidade das cápsulas durante simulação gastrointestinal humana *in vitro*.
- Analisar a composição química do óleo essencial de pimenta preta (*Piper nigrum L.*), determinar a influência do pH e da razão dos biopolímeros na formação do complexo coacervado obtido a partir da gelatina e do alginato de sódio, e encapsular o óleo essencial de pimenta preta.
- Estudar a influência do tratamento térmico da  $\beta$ -lactoglobulina, o pH e a razão dos biopolímeros na formação do complexo interpolimérico entre  $\beta$ -lactoglobulina e alginato de sódio.
- Encapsular o óleo essencial de pimenta preta (*Piper nigrum L.*) por coacervação complexa utilizando a  $\beta$ -lactoglobulina e o alginato de sódio como materiais de parede, caracterizar a eficiência de encapsulação, estrutura química, morfológica e a estabilidade das microcápsulas durante a simulação gastrintestinal humana *in vitro* e em matrizes alimentares simuladas.

**CAPÍTULO I**  
**REVISÃO DE LITERATURA**

## 1. Microencapsulação

A microencapsulação é definida como processo no qual um ingrediente ativo (encapsulado) é rodeado por um revestimento (material de parede), formando microcápsulas e protegendo o encapsulado contra condições ambientais adversas (GAONKAR et al., 2014; GANJE et al., 2016; MACHADO et al., 2016).

Os principais objetivos da microencapsulação são: obter melhor aproveitamento da substância encapsulada, reduzir sua interação com fatores ambientais, prevenir perdas sensoriais e nutricionais, mascarar substâncias com sabores indesejáveis, prolongar o prazo de validade da substância encapsulada, incorporá-los em um produto novo ou existente e proteger a substância encapsulada de fluidos gastrintestinais (ALVIM et al., 2016; GANJE et al., 2016; MACHADO et al., 2016).

As cápsulas podem ser classificadas em dois grupos. As que são definidas como sistema do **tipo reservatório** e classificadas como ‘microcápsulas verdadeiras’. Elas são caracterizadas por seu núcleo ser nitidamente concentrado na região central, circundado por um filme definido e contínuo do material de parede. E aquelas onde o núcleo é uniformemente disperso em uma matriz, classificadas como **sistema matricial**, resulta nas camadas microsferas (KING, 1995; RÉ, 1998).

O que difere as microcápsulas das microsferas, é que nas microsferas, uma pequena fração do material “encapsulado” permanece exposta na superfície, o que é evitado pela “verdadeira” encapsulação. No entanto, o termo ‘encapsulação’ tem sido usado em seu sentido amplo, englobando tanto a formação de microcápsulas quanto de microsferas (DEPYPERE et al., 2003). As microcápsulas podem ter ainda mais de um núcleo ou várias paredes para um mesmo núcleo (CONSTANT; STRINGHETA, 2002). A Figura 1 ilustra os principais modelos de microcápsulas.

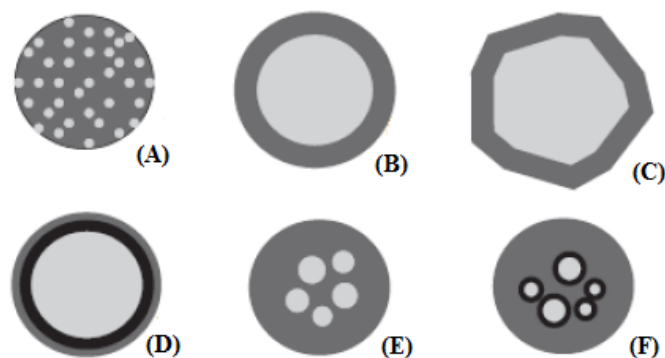


**Figura 1.** Modelos de microcápsulas

(A): matriz (microsfera) – produzido por atomização; (B): microcápsula simples; (C): microcápsula simples e irregular; (D): microcápsula de duas paredes; (E): microcápsula com vários núcleos e; (F): agrupamento de microcápsulas (ARSHADY, 1993; GIBBS, 1999).

### 1.1 Técnicas de microencapsulação

As técnicas de microencapsulação dividem-se em três grupos: físicos, químicos e físico-químicos.

São métodos físicos: *spray drying* (SARKAR et al., 2010; DE BARROS FERNANDES et al., 2014; BALASUBRAMANI et al., 2015), *spray chilling* (PELLISSARI et al., 2016; ORIANI et al., 2016), *spray cooling* (RIBEIRO et al., 2012; ALVIM et al., 2013), extrusão (DOLÇA et al., 2015; RUTTARATTANAMONGKOL et al., 2015), co-cristalização e liofilização (TURASAN et al., 2015; JAFARI et al., 2016).

Métodos químicos: coacervação simples (CHITPRASERT et al., 2014; SUTAPHANIT et al., 2014) e complexa (OZYILDZ et al 2012; PENG et al., 2014; SANTOS et al., 2014), envolvimento por lipossomas e separação em fase orgânica (ZHAO et al., 2015).

Métodos físico-químicos: emulsificação (DIMA et al., 2014; MAJEED et al., 2016), inclusão molecular e polimerização interfacial (MUNIN et al., 2011; JOYE; McCLEMENTS, 2014).

A escolha do método depende da aplicação, do tipo de material, do mecanismo de liberação desejado, do tamanho da partícula (micro ou nano), das propriedades

físicas e químicas do núcleo e da parede, da escala de produção e do custo (MUNIN, 2011; ALVIM et al., 2016; MACHADO, 2016).

Dentre as técnicas de microencapsulação, a coacervação complexa destaca-se por apresentar vantagens como: baixa concentração de materiais de parede (GIRARD et al. 2017; LEMOS et al., 2017; RUTZ et al. 2017), elevada eficiência de encapsulação ( $\cong$  90%) (DA SILVA et al., 2015), integridade do material de parede, variedade de biopolímeros que podem ser utilizados como materiais de parede, condições brandas de temperatura no processamento, uma boa liberação controlada dos ingredientes ativos e proteção a ingredientes funcionais (sensíveis a altas temperaturas) (RUTZ et al., 2017).

### **1.1.1 Coacervação**

A coacervação é definida como uma separação de um sistema coloidal em duas fases líquidas (IUPAC, 1997). A coacervação pode ser simples ou complexa, dependendo do número de polímeros envolvidos. A coacervação complexa ocorre principalmente através de interações eletrostáticas entre duas ou mais soluções poliméricas de cargas opostas, resultando em duas fases líquidas: uma pobre em polímeros e a outra rica em polímeros (coacervado), que é utilizado para revestir uma variedade de ingredientes ativos. Os coacervados possuem propriedades funcionais melhoradas em comparação com os polímeros individuais (SCHMITT;TURGEON, 2011; ZHANG et al., 2012).

A coacervação complexa consiste na interação eletrostática entre dois polímeros, normalmente uma proteína e um polissacarídeo (NESTERENKO et al., 2014). Nesse caso são formados quando uma proteína a um pH abaixo do seu ponto isoelétrico (carga positiva) é misturado com um polissacarídeo aniônico (ALVIM et al., 2010; DA SILVA et al., 2015). Tal processo pode ser afetado por vários fatores como: a natureza, peso e densidade das cargas dos polímeros, temperatura, pH e força iônica (SCHMITT;TURGEON, 2011; SOUZA et al., 2013).

O processo de microencapsulação por coacervação complexa consiste em três etapas básicas: emulsificação, coacervação e reticulação (ZHANG et al., 2012). Na Figura 2 observa-se a representação esquemática dessas etapas durante a encapsulação de um óleo por coacervação complexa.

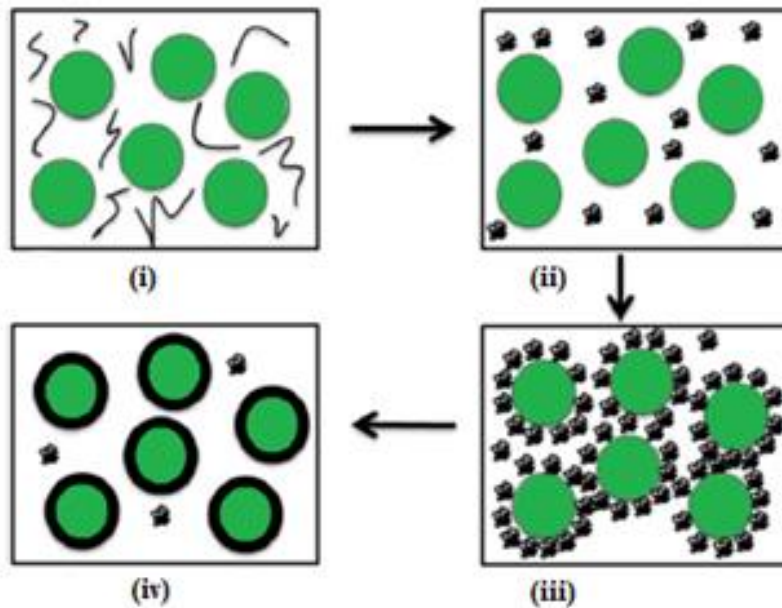


**Figura 2:** Representação esquemática das etapas de encapsulação de um óleo por coacervação complexa, (i) emulsificação óleo/água contendo polissacarídeo e proteína, (ii) início da coacervação após ajuste do pH da solução abaixo do ponto isoelétrico da proteína, (iii) formação de parede devido à deposição da fase rica em polímero em torno das gotículas hidrofóbicas, (iv) endurecimento da parede das cápsulas através da adição de agentes reticulantes.

**Fonte:** Adaptado de BAKRY et al., 2016.

Na primeira etapa o óleo é emulsificado em uma solução contendo dois polímeros (normalmente uma proteína e um polissacarídeo), ainda em um pH acima do ponto isoelétrico da proteína. Na segunda etapa ocorre o início da coacervação como resultado da atração eletrostática entre os polímeros com cargas opostas causada pelo abaixamento do pH da solução abaixo do ponto isoelétrico da proteína. Na terceira etapa, ocorre a formação da parede devido à deposição da fase rica em polímero em torno das gotículas hidrofóbicas. Na última etapa, ocorre o endurecimento da parede das microcápsulas devido a adição de agentes de reticulação (PIACENTINI et al., 2013; BAKRY et al., 2016).

As microcápsulas formadas através da coacervação complexa possuem baixa resistência mecânica devido à natureza iônica da interação entre as camadas poliméricas, sendo necessário adicionar um agente reticulante para enrijecer as paredes das microcápsulas e fornecer estabilidade as suas estruturas (ALVIM et al., 2010; ZHANG et al., 2011).

A reticulação é geralmente realizada pela adição de agentes químicos como glutaraldeído ou formaldeído que reagem com os grupos amino livres de proteínas, criando ligações covalentes (GIRARDI et al., 2017; RAKSA et al., 2017). Estes agentes são tóxicos à saúde e devem ser evitados em alimentos. Agentes reticulantes naturais como o cloreto de cálcio e a transglutaminase vem sendo utilizados na microencapsulação de ingredientes ativos pela técnica de coacervação complexa (MANAF et al., 2018).

### 1.1.1.1 Cloreto de Cálcio

O cloreto de cálcio ( $\text{CaCl}_2$ ) é um sal solúvel em água, não tóxico bastante utilizado como agente reticulante em complexos contendo alginato de sódio (SOARES et al., 2019; SHEN et al., 2016; WANG et al., 2016). Os íons de  $\text{Ca}^{2+}$  em solução podem se reticular com a composição do alginato de sódio formando uma rede tridimensional, modificando sua estrutura linear e permitindo, dessa forma, que mais íons de cálcio se liguem a essas cadeias. Dessa forma, produzindo estruturas complexas denominadas de “egg box” (BAGHERI et al., 2014; LEONG et al., 2016).

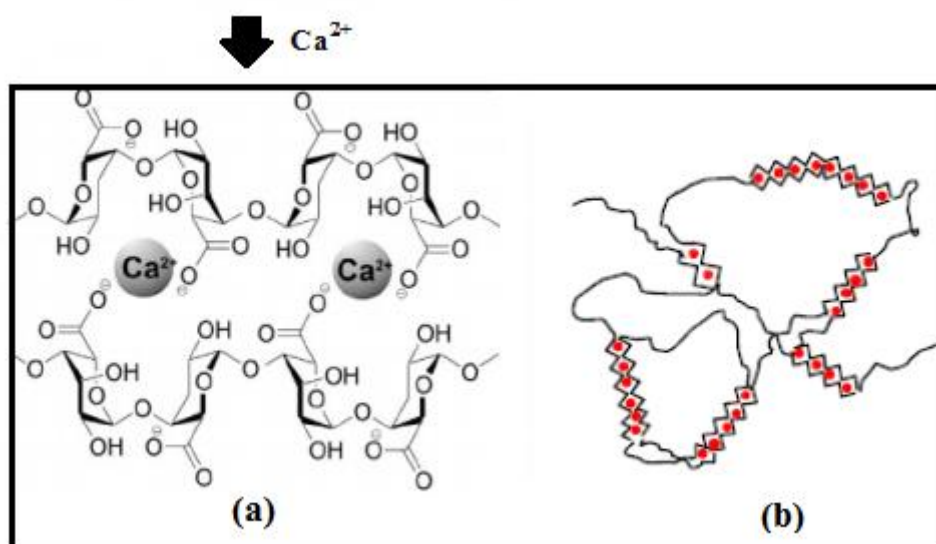


**Figura 3:**(a) Estrutura da reticulação do cloreto de cálcio no alginato de sódio, (b) modelo do “egg box” representado por proções de zig-zag e estrutura polimérica do alginato de sódio representada por partes lineares.

Fonte: Adaptado de JUAREZ et al., 2014.

### **1.1.1.2 Transglutaminase**

A transglutaminase é uma enzima natural, solúvel em água que confere modificação as proteínas em termos de solubilidade, espuma e emulsificação que afeta as propriedades funcionais dos alimentos (HUANG et al., 2014; GROSSMANN et al., 2017). Essa enzima é capaz de promover a reticulação entre proteínas pela catálise de reações de acil-transferência entre grupos carboxiamídicos e resíduos de glutamina da cadeia polipeptídica com aminas primárias, incluindo os grupos  $\epsilon$ -amino de resíduos de lisina, resultando na formação de ligações  $\epsilon$ -( $\gamma$ -glutamil) lisina intra e intermoleculares (MOTOKI; SEGURO, 1998). Diversos estudos utilizaram a transglutaminase como reticulante em microcapsulas produzidas por coacervação complexa (XIAO et al., 2014; LV et al., 2014; YUAN et al., 2017; ROJAS-MORENO et al., 2018).

## **1.2 Materiais de Parede**

O material de parede das microcápsulas tem como objetivo proteger substância do núcleo contra os fatores extrínsecos (oxigênio, luz, umidade, calor, interações com outros compostos), e reduzir as perdas dos ingredientes ativos, melhorando assim a sua estabilidade, condições de manipulação e aceitabilidade em geral. Diversos biopolímeros podem ser utilizados como materiais de parede para encapsular ingredientes ativos (TIMILSENA et al., 2017), na Tabela 1, são apresentados os principais biopolímeros que podem ser utilizados como materiais de parede na microencapsulação por coacervação complexa.



**Tabela 1:** Biopolímeros utilizados como materiais de parede na microencapsulação por coacervação complexa.

<b>Polissacarídeos (Não Modificados)</b>	<b>Polissacarídeos (Modificados)</b>	<b>Polissacarídeos (Gomas)</b>	<b>Proteínas (vegetal)</b>	<b>Proteínas (animal)</b>	<b>Polímeros</b>
Sacarose	Celulose	Xantana	Soja	Gelatina	Derivado de celulose
Amido	Ciclodextrina	Pectina	Trigo	Caseína	Quitosana
Xarope de glicose	Octenilsuccinato de amido	Carragenana	Milho (zeína)	Caseinato	PEG***
		Arábica	—	WPI*	PVA****
Maltodextrina	Dextrina	Alginato	—	WPC**	PVP*****

\*WPI: isolado protéico do soro do leite, \*\*WPC: isolado concentrado do soro do leite, \*\*\*PEG: polietileno glicol, \*\*\*\*PVA: acetato de polivinilo, \*\*\*\*\*PVP: polivinilpirrolidona.

**Fonte:** Adaptado de GAONKAR et al., 2014.

Dentre os biopolímeros utilizados como materiais de parede, destacam-se as proteínas: gelatina por ser natural não tóxica e solúvel em água (WANG et al., 2016), derivadas do soro do leite (lactoferrina e  $\beta$ -lactoglobulina), devido as suas propriedades funcionais (GARCÍA-MONTOYA et al., 2012; PEREZ et al., 2014). E o alginato de sódio, um polissacarídeo aniônico, biodegradável, biocompatível, bioativo, e de baixo valor econômico (PHILLIPS, 2009).

### 1.2.1 Gelatina

A gelatina é um material protéico derivado da degradação hidrolítica (por tratamento ácido ou alcalino) do colágeno, o principal componente de proteína do tecido conjuntivo fibroso (PICOUT; MURPHY, 2005; PHILIPS, 2009). A conversão de colágeno em gelatina é essencial na transformação que ocorre na fabricação da gelatina. A complexidade da estrutura do colágeno e a variedade de tratamentos químicos e enzimáticos que podem ser aplicados na fabricação da gelatina explicam a existência de uma grande variedade de tipos de gelatina. A principal diferença entre as formas de gelatina é a massa molar. Para a forma alfa, a massa molar varia de 80 a 125 kDa, e para a forma beta, de 160 a 250 kDa. A forma gama apresenta massa molar de 240 a 375 kDa (POPPE, 1997).

A gelatina comercial pode ser definida como uma proteína animal pura, composta de 85% a 90 % de proteína, e o restante de umidade e cinza (POPPE, 1997). De acordo com o pré-tratamento, a gelatina pode ser dividida em gelatina do tipo A e gelatina do tipo B. A gelatina tipo A é obtida pelo tratamento ácido e apresenta ponto isoelétrico de 7.0 a 9.4. A gelatina tipo B recebe tratamento neutro e ponto isoelétrico de 4.5 a 5.3 (POPPE, 1997; PHILIPS, 2009). Diversos estudos utilizaram a gelatina tipo B como material de parede para encapsular ingredientes ativos pela técnica de coacervação complexa (RAKSA et al., 2017; DE MATOS et al., 2018; DUHORANIMANA et al., 2018; SHADEL et al., 2018; DE SOUZA et al., 2018). O presente estudo utilizou a gelatina tipo B na formação do complexo gelatina/alginato de sódio e na encapsulação do óleo essencial de pimenta preta.

### **1.2.2 Lactoferrina**

A lactoferrina é comumente utilizada como emulsificante, faz parte das proteínas presentes no soro do leite. Pertence à família das transferrinas, juntamente com a transferrina sérica, ovotransferrina e melanotransferrina, sendo responsáveis principalmente pelo transporte de ferro. É produzida pelas células epiteliais da mucosa da glândula mamária de muitas espécies, como humanos, bovinos, caprinos, eqüinos e roedores. Também pode ser encontrada em diversos fluidos, como: lágrima, saliva, brônquicos, nasais, gastrointestinais e urina. Possui alta afinidade ao ferro, sendo a única proteína capaz de reter esse metal sobre diferentes valores de pH, possuindo alta resistência a proteólise (GARCÍA-MONTOYA et al., 2012).

É constituída por uma cadeia única de polipeptídeo, dobrado em dois lóbulos globulares simétricos (lóbulos N e C) ligados por uma determinada região, cada lóbulo é capaz de se unir a um átomo de  $Fe^{+2}$  ou  $Fe^{+3}$ , mas também pode se ligar ao  $Cu^{+2}$ ,  $Zn^{+2}$  e  $Mn^{+2}$  (RODRÍGUEZ-FRANCO et al., 2005). Possui peso molecular de 80 kDa, ponto isoelétrico próximo a 8.0 e sua maior concentração está presente no colostro, principalmente da espécie humana (SERRANO, 2007).

### 1.2.3 $\beta$ -lactoglobulina

A  $\beta$ -lactoglobulina é uma pequena proteína globular constituinte do soro do leite, apresenta ponto isoelétrico de  $\cong 5.1$  (VERHEUL et al., 1999; PEREZ et al., 2014; SHAFAEI et al., 2017). Estudos utilizaram a  $\beta$ -lactoglobulina na formação de complexos com polissacarídeos (HOSSEINI et al., 2013; QOMARUDIN et al., 2015; HADIAN et al., 2016; STENDER et al., 2018) e como material de parede para encapsular ingrediente ativo pela técnica de coacervação complexa (LIANG et al., 2016). O aquecimento de proteínas globulares nativas acima de suas temperaturas de desnaturação térmica faz com que elas se desdobrem e formem agregados através da formação de ligações hidrofóbicas e/ou dissulfeto. Este processo pode ser controlado para produzir nanopartículas ou micropartículas (JONES et al., 2011; PEREZ et al., 2015; KOUTINA et al., 2017; SHAFAEI et al., 2017).

### 1.2.4 Alginato de sódio

É um polissacarídeo natural, inodoro e não tóxico, pode ser extraído das algas marinhas marrons (*Phaeophyceae*) e de certas espécies de bactérias (DRAGET et al., 2005). Possui cadeias lineares solúveis em meio aquoso e é constituído por várias unidades de sais de ácido  $\beta$ -D-manurônico (M) e  $\alpha$ -L-gulurônico (G) unidas por ligações glicosídicas conforme observado na Figura 4 (a) (PHILLIPS et al., 2009).

Estas unidades são isômeros conformacionais, uma vez que possuem a mesma fórmula molecular e se diferem apenas no arranjo espacial dos átomos. Em sua estrutura química, como mostra a Figura 4 (b), regiões de blocos MM e GG (homopolímeros) são intercaladas por regiões MG (heteropolímero) (RASTOGI et al., 2007; PHILLIPS et al., 2009).

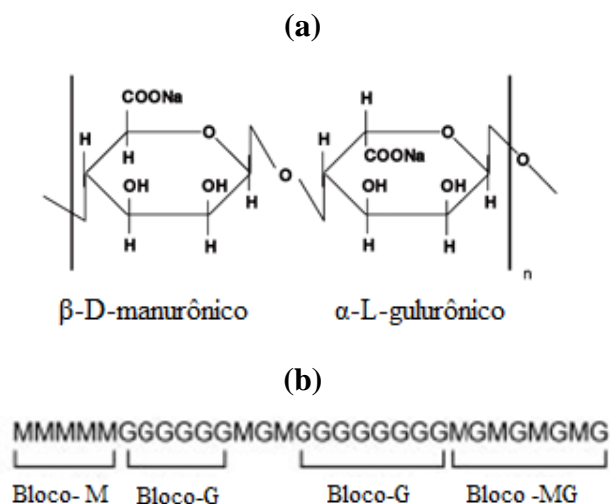


**Figura 4 (a) e (b):** Apresenta as características estruturais do alginato de sódio.

**Fonte:** (a) adaptado de MOFIDI; MOGHADAM; SARBOLOUKI (2000);

(b) adaptado de PHILLIPS; WILLIAMS (2009).

### 1.3 Óleos essenciais (OEs)

Os OEs são compostos aromáticos voláteis presentes em diversos órgãos das plantas (raízes, caules, folhas, flores e frutos), podem ser extraídos por destilação (hidrodestilação ou destilação por arraste com vapor d'água), compressão de vegetais ou com utilização de solventes (EL ASBAHANI et al., 2015). A diversidade e complexidade dos OEs agregam valor ao produto, sendo esse aplicado em diversas áreas: saúde (devido ao seu potencial terapêutico) (JEENA et al., 2014), perfumaria, cosmética e alimentícia (como aditivo flavorizante, antimicrobiano e antioxidante) (SOLORZANO-SANTOS; MIRANDA-NOVALES, 2012). Os principais componentes dos OEs são os terpenos, estes são responsáveis por suas propriedades antimicrobianas e antioxidantes. Quando expostos a determinadas condições como: oxigênio, luz, altas temperaturas, baixo pH e fluidos gastrointestinais, ocorre a degradação e redução das propriedades funcionais dos OEs. A microencapsulação pode prevenir a exposição dos óleos essenciais e reduzir suas perdas funcionais características (BAKKALI et al., 2008; DIMA et al., 2016). Conforme observado na Tabela 2, diversos estudos encapsularam os OEs utilizando diferentes biopolímeros como materiais de parede pela técnica de coacervação complexa.

**Tabela 2:** Óleos essenciais microencapsulados pela técnica de coacervação complexa utilizando diferentes biopolímeros

Óleo Essencial	Materiais de			Referências
	Parede	pH	EE (%)	
Mustarda ( <i>Sinapis alba</i> )	GE/GA	4.0	NI	PENG et al., 2014
Gengibre ( <i>Zingiber officinale</i> )	GE/NaAlg	4.0	≅ 66.0	WANG et al., 2016
Combava ( <i>Kaffir Lime</i> )	GE/GA	4.0	NI	RAKSA et al., 2017
<i>Lippia turbinata</i>	GE/GA	4.0	99.8	GIRARDI et al., 2017
Boldo do Chile ( <i>Peumus boldus</i> )	GE/GA	4.0	NI	GIRARDI et al., 2018
Citronela ( <i>Cymbopogon</i> )	GE/GA	4.5	94	MANAF et al., 2018
Citronela ( <i>Cymbopogon</i> )	GE/NaAlg	4.5	73.7	DE MATOS et al., 2018
Shiitake ( <i>Lentinula edodes</i> )	GE/CMC	4.0	85.75	YUAN et al., 2018
Laranja ( <i>Citrus aurantium</i> )	WPI e CMC	3.7	73	ROJAS-MORENO et al., 2018

GE: gelatina; GA: goma arábica; NaAlg: alginato de sódio; WPI: proteína do soro do leite isalada; CMC: carboximetilcelulose;  
NI: não informado.

### **1.3.1 Estabilidade dos óleos essenciais microencapsulados após simulação gastrointestinal**

No sistema gastrointestinal humano, os processos químicos digestivos são catalisados por enzimas digestivas que são secretadas no estômago, degradando assim os alimentos a uma escala molecular (ABRAHASSON et al., 2005). Tais fluidos e enzimas reduzem o potencial biológico dos óleos essenciais, sendo a microencapsulação uma alternativa. Estudos demonstraram que as cápsulas de OEs produzidas foram eficazes na sua proteção após simulação gastrointestinal *in vitro* (WANG et al., 2016b; VÓLIC et al., 2018).

Wang et al.(2016b) produziram cápsulas de óleo essencial de gengibre (*Zingiber officinale*), utilizando gelatina e alginato de sódio como materiais de parede e cloreto de cálcio como agente reticulante. Segundo os autores, a liberação do óleo essencial de gengibre, dependeu do pH e das soluções gástrica e intestinal simuladas. Durante a simulação gástrica, a liberação do óleo essencial de gengibre foi menor do que na simulação intestinal, os biopolímeros utilizados foram eficazes na proteção do óleo essencial durante a passagem gástrica. O mesmo foi observado por Vólic et al. (2018), o estudo encapsulou o óleo essencial de tomilho (*Thymus vulgaris*), utilizando proteína de soja e alginato como materiais de parede pelas técnicas de coacervação complexa seguida por extrusão.

### **1.3.2 Estudo da liberação dos OEs em diferentes matrizes alimentícias simuladas**

Devido as suas propriedades antioxidantes e antimicrobianas, os OEs podem ser adicionados como aditivos naturais em produtos alimentícios (BAKKALI et al., 2008), sendo assim, o estudo da liberação dos OEs encapsulados quando expostos a diferentes matrizes alimentícias é importante para sua adequada aplicação.O estudo realizado por REZAEINIA et al.(2019) avaliou a liberação do óleo de menta (*Mentha longifolia L.*) em nanocápsulas produzidas por *spray drying*. Goma de Balangu (*Lallemantia royleana*) e álcool ponivinílico foram utilizados para encapsular o óleo essencial de menta. A liberação do óleo essencial de menta ocorreu de forma crescente nos seguintes

modelos alimentícios: ácido acético (3%), etanol (50%), etanol (10%) ou água. Os resultados obtidos pelo estudo demonstraram que ocorreu menor liberação do óleo essencial em modelos alimentícios ácidos, onde as nanocápsulas foram mais resistentes a condição exposta.

#### **1.4 Pimenta preta (*Piper nigrum* L.)**

A pimenta preta (*Piper nigrum* L.) é uma das especiarias mais populares em países orientais (principalmente no sudeste da Ásia). Pertence a família da *Piperaceae* e é utilizada como agente aromatizante nos alimentos, sua característica aromática é devido aos óleos voláteis presentes em suas células (CHANDRAN et al., 2017; ORCHARD et al., 2017). Os principais terpenos presentes no OE de pimenta preta são:  $\beta$ -cariofileno, limoneno, sabineno,  $\alpha$ -pinene,  $\beta$ -pineno e sabineno (GARCÍA-DÍEZ et al., 2017; CHANDRAN et al., 2017; ORCHARD et al., 2017). Tais compostos presentes em seu óleo, vem sendo associados a diversos benefícios à saúde (ZARAI et al., 2013). A atividade antimicrobiana e antioxidante do OE de pimenta foram reportadas na literatura por vários autores (AHMAD et al., 2010; KARSHA; LAKSHMI., 2010; BAGHERI et al., 2014; KAPOOR et al., 2014; REHMAN et al., 2015). Porém na literatura são escassos estudos que microencapsularam o óleo essencial de pimenta preta (*Piper nigrum* L.) por coacervação complexa.

## 2. Referências

- ABRAHAMSSON, B., Pal, A., SJOBERG, M., CARLSSON, M., LAURELL, E., BRASSEUR, J. G. A novel in vitro and numerical analysis of shear-induced drug release from extended release tablets in the fed stomach. **Pharmaceutical Research**, 22, p.1215–1226. 2005.
- AHMAD, N; FAZAL, H; ABBASI, B. H; RASHID, M; MAHMOOD, T; FATIMA, N. Efficient regeneration and antioxidant potential in regenerated tissues of *Piper nigrum* L. **Plant Cell, Tissue and Organ Culture (PCTOC)**, v.102, n.1, p.129-134, 2010.
- ALVIM, I. D; GROSSO, C. R. F. Microparticles obtained by complex coacervation: influence of the type of reticulation and the drying process on the release of the core material. **Food Science and Technology (Campinas)**, v.30, n.4, p.1069-1076, 2010.
- ALVIM, I. D; STEIN, M. A; KOURY, I. P; DANTAS, F. B. H; CRUZ, C. L. D. C. V. Comparison between the spray drying and spray chilling microparticles contain ascorbic acid in a baked product application. **Food Science and Technology**, v.65, p. 689-694, 2016.
- ARSHADY, R. Microcapsules for food. **Journal of Microencapsulation**, v. 10, n. 4, p. 413-435, 1993.
- BAGHERI, H. N; MANAP, M.Y.B.A; ZEINA, S. Antioxidant activity of *Piper nigrum* L. essential oil extracted by supercritical CO<sub>2</sub> extraction and hydro-distillation. **Talanta**, v.121, p.220–228, 2014.
- BAKRY, A. M; ABBAS, S; ALI, B; MAJEED, H; ABOUELWAFI, M. Y; MOUSA, A; LIANG, L. Microencapsulation of Oils: A Comprehensive Review of Benefits, Techniques, and Applications. **Comprehensive Reviews in Food Science and Food Safety**, v.15, n.1, p.143-182, 2016.
- BAKKALI, F., AVERBECK, S., AVERBECK, D., IDAOMAR, M. Biological effects of essential oils – a review. **Food and Chemical Toxicology**, 46, p.446–475.2008.
- BALASUBRAMANI, P; PALANISWAMY, P. T; VISVANATHAN, R; THIRUPATHI, V; SUBBARAYAN, A; MARAN, J. P. Microencapsulation of garlic oleoresin using maltodextrin as wall material by spray drying technology. **International journal of biological macromolecules**, v.72, p.210-217, 2015.
- CHANDRAN, Janu et al. Oxidative stability, thermal stability and acceptability of coconut oil flavored with essential oils from black pepper and ginger. **Journal of food science and technology**, v. 54, n. 1, p. 144-152, 2017.
- CHITPRASERT, P; SUTAPHANIT, P. Holy Basil (*Ocimum sanctum* Linn.) Essential Oil Delivery to Swine Gastrointestinal Tract Using Gelatin Microcapsules Coated with Aluminum Carboxymethyl Cellulose and Beeswax. **Journal of agricultural and food chemistry**, v.62, n.52, p.12641-12648, 2014.



CONSTANT, P.B.L.; STRINGHETA, P.C. Microencapsulação de ingredientes alimentícios. **Boletim da Sociedade Brasileira de Ciência e Tecnologia de Alimentos**, v.36, n.1, p.12-18, 2002.

DA SILVA, THAIANE MARQUES. Encapsulação de compostos bioativos por coacervação complexa. **Ciência e Natura**, v. 37, n. 5, p. 56-64, 2015.

DA SILVA SOARES, BARBARA; SIQUEIRA, PINTO, RODRIGO; CARVALHO, GERALDO, MÁRIO; VICENTE, JUAREZ; GARCIA-ROJAS, ELARD, EDWIN. Microencapsulation of Sacha Inchi Oil (*Plukenetia volubilis* L.) using Complex Coacervation: Formation and Structural Characterization. **Food Chemistry**, p. 125045, 2019.

DE BARROS FERNANDES, R. V; MARQUES, G. R; BORGES, S. V; BOTREL, D. A. Effect of solids content and oil load on the microencapsulation process of rosemary essential oil. **Industrial Crops and Products**, v.58, n.1, p.73-181, 2014.

DE MATOS, E. F., SCOPEL, B. S., DETTMER, A. Citronella essential oil microencapsulation by complex coacervation with leather waste gelatin and sodium alginate. **Journal of Environmental Chemical Engineering**, 6(2), p.1989-1994. 2018.

DEPYPERE, F.; DEWETTINCK, K.; RONSSE, F.; PIETERS, J.G. Food powder microencapsulation: principles, problems and opportunities. **Applied Biotechnology, Food Science and Policy**, v.1, n.2, p.75-94, 2003.

DE SOUZA, VOLNEI BRITO. Functional properties and encapsulation of a proanthocyanidin-rich cinnamon extract (*Cinnamomum zeylanicum*) by complex coacervation using gelatin and different polysaccharides. **Food Hydrocolloids**, v. 77, p. 297-306, 2018.

DIMA, C; PĂTRAȘCU, L; CANTARAGIU, A; ALEXE, P; DIMA, Ș. The kinetics of the swelling process and the release mechanisms of *Coriandrum sativum* L. essential oil from chitosan/alginate/inulin microcapsules. **Food chemistry**, 195, p.39-48. 2016.

DOLÇA, C; FERRÁNDIZ, M; CAPABLANCA, L; FRANCO, E; MIRA, E; LÓPEZ, F; GARCÍA, D. Microencapsulation of Rosemary Essential Oil by Co-Extrusion/Gelling Using Alginate as a Wall Material. **Journal of Encapsulation and Adsorption Sciences**, 5 (03), p.121. 2015.

DRAGET, K. I; SMIDSRØD, O; SKJÅK-BRÆK, G. Alginates from algae. **Biopolymers Online**, 2005.

DUHORANIMANA, EMMANUEL. Effect of sodium carboxymethyl cellulose on complex coacervates formation with gelatin: Coacervates characterization, stabilization and formation mechanism. **Food hydrocolloids**, v. 69, p. 111-120, 2017.

EL ASBAHANI, A. et al. Essential oils: from extraction to encapsulation. **International journal of pharmaceutics**, v. 483, n. 1-2, p. 220-243, 2015.

GARCÍA-DÍEZ, JUAN et al. Chemical characterization and antimicrobial properties of herbs and spices essential oils against pathogens and spoilage bacteria associated to dry-cured meat products. **Journal of Essential oil research**, v. 29, n. 2, p. 117-125, 2017.

GARCÍA-MONTOYA, I. A; CENDÓN, T. S; ARÉVALO-GALLEGOS, S; RASCÓN-CRUZ, Q. Lactoferrin a multiple bioactive protein: an overview. **Biochimica et Biophysica Acta (BBA)-General Subjects**, v. 1820, n. 3, p. 226-236, 2012.

GANJE, M; JAFARI, S. M; DUSTI, A; DEHNAD, D; AMANJANI, M., GHANBARI, V. Modeling quality changes in tomato paste containing microencapsulated olive leaf extract by accelerated shelf life testing. **Food and Bioproducts Processing**, v.97, p.12-19, 2016.

GAONKAR, A. G; VASISHT, N; KHARE, A. R; SOBEL, R. Microencapsulation in the food industry: a practical implementation guide. San Diego: Elsevier, 2014.

GIBBS, B.F., KERMASHA, S., ALLI, I., MULLIGAN, C.N. Encapsulation in the food industry: A review. **International Journal Food Science Nutritional**.50, p.213-224.1999.

GIRARDI, NATALIA S. et al. Microencapsulation of Lippia turbinata essential oil and its impact on peanut seed quality preservation. **International biodeterioration & biodegradation**, v. 116, p. 227-233, 2017.

GROSSMANN, LUTZ et al. Accessibility of transglutaminase to induce protein crosslinking in gelled food matrices-Influence of network structure. **LWT**, v. 75, p. 271-278, 2017.

HADIAN, M. HOSSEINI, S. M. H.FARAHNAKY, A.MESBAHI, G. R. YOUSEFI, G. H.SABOURY, A. A. Isothermal titration calorimetric and spectroscopic studies of  $\beta$ -lactoglobulin-water-soluble fraction of Persian gum interaction in aqueous solution, **Food Hydrocolloids** 55 p.108-118. 2016.

HOSSEINI, SEYED MOHAMMAD HASHEM et al. Complex coacervation of  $\beta$ -lactoglobulin- $\kappa$ -Carrageenan aqueous mixtures as affected by polysaccharide sonication. **Food chemistry**, v. 141, n. 1, p. 215-222, 2013.

HUANG, G. Q; XIAO, J. X; QIU, H. W; Yang, J. Cross-linking of soybean protein isolate-chitosan coacervate with transglutaminase utilizing capsanthin as the model core. **Journal of microencapsulation**, v.31, n.7, p.708-715, 2014.

IUPAC. IUPAC Compendium of Chemical Technology, North Carolina, USA.1997.

JAFARI, S. M; MAHDAVI-KHAZAEI, K; HEMMATI-KAKHKI, A. Microencapsulation of saffron petal anthocyanins with cress seed gum compared with Arabic gum through freeze drying. **Carbohydrate polymers**, v.140, p.20-25, 2016.

JEENA, K; LIJU, V. B; UMADEVI, N. P; KUTTAN, R. Antioxidant, antiinflammatory and antinociceptive properties of black pepper essential oil (*Piper nigrum L*). **Journal of Essential oil Bearing Plants**, v.17, n.1, p. 1-12, 2014.

JONES, OWEN G.; McCLEMENTS, DAVID JULIAN. Recent progress in biopolymer nanoparticle and microparticle formation by heat-treating electrostatic protein–polysaccharide complexes. **Advances in colloid and interface science**, v. 167, n. 1-2, p. 49-62, 2011.

JOYE, I. J; DAVIDOV-PARDO, G; McCLEMENTS, D. J. Nanotechnology for increased micronutrient bioavailability. **Trends in Food Science & Technology**, v. 40, n.2, p.168-182, 2014.

JUAREZ, G. A. P.; SPASOJEVIC, M.; FAAS, M. M.; DE VOS, P. Immunological and technical considerations in application of alginate-based microencapsulation systems. **Frontiers in Bioengineering and Biotechnology**. v. 2, Article 26, 2014.

KAPOOR, I. P. S; SINGH, B; SINGH, G; DE HELUANI, C. S; DE LAMPASONA, M. P; CATALAN, C. A. Chemistry and in Vitro Antioxidant Activity of Volatile Oil and Oleoresins of Black Pepper (*Piper nigrum*). **Journal of agricultural and food chemistry**, 57(12), p.5358-5364. 2009

KARSHA, PAVITHRA VANI; LAKSHMI, O. BHAGYA. Antibacterial activity of black pepper (*Piper nigrum* Linn.) with special reference to its mode of action on bacteria. 2010.

KING, A.H. Encapsulation of food ingredients. In: RISCH, S.J.; REINECCIUS, G.A. **Encapsulation and controlled release of food ingredients**. ACS Symposim Series, 590. Washington. DC: ACS, p.26-39. 1995

KOUTINA, GLYKERIA. The effect of protein-to-alginate ratio on in vitro gastric digestion of nanoparticulated whey protein. **International dairy journal**, v. 77, p. 10-18, 2018.

LEMO, YURI PESSOA; MARIANO MARFIL, PAULO HENRIQUE; NICOLETTI, VÂNIA REGINA. Particle size characteristics of buriti oil microcapsules produced by gelatin-sodium alginate complex coacervation: Effect of stirring speed. **International journal of food properties**, v. 20, n.2, p. 1438-1447, 2017.

LEONG, J. Y., LAM, W. H., HO, K. W., VOO, W. P., LEE, M. F. X., LIM, H. P., Chan, E. S. Advances in fabricating spherical alginate hydrogels with controlled particle designs by ionotropic gelation as encapsulation systems. *Particuology*, 24, 44-60. 2016.

LIANG, J., YAN, H., YANG, H. J., KIM, H. W., WAN, X., LEE, J., KO, S. Synthesis and controlled-release properties of chitosan/ $\beta$ -Lactoglobulin nanoparticles as carriers for oral administration of epigallocatechin gallate. **Food science and biotechnology**, 25 (6), p.1583-1590. 2016.

LV, Yi et al. Formation of heat-resistant nanocapsules of jasmine essential oil via gelatin/gum arabic based complex coacervation. **Food Hydrocolloids**, v. 35, p. 305-314, 2014.

MACHADO, L. C; PELEGATI, V. B; OLIVEIRA, A. L. Study of simple microparticles formation of limonene in modified starch using PGSS–Particles from

gas-saturated suspensions. **The Journal of Supercritical Fluids**, v. 107, p. 260-269, 2016.

MAJEED, H; ANTONIOU, J; HATEGEKIMANA, J; SHARIF, H. R; HAIDER, J; LIU, F; ZHONG, F. Influence of carrier oil type, particle size on in vitro lipid digestion and eugenol release in emulsion and nanoemulsions. **Food Hydrocolloids**, v.52, p.415-422, 2016.

MANAF, M. A. et al. Encapsulation of volatile citronella essential oil by coacervation: efficiency and release study. In: **IOP conference series: materials science and engineering**. IOP Publishing, p. 012072. 2018.

MOFIDI, N; AGHAI-MOGHADAM, M; SARBOLOUKI, M. N. Mass preparation and characterization of alginate microspheres. **Process Biochemistry**, 35(9), p.885-888. 2000.

MOTOKI, M; SEGURO, K. Transglutaminase and its use for food processing. **Trends in food science & technology**,9(5), p. 204-210. 1998.

MUNIN, A; EDWARDS-LÉVY, F. Encapsulation of natural polyphenolic compounds; a review. **Pharmaceutics**, v. 3, n. 4, p. 793-829, 2011.

NESTERENKO, A., ALRIC, I., VIOLLEAU, F., SILVESTRE, F; DURRIEU, V. The effect of vegetable protein modifications on the microencapsulation process. **Food Hydrocolloids**, 41, p. 95-102. 2014.

ORCHARD, ANÉ. The in vitro antimicrobial activity and chemometric modelling of 59 commercial essential oils against pathogens of dermatological relevance. **Chemistry & biodiversity**, v. 14, n. 1, p.1600218, 2017.

ORIANI, V. B; ALVIM, I. D; CONSOLI, L; MOLINA, G; PASTORE, G. M; HUBINGER, M. D. Solid lipid microparticles produced by spray chilling technique to deliver ginger oleoresin: Structure and compound retention. **Food Research International**, 80, 41-49. 2016.

OZYILDIZ, F; KARAGONLU, S; BASAL, UZEL, G. A; BAYRAKTAR, O. Microencapsulation of ozonated red pepper seed oil with antimicrobial activity and application to nonwoven fabric. **Letters in Applied Microbiology**, v.56, p.168-179,2012.

PELISSARI, J. R; SOUZA, V. B; PIGOSO, A. A; TULINI, F. L; THOMAZINI, M; RODRIGUES, C. E; FAVARO-TRINDADE, C. S. Production of solid lipid microparticles loaded with lycopene by spray chilling: Structural characteristics of particles and lycopene stability. **Food and Bioproducts Processing**, 98, p. 86-94. 2016.

PENG, C; ZHAO, S. Q; ZHANG, J; HUANG, G. Y; CHEN, L. Y; ZHAO, F. Y. Chemical composition, antimicrobial property and microencapsulation of Mustard (*Sinapis alba*) seed essential oil by complex coacervation. **Food chemistry**, v.165, p.560-568, 2014.

PEREZ, A. A., ANDERMATTEN, R. B., RUBIOLO, A. C; SANTIAGO, L. G.  $\beta$ -Lactoglobulin heat-induced aggregates as carriers of polyunsaturated fatty acids. **Food chemistry**, **158**, p.66-72. 2014.

PEREZ, ADRIÁN A. Biopolymer nanoparticles designed for polyunsaturated fatty acid vehiculization: Protein–polysaccharide ratio study. **Food chemistry**, v. 188, p. 543-550, 2015.

PHILLIPS, O.G; WILLIAMS, P. A. **Handbook of hydrocolloids**. 2. ed. Florida: CRC Press, 2009.

PIACENTINI, E; GIORNO, L; DRAGOSAVAC, M. M; VLADISAVLJEVIC, G.T; HOLDICH, R.G. Microencapsulation of oil droplets using cold water fish gelatine/gum arabic complex coacervation by membrane emulsification. **Food Research International**, v.53, p.362–72, 2013.

PICOUT, D. R; MURPHY, S. B. R. Thermoreversible and Irreversible Physical Gels from Biopolymers. In: *Polymer Gels and Networks*. OSAKA, Y; KHOKHLOV, A. Marcel Dekker, Inc. All Rights Reserved, p. 36-46. 2005.

POPPE, J. Gelatin. In: *Thickening and Gelling Agents for Food*. IMESON, A. Springer Science Business Media Dordrecht, Second Edition, p. 144-168. 1997.

QOMARUDIN, Q., ORBELL, J. D., RAMCHANDRAN, L., GRAY, S. R., STEWART, M. B; VASILJEVIC, T. Properties of beta-lactoglobulin/alginate mixtures as a function of component ratio, pH and applied shear. **Food Research International**, 71, p. 23-31.2015.

RAKSA, A., SAWADDEE, P., RAKSA, P., ALDRED, A. K. Microencapsulation, chemical characterization, and antibacterial activity of Citrus hystrix DC (*Kaffir Lime*) peel essential oil. *Monatshefte für Chemie-Chemical Monthly*, 148(7), p.1229-1234. 2017.

RASTOGI, R; SULTANA, Y; AQIL, M; ALI, A; KUMAR, S; CHUTTANI, K; MISHRA, A. K. Alginate microspheres of isoniazid for oral sustained drug delivery. **International journal of pharmaceutics**, v.334, n.1, p. 71-77, 2007.

RÉ, M.I. Microencapsulation by spray drying. **Drying Technology**, v.16, p.1195-1236, 1998.

REHMAN, A; MEHMOOD, M. H; HANEEF, M; GILANI, A. H; ILYAS, M; SIDDIQUI, B. S; AHMED, M. Potential of black pepper as a functional food for treatment of air ways disorders. **Journal of Functional Foods**, v.19, p.126-140, 2015.

REZAEINIA, HASSAN et al. Electrohydrodynamic atomization of Balangu (*Lallemantia royleana*) seed gum for the fast-release of *Mentha longifolia* L. essential oil: Characterization of nano-capsules and modeling the kinetics of release. **Food Hydrocolloids**, v. 93, p. 374-385, 2019.

RIBEIRO, MARILENE DM MORSELLI; ARELLANO, DANIEL BARRERA; GROSSO, CARLOS R. FERREIRA. The effect of adding oleic acid in the production of stearic acid lipid microparticles with a hydrophilic core by a spray-cooling process. **Food Research International**, v. 47, n. 1, p. 38-44, 2012.

RODRÍGUEZ-FRANCO, D. A; VÁZQUEZ-MORENO, L; RAMOS-CLAMONT, M. G. Actividad antimicrobiana de la lactoferrina: Mecanismos y aplicaciones clínicas potenciales. **Revista Latino-americana de Microbiología**, v. 47, p. 101-111, 2005.

ROJAS-MORENO, SANDRA. Effects of complex coacervation-spray drying and conventional spray drying on the quality of microencapsulated orange essential oil. **Journal of Food Measurement and Characterization**, v. 12, n. 1, p. 650-660, 2018.

RUTTARATTANAMONGKOL, K; AFIZAH, M. N; RIZVI, S. S. Stability and rheological properties of corn oil and butter oil emulsions stabilized with texturized whey proteins by supercritical fluid extrusion. **Journal of Food Engineering**, 166, 139-147. 2015.

RUTZ, JOSIANE K. Microencapsulation of palm oil by complex coacervation for application in food systems. **Food chemistry**, v. 220, p. 59-66, 2017.

SANTOS, M. G; CARPINTEIRO, D.A; THOMAZINI, M; ROCHA-SELMÍ, G. A; DA CRUZ, A. G; RODRIGUES, C. E; FAVARO-TRINDADE, C. S. Coencapsulation of xylitol and menthol by double emulsion followed by complex coacervation and microcapsule application in chewing gum. **Food Research International**, v.66, p.454-462, 2014

SARKAR, A; HORNE, D. S; SINGH, H. Interactions of milk protein-stabilized oil-in-water emulsions with bile salts in a simulated upper intestinal model. **Food Hydrocolloids**, v. 24, n.2-3, p.142-151, 2010.

SCHMITT, C. TURGEON, S. L. Protein/polysaccharide complexes and coacervates in food systems. **Advances in Colloid and Interface Science** 167 p.63-70. 2011.

SERRANO, M. E. D. Lactoferrina: producción industrial y aplicaciones. **Revista Mexicana de Ciências Farmacêuticas**, v. 38, n. 3, p. 30-38, 2007.

SHADDEL, R., HESARI, J., AZADMARD-DAMIRCHI, S., HAMISHEHKAR, H., FATHI-ACHACHLOUEI, B., HUANG, Q. Double emulsion followed by complex coacervation as a promising method for protection of black raspberry anthocyanins. **Food hydrocolloids**, 77, 803-816. 2018.

SHAFAEI, ZAHRA.  $\beta$ -Lactoglobulin: An efficient nanocarrier for advanced delivery systems. **Nanomedicine: Nanotechnology, Biology and Medicine**, v. 13, n. 5, p. 1685-1692, 2017.

SHEN, L., CHEN, J., BAI, Y., MA, Z., HUANG, J., FENG, W. Physical properties and stabilization of microcapsules containing thyme oil by complex coacervation. **Journal of food science**, 81(9), p. 2258-2262. 2016.

SOLÓRZANO-SANTOS, F; MIRANDA-NOVALES, M. G. Essential oils from aromatic herbs as antimicrobial agents. **Current opinion in biotechnology**, v. 23, n. 2, p. 136-141, 2012.

SOUZA, CLITOR, J, F. Complex coacervates obtained from interaction egg yolk lipoprotein and polysaccharides. **Food hydrocolloids**, v. 30, n. 1, p. 375-381, 2013.

STENDER, E. G., KHAN, S., IPSEN, R., MADSEN, F., HÄGGLUND, P., HACHEM, M. A; SVENSSON, B. Effect of alginate size, mannuronic/guluronic acid content and pH on particle size, thermodynamics and composition of complexes with  $\beta$ -lactoglobulin. **Food hydrocolloids**, 75, 157-163. 2018.

SUTAPHANIT, P; CHITPRASERT, P. Optimisation of microencapsulation of holy basil essential oil in gelatin by response surface methodology. **Food chemistry**, v.150, p.313-320, 2014.

TIMILSENA, YAKINDRA PRASAD et al. Digestion behaviour of chia seed oil encapsulated in chia seed protein-gum complex coacervates. **Food hydrocolloids**, v. 66, p. 71-81, 2017.

TURASAN, H; SAHIN, S; SUMNU, G. Encapsulation of rosemary essential oil. **LWT-Food Science and Technology**, v.64, n.1, p.112-119, 2015.

VERHEUL, MARLEEN; ROEFS, SEBASTIANUS PFM; DE KRUIF, Kees G. Kinetics of heat-induced aggregation of  $\beta$ -lactoglobulin. **Journal of Agricultural and Food Chemistry**, v. 46, n. 3, p. 896-903, 1998.

VOLIĆ, M., PAJIĆ-LIJAKOVIĆ, I., DJORDJEVIĆ, V., KNEŽEVIĆ-JUGOVIĆ, Z., PEĆINAR, I., STEVANOVIĆ-DAJIĆ, Z; BUGARSKI, B. Alginate/soy protein system for essential oil encapsulation with intestinal delivery. **Carbohydrate polymers**, 200, 15-24. 2018.

WANG, L; YANG, S; CAO, J; ZHAO, S; WANG, W. Microencapsulation of Ginger Volatile Oil Based on Gelatin/Sodium Alginate Polyelectrolyte Complex. **Chemical and Pharmaceutical Bulletin**, 64(1), 21-26. 2016.

XIAO, ZUOBING et al. Production and characterization of multinuclear microcapsules encapsulating lavender oil by complex coacervation. **Flavour and fragrance journal**, v. 29, n. 3, p. 166-172, 2014.

YUAN, YANG et al. Complex coacervation of soy protein with chitosan: Constructing antioxidant microcapsule for algal oil delivery. **LWT**, v. 75, p. 171-179, 2017.

ZARAI, Z; BOUJELBENE, E; SALEM, N. B; GARGOURI, Y; SAYARI, A. Antioxidant and antimicrobial activities of various solvent extracts, piperine and piperic acid from *Piper nigrum*. **Lwt-Food science and technology**, v.50, n.2, p.634-641, 2013.

ZHANG, K., ZHANG, H., HU, X., BAO, S; HUANG, H. Synthesis and release studies of microalgal oil-containing microcapsules prepared by complex coacervation. **Colloids and surfaces B: Biointerfaces**, 89, 61-66. 2012.

ZHAO, J; WEI, T; WEI, Z; YUAN, F; GAO, Y. Influence of soybean soluble polysaccharides and beet pectin on the physicochemical properties of lactoferrin-coated orange oil emulsion. **Food Hydrocolloids**, 44, 443-452. 2015.



**CAPÍTULO II**  
**FORMATION AND CHARACTERIZATION OF THE COMPLEX**  
**COACERVATES OBTAINED BETWEEN LACTOFERRIN AND SODIUM**  
**ALGINATE**

Published at **International Journal of Biological Macromolecules**, v. 120, p.332-338,  
2018.

## Abstract

The aim of this study was to evaluate the influence of some parameters (pH, NaCl, and ratio of biopolymers) on the formation of the complex coacervates of lactoferrin and sodium alginate. Different ratios of lactoferrin:sodium alginate were tested (1:1, 1:2, 1:4, 1:8, 2:1, 4:1, and 8:1) at pH levels ranging from 2.0 to 7.0 with different concentrations of NaCl (0, 50, 100, 150, and 200mM). Sodium alginate has a molecular weight of  $138 \text{ kDa} \pm 0.07$ . The ratio of 8:1 (lactoferrin: sodium alginate) at a pH of 4.0 with a low salt concentration was the optimal condition for the formation of the complex. The thermodynamic parameters demonstrated that the interaction between lactoferrin and sodium alginate was exothermic and spontaneous with a favorable enthalpic and unfavorable entropic contribution during the interaction. The chemical, thermal and morphological characteristics of the biopolymers and the complex coacervates demonstrated their nature and changes due to electrostatic interactions. The formation of complex coacervates between lactoferrin and sodium alginate can serve as an alternative to the incorporation of lipophilic functional ingredients sensitive to high temperatures in various food systems.

**Keywords:** Electrostatic interaction, Whey protein, Biopolymers, Thermodynamic parameters, Enthalpy

## 1. Introduction

Proteins and polysaccharides are present in many food systems and both contribute to the structure, texture, and stability of food. The properties of proteins and polysaccharides are enhanced when the formation of complex coacervates occurs. These coacervates can be used as biomaterials in microencapsulation systems [1].

The interaction between polysaccharides and proteins in an aqueous dispersion is often accompanied by phase separation. These can occur through two distinct paths: (i) segregation (thermodynamic incompatibility) and (ii) association (complex coacervation). Complex coacervation occurs through electrostatic interaction between oppositely charged biopolymers [2]. Several parameters have been shown to influence electrostatic interactions between polysaccharides and proteins: pH, temperature, biopolymer ratio and concentration, charge density, and salt concentration [3-6].

The formation of complex coacervates between proteins and polysaccharides typically occurs between the isoelectric point (pI) of the protein and the pKa of the reactive groups of the polysaccharides. The following sequential processes are involved in the formation of the complexes: (1) the primary soluble formation of complex coacervates ( $\text{pH}_c$ ); (2) a sharp increase in turbidity ( $\text{pH}_{\phi 1}$ ); (3) the maximum point ( $\text{pH}_{\text{max}}$ ), which is reached when electrical equivalence occurs between the biopolymers; and (4) the point when the insoluble complexes begin to dissociate due to protonation of the anionic groups ( $\text{pH}_{\phi 2}$ ). Such processes having been demonstrated by several studies reported in the literature [6,7].

Due to their functional and nutritional properties, whey proteins are used in combination with polysaccharides to form complex coacervates such as: protein isolate[8], bovine serum albumin[7],  $\beta$ -lactoglobulin[9,10],  $\alpha$ -lactoglobulin[11], and lactoferrin[3,4,5,12].

Lactoferrin (Lf) has a molecular weight of 80 kDa, approximately 700 amino acid residues and an isoelectric point (pI) near 8.0. It consists of a single chain of polypeptides folded into two symmetric globular lobes (lobes N and C) connected by a given region. Each lobe is able to bind to an  $\text{Fe}^{+2}$  or  $\text{Fe}^{+3}$  atom, but it can also bind to  $\text{Cu}^{+2}$ ,  $\text{Zn}^{+2}$ , and  $\text{Mn}^{+2}$ [13].

Sodium alginate (NaAlg) is a natural, anionic, odorless, and non-toxic polysaccharide that can be extracted from brown marine algae (*Phaeophyceae*) and

certain species of bacteria. It has linear chains that are soluble in aqueous media and consists of several units of the salts of  $\beta$ -D-mannuronic acid (M) and  $\alpha$ -L-guluronic acid (G) linked by glycosidic bonds. These units are conformational isomers since they have the same molecular formula and differ only in the spatial arrangement of their atoms. In the chemical structure, regions of MM and GG blocks (homopolymers) are intercalated by MG (heteropolymer)[14].

The present study aimed to determine the influence of pH, biopolymer ratio, and NaCl concentration on the formation of the complex coacervates obtained from Lf and NaAlg. The complexes of Lf/NaAlg, Lf and NaAlg were further characterized by their thermal, chemical, and morphological properties.

## **2. Materials and Methods**

### *2.1 Materials*

Sodium alginate was purchased from the company Sigma-Aldrich<sup>®</sup> (St. Louis–USA); dehydrated lactoferrin (Bioferrin<sup>®</sup>2000) was acquired from the company Glanbia Nutritionals (Fitchburg, USA); sodium chloride p.a. (99%) was obtained from the company Cinética<sup>®</sup> (Paraná-BR); citric acid monohydrate and tribasic sodium citrate were obtained from VETEC<sup>®</sup>Ltda (Rio de Janeiro, Brazil); and the water used was ultrapure with a conductivity of 0.05  $\mu$ S/cm (Master System P&D, Gehaka, Brazil).

### *2.2 Determination of the molecular weight of NaAlg*

The molecular weight of NaAlg was determined by the viscosimetric method adapted from Pamies[15]. The dynamic viscosity was calculated using the data obtained from Cannon-Fenske capillary viscometers (Schott-Gerate, Germany). The capillaries were immersed in a thermostatic bath (Schott-Gerate, CT-52, Germany) to control the temperature, which was maintained at approximately  $25 \pm 0.05^\circ\text{C}$ . The NaAlg solution was prepared with 0.1M NaCl with the following concentrations: 0.1, 0.2, 0.3, 0.4, 0.5, 0.6 and 0.75%[15]. The solution and solvent densities were measured in a densimeter (Anton Paar, DMA 4500M, Austria) with an autoinjector (Anton Paar, Xsample 452, Austria). Sample readings were performed in triplicate. The intrinsic viscosity ( $[\eta]$ ) was

estimated by extrapolation of Martin curves to concentration of "zero"[16] using the following equations:

$$\ln(\eta_{sp}/c) = \ln[\eta] + K[\eta]c \quad (1)$$

$$\eta_{sp} = \frac{\eta - \eta_0}{\eta} \quad (2)$$

Where  $[\eta]$  is the intrinsic viscosity ( $\text{cm}^3/\text{g}$ ),  $\eta_{sp}$  is the specific viscosity,  $c$  is the concentration of NaAlg ( $\text{g/mL}$ ),  $\eta$  is the viscosity of the solution of NaAlg ( $\text{g/cm.s}$ ),  $\eta_0$  is the viscosity of the solvent ( $\text{g/cm.s}$ ), and  $K$  is Martin's constant. The molecular weight was determined by the following viscosimetric equation[17,18]:

$$[\eta] = K \cdot M^a \quad (3)$$

where  $[\eta]$  is the intrinsic viscosity ( $\text{cm}^3/\text{g}$ ),  $M$  is the molecular weight, and  $K$  and  $a$  are the constants that depend on the polymer, solvent, and temperature. The constants  $a=0.92$  and  $K=7.3 \times 10^{-6} \text{ dm}^3/\text{g}$  were used, as reported by Pamies[15].

### 2.3 Formation of the Lf/NaAlg complex

#### 2.3.1 Preparation of the solutions of Lf and NaAlg

The polysaccharide and protein were weighed in an analytical balance (Shimadzu, AY220, Philippines) for the preparation of a solution containing a fixed concentration of 0.1% (w/w). The NaAlg was homogenized for 24h using a magnetic stirrer (NT101, Novatecnica, Brazil), and the Lf was homogenized for 30 minutes, as performed by Gulão[4]. Ratios of 1:1, 1:2, 1:4: 1:8, 2:1, 4:1, and 8:1 (protein: polysaccharide) were tested. After determining the best ratio, different NaCl concentrations (0, 50, 100, 150, and 200mM) were tested and evaluated.

#### 2.3.2 Turbidimetric measurements

The pH-dependent turbidity was measured at a wavelength of 600 nm using a spectrophotometer (Biomate 3S, Thermo Fisher Scientific, USA) calibrated with ultrapure water to 100% transmittance (%T). Turbidity was defined as  $100 - \%T$ . With the aid of a magnetic stirrer (NT101, Novatecnica, Brazil) and pHmeter (Tecnoyon,

mPA210, Brazil), the pH values of the solutions were adjusted with 0.5M HCl. The pH was adjusted from 7.0 to 2.0 by 0.5-unit increments with a confidence interval of  $\pm 0.1$  unit. Different concentrations of NaCl were added to the ratio of 8:1 (Lf:NaAlg). Measurements of complexes and solutions with biopolymer isolates were performed three times. Sample readings were performed in triplicate at 25°C, as adapted from Souza [6].

### 2.3.3 $\zeta$ -Potential

A Zetasizer Nano ZS90 (Malvern Instruments, UK) was used to determine the zeta ( $\zeta$ )-potential. Lf and NaAlg stock solutions, and the mentioned ratios of complexes were diluted to 0.1% w/w and transferred to an MPT-2 autotitrator (Malvern Instruments, UK). Different concentrations of NaCl were added to the ratio of 8:1 (Lf:NaAlg). The pH was titrated using 0.5M NaOH, 0.25M HCl, and 0.025M HCl solutions. The pH was adjusted from 7.0 to 2.0 by 0.5-unit increments with a confidence interval of  $\pm 0.1$  unit.  $\zeta$ -potentials were calculated using the Smoluchowski mathematical model. Each experiment was performed three times, and sample readings were made in triplicate at 25°C, as adapted from Souza [6].

### 2.3.4 Isothermal titration calorimetry (ITC)

To perform a thermodynamic analysis by isothermal titration calorimetry (ITC), Nano-ITC equipment (TA Instruments, New Castle, USA) was used. The titration solutions (Lf) at 0.15mM and 0.0015mM NaAlg were prepared in a 10 mM citrate buffer (pH 4.0). A pH level of 4.0 was chosen as the best condition after evaluating the results obtained in the zeta and turbidity analyses. Additionally, as described in previous literature [3, 5, 13], the complex formation pH should be higher than the pKa of the alginate to avoid aggregate formation.

After dissolution of the biopolymers, the solutions were dialyzed using 3.5 kDa membranes (Sigma–Aldrich, Midi 3500, USA) to equilibrate ionic strength and pH ( $4.0 \pm 0.05$ ). The solutions were filtered (0.45  $\mu$ m) and degassed under vacuum using a degassing station (TA Instruments, New Castle, USA). The control was prepared by titration of lactoferrin in the buffer that was in the sample cell, and the reference cell was filled with ultrapure water. In total, 250  $\mu$ L of the titration solution (Lf) was titrated

in the sample cell containing the NaAlg solution at 310 rpm, an injection interval of 300 seconds and an injection volume of 10  $\mu\text{L}$ . The dilution energy was subtracted from the raw data, and the thermodynamic parameters were obtained through the program TANanoAnalyze<sup>®</sup>. The results were expressed at the significance level of 0.1.

The final concentration of Lf was measured by a spectrophotometer (Biochrom, LIBRA S12, England) at a wavelength of 280 nm and a coefficient of  $92.35 \text{ M}^{-1} \cdot \text{cm}^{-1}$ , which was obtained from the calibration curve of the protein at concentrations of 0.010 to 0.002mM. This method was adapted from Hosseini [19].

## 2.4 Characterization of the complex coacervate formed by Lf-NaAlg

### 2.4.1 *Fourier transform infrared spectroscopy (FT-IR)*

FT-IR spectra were obtained from the Lf and NaAlg samples at the ratio of 8:1 (Lf:NaAlg) and a pH of 4.0. The samples were frozen in an ultra-freezer (Terroni, COLD120, Brazil) at  $-40^{\circ}\text{C}$  for approximately 24 h. Soon after, they were placed in a benchtop freeze dryer (Terroni, Enterprise I, Brazil) for drying and stored in a desiccator with silica gel until use. The analyses were performed with an FT-IR spectrometer (Bruker, Ver-tex 70, Germany) using KBr (potassium bromide) pellets and read in the range of  $4000\text{--}400 \text{ cm}^{-1}$ .

### 2.4.2 *Differential Scanning Calorimetry (DSC)*

The moisture of the samples was determined in a gravimetric isotherm analyzer Q5000SA (TA Instruments, USA) under a controlled relative humidity of 0% at a temperature of  $60^{\circ}\text{C}$  until the mass change was less than 0.001%.  $\text{N}_2$  was used for purging at a flow rate of 200 mL/min. A differential scanning calorimetry (DSC) analysis was performed using a differential scanning calorimeter Q200 (TA Instruments, USA). An indium (In) standard was used to calibrate the energy and temperature of the equipment, and nitrogen was used as the drag gas. The lyophilized samples ( $\sim 5 \text{ mg}$ ) in which the moisture content was determined were weighed in hermetic aluminum crucibles with the aid of a precision scale (Mettler Toledo, Mx5, USA). Samples were analyzed over a temperature range of 20 to  $200^{\circ}\text{C}$  at the rate of  $5^{\circ}\text{C}/\text{min}$ , and an empty, sealed crucible was used as a reference [20]. The determination

of the transition temperature at the maximum peak and the enthalpy variation were analyzed by the Universal V4.5A<sup>®</sup> software (TA Instruments, USA).

#### 2.4.3 Scanning electron microscopy (SEM)

Micrographs of the Lf (1500x), NaAlg (50x) and freeze-dried (Terroni, Enterprise I, Brazil) complex of Lf/NaAlg at a ratio of 8:1 and pH of 4.0 (1500x) were obtained with a scanning electron microscope TM3000 (Hitachi, Tokyo, Japan) using a tungsten filament that was operated in secondary electron mode with an acceleration voltage of 15 kV.

### 3. Results and discussion

#### 3.1 Intrinsic viscosity and molecular weight of NaAlg

In the present study, NaAlg presented  $[\eta]= 0,3911 \text{ cm}^3/\text{g}$  and  $138 \text{ kDa} \pm 0.07$  molecular weight. This molecular weight value is similar to those reported in the literature [15, 21] when the molecular weight of sodium alginate was determined using the viscosimetric method. Additionally, the studies carried out by Pamies [15] and Dávila [21] obtained molecular weight values of NaAlg of 143 and 99.9 kDa, respectively.

NaAlg can vary its molecular weight from 100 to 270 kDa depending on its origin and extraction [22]. In this sense, alginate characterization is necessary to determine the exact molecular weight that should be inserted in ITC equipment to determine the interactions between Lf and NaAlg.

#### 3.2 Effect of the pH and ratio on the formation of the Lf/NaAlg complex

Fig. 1 shows the effect of the pH and ratio on the formation of the Lf/NaAlg complex. The variation of the zeta potential as a function of the pH of the biopolymers, both individually and in the respective ratios (1:1, 1:2, 1:4, 1:8, 2:1, 4:1, and 8:1) of Lf/NaAlg, is presented in Fig. 1(A). Lf showed a positive charge through out the studied pH range, and NaAlg presented a negative charge. According to the literature, the pI of



Lf is near pH 8.0, and the pKa of NaAlg is in the range of pH 3.4 - 3.7[3,5,13]. Thus, the ideal pH for the formation of the Lf/NaAlg complex is in the range of pH 3.7 to 8.0.

For the ratios of 1:1, 1:2, 1:4, 1:8, and 2:1 Lf/NaAlg, the zeta potential was negative over the pH range studied. This can be explained due to the stoichiometric balance of the charges, the electric charge density present in Lf was not sufficient to balance the charge of the Lf/NaAlg complexes[23]. As opposed to this situation, for the 4:1 ratio (Fig. 1A), the zeta potential was positive up to pH 3.0, and at this point, charge balance was achieved, allowing for a better interaction for complex formation.

The 8:1 ratio of Lf:NaAlg showed a positive zeta potential until the pH was close to 4.0, and above that pH, the zeta potential remained negative (Fig. 1A). Such behavior can be attributed to the protonation of the carboxylic groups when  $\text{pH} < \text{pKa}$  of sodium alginate for all the ratios[3,5]. Electrostatic interaction occurs between the  $\text{NH}_3^+$  positive cells present on the surface of the protein and the  $-\text{COO}^-$  negatively charged on sodium alginate. The greatest electrostatic interaction occurred near pH 4.0 where the charge approached neutrality, which represents a balance between the biopolymer charges. Similar results were obtained by Peinado[3] and Wang [12]. Peinado [3] observed that Lf/NaAlg samples exhibited extensive sedimentation at pH 2.0 and 3.0 (can be attributed to the protonation of the carboxylic groups), and the best pH was 4.0. According to Wang [12], the best pH was 4.5, at which the yield (w/w) and turbidity values increased significantly (91%) ( $p < 0.05$ ) at the Lf:NaAlg ratio of 8:1.

Fig. 1 (B) shows the variation of turbidity as a function of pH for the individual biopolymers and the Lf/NaAlg complex. As observed in Fig. 1 (B), the turbidity of the individual biopolymers remained constant over the studied pH range with a slight increase in the turbidity of Lf at pH 2.5. The ratios of 1:2, 1:4, and 1:8 showed higher turbidity at pH 2.0, while the ratios of 1:1, 2:1, and 4:1 showed higher turbidity at pH 2.5, decreasing as the pH was increased. By reducing the pH substantially below the pKa of the anionic polysaccharide, a loss of its charge and, consequently, a reduction in the electrostatic attraction of the complex coacervates occurs. The turbidity observed at  $\text{pH} < \text{pKa}$  can be attributed to the protonation of the carboxylic groups ( $-\text{CO}_2^- \rightarrow -\text{CO}_2\text{H}^+$ ) and possible aggregation of these groups [3,5]. This was observed by Peinado [3]. According to the author, at low pH values, extensive aggregation was observed in some of the samples (NaAlg), as indicated by the formation of white sediment at the bottom of the tubes. In the present study, the ideal ratio for formation of the Lf/NaAlg complexes was 8:1, which presented a higher turbidity at pH 4.0,  $\text{pH} > \text{pKa}$

of the alginate and below the pI of Lf. Moreover, at pH 4.0, the ratio of 8:1 presented a charge near neutral ( $-8 \text{ mV} \pm 0.173$ ), representing a balance between the charges of the biopolymers. The same was observed by Wang [12]. The better ratio of Lf/ NaAlg was 8:1 but the ideal pH was 4.5. The difference can be explained because the type of Lf was different and the author heated the protein.

In the zeta potential measurements, the highest coefficient of variation (CV) obtained in triplicate was 4.55% for the ratio of 8:1. Under this condition, the pH and ratio showing the best balance of charges were evaluated. When evaluating the turbidity of the ratios as a function of pH, it was possible to observe a higher CV (3.44%) in the triplicate measurements of the 1:2 ratio. When evaluating the 8:1 ratio as a function of salt, the highest CV was 1.6% in the triplicate measurements of the 150mM NaCl concentration. CV is a statistical measure of the dispersion of data points in a data series around the average, indicating variability. It is used when one wants to determine if observations vary from the average. According to the literature [24], when the CV is less than or equal to 10%, the data dispersion is low, and the accuracy of the values is optimal. Thus, the results obtained in the zeta potential and turbidity measurements are considered reliable and accurate because they are below 10%.

The critical pH transition points ( $\text{pH}_{\phi_1}$ ,  $\text{pH}_{\text{max}}$ , and  $\text{pH}_{\phi_2}$ ) for the 8:1 ratio of Lf/NaAlg can be observed in Fig. 1(C). The  $\text{pH}_c$  was not clearly determined from the turbidity measurements. Before  $\text{pH}_{\phi_1}$ , the turbidity remained constant. Such behavior may be due to protonation of the alginate because  $\text{pH} < \text{pK}_a$ , which reduces the covalent attractions between the biopolymers [25].

The first point observed was  $\text{pH}_{\phi_1}$  (2.5 to 3.7). This point indicates a higher interaction between the biopolymers due to the formation of insoluble complexes. However, the pH is below the pKa of alginate, which may indicate possible aggregation of the carboxylic groups [3,5]. The  $\text{pH}_{\text{max}}$  was between pH 4.0 to 4.5. In this range, the formation of the complexes occurred due to the higher positive charge density of Lf because it was at a pH below its pI. Alginate had the highest negative charge density because it was at a  $\text{pH} > \text{pK}_a$ , resulting in an electrostatic attraction between the biopolymers. In the present study, the optimum pH for complex formation was pH 4.0, this pH is most commonly encountered in food products. The Lf/NaAlg complex thus presenting its potential to be used as a wall material in the incorporation of functional ingredients in various food systems [5].

A similar result was obtained by Peinado [3], according to the author, the ideal pH for the formation of the Lf/NaAlg complex was pH 4.0. The same pH (4.0) was used by Gulão [4] to form a complex between Lf and gum arabic. In the present study, the last critical point observed (Fig. 1C) was  $pH_{\phi_2}$  (pH5.9), in which the dissociation of the complex occurred due to electrostatic repulsion, which was also observed by Peinado [3].

### 3.3 *Effect of NaCl concentration on the formation of the coacervate complex of Lf/NaAlg*

Fig. 2 presents the effect of different NaCl concentrations as a function of the turbidity on the 8:1 ratio of the Lf/NaAlg complex in the pH range from 2.0 to 7.0. As observed in Fig. 2, the ratio with 50mM NaCl was the one with the highest turbidity over the studied pH range. The addition of the salt (all concentrations) favored the formation of the Lf/NaAlg complex.

However, the increased turbidity at all salt concentrations can be attributed to the aggregation of alginate carboxyl groups. Monovalent or multivalent ions, such as sodium or calcium, bind to the groups loaded in the biopolymer chain by altering the general charge characteristics and promoting the protonation of these groups[26]. Thus, a possible disadvantage in the formation of the Lf/NaAlg complex can be attributed to the interaction of salt ions with groups of opposite charge in the protein. These form a double layer of ionic groups, which decreases the electrostatic interaction between protein molecules. This causes more solvation of proteins and, thus, increases the solubility of the protein [6, 27]. This may be because the behavior resulting from the increase in the saline concentration is related to the internal characteristics of the proteins (amino acid composition, isoelectric point, hydrophobicity, molecular weight, and charge density). At high salt concentrations, most water molecules are strongly bound to salt ions, and the reorganization of water molecules around proteins occurs. This could result in a stronger protein-protein interaction (mainly through surface hydrophobic interactions) than protein-water interaction [27]. Dubin [28], Wang [29] and Seyrek[30] observed that salt reduces the attractive force interaction between oppositely charged protein-polyelectrolytes by reducing complex coacervation. The same was observed by other authors when studying the effect of salt on oppositely charged biopolymers[3,4,31]. Peinado[3] observed that up to 100mM of NaCl presented

an increase in the turbidity of the Lf/NaAlg complex, and when the salt concentration further increased, the turbidity decreased. According to the author, intermediate salt levels promoted flocculation of particles, and higher salt levels promoted the separation of these particles. Gulão[4] observed that the concentrations of 300 and 500mM contributed to the reduction of the formation of the Lf/gum arabic complex. The same was observed by Bengoechea [31] when studying the formation of the Lf/pectin complex.

According to the results presented in the present study, the LF/NaAlg complex can be used to incorporate functional ingredients in to food matrices with low salt concentration. Higher salt concentrations weakened the attraction between the protein and the polysaccharide molecules due to the characteristics of the biopolymers.

### 3.4 Isothermal Titration Calorimetry

The thermograms of the heat flux over time (obtained from the titration of Lf in NaAlg at 25°C and pH 4.0) are shown in Fig. 3(A). According to the figure, the titration profile was exothermic for all injections. The binding isotherm of the Lf/NaAlg complex, shown in Fig. 3 (B), was characterized by one stage. Several studies have reported the same behavior when studying the interaction between proteins and polysaccharides, such as  $\beta$ -lactoglobulin/carrageenan [19],  $\beta$ -lactoglobulin/Persian gum[10], ovalbumin/chitosan[32], and soy protein/gum arabic [33].

The ITC data were better adjusted using an independent model supplied by the TA NanoAnalyze<sup>®</sup> software. The thermodynamic parameters used included the reaction stoichiometry (N), binding constant (K), enthalpy ( $\Delta H$ ), change of entropy (T $\Delta S$ ), and Gibbs free energy change ( $\Delta G$ ), which can be calculated from the equation  $\Delta G = \Delta H - T\Delta S$ , where T is the temperature in Kelvin (298.15). In the present study, the following parameters were obtained:  $K(M^{-1}) = 0.24 \times 10^7 \pm 1.574 \times 10^7$ ,  $N = 6.89 \pm 0.1975$ ,  $\Delta H$  (kcal/mol) =  $-15.96 \pm 0.8996$ , T $\Delta S$  (kcal/mol) =  $-7.25$ , and  $\Delta G$  (kcal/mol) =  $-8.70$ .

In regards to the binding stoichiometry, that is, the number of Lf molecules that interacted with NaAlg, the value of  $N \cong 7$  indicates that 7 Lf molecules interacted with 1 molecule of NaAlg.

The binding constant was on the order of  $10^7 M^{-1}$ , indicating a strong binding affinity between Lf and NaAlg[34]. The  $\Delta G$  value was negative, indicating the spontaneous nature of the interaction between Lf and NaAlg. According to the

literature, enthalpy ( $\Delta H$ ) is related to the energy involved in molecular interactions and reflects the contribution of hydrogen bonds, electrostatic interactions and van der Waals, while the change in entropy ( $T\Delta S$ ) reflects a change in the order of the system and is related to hydrophobic interactions[35,36]. The  $\Delta H$  and  $T\Delta S$  values were negative, indicating that the complexation process between the protein and NaAlg is favorable enthalpically and unfavorable entropically.

The enthalpic contribution is regulated by the mixing ratio and the nature and density of the charges of the biopolymers. The unfavorable entropic effects resulted mainly from the loss of conformational independence by the biopolymer after complexation [1]. Similar behavior was described in the literature when studying the thermodynamic parameters of  $\beta$ -lactoglobulin-gum acacia[9], ovalbumin-chitosan[31]  $\beta$ -lactoglobulin- $\kappa$ -carrageenan[19],  $\beta$ -lactoglobulin-Persian gum[10], ovalbumin-carboxymethylcellulose[37], and egg white proteins-carrageenan [38].

### 3.5 Chemical and morphological characterization of the Lf/NaAlg complex

Fig. 4 shows the infrared (FT-IR) spectroscopy results of NaAlg, Lf and the complex of Lf /NaAlg (8:1) at pH 4.0. The selected wavelength region ( $4000$  to  $400$   $\text{cm}^{-1}$ ) includes the amide bands of the protein: group I ( $1625$ - $1750$   $\text{cm}^{-1}$ ), group II ( $1475$ - $1575$   $\text{cm}^{-1}$ ), and group III ( $1225$  -  $1425$   $\text{cm}^{-1}$ ). The amide band I refers to the stretching of the C=O, the amide band II corresponds to the stretching of the N-H, and the amide band III is attributed to the stretching of the C-N and N-H groups [39]. In Lf, the amide bands I, II and III were observed at  $1632$ ,  $1521$ , and  $1393$  $\text{cm}^{-1}$ , respectively (Fig.4). Similar values were demonstrated by Bokkhim[5].

The free amino acid O-H groups [40] can be identified between the bands  $3300$  and  $3170$   $\text{cm}^{-1}$ . In Lf, the O-H group of the free amino acid can be identified by the  $3278$  band [39].

For NaAlg, the first band is at  $1591$  $\text{cm}^{-1}$ , representing the presence of  $\text{CO}_2^-$  in the carboxylic acid salts ( $\text{RCOO}^-$ ) in the range of  $1650$ - $1550$  $\text{cm}^{-1}$ [40]. Band 2, at  $1404$  $\text{cm}^{-1}$ , refers to the C-O bond of the acid group ( $\text{RCOOH}$ ) in the range of  $1440$ - $1395$  $\text{cm}^{-1}$ [41]. Band 3 ( $1024$   $\text{cm}^{-1}$ ) is attributed to the vibrational stretch of the C-O and C-C of the pyranose ring[5].

The 8:1 ratio of Lf/NaAlg is similar to the spectra of the two biopolymers individually, with bands at 3278, 1521, and 1393  $\text{cm}^{-1}$  for Lf that were observed in the complex. The 3278  $\text{cm}^{-1}$  band represents the O-H group of the free amino acids. The 1521  $\text{cm}^{-1}$  band corresponds to the stretching of the N-H groups. The region represented by amide III (1393  $\text{cm}^{-1}$ ) for Lf is attributed to the stretching of the C-N and N-H groups, which was also observed in the complex.

The region represented by the amide I observed in Lf was observed in the complex with a displacement of 1  $\text{cm}^{-1}$  in the region of 1631  $\text{cm}^{-1}$ . Such displacement indicates that the negative groups of NaAlg were associated with the positive groups of Lf, as observed by Devi [42]. Nevertheless, for the 8:1 ratio of Lf/NaAlg, the 1024  $\text{cm}^{-1}$  band may indicate the formation of an electrostatic interaction between the carboxylic groups (-COO) of NaAlg and the amine groups (-NH<sub>3</sub><sup>+</sup>) of Lf [6].

For a better understanding of the internal structure of the complex coacervate, SEM images of the individual biopolymers and the Lf/NaAlg complex were taken in order to examine the new structures that were formed (Fig. 5). The NaAlg presented blocks in different sizes that had irregular shapes and surfaces (Fig. 5A), which was also observed by Borba [43]. Lf presented a globular and irregular shape (Fig. 5B), as reported by Wang [12]. The complexes of Lf/NaAlg (8:1) at pH 4.0 can be observed in Fig. 5C. The formation of a three-dimensional network during complexation is noted, and the sample had a heterogeneous structure [44].

### 3.6 *Differential scanning calorimetry*

Fig. 6 shows the isolated thermograms of NaAlg, Lf, and the Lf/NaAlg complex (8:1, pH 4.0). The main endothermic events corresponding to Lf denaturation, the interactions of the Lf/NaAlg complex (8:1) and the T<sub>g</sub> value were observed at different temperatures.

The denaturation temperature of isolated Lf was 53°C. The T<sub>g</sub> of NaAlg is 120.27°C, [45]. The Lf/NaAlg complex (8:1) degraded at 116.67°C, indicating that the degradation temperature of the complex was between the denaturation temperature of Lf and the T<sub>g</sub> of NaAlg. The same was observed by Duhoranimama [46] when evaluating the thermal characteristics of gelatin (G), carboxymethyl cellulose (CMC) and G-CMC complex coacervates. The denaturation temperature of the isolated gelatin was

104.21°C, CMC presented a melting temperature of 167.17°C and the G-CMC complex coacervates degraded at 118.26°C.

The enthalpy of denaturation ( $\Delta H_d$ ) indicates the amount of energy needed to denature structures native to biopolymers[47]. The  $\Delta H_d$  of Lf, and the complex of Lf/NaAlg were 1.487 J/g, 129.5 J/g, respectively. The results indicated that the degradation of Lf in complex coacervates requires a higher thermal energy compared to isolated Lf. The high  $\Delta H_d$  value of the Lf/NaAlg complex (129.5 J/g) indicates that it can be used as a thermally resistant wall material, and it is possible to use it to microencapsulate components sensitive to high temperatures.

These results are in agreement with the findings of Duhoranimama [46], who reported that enthalpy values of G-CMC complex coacervates (236.033 J/g) were higher than the corresponding values of pure G (4.524 J/g). The same was observed by Bokkhim [5] and Timilsena [47]. Bokkhim [5] determined that native Lf presented a better thermal stability in the Lf/NaAlg complex, which was different from the other Lf types studied by the author. Timilsena [47] reported that enthalpy values of chia seed protein isolate (CPI) and chia seed gum complex coacervates were higher than the corresponding values of pure CPI.

#### **4. Conclusion**

In this study, NaAlg had a low molecular weight and its interaction with Lf in the formation of soluble or insoluble complexes was a function of pH. The best ratio and pH for complex formation were 8:1 Lf/NaAlg and 4.0, respectively. A low salt concentration favored electrostatic interaction; however, higher concentrations weakened the attraction between the protein and the polysaccharide molecules due to the characteristics of Lf and NaAlg. The ITC data indicated a strong binding affinity between Lf and NaAlg with a favorable enthalpic and unfavorable entropic contribution during their interaction. The chemical and morphological characteristics of the complex coacervates showed changes produced by the electrostatic interaction between lactoferrin and sodium alginate. The Lf/NaAlg complex presented a higher thermal resistance, thus presenting its potential to be used as a wall material in the incorporation of functional ingredients sensitive to high temperatures in various food systems.

**Conflict of interest**

The authors declare no conflict of interest.

**Acknowledgment**

The authors thank to FAPERJ and CNPq for the financial support.



## 5. References

- [1] Dickinson, E. Interfacial structure and stability of food emulsions as affected by protein–polysaccharide interactions, *Soft Matter* 4 (2008) 932-942.
- [2] Tolstoguzov, V. B. Functional properties of food proteins and role of protein polysaccharide interaction, *Food Hydrocolloid* 4 (1991) 429-468.
- [3] Peinado, I. Lesmes, U. Andres, A. McClements, D. J. Fabrication and morphological characterization of biopolymer particles formed by electrostatic complexation of heat treated lactoferrin and anionic polysaccharides, *Langmuir* 26 (2010) 9827- 9834.
- [4] Gulão, E. D. S. D. Souza, C. J. F. D. Silva, F. A. S. Coimbra, J. S. R. Garcia-Roja, E. E. Complex coacervates obtained from lactoferrin and gum arabic: Formation and characterization, *Food Research International* 65 (2014) 367-374.
- [5] Bokkhim, H. Bansal, N. Grøndahl, L. Bhandari, B. Interactions between different forms of bovine lactoferrin and sodium alginate affect the properties of their mixtures, *Food Hydrocolloids* 48 (2015) 38-46.
- [6] Souza, C. J. Garcia-Rojas, E. E. Interpolymeric complexing between egg white proteins and xanthan gum: Effect of salt and protein/polysaccharide ratio, *Food Hydrocolloids* 66 (2017) 268-275.
- [7] Liu, J. Shim, Y. Y. Wang, Y. Reaney, M. J. Intermolecular interaction and complex coacervation between bovine serum albumin and gum from whole flaxseed (*Linum usitatissimum* L.), *Food Hydrocolloids* 49 (2015) 95-103.
- [8] Zeeb, B. Mi-Yeon, L. Gibis, M. Weiss, J. Growth phenomena in biopolymer complexes composed of heated WPI and pectin, *Food Hydrocolloids* 74 (2018) 53-61.
- [9] Aberkane, L. Jasniewski, J. Gaiani, C. Scher, J. Sanchez, C. Thermodynamic characterization of acacia gum–  $\beta$ -lactoglobulin complex coacervation, *Langmuir* 26 (2010) 12523-12533.
- [10] Hadian, M. Hosseini, S. M. H. Farahnaky, A. Mesbahi, G. R. Yousefi, G. H. Saboury, A. A. Isothermal titration calorimetric and spectroscopic studies of  $\beta$ -lactoglobulin-water-soluble fraction of Persian gum interaction in aqueous solution, *Food Hydrocolloids* 55 (2016) 108-118.
- [11] Du, J. Reuhs, B. L. Jones, O. G. Influence of PEGylation on the ability of carboxymethyl-dextran to form complexes with  $\alpha$ -lactalbumin, *Food chemistry* 196 (2016) 853-859.
- [12] Wang, B. Blanch, E. Barrow, C. J. Adhikari, B. Preparation and study of digestion behavior of lactoferrin-sodium alginate complex coacervates, *Journal of Functional Foods* 37 (2017) 97-106.

- [13] García-Montoya, I. A. Cendón, T.S. Arévalo-Gallegos, S. Rascón-Cruz, Q. Lactoferrin a multiple bioactive protein: na overview, *Biochimica et Biophysica Acta(BBA)-General Subjects* 1820 (2012), 226-236.
- [14] Phillips, O. G. Williams, P. A. *Handbook of hydrocolloids*, (2 Ed), Florida, Boca Raton, 2009, pp. 902.
- [15] Pamies, R. Schmidt, R. R. Martínez, M. D. C. L. de la Torre, J. G. The influence of mono and divalent cations on dilute and non-dilute aqueous solutions of sodium alginates, *Carbohydrate Polymers* 80 (2010) 248-253.
- [16] Guo, X. Zhao, W. Liao, X. Hu, X. Wu, J. Wang, X. Extraction of pectin from the peels of pomelo by high-speed shearing homogenization and its characteristics, *LWT-Food Science and Technology* 79 (2017) 640-646.
- [17] Mark, H, in: *Der feste Körper*, Hirzel, Leipzig, 1938, pp. 65-104.
- [18] Houwink, R. The interrelationship between viscosimetric and osmotic identified degree of polymerisation in high polymers, *Journal Fur Praktische Chemie-Leipzig* 157 (1940) 15-18.
- [19] Hosseini, S. M. H. Emam-Djomeh, Z. Razavi, S. H. Moosavi-Movahedi, A. A. Saboury, A. A. Atri, M. S. Van der Meeren, P.  $\beta$ -Lactoglobulin–sodium alginate interaction as affected by polysaccharide depolymerization using high intensity ultrasound, *Food hydrocolloids* 32 (2013) 235-244.
- [20] Fareez, I. M. Lim, S. M. Mishra, R. K. Ramasamy, K. Chitosan coated alginate–xanthan gum bead enhanced pH and thermotolerance of *Lactobacillus plantarum* LAB12, *International journal of biological macromolecules* 72 (2015) 1419-1428.
- [21] Dávila, J. L. d'Ávila, M. A. Laponite as a rheology modifier of alginate solutions: Physical gelation and aging evolution, *Carbohydrate polymers* 157 (2017) 1-8.
- [22] Launey, B. Doublier, J. L. Cuvelier, G. Flow properties of aqueous solutions and dispersions of polysaccharides, in: J. R. Mitchell, D. A. Ledward, *Functional Properties of Food Macromolecules*, London, Elsevier, 1985, pp. 1-78.
- [23] Schmitt, C. Turgeon, S. L. Protein/polysaccharide complexes and coacervates in food systems. *Advances in Colloid and Interface Science* 167 (2011) 63-70.
- [24] Pimentel Gomes, F. *Curso de Estatística Experimental*. São Paulo: Nobel, 1985. 467p.
- [25] Ru, Q. Wang, Y. Lee, J. Ding, Y. Huang, Q. Turbidity and rheological properties of bovine serum albumin/pectin coacervates: effect of salt concentration and initial protein/polysaccharide ratio, *Carbohydrate Polymers* 88 (2012) 838-846.
- [26] Matalanis, A. Jones, O. G. McClements, D. J. Structured biopolymer-based delivery systems for encapsulation, protection, and release of lipophilic compounds, *Food Hydrocolloids* 25 (2011) 1865-1880.

- [27] Vojdani, F. Solubility, in: G. M. Hall, *Methods of testing protein functionality*, London, Blackie Academic & Professional, 1996, pp.11-60.
- [28] Dubin, P. L. Gao, J. Mattison, K. Protein purification by selective phase separation with polyelectrolytes, *Separation and Purification Methods* 23 (1994)1-16.
- [29] Wang, Y.L.Kimura, K. Huang, Q.R. Dubin, P.L. Jaeger, W. Effects of Salt on Polyelectrolyte-Micelle Coacervation, *Macromolecules* 32 (1999) 7128–7134.
- [30] Seyrek, E. Dubin, P. L. Tribet, C. Gamble, E. A. Ionic strength dependence of protein-polyelectrolyte interactions, *Biomacromolecules* 4 (2003) 273-282.
- [31] Bengoechea, C. J. O. G. Guerrero, A. McClements, D. J. Formation and characterization of lactoferrin/pectin electrostatic complexes: Impact of composition, pH and thermal treatment, *Food Hydrocolloids* 25 (2011) 1227–1232.
- [32] Xiong, W. Ren, C.Jin, W. Tian, J. Wang, Y. Shah, B. R. Li, B. Ovalbumin-chitosan complex coacervation: Phase behavior, thermodynamic and rheological properties, *Food Hydrocolloids* 61 (2016) 895-902.
- [33] Dong, D. Li, X. Hua, Y. Chen, Y. Kong, X. Zhang, C. Wang, Q. Mutual titration of soy proteins and gum arabic and the complexing behavior studied by isothermal titration calorimetry, turbidity and ternary phase boundaries, *Food Hydrocolloids* 46 (2015) 28-36.
- [34] Ferstl, M. Drechsler, M. Rachel, R. Rischer, M. Engel, J. Backofen, M. Goepferich, A. The impact of polyelectrolyte structure on the shape of nano assemblies with cationic peptides, *Journal of pharmaceutical sciences* 102 (2013) 2599-2607.
- [35] Bou-Abdallah, F.Terpstra, T. R. The thermodynamic and binding properties of the transferrins as studied by isothermal titration calorimetry. *Biochimica et Biophysica Acta (BBA)-General Subjects*1820 (3) (2012) 318-325.
- [36] Pires, A.C.S, Silva, M.C.H, Silva, L.H.M. Microcalorimetry a food science and engineering approach, in: J. Coimbra, J.A. Teixeira (Eds.), *Engineering Aspects of Milk and Dairy Products*, CRC Press, Boca Raton, 2009, pp. 201–218.
- [37] Xiong, W. Ren, C. Tian, M. Yang, X. Li, J. Li, B. Complex coacervation of ovalbumin-carboxymethylcellulose assessed by isothermal titration calorimeter and rheology: Effect of ionic strength and charge density of polysaccharide, *Food Hydrocolloids* 73 (2017) 41-50.
- [38] Souza, C. J, Souza, C. S, Bastos, L. P. H, Garcia-Rojas, E. E. Interpolymer complexation of egg white proteins and carrageenan: Phase behavior, thermodynamics and rheological properties. *International journal of biological macromolecules* 109 (2018) 467-475.
- [39] Huang, C.Y. Balakrishnan, G. Spiro, T. G. Protein secondary structure from deep-UV resonance Raman spectroscopy, *Journal of Raman Spectroscopy* 37 (2006) 277-282.

- [40] Barth, A. Zscherp, C. What vibrations tell about proteins, *Quarterly Reviews of Biophysics* 35 (2002) 369-430.
- [41] Barbosa, A.D.C.L. Espectroscopia no Infravermelho na caracterização de compostos orgânicos, Minas Gerais, UFV, 2007, pp.189.
- [42] Devi, N. Hazarika, D. Deka, C. Kakati, D. K. Study of complex coacervation of gelatin A and sodium alginate for microencapsulation of olive oil, *Journal of Macromolecular Science, Part A* 49 (2012) 936-945.
- [43] Borba, P. A. A. Pinotti, M. de Campos, C. E. M. Pezzini, B. R. Stulzer, H. K. Sodium alginate as a potential carrier in solid dispersion formulations to enhance dissolution rate and apparent water solubility of BCS II drugs, *Carbohydrate polymers* 137 (2016) 350-359.
- [44] Kayitmazer, A. B. Bohidar, H. B. Mattison, K. W. Bose, A. Sarkar, J. Hashidzume, A. Dubin, P. L. Mesophase separation and probe dynamics in protein–polyelectrolyte coacervates, *Soft Matter* 3 (2007) 1064-1076.
- [45] Flynn, E. J, Keane, D, Holmes, J. D, Morris, M. A. Unusual trend of increasing selectivity and decreasing flux with decreasing thickness in pervaporation separation of ethanol/water mixtures using sodium alginate blend membranes. *Journal of colloid and interface science*, 370 (2012), 176-182.
- [46] Duhoranimana, E. Karangwa, E. Lai, L. Xu, X. Yu, J. Xia, S. Habinshuti, I. Effect of sodium carboxymethyl cellulose on complex coacervates formation with gelatin: Coacervates characterization, stabilization and formation mechanism. *Food Hydrocolloids* 69 (2017) 111-120.
- [47] Timilsena, Y. P. Wang, B. Adhikari, R. Adhikari, B. Preparation and characterization of chia seed protein isolate–chia seed gum complex coacervates, *Food hydrocolloids* 52 (2016) 554-563.

## Figure Captions

**Fig. 1:** (A)  $\zeta$  potential of the isolated biopolymers (Lf and NaAlg) and the Lf/NaAlg complex at different ratios. (B) Turbidity ( $\text{cm}^{-1}$ ) as a function of pH in the system containing Lf/NaAlg complexes with different ratios. (C)  $\text{pH}_{\phi 1}$ ,  $\text{pH}_{\text{máx}}$  and  $\text{pH}_{\phi 2}$  of the Lf/NaAlg complex at a ratio of 8:1.

**Fig. 2:** Turbidity ( $\text{cm}^{-1}$ ) as a function of pH in the system containing complex Lf/NaAlg ratio  $r=8:1$  at different concentrations of NaCl.

**Fig. 3:** (A) Heat flow thermogram ( $\mu\text{cal/s}$ ) as a function of time (s), obtained during the titration of 0.15mM Lf in 0.0015mM NaAlg in a 10mM citrate buffer (pH 4.0) at 25°C. (B) Graphical representation of the integral of the area under each peak (kcal/mol) as a function of the molar ratio ( $r_m$ ) of Lf/NaAlg, ( $p < 0.1$ ).

**Fig. 4:** FT-IR spectra of NaAlg, Lf and the Lf/NaAlg complex at a ratio of 8:1 at pH 4.0.

**Fig. 5:** SEM of the (A) NaAlg, (B) Lf, and (C) complex of Lf/NaAlg at a ratio of 8:1 at pH 4.0.

**Fig. 6:** (A) Thermogram generated by DSC analysis of Lf, NaAlg and samples from the Lf/NaAlg complex at a ratio of 8:1 at pH 4.0. (B) Thermogram generated by DSC analysis of Lf.

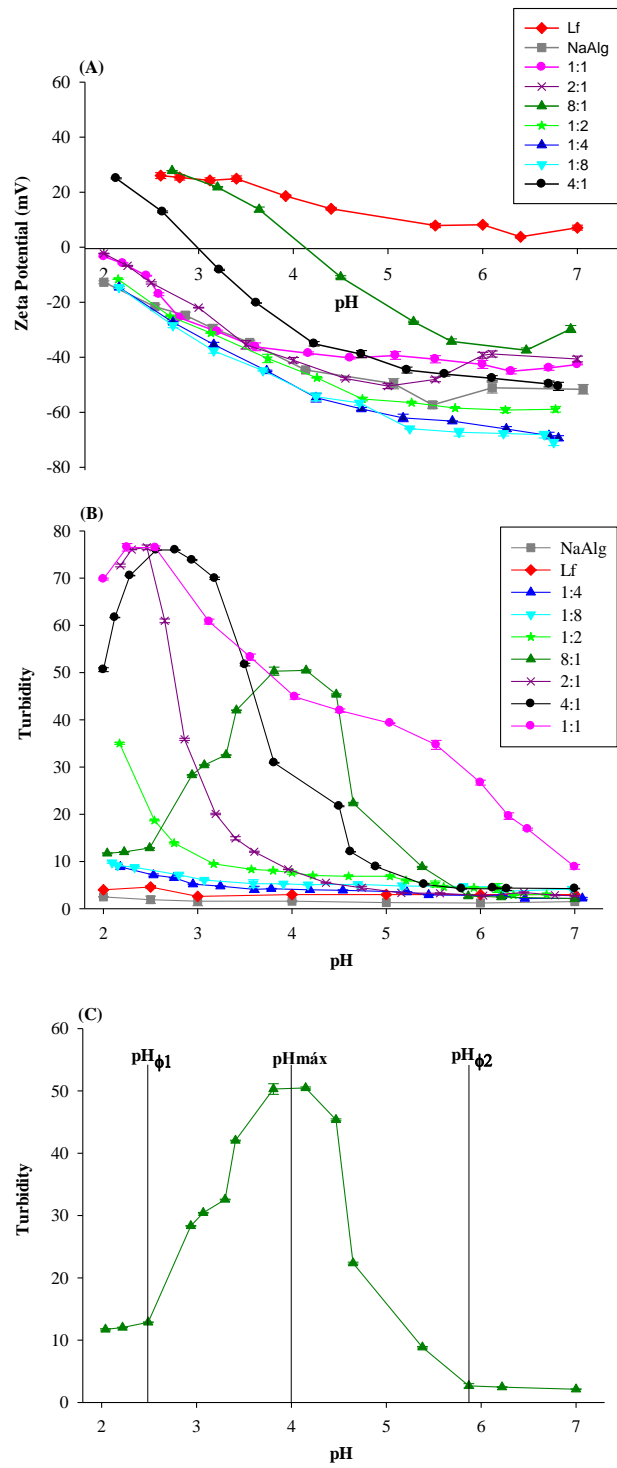


**Fig.1.**

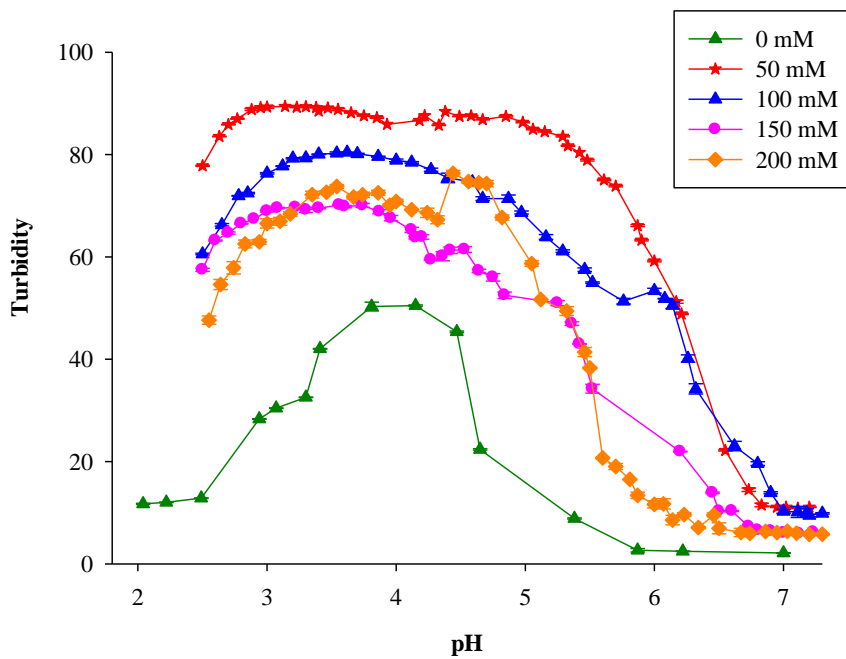


Fig.2.

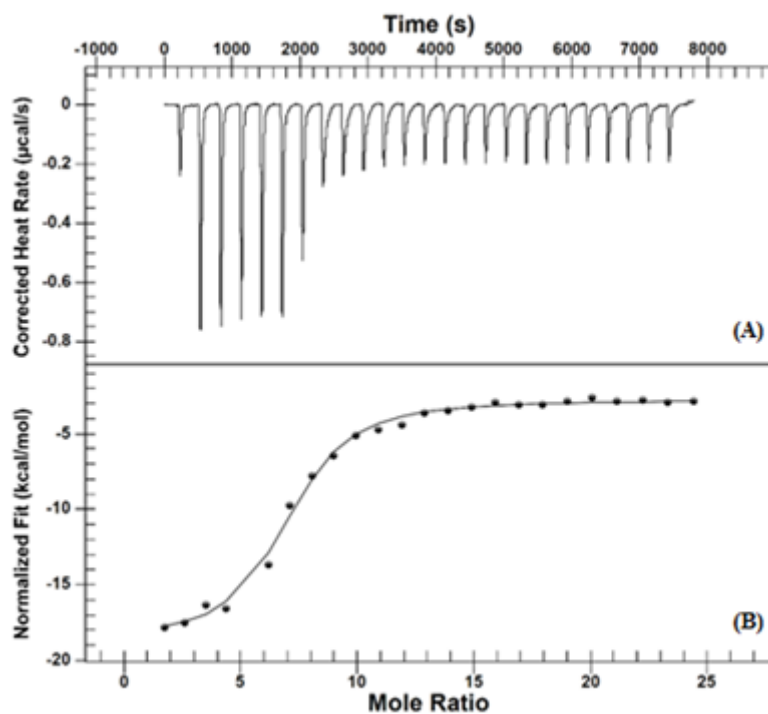
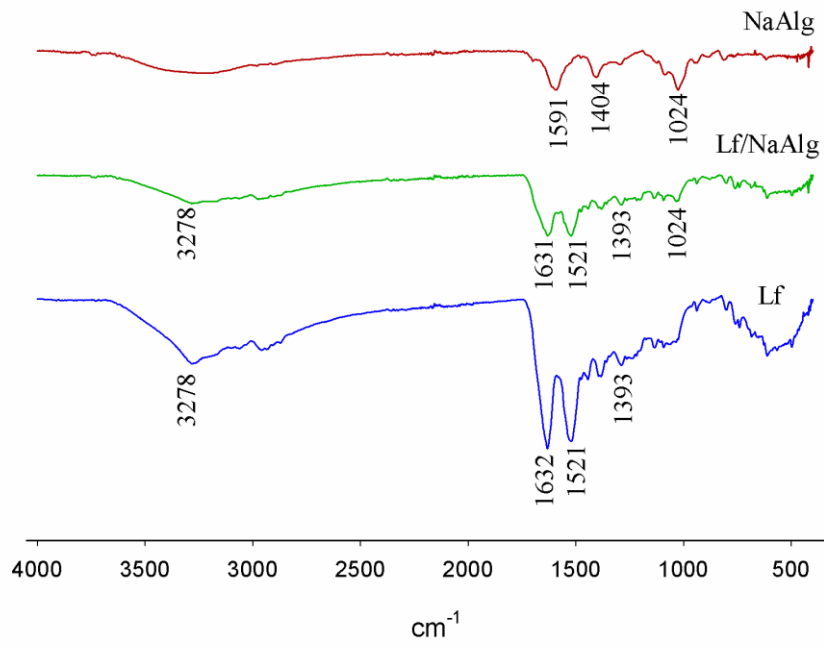
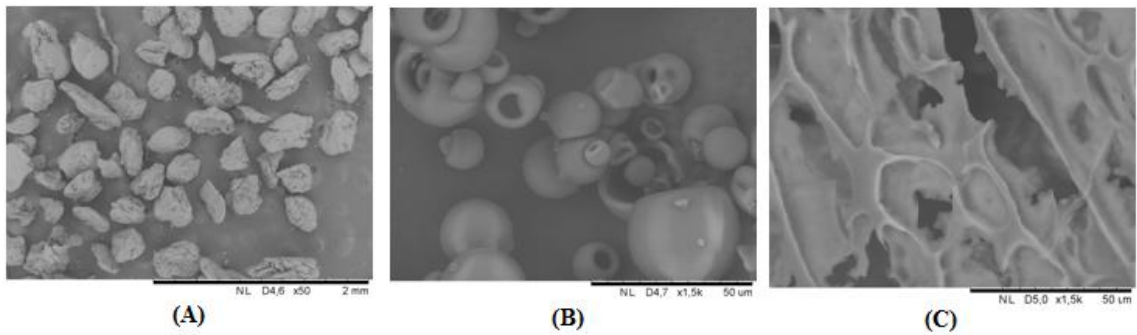


Fig.3.



**Fig.4.**



**Fig.5.**



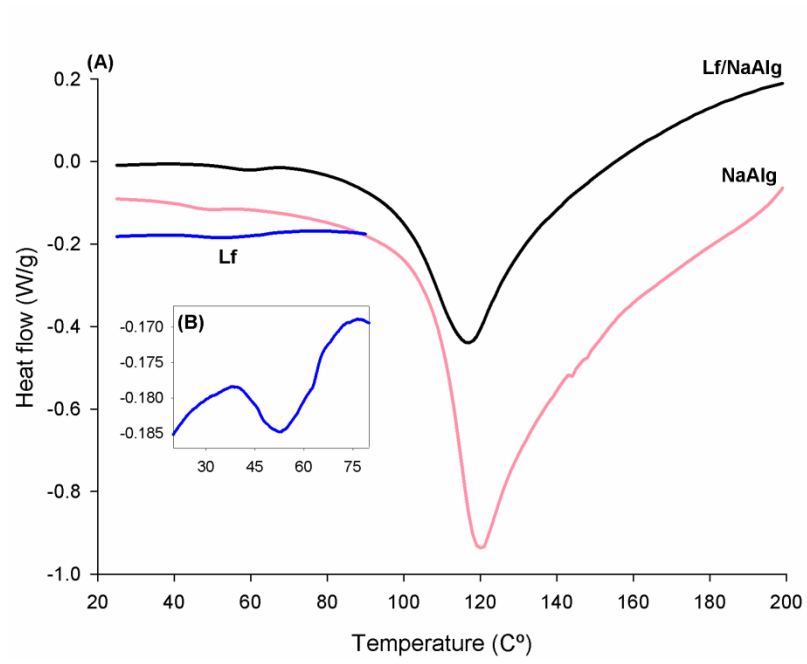


**Fig.6.**

**CAPÍTULO III**  
**ENCAPSULATION OF THE BLACK PEPPER (*PIPER NIGRUM L.*)**  
**ESSENTIAL OIL BY LACTOFERRIN-SODIUM ALGINATE COMPLEX**  
**COACERVATES: STRUCTURAL CHARACTERIZATION AND SIMULATED**  
**GASTROINTESTINAL CONDITIONS**

Submitted to **Food chemistry**.

## Abstract

The black pepper essential oil (EO) was encapsulated by complex coacervation with lactoferrin and sodium alginate using transglutaminase as a cross-linking. Encapsulation efficiency varied from 31.66 to 84.48 %. Chemical and morphological characteristics showed that EO was encapsulated in a lactoferrin/sodium alginate shell. The chemical composition of the EO unencapsulated and encapsulated was identified by gas chromatography (GC) and nuclear magnetic resonance (NMR). GC and NMR analysis indicated good core protection with the materials used. The stability of the black pepper EO capsules under *in vitro* digestion was evaluated. Capsules demonstrated the low release of the EO during gastric digestion and higher release in intestinal digestion. The biopolymers used as wall materials shown to protect black pepper essential oil effectively. The capsules developed in this study can be used to transport active ingredients because they are resistant to the human oral and gastric conditions tested *in vitro*.

**Keywords:** Terpenes, whey protein, polysaccharides, encapsulation efficiency, nuclear magnetic resonance.

## 1. Introduction

Black pepper (*Piper nigrum L.*) is a plant of *Piperaceae* family, is used as a spice. The essential oil (EO) of *Piper nigrum* presented antioxidant and antimicrobial activity (Ravindran & Kallapurackal, 2004; Saha et al., 2013). Essential oils (EOs) are aromatic and volatile oily liquids obtained from plants and are rich sources of biologically active compounds such terpenoids and phenolic acids (Oussalah, Caillet, Saucier, & Lacroix, 2006). Certain conditions (oxygen, light, high temperatures, low pH and gastrointestinal fluids) contribute to the degradation and decrease of their biological potential of the EOs. Encapsulation can prevent exposure of EOs and their degradation (Bakkali et al., 2008; Dima et al., 2016).

Microencapsulation creates a physical barrier between the core and wall materials protecting sensitive ingredients from the external environment. Among the techniques of microencapsulation, complex coacervation has been used to encapsulate EOs (Koupantsis et al., 2016; Ghasemi et al., 2017; Rojas-Moreno et al., 2018; Girardi et al., 2017). The main advantages of complex coacervation over other microencapsulation methods include generally high encapsulation efficiency and the possibility of controlled release application (Kravolec et al., 2012). The complex coacervation process principally consists of three basic steps: emulsification, coacervation, and shell formation and/or hardening (Zhang et al., 2012). Coacervation is the separation of a colloidal system into two liquid phases (International Union of Pure and Applied Chemistry-IUPAC, 1997). The complex coacervation consists of the electrostatic interaction between two polymers with opposite charges, usually a protein and polysaccharide (Nesterenko et al., 2014).

Due to their functional and nutritional properties, whey proteins are used in combination with polysaccharides to encapsulate EOs and other compounds by complex coacervation: whey protein isolate (WPI)/carboxymethylcellulose (CMC) (Koupantsis et al., 2014; Koupantsis et al., 2016), WPI/pectin (Ghasemi et al., 2017), WPI/ Sodium alginate (Rojas-Moreno et al., 2018). In this study, lactoferrin (Lf) and sodium alginate (NaAlg) were used as wall materials. Lf is an iron-binding protein which is commercially extracted and manufactured from bovine milk, presented isoelectric point (pI) near to 8.0 and has 80kDa (Tomita et al., 2009; Bengoechea, Jones, et al., 2011). NaAlg is natural, biocompatible, biodegradable anionic polysaccharide extracted from brown seaweed (*Phaeophyceae*), or certain species. The structure

consists of linear chains (1→4 linked blocks of poly β-D-mannuronic acid (M), α-D-guluronic acid (G) and mixed MG blocks (Pamies, Rodríguez-Schmidt, López-Martínez, & García-de la Torre, 2010; Lemos, Marfil & Nicoletti, 2017).

Studies showed that formation of complex coacervates between Lf and NaAlg can serve as an alternative to the incorporation of active ingredients (Bokking et al., 2015; Wang et al., 2017; Bastos, De Carvalho & Garcia-Rojas, 2018). Wang et al., 2017 demonstrated the Lf/NaAlg complex protect the degradation of the Lf alone when compared both in gastrointestinal delivery. The Lf/NaAlg complex presented good stability in simulated oral and gastric conditions. In the human gastrointestinal tract, foods are digested by a combination of physical and chemical processes. Chemical digestive processes are catalyzed by digestive enzymes that are secreted in the stomach, thereby degrading the foods to a molecular scale (Abrahamsson et al., 2005; Schwizer, Steingoetter, & Fox, 2006). Studies have been investigating the digestion of EOs microcapsules (Li et al., 2018; Volić et al., 2018).

Specific compounds are used as cross-linking agent in order to obtain more resistant structures for the capsules produced by complex coacervation (Peng et al., 2014). Transglutaminase (TG), is a naturally enzyme, catalyzes the formation of isopeptide bonds between the ε- amino group of polypeptide-bound lysines and the γ-carboxamide group of polypeptide-bound glutamines (Motoki & Seguro, 1998). It is used as cross-linking agent for fabricated EOs microcapsules by complex coacervation (Xiao et al., 2014; Lv et al., 2014; Rojas-Moreno et al., 2018).

The objective of this study was encapsulate the black pepper EO by complex coacervation using Lf and NaAlg as wall materials, to characterize the encapsulation efficiency, chemical structure, composition and stability of the capsules under human gastrointestinal simulation *in vitro*.

## 2. Materials and Methods

### 2.1. Materials

Sodium alginate, calcium chloride, α-amylase (A0521), porcine pepsin (P6887), pancreatin from porcine pancreas (P7545), porcine bile extract (B3883) was purchased from the company Sigma-Aldrich® (St. Louis, USA), dehydrated lactoferrin (Bioferrin® 2000) was acquired from the company Glanbia Nutricionals (Fitchburg, USA), Transglutaminase was acquired from the Ajinomoto (São Paulo, Brazil). Black pepper

essential oil was obtained from Ferquima (São Paulo, Brazil). The reagents used were of grade P.A. The water used was ultrapure with a conductivity of 0.05  $\mu\text{S}/\text{cm}$  (Master System P&D, Gehaka, Brazil).

## 2.2. Methods

### 2.2.1. Chemical composition of black pepper EO

#### 2.2.1.1. Gas Chromatography (GC)

Analyses of volatile oils were carried out on a gas chromatograph coupled with a mass spectrometer-MS (QP2010, Plus-Shimadzu, Japan) with a Factor Four-VF-5ms capillary column (Varian) (30 m  $\times$  0.25 mm, 0.25  $\mu\text{m}$  film thickness). The injection volume of the sample was 1  $\mu\text{L}$  (split 1:30) and the injector, GC-MS interface and ion source temperatures were maintained at 220, 310, and 250 $^{\circ}\text{C}$ , respectively, with an ionization energy of 70eV. The oven temperature was programmed as follows: 60 $^{\circ}\text{C}$  at 2 min, 60 to 260 $^{\circ}\text{C}$  at 3 $^{\circ}\text{C min}^{-1}$ , 260 to 290  $^{\circ}\text{C}$  at 10 $^{\circ}\text{C min}^{-1}$ , and 290 $^{\circ}\text{C}$  at 5 $^{\circ}\text{C min}^{-1}$ . The identified of the EO compounds were by visual comparison of their spectra in the literature (Adams, 2007) and by the spectra provided by the device database (NIST21 and NIST107). A standard solution of n-alkanes ( $\text{C}_8\text{-C}_{20}$ ) was injected under the same chromatographic conditions as the sample to obtain the retention indices (IK value).

A gas chromatograph (5890-series II, Hewlett Packard, USA) coupled with a flame ionization detector (CG-FID) and equipped with a Factor Four-VF-5ms capillary column (Varian) (30 m  $\times$  0.25 mm, 0.25  $\mu\text{m}$  film thickness) was used for the quantification of EOs. The injector and detector temperatures were maintained at 220 and 250 $^{\circ}\text{C}$ , respectively. For each sample, 1 $\mu\text{L}$  was injected in split mode (1:30). The carrier gas was helium at a flow rate of 1  $\text{mL}\cdot\text{min}^{-1}$  (12 psi). The oven ramp temperature was programmed as follows: 60 $^{\circ}\text{C}$  for 2 min, increased to 260 $^{\circ}\text{C}$  at 3 $^{\circ}\text{C min}^{-1}$ , and 260 to 290 $^{\circ}\text{C}$  at 10 $^{\circ}\text{C min}^{-1}$ . The relative percentage of the oil constituents was expressed as a percentage by area normalization.

#### 2.2.1.2. Nuclear Magnetic Resonance (NMR)

NMR spectra were recorded using a spectrometer (Advance III, Bruker, USA) operated at 500MHz. The sample was measured in  $\text{CDCl}_3$  (TMS was used as internal

reference) at 298.15K, adapted from Vicente et al., (2015). The spectra were processed using the MestReNova software 9.0 (Mestrelab research).

### 2.2.2. Preparation of the black pepper EO capsules

The production of the capsules was performed as described a previous study by Bastos, De Carvalho & Garcia-Rojas, 2018. The biopolymers were weighed in an analytical balance (B-TEC-210, Tecnal, Brazil) for the preparation of a solution containing a fixed concentration of 0.1% (w/w). The NaAlg was homogenized for 24h and the Lf was homogenized for 30 minutes using a magnetic stirrer (NT101, Novatecnica, Brazil). In previous study (Bastos, De Carvalho & Garcia-Rojas, 2018), was obtained the ratio of 8:1(Lf/NaAlg) at a pH 4.0 were the ideal conditions for the formation of the Lf/NaAlg complex and which was used to prepare the microcapsules.

The Lf/NaAlg microcapsules were tested using a solution with total concentration of 0.36, 0.72 and 1.4% (w/w) and different core/wall concentrations were tested (1:1, 1:2 and 2:1). Black pepper EO added with Lf solution and was emulsified with ultra-turrax (T25D, IKA, Germany) at the stirring rate of 10.000 rpm for 3 min (Lv et al., 2014). The NaAlg was added, the mixture was homogenized (NT101, Novatecnica, Brazil) and acidification at pH 4.0 with acetic acid (20%, v/v). The temperature of the suspension of the microcapsule will be reduced to 5 °C in an ice-water bath for 60 minutes (Peng et al., 2014). Transglutaminase solution (0.25% w/w) is added under magnetic stirred at 400 rpm for 3 hours at 25 °C to induce cross-linking (Lv et al., 2014). The microcapsules were kept at 10°C for 48 hours and then the supernatant was removed. Finally, the microcapsules were frozen in liquid nitrogen and freeze-dried (Enterprise I, Terroni, Brazil) for 24 hours.

## 2.3.Characterization of the microcapsules

### 2.3.1. Determination of standard curve and encapsulation efficiency

The black pepper EO was dissolved and diluted with hexane (80%) and ethanol (20%) solution, and then formulated into 0.0 to 1.2 mg/mL standards solutions. The absorption with solutions standard were measured using a spectrophotometer (Biomate 3S, Thermo Fisher Scientific, USA) at 288 nm. A mixture of ethanol and hexane solution was used as a blank. The linear regression of absorption on concentration was

made and the regression equation was constructed. In addition, the standard curve was drawn and its equation is  $y = 0.300x$ ,  $R^2=0.986$ .

Ten milligrams of black pepper EO microcapsules powder was weighed (B-TEC-210, Tecnal, Brazil) and 10 mL of the solvent was added (Hexane and Ethanol). The sample was put in 20°C water bath (2510, Soni-tech, Brazil) for 10 min by ultrasonic (80 W), after the sample was incubated in the shaker (TE-424, Tecnal, Brazil) for 2 hours at 25°C. The sample was homogenized on a Vortex (AP 56, Phoenix, Brazil) and centrifuged (Digicen 21 R, OrtoAlresa, Spain) at 8000 rpm for 15 min, adapted from Li et al. (2018). The supernatant phase was collected, to enable measurement (Biomate 3S, Thermo Fisher Scientific, USA) of its absorption as well as calculating its content. The microcapsule EE is the significant indicator to appraise the quality of the prepared microcapsule products. The oil mass was measured, and theoretical oil value ( $OT\%$ ) was given by equation (1) and the loaded oil content ( $OC\%$ ) was given by equation (2).

$$OT(\%) = \frac{W_{oil}}{W_{ic}} \times 100 \quad (1)$$

$$OC(\%) = \frac{W_{foil}}{W_{fc}} \times 100 \quad (2)$$

Where  $W_{oil}$  is the initial mass of oil added in the system,  $W_{ic}$  is the initial mass of the capsule and  $W_{foil}$  is the oil content after encapsulation and  $W_{fc}$  final capsule mass after freeze-dried. The EE is the percentage of loaded oil content divided by the percentage of theoretical oil (Timilsena et al., 2016), given by equation (3).

$$EE(\%) = \frac{OC(\%)}{OT(\%)} \times 100 \quad (3)$$



### 2.3.2. Fourier transform infrared spectroscopy (FT-IR)

The FT-IR spectra of the dried samples (Lf, NaAlg, EO and the capsule) were obtained. The analyses were performed with an FT-IR spectrometer (Ver-tex 70, Bruker, Germany) read in the range of 4000–400  $\text{cm}^{-1}$ .

### 2.3.3. Chemical composition of the black pepper EO after encapsulation

The EO extraction was performed as described in section 2.3.1. The supernatant phase was removed and analyzed by GC and NMR as described in section 2.2.1.

### 2.3.4. Morphology

#### 2.3.4.1. Optical microscopy

An aliquot of the sample were placed between the lamina and cover-slip and taken to the optical microscope (K220, Kasvi, Brazil) coupled to an Moticam camera (5MP, Kasvi, Brazil) that was viewed at 100 $\times$  magnification with immersion oil.

#### 2.3.4.2. Scanning Electron Microscopy (SEM)

Micrograph of the black pepper capsule after freeze-dried (1000x) (Enterprise I, Terroni, Brazil) was obtained with a scanning electron microscope TM3000 (Hitachi, Japan) equipped with a tungsten filament and operated in secondary electron mode at an acceleration voltage of 15 Kv.

## 2.4. *In vitro* digestion

*In vitro* digestion was simulated in three stages: oral, gastric and intestinal (Minekus et al., 2014 and Timilsena et al., 2017). Simulated oral, gastric and intestinal digestions were prepared according to Minekus et al., 2014.

#### 2.4.1. Simulated oral digestion

Briefly, 0.33g of the microcapsule lyophilized was weighed in an analytical balance (B-TEC-210, Tecnal, Brazil), and then mixed with 0.7mL pre-warmed of simulated salivary fluid (SSF) containing 0.1mL salivary  $\alpha$ -amylase (75 U/mL in final oral solution), the mixture was added followed by 5 $\mu$ L of 0.3 M CaCl<sub>2</sub> and 195 $\mu$ L of water. The pH of the mixture was adjusted to 7.0 with pHmeter (mPA210, Tecnoyon, Brazil) and stirred at 95 rpm for 2 minutes at 37°C using the shaking (TE-424, Tecnal, Brazil).

#### 2.4.2. Simulated gastric digestion

After mouth digestion, 1.5mL pre-warmed of simulated gastric fluid (SGF) was added to the oral digested mixture with 0.32 mL of the pepsin (2.000U/mL in final gastric solution), the mixture was added followed by 1 $\mu$ L of 0.3 M CaCl<sub>2</sub>, 40 $\mu$ L of 1M HCl and 139 $\mu$ L of water. The pH of the mixture was adjusted to 3.0 with pHmeter (mPA210, Tecnoyon, Brazil) and stirred at 95 rpm for 2 h at 37°C using the shaking (TE-424, Tecnal, Brazil).

#### 2.4.3. Simulated intestinal digestion

After the completion of gastric digestion, 2.2mL pre-warmed of simulated intestinal fluid (SIF) was added into the mixture with 1mL of the pancreatin (100U/mL in final intestinal volume) and 0.5mL of the bile extract solution (10mM). The mixture was added followed by 8 $\mu$ L of 0.3 M CaCl<sub>2</sub>, 30 $\mu$ L of 1M NaOH and 262 $\mu$ L of water. The pH of the mixture was adjusted to 7.0 with pHmeter (mPA210, Tecnoyon, Brazil) and stirred at 95 rpm for 2 h at 37°C using the shaking (TE-424, Tecnal, Brazil). Aliquots (120 $\mu$ L) of gastric and intestinal juice were taken at 0, 15, 30, 60 and 120 minutes. After withdrawal of each aliquot, 120  $\mu$ L of gastric or intestinal juice was added to continue the digestion process. The quantity of EO released was calculated from the absorbance according to section (2.3.1).

## 2.5. Statistical analysis

All experimental measurements were conducted in triplicate, and the data are expressed as the mean  $\pm$  standard deviation. The statistical analyses were performed using Origin<sup>®</sup> Pro 9.0. The Kolmogorov-Smirnov normality test was performed for the populations. After confirming normality for all populations, one-way variance (ANOVA) was performed to determine the existence of significant difference between populations. Significant differences at a level of significance  $\alpha = 0.05$  were identified by Tukey's test.

## 3. Results and Discussion

### 3.1. Composition of black pepper EO

#### 3.1.1. GC analysis

The black pepper EO compounds were identified by GC-FID and GC-MS analysis, and are given in Table 1. The black pepper EO contains a complex mixture consisting mainly of monoterpenes and sesquiterpenes. The predominant component was  $\beta$ -caryophyllene (28%), followed by limonene (15%), sabinene (11.4%),  $\beta$ -pinene (11%),  $\alpha$ -pinene (10.5%), 3-carene (6%),  $\alpha$ -copaene (3.6%), elemene (2%), mircene (1.6%),  $\alpha$ -caryophyllene (1%). The other terpenes identified had a percentage below 1%:  $\alpha$ -thujene (0.93%), p-cymene (0.47%), 2-carene (0.4%), linalool (0.3%), 4-terpineol (0.28%).

Several studies presented the  $\beta$ -caryophyllene as a major component in black pepper EO, but in different concentrations: 57.6% (García-Díez et al., 2016), 15.03% (Chandran et al., 2017) and 28% (Orchard et al., 2017). The variation of the chemical composition of the terpenes in the black pepper EO can be attributed to the origin, climate, type of culture and type of extraction of the identified samples (García-Díez et al., 2016).

#### 3.1.2. NMR

The main five terpenes identified by CG were confirmed by <sup>1</sup>H and <sup>13</sup>C NMR, as observed in Table 2. Some signals of the major compounds of black pepper EO were

identified mostly due to the presence of the  $sp^2$  protons at  $\delta_H$  4.51 – 5.41 ppm and the correlations at  $^1J_{H-C}$  with respective  $sp^2$  carbons at  $\delta_C$  101 – 125. The presence of several methyl group signals was also very informative to assign some major compounds, mostly due to their long-range correlation signals ( $^{2,3}J_{H-C}$ ).

The main components identified in black pepper EO are known and its NMR data were compared to the literature data. The sabinene was detected especially by the signal at  $\delta_H$  0.67 and  $\delta_C$  16.0 ppm of the methylene carbon of the cyclopropyl ring (CH<sub>2</sub>-6) (Guerrini et al., 2006). Some characteristic signals of methyl groups were also detected and compared to the literature data, for instance, the methyl groups at  $\delta_H$  0.86 ( $\alpha$ -pinene), 0.91, 0.97 (sabinene), 0.96 and 0.98 ( $\beta$ -caryophyllene) ppm (Guerrini et al., 2006). Limonene was detected, especially due the presence of some characteristic carbon  $sp^2$  signals at  $\delta_C$  133.7 (C-1), 120.6 (CH-2), 150.2 (C-8) and 108.4 (CH<sub>2</sub>-10) ppm and its respective proton signals at  $\delta_H$  5.40 (brs, CH-2) and 4.70 (brs, CH<sub>2</sub>-10) ppm. Also  $\beta$ -pinene was detected due the presence of  $sp^2$  carbons signals at  $\delta_C$  152.3 (C-2), 105.9 (CH<sub>2</sub>-10) ppm and the methyl groups at  $\delta_C$  26.1 (CH<sub>3</sub>-8) and 21.8 (CH<sub>3</sub>-9) ppm (Skakovskii et al., 2006).

It was possible to detect the presence of the quaternary  $sp^2$  carbons at  $\delta_C$  133.7 – 154.7 ppm and methyl groups at  $\delta_C$  16.3 – 30.1 ppm, which had its positions assigned by HMBC experiment and comparison with the literature data (Guerrini et al., 2006). Limonene, sabinene,  $\beta$ -pinene and  $\alpha$ -pinene has the same molar weight that can be justified because they are isomers, these were differentiated by their fragments (Table 2).

The same terpenes were identified by NMR in others EOs.  $\beta$ -caryophyllene, was identified in *Rosmarinus officinalis* (Da Silva Bomfim et al., 2015), *Syzigium aromaticum* (Owen et al., 2017) and *Myrtus communis* (Bouzabata et al., 2015) EOs.  $\beta$ -pinene and limonene was identified in *Ocoteabofa Kunth* (Guerrini et al., 2006), *Rosmarinus officinalis* (Da Silva Bomfim et al., 2015) and *Myrtus communis* (Bouzabata et al., 2015) EOs.  $\alpha$ -pinene and  $\beta$ -pinene in *Rosmarinus officinalis* (Da Silva Bomfim et al., 2015) EO. Sabinene was identified in *Ocoteabofa Kunth* (Guerrini et al., 2006).

### 3.2.Characterization of the microcapsules

In Table 3 was showed the composition of the formulations and the EE of the capsules produced by complex coacervation. The theoretical oil value, oil content and EE (equation 3) of microcapsules prepared with different samples were presented (Table 3). The theoretical oil values was that 33.33, 50 and 66.66%. Loaded oil content varied from 13.44 (S6) to 31.86% (S7). EE varied from 31.66 (S8) to 84.48 (S9). The core material was black pepper EO and wall material weight was the biopolymers and cross-linking agent.

#### 3.2.1. Encapsulation Efficiency (EE)

The samples S3 and S9 presented higher EE ( $81.33 \pm 2.76$  and  $84.48 \pm 2.0$ , respectively) and did not present significant differences ( $p < 0.05$ ) of EE. The samples had different percentages of biopolymers, core material and wall material weight. The samples were formulated with different EO and biopolymers concentrations (Table 3). Core material of the S9 was four times high than S3, 0.36g and 0.09g, respectively. The similarity in the composition of the samples was the EO concentrations were lower than that of biopolymers and the same core/wall ratio was using (1:2). The high EE using core/wall ratio of 1:2 was observed by Rojas-Moreno et al. (2018) when encapsulated orange EO with WPI and different polysaccharides was wall materials. In present study, the samples S3 and S9 presented concentrations of biopolymers sufficient to cover a greater amount of core, ensuring that the active material is trapped inside the capsule (Da Cruz et al., 2019).

The sample S6 was prepared using 1:2 core/wall ratio, but differed significant of EE from the others (S3 and S9) with the same core/wall ratio. S6 presented lower EE ( $41.88 \pm 3.36$ ), and used intermediary concentrations of biopolymers (%), core concentration and wall material weight when compared to S3 and S9, this contributed to the S6 had significant differences of EE.

The samples S1, S2 and S5 were prepared with different conditions (percentages and concentrations of biopolymers, EO concentrations and core/wall ratio), as presented in Table 3. S2 and S5 were formulated using core/ wall ratio of 1:1, and S1 using 2:1. Samples S1 and S2 were formulated with 0.36% of the biopolymers concentrations, and

S5 with 0.72%. The core material concentration between S1 and S5 has similar, and the wall weight material between S1 and S2 was the same. The different conditions to formulated these samples not contributed to exert a significant difference in the EE. S1, S2 and S5 presented lower EE, this fact may have occurred due to that an insufficient amount of wall materials was available to cover the entire core, resulting in a high free core concentration, high amount of core that was not encapsulated and hence was lost during the encapsulation process (Timilsena et al., 2016; Wang et al., 2016; Da Cruz et al., 2019).

The samples S4 and S8 did not present significant differences ( $p < 0.05$ ) of EE. The samples using the same core concentration (0.72 g), but differs the wall material weight, the percentage of the biopolymers and core/wall ratio. These core concentration using not exert a significant difference in the EE in different core/wall ratio tested (2:1 and 1:1).

The sample S7 was prepared with 2:1 core/wall ratio, with higher concentration of core material (1.44 g) and total of the materials (2.16 g). S7 was different from the other samples with the same core/wall ratio (S1 and S4), the EE of the S7 ( $54.84 \pm 3.7$ ) was higher than S1 ( $36.61 \pm 0.7$ ) and S4 ( $33.12 \pm 2.75$ ). Twice the concentration of the core material did not exert a significant difference in the EE of the samples (S1 and S4), but by increasing the concentration of the core material four times, the percentage of EE was high (S7). The opposite was observed by Wang et al. (2016), the study observed that higher concentration of ginger EO (core material), reduced the EE of the capsules using the 2:1 core/wall ratio with gelatin and sodium alginate as wall materials.

### 3.2.2. Chemical characterization of the black pepper EO microcapsule

FT-IR spectra of the biopolymers, black pepper EO and microcapsule (S9) at pH 4.0 were demonstrated in Figure 1. Samples of the biopolymers were presented in previous study (Bastos et al., 2018). The selected wavelength region ( $4000$  to  $400$   $\text{cm}^{-1}$ ) includes the amide bands of the protein: group I ( $1625$ - $1750$   $\text{cm}^{-1}$ ), group II ( $1475$ - $1575$   $\text{cm}^{-1}$ ), and group III ( $1225$  -  $1425$   $\text{cm}^{-1}$ ). The free amino acid O-H groups can be identified between the bands  $3300$  and  $3170$   $\text{cm}^{-1}$ . The amide group I refers to the stretching of the C=O, the amide group II corresponds to the stretching of the N-H, and the amide group III is attributed to the stretching of the C-N and N-H groups (Barth et al., 2007). In Lf, the amide groups I, II and III were observed at  $1632$ ,  $1521$ , and

1393 $\text{cm}^{-1}$ , respectively. The amide groups of the Lf were demonstrated by Martins et al., 2016 and Yan et al., 2017. The O-H group of the free amino acid can be identified by the 3278 band, the same was observed by Martins et al. (2016).

For NaAlg, the first band is at 1591 $\text{cm}^{-1}$ , representing the presence of  $\text{CO}_2^-$  in the carboxylic acid salts ( $\text{RCOO}^-$ ) in the range of 1650-1550 $\text{cm}^{-1}$  (Abreu et al., 2008). Band 2, at 1404 $\text{cm}^{-1}$ , refers to the C-O bond of the acid group ( $\text{RCOOH}$ ) in the range of 1440-1395 $\text{cm}^{-1}$  (Abreu et al., 2008). Band 3 (1024  $\text{cm}^{-1}$ ) is attributed to the vibrational stretch of the C-O and C-C of the pyranose ring (Bokkhim et al., 2015). The characteristic bands of the NaAlg were observed by Abreu et al. (2008), Bokkhim et al. (2015) and Zhang et al. (2019).

Spectrum peak of black pepper EO shows CH stretching vibration at 2922  $\text{cm}^{-1}$  (Raksa et al., 2017), vibration of the aliphatic C-H in  $\text{CH}_2$  at 2868 (Alizadeh-Sani et al., 2018), C=C stretching at 1643  $\text{cm}^{-1}$  (Alizadeh-Sani et al., 2018), C-OH absorption bending vibration at 1446  $\text{cm}^{-1}$  and  $\text{CH}_3$  bending at 1381  $\text{cm}^{-1}$  (Volić et al., 2018; Alizadeh-Sani et al., 2018). The peak 886  $\text{cm}^{-1}$  assigned to the bending vibrations (out of the plane) in  $=\text{CH}_2$  (Volić et al., 2018), the peak at 786  $\text{cm}^{-1}$  is assigned to benzene rings  $=\text{CH}$  vibration absorption (Raksa et al., 2017).

In black pepper EO microcapsule, it shows amide bands III at 1393  $\text{cm}^{-1}$ , and O-H group of the free amino acid can be identified by the 3278 band characteristics of the Lf. The peak 1024  $\text{cm}^{-1}$  is attributed to the vibration stretch of the C-O and C-C of the pyranose ring presented on NaAlg. The band 1643 refers to C=C stretching present in black pepper EO. The results show that the black pepper EO is successfully encapsulated in the Lf/NaAlg shell.

### 3.2.3. Composition of the black pepper EO after encapsulation

Black pepper EO after encapsulation was identified by GC-FID, GC-MS and NRM analysis.

#### 3.2.3.1. GC

In Table 1 was showed the components of the black pepper EO after encapsulation analyzed by GC. The  $\beta$ -caryophyllene was at 27.3% after the

encapsulation, at low levels (2.5%) compared to the relative content in the original (28%) EO. Therefore, the high percentage of this terpene was preserved (97.5%) after encapsulation.

The other terpenes in the original EO were identified after encapsulation at the following percentages: limonene (13.14%), sabinene (10.29%),  $\beta$ -pinene (8.77%), and  $\alpha$ -pinene (8.53%). The other compounds were present at low concentrations. The minor compounds present in the original EO were not identified after microencapsulation (linalool and 4-terpineol).

There was a decrease in all terpenes percentages after encapsulation, perhaps because these components are volatile and sensitive to adverse factors (oxygen, light and low pH), which may have contributed to its reduction during the fabrication of the microcapsules (Jun-Xia, Hai-Yan & Jian, 2011; Dima et al., 2016). The same was observed in other studies of encapsulated EOs (Jun-Xia, Hai-Yan & Jian, 2011, Peng et al., 2014; Lv et al., 2014).

The results obtained in the present study showed that encapsulated Black pepper EO has great retention capacity. The main terpenes identified in the EO were preserved above 87% of their original content (unencapsulated EO). The great retention of EOs has been reported in other studies: sweet orange (Jun-Xia, Hai-Yan & Jian, 2011), mustard (Peng et al., 2014), and jasmine (Lv et al., 2014). Jun-Xia et al. (2011) identified D-limonene as major compound in the sweet orange EO after microencapsulation by complex coacervation using soybean protein isolate/gum arabic. The same method was used for encapsulated mustard (*Sinapis alba*) EO (Peng et al., 2014), for which the authors confirmed the presence of allyl isothiocyanate in EO after microencapsulation. Linalool was identified in jasmine EO after microencapsulation by complex coacervation with gelatin/gum arabic (Lv et al., 2014).

### 3.2.3.2. <sup>1</sup>H NMR

The black pepper EO was extracted from the microcapsule (S9) according to section (2.3.1) and also submitted to <sup>1</sup>H NMR analysis to check the preservation of the terpenes. Stacked <sup>1</sup>H NMR spectrum of black pepper EO unencapsulated (1) and encapsulated (2) can be observed in Figure 2. Some high intensity signals of solvents used in the extraction (ethanol and hexane) were observed, after its removal it was possible to observe the signals of the compounds belonging to the extracted EO,



specially the protons of the  $sp^2$  carbons ( $\delta_H$  4.5 – 5.5 ppm). The shielded protons at  $\delta_H$  0.5 – 2.5 ppm presented a slight change in absorption that can be justified due the presence of the solvents used in the extraction of the EO.

#### 3.2.4. Morphology

The morphology of the black pepper EO capsule (S9) using Lf/NaAlg as wall material and transglutaminase as cross-linking agent can be observed in the Figure 3. The optical image show the microscopic structure of black pepper EO capsules formed with the ratio 1:2 oil/polymers showing a spherical and intact shape (Figure 3A). The same was demonstrated by Lv et al. (2012) and Matos et al. (2018). Lv et al. (2012) obtained spherical particles containing jasmine EO using gelatin/CMC as encapsulants. Matos et al. (2018) observed these when encapsulated citronella EO using gelatin and sodium alginate as wall materials.

The SEM images of the Lf, NaAlg and the complex Lf/NaAlg was demonstrated in previous study by Bastos et al. (2018). SEM was used to observe the morphology of the dried black pepper EO capsule (Figure 3B). The three-dimensional network was observed, maintaining a structure similar to the complex coacervates formed prior to encapsulation (Bastos et al. 2018). The sample showed the sponge-like structure, particularly of the capsule. Black pepper EO single droplets or small aggregates were observed (droplets are indicated by the red arrows). The similar structure was observed by Koupantsis et al. (2016) when encapsulated  $\beta$ -pinene in WPI/CMC complex coacervates.

#### 3.3. *In vitro* digestion

The extent of oil release from the black pepper EO capsule (S9) at different time intervals in gastric and intestinal environments is shown in Figure 4. The sample was submitted in oral condition simulated for 2 minutes. The hypothesis were, the slight release can be occurred because at pH 7.0 (oral digestion) the complex was insoluble due to electrostatic repulsion (initially in pH 5.9) demonstrated in previous study (Bastos, De Carvalho & Garcia-Rojas, 2018). The  $\alpha$ -amylase presented in oral conditions hydrolyzes amylase and amylopectin molecules in starch foods (Sarkar et al.,

2009), but the biopolymers used in present study don't have this composition and the  $\alpha$ -amylase not contributed for the release in oral digestion.

During exposure to gastric conditions (2 hours), the initial EO loads released about 24.30%. The capsule protect the release of the initial EO load during gastric conditions, the release remained almost constant. Protein digestion is initiated in the stomach by pepsin (Tomé & Debabbi, 1998), but the capsule was not totally ruptured and 75.7% the EO was preserved. This can be explained because the NaAlg protect the disintegrated of the Lf in Lf/NaAlg complex coacervates. This is observed by Wang et al. (2017) when study the protect effect of the NaAlg in Lf on the complex Lf/NaAlg. Alginates have previously been shown to inhibit pepsin activity *in vitro* (Sunderland et al., 2000; Strugala et al., 2005; Chater et al., 2015). Sunderland et al. (2000) showed alginates could inhibit pepsin activity by 52% *in vitro*. Strugala et al. (2005) showed significant correlations between alginate structure and levels of inhibition, with high frequency of mannuronic acid residues alginates tending to inhibit better than those high in guluronic acid residues. However the mechanism of pepsin inhibition is poorly understood.

In pH 3.0 (gastric conditions), electrostatic interaction between Lf and NaAlg is favorable and the capsules was stronger. However this pH is below the pKa of the NaAlg and is possible aggregation of the carboxylic groups (Bastos et al., 2018).

The release of the EO at intestinal stage was found to be faster compared to that gastric stage. In 2 hours of intestinal digestion the release EO was increased in function of the time (47.7-84.87%). Occurred the rupture the capsule and only 15.13% of the EO was preserved. The same was observed by Wang et al. (2017). The protein continually digestion occurred in intestinal digestion by pancreatic and intestinal proteases such as trypsin, chymotrypsin, and membrane peptidases (Tomé & Debabbi, 1998). In this case the NaAlg not protect the Lf in Lf/NaAlg complex coacervates because they cannot survive from trypsin attack (Chater et al., 2015) and the capsule was reputed. The catalytic mechanisms of pepsin and trypsin are distinct, it is therefore possible that alginate is able to interact with and disrupt the catalytic mechanism of pepsin, but not of trypsin. Pepsins are aspartate proteases, and broad specificity end peptidases with a preference for cleavage between hydrophobic amino acids (Powers, Harley, & Myers, 1977). Trypsin on the other hand is a serine protease. Serine proteases are usually end peptidases and preferentially cleave within the polypeptide chain, preferentially

cleaving on the carboxyl side of lysine and arginine (Hedstrom, 2002; Chater et al., 2015).

It is perhaps due to neutral pH (7.0) of intestine, the protective coatings are destroyed and thus the capsule was degraded that resulted in the sustained release of EO from capsules in stimulated intestinal fluids. The results of this study showed that Lf and NaAlg effectively prevent the release of EO in oral and gastric conditions which minimizing the chemical degradation of EO in gut environment. Our results are in accordance with those obtained for others EOs (Li et al., 2018; Vólic et al., 2018).

#### **4. Conclusion**

Black pepper EO capsules produced by complex coacervation using Lf and NaAlg as wall materials, and transglutaminase as cross-linking agent have a good encapsulation efficiency. The encapsulated black pepper EO was confirmed by the chemical and morphological characteristics. The presence of the terpenes in the encapsulated black pepper EO indicated good core protection with the biopolymers used. The black pepper EO capsule demonstrated resistance under oral and gastric conditions and release in the intestine contributing to your absorption. The Lf and NaAlg showed potential used as wall materials in encapsulated black pepper EO by complex coacervation.

##### **Conflict of interest**

The authors declare no conflict of interest.

##### **Acknowledgment**

The authors thank to CNPq, FAPERJ and CAPES (Finance code 001) for financial support.

## 5. References

- Abrahamsson, B., Pal, A., Sjöberg, M., Carlsson, M., Laurell, E., Brasseur, J. G. (2005). A novel *in vitro* and numerical analysis of shear-induced drug release from extended release tablets in the fed stomach. *Pharmaceutical Research*, 22, 1215–1226.
- Abreu, F. O., Bianchini, C., Forte, M. M., & Kist, T. B. (2008). Influence of the composition and preparation method on the morphology and swelling behavior of alginate–chitosan hydrogels. *Carbohydrate Polymers*, 74(2), 283-289.
- Adams, R. P. (2007). Identification of essential oil components by gas chromatography/mass spectrometry (4th ed.). Illinois USA: Allured Publishing Corporation.
- Alizadeh-Sani, M., Khezerlou, A., & Ehsani, A. (2018). Fabrication and characterization of the bionanocomposite film based on whey protein biopolymer loaded with TiO<sub>2</sub> nanoparticles, cellulose nanofibers and rosemary essential oil. *Industrial Crops and Products*, 124, 300-315.
- Bakkali, F., Averbeck, S., Averbeck, D., Idaomar, M. (2008). Biological effects of essential oils – a review. *Food and Chemical Toxicology*, 46, 446–475.
- Barth, A. (2007). Infrared spectroscopy of proteins. *Biochimica et Biophysica Acta (BBA)-Bioenergetics*, 1767(9), 1073-1101.
- Bastos, L. P. H., De Carvalho, C. W. P., & Garcia-Rojas, E. E. (2018). Formation and characterization of the complex coacervates obtained between lactoferrin and sodium alginate. *International Journal of Biological Macromolecules*, 120, 332-338.
- Bengoechea, C., Jones, O. G., Guerrero, A., & McClements, D. J. (2011). Formation and characterization of lactoferrin/pectin electrostatic complexes: Impact of composition, pH and thermal treatment. *Food Hydrocolloids*, 25(5), 1227-1232.
- Bokkhim, H., Bansal, N., Grøndahl, L., Bhandari, B. (2015). Interactions between different forms of bovine lactoferrin and sodium alginate affect the properties of their mixtures. *Food Hydrocolloids*, 48, 38-46.
- Bouzabata, A., Cabral, C., Gonçalves, M. J., Cruz, M. T., Bighelli, A., Cavaleiro, C., & Salgueiro, L. (2015). *Myrtus communis* L. as source of a bioactive and safe essential oil. *Food and Chemical Toxicology*, 75, 166-172.
- Chandran, J., Nayana, N., Roshini, N., & Nisha, P. (2017). Oxidative stability, thermal stability and acceptability of coconut oil flavored with essential oils from black pepper and ginger. *Journal of Food Science and Technology*, 54(1), 144-152.
- Chater, P. I., Wilcox, M. D., Brownlee, I. A., & Pearson, J. P. (2015). Alginate as a protease inhibitor *in vitro* and in a model gut system; selective inhibition of pepsin but not trypsin. *Carbohydrate Polymers*, 131, 142–151.
- Da Cruz, M. C. R., Dagostin, J. L. A., Perussello, C. A., & Masson, M. L. (2019). Assessment of physicochemical characteristics, thermal stability and release profile of

ascorbic acid microcapsules obtained by complex coacervation. *Food hydrocolloids*, 87, 71-82.

Da Silva Bomfim, N., Nakassugi, L. P., Oliveira, J. F. P., Kohiyama, C. Y., Mossini, S. A. G., Grespan, R., & Machinski Jr, M. (2015). Antifungal activity and inhibition of fumonis in production by *Rosmarinus officinalis* L. essential oil in *Fusarium verticillioides* (Sacc.) Nirenberg. *Food Chemistry*, 166, 330-336.

Dima, C., Pătrașcu, L., Cantaragiu, A., Alexe, P., & Dima, Ș. (2016). The kinetics of the swelling process and the release mechanisms of *Coriandrum sativum* L. essential oil from chitosan/alginate/inulin microcapsules. *Food Chemistry*, 195, 39-48.

García-Díez, J., Alheiro, J., Pinto, A. L., Soares, L., Falco, V., Fraqueza, M. J., & Patarata, L. (2016). Behaviour of food-borne pathogens on dry cured sausage manufactured with herbs and spices essential oils and their sensorial acceptability. *Food Control*, 59, 262-270.

Ghasemi, S., Jafari, S. M., Assadpour, E., & Khomeiri, M. (2017). Production of pectin-whey protein nano-complexes as carriers of orange peel oil. *Carbohydrate polymers*, 177, 369-377.

Girardi, N. S., García, D., Passone, M. A., Nesci, A., & Etcheverry, M. (2017). Microencapsulation of *Lippia turbinata* essential oil and its impact on peanut seed quality preservation. *International Biodeterioration & Biodegradation*, 116, 227-233.

Guerrini, A., Sacchetti, G., Muzzoli, M., Rueda, G. M., Medici, A., Besco, E., Bruni, R. (2006). Composition of the volatile fraction of *Ocoteabofo Kunth* (*Lauraceae*) Calyces by GC-MS and NMR finger print and its antimicrobial and antioxidant activity. *Journal of Agricultural and Food Chemistry*, 54, 7778-7788.

Hedstrom, L. (2002). Serine protease mechanism and specificity. *Chemical Reviews*, 102(12), 4501-4524.

IUPAC. (1997). IUPAC Compendium of Chemical Technology, North Carolina, USA.

Jun-xia, X., Hai-yan, Y., & Jian, Y. (2011). Microencapsulation of sweet orange oil by complex coacervation with soybean protein isolate/gum Arabic. *Food Chemistry*, 125(4), 1267-1272.

Koupantsis, T., Pavlidou, E., Paraskevopoulou, A. (2014). Flavour encapsulation in milk proteins–CMC coacervate-type complexes. *Food Hydrocolloids*, 37, 134-142.

Koupantsis, T., Pavlidou, E., & Paraskevopoulou, A. (2016). Glycerol and tannic acid as applied in the preparation of milk proteins–CMC complex coacervates for flavour encapsulation. *Food Hydrocolloids*, 57, 62-71.

Kralovec, J. A., Zhang, S., Zhang, W., & Barrow, C. J. (2012). A review of the progress in enzymatic concentration and microencapsulation of omega-3 rich oil from fish and microbial sources. *Food Chemistry*, 131(2), 639-644.

- Lemos, Y. P., Mariano Marfil, P. H., & Nicoletti, V. R. (2017). Particle size characteristics of buriti oil microcapsules produced by gelatin-sodium alginate complex coacervation: Effect of stirring speed. *International Journal of Food Properties*, 20(2), 1438-1447.
- Li, D., Wu, H., Huang, W., Guo, L., & Dou, H. (2018). Microcapsule of Sweet Orange Essential Oil Encapsulated in Beta-Cyclodextrin Improves the Release Behaviors In Vitro and In Vivo. *European Journal of Lipid Science and Technology*, 120(9), 1-11.
- Lv, Y., Zhang, X., Abbas, S., & Karangwa, E. (2012). Simplified optimization for microcapsule preparation by complex coacervation based on the correlation between coacervates and the corresponding microcapsule. *Journal of Food Engineering*, 111, 225-233.
- Lv, Y., Yang, F., Li, X., Zhang, X., & Abbas, S. (2014). Formation of heat-resistant nanocapsules of jasmine essential oil via gelatin/gum arabic based complex coacervation. *Food Hydrocolloids*, 35, 305-314.
- Martins, J. T., Santos, S. F., Bourbon, A. I., Pinheiro, A. C., González-Fernández, Á., Pastrana, L. M., & Vicente, A. A. (2016). Lactoferrin-based nanoparticles as a vehicle for iron in food applications—Development and release profile. *Food Research International*, 90, 16-24.
- Matos, E. F., Scopel, B. S., & Dettmer, A. (2018). Citronella essential oil microencapsulation by complex coacervation with leather waste gelatin and sodium alginate. *Journal of Environmental Chemical Engineering*, 6(2), 1989-1994.
- Minekus, M., Alminger, M., Alvito, P., Ballance, S., Bohn, T. O. R. S. T. E. N., Bourlieu, C., & Dufour, C. (2014). A standardised static in vitro digestion method suitable for food—an international consensus. *Food & Function*, 5(6), 1113-1124.
- Motoki, M., & Seguro, K. (1998). Transglutaminase and its use for food processing. *Trends in Food Science & Technology*, 9(5), 204-210.
- Nesterenko, A., Alric, I., Violleau, F., Silvestre, F., & Durrieu, V. (2014). The effect of vegetable protein modifications on the microencapsulation process. *Food Hydrocolloids*, 41, 95-102.
- Orchard, A., Sandasi, M., Kamatou, G., Viljoen, A., & Van Vuuren, S. (2017). The in vitro antimicrobial activity and chemometric modelling of 59 commercial essential oils against pathogens of dermatological relevance. *Chemistry & Biodiversity*, 14(1), 160-218.
- Owen, L., Grootveld, M., Arroo, R., Ruiz-Rodado, V., Price, P., & Laird, K. (2017). A Multifactorial Comparison of Ternary Combinations of Essential Oils in Topical Preparations to Current Antibiotic Prescription Therapies for the Control of Acne Vulgaris-Associated Bacteria. *Phytotherapy Research*, 31(3), 410-417.

Oussalah, M., Caillet, S., Saucier, L., & Lacroix, M. (2006). Antimicrobial effects of selected plant essential oils on the growth of a *Pseudomonas putida* strain isolated from meat. *Meat Science*, 73(2), 236-244.

Pamies, R. Schmidt, R. R. Martínez, M. D. C. L. de la Torre, J. G. (2010). The influence of mono and divalent cations on dilute and non-dilute aqueous solutions of sodium alginates, *Carbohydrate Polymers*, 80, 248-253.

Peng, C., Zhao, S. Q., Zhang, J., Huang, G. Y., Chen, L. Y., & Zhao, F. Y. (2014). Chemical composition, antimicrobial property and microencapsulation of Mustard (*Sinapis alba*) seed essential oil by complex coacervation. *Food Chemistry*, 165, 560-568.

Powers, J.C., Harley, A.D., & Myers, D.V. (1977). Subsite specificity of porcine pepsin. *Advances in Experimental Medicine and Biology*, 95, 141-157.

Raksa, A., Sawaddee, P., Raksa, P., & Aldred, A. K. (2017). Microencapsulation, chemical characterization, and antibacterial activity of Citrus hystrix DC (*Kaffir Lime*) peel essential oil. *Monatshefte für Chemie-Chemical Monthly*, 148(7), 1229-1234.

Ravindran, P. N., Kallapurackal, J. A. (2004). Black Pepper. In K. Peter (Ed.), *Handbook of Herbs and Spices* (pp.62-110). New York: CRC Press, Taylor & Francis Group.

Rojas-Moreno, S., Osorio-Revilla, G., Gallardo-Velázquez, T., Cárdenas-Bailón, F., & Meza-Márquez, G. (2018). Effect of the cross-linking agent and drying method on encapsulation efficiency of orange essential oil by complex coacervation using whey protein isolate with different polysaccharides. *Journal of Microencapsulation*, 35(2), 165-180.

Saha, K. C., Seal, H. P., & Noor, M. A. (2013). Isolation and characterization of piperine from the fruits of black pepper (*Piper nigrum*). *Journal of the Bangladesh Agricultural University*, 11, 11-16.

Schwizer, W., Steingoetter, A., & Fox, M. (2006). Magnetic resonance imaging for the assessment of gastrointestinal function. *Scandinavian Journal of Gastroenterology*, 41, 1245-1260.

Skakovskii, E.D., Lamotin, S.A., Shpak, S.I., Tychinskaya, L.Y., Gaidukevich, O. A., Lamotkin, A.I. (2006). Application of NMR spectroscopy for analysis of the composition of pine needle essential oil. *Journal of Applied Spectroscopy*, 73(2), 275-279.

Strugala, V., Kennington, E.J., Campbell, R.J., Skjak-Braek, G., & Dettmar, P.W. (2005). Inhibition of pepsin activity by alginates in vitro and the effect of epimerization. *International Journal of Pharmaceutics*, 304(1-2), 40-50.

Sunderland, A., Dettmar, P., & Pearson, J. (2000). Alginates inhibit pepsin activity invitro; a justification for their use in gastroesophageal reflux disease (GORD). *Gastroenterology*, 118(4), 347.

- Timilsena, Y. P., Adhikari, R., Barrow, C. J., & Adhikari, B. (2016). Microencapsulation of chia seed oil using chia seed protein isolate chia seed gum complex coacervates. *International Journal of Biological Macromolecules*, 91, 347-357.
- Timilsena, Y. P., Adhikari, R., Barrow, C. J., & Adhikari, B. (2017). Digestion behaviour of chia seed oil encapsulated in chia seed protein-gum complex coacervates. *Food Hydrocolloids*, 66, 71-81.
- Tomita, M., Wakabayashi, H., Shin, K., Yamauchi, K., Yaeshima, T., & Iwatsuki, K. (2009). Twenty-five years of research on bovine lactoferrin applications. *Biochimie*, 91(1), 52-57.
- Tomé, D., & Debabbi, H. (1998). Physiological effects of milk protein components. *International Dairy Journal*, 8, 383-392.
- Vicente, J., de Carvalho, M. G., & Garcia-Rojas, E. E. (2015). Fatty acids profile of sacha inchi oil and blends by <sup>1</sup>H NMR and GC-FID. *Food chemistry*, 181, 215-221.
- Volić, M., Pajić-Lijaković, I., Djordjević, V., Knežević-Jugović, Z., Pećinar, I., Stevanović-Dajić, Z., & Bugarski, B. (2018). Alginate/soy protein system for essential oil encapsulation with intestinal delivery. *Carbohydrate polymers*, 200, 15-24.
- Wang, L., Yang, S., Cao, J., Zhao, S., & Wang, W. (2016). Microencapsulation of Ginger Volatile Oil Based on Gelatin/Sodium Alginate Polyelectrolyte Complex. *Chemical and Pharmaceutical Bulletin*, 64(1), 21-26.
- Wang, B., Blanch, E., Barrow, C. J., & Adhikari, B. (2017). Preparation and study of digestion behavior of lactoferrin-sodium alginate complex coacervates. *Journal of Functional Foods*, 37, 97-106.
- Xiao, Z., Liu, W., Zhu, G., Zhou, R., & Niu, Y. (2014). Production and characterization of multinuclear microcapsules encapsulating lavender oil by complex coacervation. *Flavour and Fragrance Journal*, 29 (3), 166-172.
- Yan, J. K., Qiu, W. Y., Wang, Y. Y., & Wu, J. Y. (2017). Biocompatible polyelectrolyte complex nanoparticles from lactoferrin and pectin as potential vehicles for antioxidant vecurcumin. *Journal of Agricultural and Food Chemistry*, 65(28), 5720-5730.
- Zhang, K., Zhang, H., Hu, X., Bao, S., & Huang, H. (2012). Synthesis and release studies of microalgal oil-containing microcapsules prepared by complex coacervation. *Colloids and Surfaces B: Biointerfaces*, 89, 61-66.
- Zhang, H., Fu, Y., Xu, Y., Niu, F., Li, Z., Ba, C., & Li, X. (2019). One-step assembly of zein/caseinate/alginate nanoparticles for encapsulation and improved bioaccessibility of propolis. *Food & Function*, 10(2), 635-645.



## Figure Caption

**Fig. 1:** FT-IR spectra of NaAlg, Lf, black pepper EO and black pepper EO capsule (Lf/NaAlg ratio  $r= 8:1$ ) at pH 4.0.

**Fig. 2:**  $^1\text{H}$  NMR spectrum of the black pepper (BP) EO unencapsulated (1) and encapsulated (2) (500 MHz,  $\text{CDCl}_3$ )

**Fig. 3:** (A) Optical microscopy image at 100x of black pepper EO capsules at ratio 1:2 (core/ wall material), and (B) SEM of the black pepper EO capsule.

**Fig. 4:** Release of the black pepper EO from the capsule during *in-vitro* digestion.

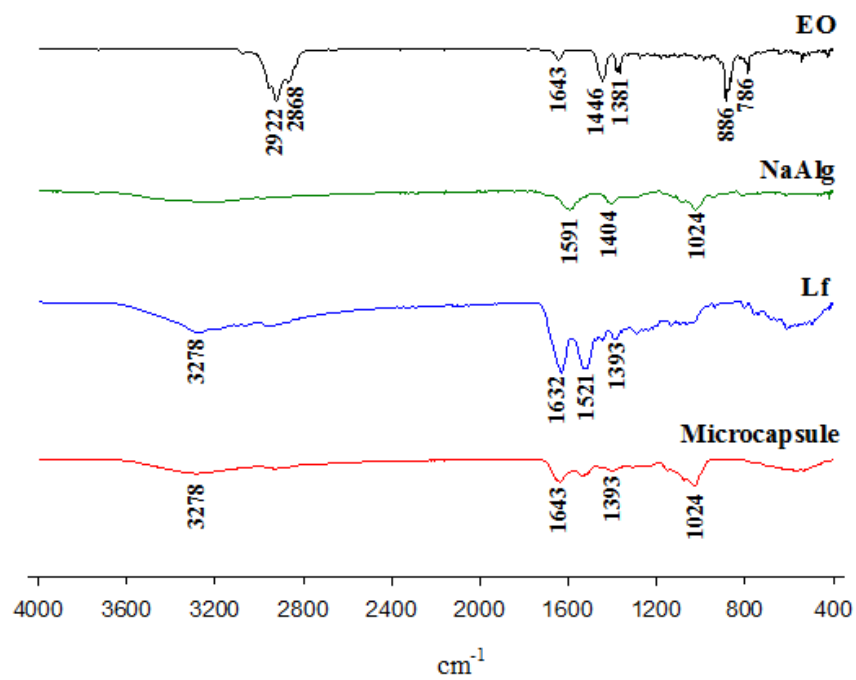


**Fig1.**

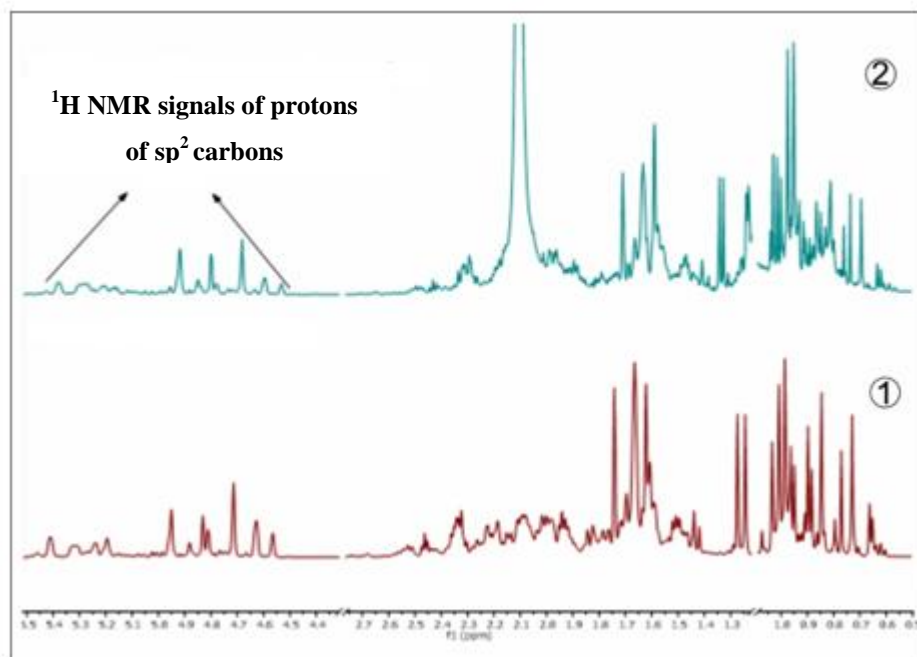


**Fig. 2.**

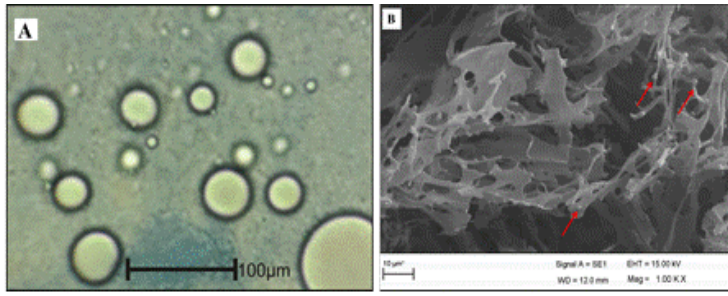


Fig. 3.

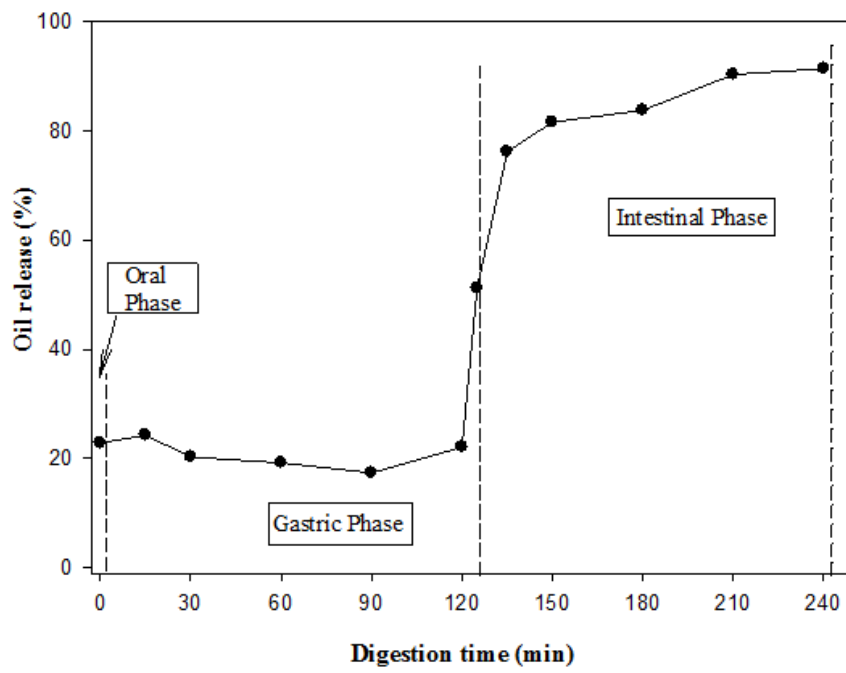
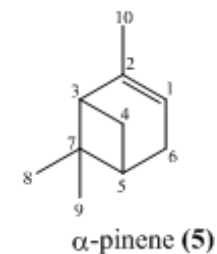
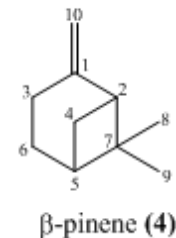
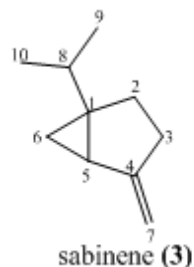
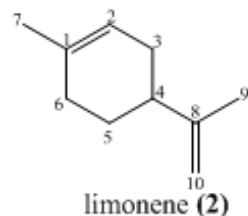
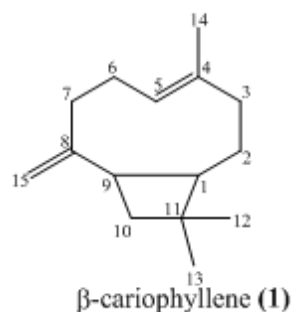


Fig. 4.

**Table 1.** Chemical composition of the original black pepper EO and content in capsule by GC.<sup>a</sup>KI= Kovats indices to n-alkanes (C<sub>8</sub>–C<sub>20</sub>) on an HP- 5MS column, <sup>b</sup>KI=identification based on comparison of retention index with those of published data (Adams, 2007), <sup>c</sup>RT= Retention time, <sup>d</sup>Relative content obtained by GC-FID.

<b>Component</b>	<b>KI<sup>a</sup></b>	<b>KI<sup>b</sup></b>	<b>RT<sup>c</sup> (min)</b>	<b>Relative content in original EO<sup>d</sup> (%)</b>	<b>Relative content EO in microcapsule<sup>d</sup> (%)</b>
β-caryophyllene (1)	1429	1419	26.046	28	27.3
Limonene (2)	1033	1029	9.400	15	13.140
Sabinene (3)	975	975	7.434	11.4	10.29
β-pinene (4)	982	979	7.546	11	9.77
α-pinene (5)	934	939	6.196	10.5	9.53
3-carene (8)	1012	1011	8.672	6	3.7
α-copaene (14)	1379	1376	24.061	3.6	2.56
Elemene (13)	1336	1338	22.428	2	1.36
Mircene (7)	989	990	7.961	1.6	1.07
α-cariophyllene (15)	1457	1454	27.235	1	0.73
α-thujene (6)	924	930	5.967	0.93	0.59
p-cymene (9)	1027	1024	9.168	0.47	0.33
2-carene (10)	1086	1002	11.652	0.4	0.3
Linalool (11)	1101	1096	12.152	0.3	-
4-terpineol (12)	1117	1177	15.421	0.28	-

**Table 2.**  $^{13}\text{C}$  and  $^1\text{H}$  NMR data of identified major compounds in the black pepper EO ( $\delta_{\text{C}}$  and  $\delta_{\text{H}}$  in ppm).



C	$\delta_{\text{C}}$	$\delta_{\text{H}}$ (J in Hz)	$\delta_{\text{C}}$	$\delta_{\text{H}}$	$\delta_{\text{C}}$	$\delta_{\text{H}}$ (J in Hz)	$\delta_{\text{C}}$	$\delta_{\text{H}}$ (J in Hz)	$\delta_{\text{C}}$	$\delta_{\text{H}}$
1	53.5	1.68( <i>m</i> )	133.7	-	37.6	-	152.3	-	116.0	5.18(br s)
2			120.6	5.40(brs)			51.8	2.45( <i>t</i> , 5.3)	144.5	
3	40.0									
4	135.5		41.1		154.5	-				
5	124.3	5.30( <i>dd</i> , 5, 10.5)							40.7	
6			30.6	2.10( <i>m</i> )	16.0	0.64( <i>d</i> , 5.5)			37,6	
7	34.8	1.98 ( <i>m</i> ), 2.20( <i>m</i> )	23.5	1.65(br s)	101.5	4.61(brs) 4.79(brs)				
8	157.4		150.2		32.6	1.52 ( <i>m</i> )	26.1	1.23 ( <i>s</i> )	26.4	1.26 ( <i>s</i> )
9	48.5		20.8	1.72( <i>s</i> )	19.7	0.88( <i>d</i> , 7)	21.8	0.71 ( <i>s</i> )	20.8	0.83( <i>s</i> )
10	40.3	1.64( <i>m</i> ), 1.93( <i>m</i> )	108.4	4.70(brs)	19.8	0.95( <i>d</i> , 7)	105,9	4.55(brs), 4.61(brs)	23.0	1.65( <i>s</i> )
11	33.9									
12	22.6	0.97( <i>s</i> )								
13	30.1	0.99( <i>s</i> )								
14	16.3	1.60( <i>s</i> )								
15	111.6	4.81(brs), 4.93(brs)								
<b>m/z</b>		204		136		136		136		136

**Table 3.** Composition of the formulations and encapsulation efficiency of the microcapsules produced by complex coacervation.

Samples	Core Material (g)	Wall Material Weight (g)			core/wall (w/w)	Transglutaminase solution (g)	Loaded oil content(%)	Theoretical oil value (%)	EE (%)
		Lf (g)	NaAlg (g)	Total (g)					
S1	0.36	0.16	0.02	0.54	2:1	10	23.82 ± 1.5	66.66	36.61 <sup>cd</sup> ± 0.7
S2	0.18	0.16	0.02	0.36	1:1	10	17.83 ± 0.6	50	35.65 <sup>cd</sup> ± 1.36
S3	0.09	0.16	0.02	0.27	1:2	10	27.38 ± 0.63	33.33	81.33 <sup>a</sup> ± 2.76
S4	0.72	0.32	0.04	1.08	2:1	10	25.37 ± 2.0	66.66	33.12 <sup>d</sup> ± 2.75
S5	0.36	0.32	0.04	0.72	1:1	10	20.09 ± 1.10	50	37.89 <sup>cd</sup> ± 1.97
S6	0.18	0.32	0.04	0.54	1:2	10	13.44 ± 0.8	33.33	41.88 <sup>c</sup> ± 3.36
S7	1.44	0.64	0.08	2.16	2:1	10	31.86 ± 2.64	66.66	54.84 <sup>b</sup> ± 3.7
S8	0.72	0.64	0.08	1.44	1:1	10	15.3 ± 0.7	50	31.66 <sup>d</sup> ± 0.56
S9	0.36	0.64	0.08	1.08	1:2	10	27.86 ± 0.27	33.33	84.48 <sup>a</sup> ± 2.0

The analyses were performed in three replicates. The same letters in the same column do not differ significantly by the Tukey test with a probability of 5%

**CAPÍTULO IV**  
**ENCAPSULATION OF BLACK PEPPER (*PIPER NIGRUM L.*) ESSENTIAL**  
**OIL WITH GELATIN AND SODIUM ALGINATE BY COMPLEX**  
**COACERVATION**

Submitted to **Food Hydrocolloids**.

## Abstract

Black pepper essential oil (EO) was analyzed by gas chromatography (GC) and nuclear magnetic resonance (NMR). The main component was  $\beta$ -caryophyllene (28%). The molecular weights of the biopolymers were determined. Sodium alginate and gelatin had molecular weights of 138 kDa and 249 kDa, respectively. The effect of ratio and pH on complex formation was evaluated. The ratio of 6:1 (gelatin/sodium alginate) at pH 4.0 were the ideal conditions. The EO was encapsulated in a complex coacervate with gelatin and sodium alginate using calcium chloride as a cross-linking agent. The encapsulation efficiency varied from 49.13 to 82.36%, and the chemical composition of the encapsulated EO was identified by GC. GC analysis indicated good core protection with the materials used. The chemical characteristics showed that the EO was encapsulated in a gelatin/sodium alginate shell. These biopolymers can serve as a potential vehicle for black pepper EO.

**Keywords:** chemical composition, molecular weights, electrostatic interaction, encapsulation efficiency, biopolymers.



## 1. Introduction

Essential oils (EOs) are natural aromatic volatile liquids extracted from different parts of plants, such as flowers, buds, seeds, leaves, stems and bark. The composition and physicochemical properties of EOs are greatly influenced by the species, part of plant, geographic origin, time of harvest, stage of development, age of plants and extraction method (Bakkali et al., 2008; Dima et al., 2016). EOs are composed of the following classes of compounds: tertiary terpene alcohols and related esters, aliphatic terpene ethers, aliphatic and aromatic terpene hydrocarbons (Bakkali et al., 2008). The identification of the compounds can be achieved by gas chromatography (GC) and nuclear magnetic resonance (NMR) (Guerrini et al., 2006). Previous studies revealed that, of these classes, a series of compounds have antioxidant and antibacterial activity. For this reason, EOs are an alternative to chemical preservatives and, therefore, are used in preparing safe foods with a positive impact on consumers health (Dima et al., 2016).

Black pepper (*Piper nigrum L*) is a plant of the *Piperaceae* family, largely used as a flavoring agent in foods (Chandran et al., 2017). The black pepper EO is sensitive to oxygen, light and high temperature. These factors contribute to the degradation of the EOs and, subsequently, to the decrease in their biological potential. Therefore, encapsulation is required in order to prevent this occurrence (Dima et al., 2016).

Microencapsulation is a process that retains a bioactive material (solid, liquid or gas) inside another (wall material) to protect the bioactive material against adverse environmental conditions, thereby increasing the shelf life and promoting the controlled release of the active compound in the microcapsule. As one of the microencapsulation technologies used in the foods industry, the complex coacervation process has been used for encapsulating reactive, sensitive, or volatile additives or nutrients (Schmitt & Turgeon, 2011). The complex coacervation process principally consists of three basic steps: emulsification, coacervation, and shell formation and/or hardening (Zhang et al., 2012).

Coacervation is the separation of a colloidal system into two liquid phases (International Union of Pure and Applied Chemistry-IUPAC, 1997). Complex coacervation is based on the associative interaction between oppositely charged polymers, usually a protein and a polysaccharide (Schmitt & Turgeon, 2011). Many wall materials using proteins and polysaccharides are reported in the literature: whey protein isolate/sodium alginate (Rojas-Moreno et al., 2018), gelatin/

carboxymethylcellulose (Yuan et al., 2018), gelatin/ arabic gum (Lv et al., 2014; Girardi et al., 2017; Raksa et al., 2017), and gelatin/sodium alginate (Wang et al., 2016; De Matos, Scopel & Dettmer, 2018). In this study, the biopolymers used as wall materials were gelatin (GE) and sodium alginate (NaAlg).

Gelatin (GE) is a natural nontoxic water-soluble protein derived from collagen. The polypeptide structure of the GE molecule facilitates its interactions with other oppositely charged ingredients, which makes it an important wall material used for microcapsules production by complex coacervation (Wang et al., 2016). Sodium alginate (NaAlg) is an anionic linear polysaccharide containing 1,4-linked D-mannuronic acid and L-guluronic acid residues, and is obtained from brown seaweed. NaAlg is a natural, biocompatible, biodegradable, and hydrophilic polymer, which has been used in microparticulate formulations (Dima et al., 2016).

Microcapsules obtained by complex coacervation are fragile under certain conditions. For this reason, specific compounds are used for cross-linking in order to obtain more resistant structures. An alginate matrix can be prepared through physical and/or chemical cross-linking of the polymer chains. The ionic cross-linking generates a three-dimensional network mainly by interaction of the carbonyl groups of guluronate moieties with multivalent cations, giving rise to the well-known “egg-box” conformation. The  $\text{Ca}^{2+}$  ion is the most used, perhaps because of the adequate network of the Ca-alginate gel and the acceptability of calcium by human organism (Phillips, 2009; Bagheri et al., 2014). Studies have shown that calcium chloride was efficient as a cross-linking agent (Wang et al., 2016; Li et al., 2018).

Several studies in the literature describe the potential use of the complex coacervation process in the encapsulation of EOs (Lv et al., 2014; Wang et al., 2016; Girardi et al., 2017; Raksa et al., 2017; De Matos, Scopel & Dettmer, 2018; Rojas-Moreno et al., 2018; Yuan et al., 2018). Thus, the present study aimed to analyze the compositions of black pepper EO, and to determine the influence of pH and biopolymer ratios on the formation of the complex coacervate obtained from GE and NaAlg, for use in the encapsulation of black pepper EO.

## 2. Materials and Methods

### 2.1. Materials

Gelatin, sodium alginate, calcium chloride and Tween 20 were obtained from Sigma-Aldrich (St. Louis, USA). Black pepper EO was obtained from Ferquima (São Paulo, Brazil) with the following characteristics: transparent/straw yellow, free of impurities, density (20°C) of 0.870 – 0.900 g.cm<sup>-3</sup>, and refraction index (20°C) of 1.480 – 1.500. Ultrapure water with a conductivity of 0.05 µS/cm was used (Master System P&D, Gehaka, Brazil).

### 2.2 Methods

#### 2.2.1 Chemical composition of black pepper (*Piper nigrum L.*) EO

##### 2.2.1.1 GC analysis

Analyses of volatile oils were carried out on a gas chromatography coupled with a mass spectrometer (QP2010, Plus-Shimadzu, Japan) with a Factor Four-VF-5ms capillary column (Varian) (30 m × 0.25 mm, 0.25 µm film thickness). The injection volume of the sample was 1 µl (split 1:30) and the injector, gas chromatography coupled with a mass spectrometer (GC-MS) interface and ion source temperatures were maintained at 220, 310, and 250°C, respectively, with an ionization energy of 70eV. The oven temperature was programmed as follows: 60°C at 2 min, 60 to 260°C at 3°C min<sup>-1</sup>, 260 to 290 °C at 10°C min<sup>-1</sup>, and 290°C at 5°C min<sup>-1</sup>. The EO constituents were identified by visual comparison of their spectra in the literature (Adams, 2007) and by the spectra provided by the device database (NIST21 and NIST107). A standard solution of n-alkanes (C<sub>8</sub>-C<sub>20</sub>) was injected under the same chromatographic conditions as the sample to obtain the retention indices (IK value).

A gas chromatograph (5890-series II, Hewlett Packard, USA) coupled with a flame ionization detector (CG-FID) and equipped with a Factor Four-VF-5ms capillary column (Varian) (30 m × 0.25 mm, 0.25 µm film thickness) was used for the quantification of EO. The injector and detector temperatures were maintained at 220 and 250°C, respectively. The amount of the injection of the samples was 1µL in split mode (1:30). The carrier gas was helium at a flow rate of 1 mL.min<sup>-1</sup>(12 psi). The oven

ramp temperature was programmed as follows: 60 °C for 2 min, increased to 260°C at 3°C min<sup>-1</sup>, and 260 to 290°C at 10°C min<sup>-1</sup>. The relative percentage of the oil constituents was expressed as a percentage by area normalization.

#### 2.2.1.2 NMR analysis

The NMR spectra were recorded on a spectrometer (Advance III, Bruker, USA) operating at 500.13MHz. The sample was measured in CDCl<sub>3</sub> (TMS was used as internal reference) at 298.15K, adapted from Vicente et al. (2015). The spectra were processed using the BrukerTopSpin 3.5 software. The spectra were processed using the MestreNova<sup>®</sup> Software 9.0 (Mestrelab research).

#### 2.2.2 Determination of the molecular weights of the biopolymers

The molecular weights of the biopolymers were determined by the viscosimetric method, adapted from Pamies et al. (2010) and Masueli (2014). The dynamic viscosity was calculated from the data obtained using Cannon-Fenske viscosimetric capillaries, (Schott-Gerate, Germany). The capillaries were immersed in a thermostatic bath (CT-52, Schott-Gerate, Germany) to control the temperature, which was maintained at approximately 25°C± 0.05. The biopolymers solutions were prepared with 0.1 M NaCl, and the NaAlg content was determined as in a previous study (Bastos, De Carvalho & Garcia-Rojas, 2018) with the concentrations 0.1, 0.2, 0.3, 0.4, 0.5, 0.6 and 0.75% (Pamies et al., 2010) and GE concentrations ranging from 0.1-1.0 % with a variation of 0.1% (Masueli, 2014). The solutions and solvent densities were measured in a densimeter (DMA 4500M, Anton Paar, Austria) with an autoinjector (Xsample 452, Anton Paar, Austria). The intrinsic viscosity ([ $\eta$ ]) was estimated by extrapolation of Martin curves to concentration "zero" (Guo et al., 2017), using the following equations:

$$\ln(\eta_{sp}/c) = \ln[\eta] + K[\eta]c \quad (1)$$

$$\eta_{sp} = \frac{\eta - \eta_0}{\eta} \quad (2)$$

where  $[\eta]$  is the intrinsic viscosity ( $\text{cm}^3/\text{g}$ ),  $\eta_{sp}$  is the specific viscosity,  $c$  is the concentration of the biopolymers ( $\text{g/mL}$ ),  $\eta$  is the viscosity of the solution of the biopolymers ( $\text{g/cm.s}$ ),  $\eta_0$  is the viscosity of the solvent ( $\text{g/cm.s}$ ), and  $K$  is Martin's constant.

The molecular weights were determined by the following viscosimetric equation (Mark, 1938; Houwink, 1940):

$$[\eta] = K \cdot M^a \quad (3)$$

where  $[\eta]$  is the intrinsic viscosity ( $\text{cm}^3/\text{g}$ ),  $M$  is the molecular weight, and  $K$  and  $a$  are constants that depend on the polymer, the solvent, and the temperature. The NaAlg constants  $a=0.92$  and  $K=7.3 \times 10^{-3} \text{cm}^3/\text{g}$  were used as reported by Pamies et al. (2010), and the GE constants  $a=0.62$  and  $K= 2.9 \times 10^{-3} \text{cm}^3/\text{g}$  were used as reported by Masueli (2014).

### 2.2.3 Formation of the complex GE/NaAlg

#### 2.2.3.1 Preparations of the solutions of GE and NaAlg

The biopolymers were weighted on an analytical balance (B-TEC-210, Tecnal, Brazil) for preparation of solutions containing a fixed concentration of 0.1% w/w. The biopolymers were dissolved in ultrapure water using a magnetic stirrer (NT101, Novatecnica, Brazil). NaAlg was homogenized for 24 hours, and GE was homogenized for 15 minutes at 50°C (Girardi et al., 2017). The ratios of 1:1, 1:2, 1:4, 1:6, 2:1, 4:1, and 6:1 (protein/polysaccharide) were tested.

#### 2.2.3.2 Effect of protein ratio on the formation of the GE/NaAlg complex

To determine the ideal ratio at which protein and polysaccharide form a complex coacervation, GE and NaAlg were mixed at different ratios (w/w). After mixing the biopolymers solutions at varying ratios, the pH of the mixture was adjusted to 4.0 using NaOH and HCl solutions, with a pHmeter (mPA210, Tecnoyon, Brazil). Individual biopolymers and the ratios were measurements by turbidity and  $\zeta$ -potential. Turbidity was measured at a wavelength of 600nm on a spectrophotometer (Biomate 3S, Thermo

Fisher Scientific, USA) calibrated with ultrapure water to 100% transmittance (%T). Turbidity was defined as 100-%T. A Zetasizer Nano ZS90 (Malvern Instruments, UK) was used to determine  $\zeta$ -potential, with a confidence interval of  $\pm 0.1$  unit. Each experiment was performed three times. Samples readings were performed in triplicate at 25°C. The ratio of GE/NaAlg (w/w) where the maximum interaction between GE and NaAlg occurred was selected to study the effect of pH on the formation of the GE/NaAlg complex, adapted from Diarrassouba et al. (2015).

#### 2.2.3.3 Effect of pH on the formation of the GE/NaAlg complex

The pH of the mixture at the selected ratio was varied from 7.0 to 2.0, turbidity and  $\zeta$ -potential. In Zetasizer Nano ZS90 (Malvern Instruments, UK), the GE/NaAlg mixture was transferred to an MPT-2 autotitrator (Malvern Instruments, UK). The pH was titrated using 0.5M NaOH, 0.25M HCl, and 0.025M HCl solutions. The pH was varied by 0.5 unit increments with a confidence interval of  $\pm 0.1$  unit, adapted from Diarrassouba et al. (2015).

#### 2.2.4 Preparation of microcapsules

The GE/NaAlg microcapsules were tested using a solution with a total concentration of 0.7, 1.4 or 2.1% (w/w) and biopolymer mixing ratio of 6:1. Different core/wall ratios were tested (0.3:1, 0.6:1 and 1.2:1). Black pepper EO was initially mixed with 40% (w/w) of Tween 20, and then added to the GE and NaAlg solutions. Subsequently, the whole solution was emulsified using a Ultra-Turrax (T25D, IKA, Germany) at the stirring rate of 10.000 rpm for 3 min, adapted from Lv et al. (2014). The mixture was homogenized (NT101, Novatecnica, Brazil) for 30 minutes at 25°C, then, 25mL of a calcium chloride solution (30mg.mL<sup>-1</sup>) (Bagheri et al., 2014) was added and dissolved with magnetic stirring (NT101, Novatecnica, Brazil). Acetic acid (20%, v/v) was used for acidification at pH 4.0. The microcapsules were stored at 10°C for 48 hours, and then the supernatant was removed. Finally, the microcapsules were frozen at -80°C using dry ice and freeze-dried (Enterprise I, Terroni, Brazil) for 24 hours.

## 2.2.5 Characterization of the microcapsules

### 2.2.5.1 . Loaded oil content and Encapsulation Efficiency (EE)

According to Karaca, Nickerson & Low (2013), approximately 300 mg of microcapsules were weighted in a Falcon tube (15 mL) to which 5 mL of isopropanol, 2 mL of ultrapure water, and 2 mL of hexane were added. The components were homogenized on a Vortex (AP 56, Phoenix, Brazil) and centrifuged (Digicen 21R, OrtoAlresa, Spain) at 8.000rpm for 15 minutes. Then, the supernatant phase was removed, washed twice with hexane, and placed in a petri dish for drying and the evaporation of hexane. The mass was measured gravimetrically, the theoretical oil value ( $OT\%$ ) was given by equation (4) and the loaded oil content ( $OC\%$ ) was given by equation (5).

$$OT(\%) = \frac{W_{oil}}{W_c} \times 100 \quad (4)$$

$$OC(\%) = \frac{W_{oil}}{W_c} \times 100 \quad (5)$$

where  $W_{oil}$  is the initial mass of oil added to the system,  $W_c$  is the initial mass of the capsule,  $W_{oil}$  is the oil content after encapsulation and  $W_c$  is the final capsule mass after freeze-dried used in this analysis. The encapsulation efficiency (EE) is the percentage of loaded oil content divided by the percentage of theoretical oil (Timilsena et al., 2016), given by equation (6).

$$EE(\%) = \frac{OC(\%) \times 100}{OT(\%)} \quad (6)$$

### 2.2.5.2 Fourier transform infrared spectroscopy (FT-IR)

The FT-IR spectra of the dried samples (GE, NaAlg, black pepper EO and the capsule) were obtained. The analyses were performed with an FT-IR spectrometer (Vertex 70, Bruker, Germany) read in the range of 4000–400  $\text{cm}^{-1}$ .

### 2.2.5.3 Chemical composition of the black pepper EO microencapsulated

In the sample with a higher EE (S3), oil extraction was performed as described in section 2.2.5.1. The supernatant phase was removed and analyzed by GC, under the same conditions as before (section 2.2.1.1).

### 2.2.6 Statistical analysis

All experimental measurements were conducted in triplicate, and the data are expressed as the mean  $\pm$  standard deviation. The statistical analyses were performed using Origin<sup>®</sup> Pro 9.0. The Kolmogorov-Smirnov normality test was performed for the populations. After confirming normality for all populations, one-way variance (ANOVA) was performed to determine the existence of significant difference between populations. Significant differences at a level of significance  $\alpha = 0.05$  were identified by Tukey's test.

## 3. Results and Discussion

### 3.1. Composition of black pepper EO

#### 3.1.1 GC analysis

Compounds were identified by GC-FID and GC-MS analyses of black pepper EO and are given in Table 1. The GC-MS chromatograph can be observed in Figure S1. In total, fifteen components were identified, representing 92% of the total components of the black pepper EO. The EO is a complex mixture consisting mainly of monoterpenes and sesquiterpenes. The predominant component was  $\beta$ -caryophyllene (28%), followed by limonene (15%), sabinene (11.4%),  $\beta$ -pinene (11%),  $\alpha$ -pinene (10.5%), 3-carene (6%),  $\alpha$ -copaene (3.6%), elemene (2%), mircene (1.6%),  $\alpha$ -caryophyllene (1%). The others terpenes identified had a percentage below 1%:  $\alpha$ -thujene (0.93%), p-cymene (0.47%), 2-carene (0.4%), linalool (0.3%), 4-terpineol (0.28%).

Previous studies reported a similar qualitative chemical composition for black pepper EO, although in different quantities (García-Díez et al., 2016; Chandran et al., 2017, Orchard et al., 2017). The studies identified  $\beta$ -caryophyllene as a major



component of black pepper EO, but at different concentrations: 57.6% (García-Díez et al., 2016), 15.03% (Chandran et al., 2017) and 28% (Orchard et al., 2017). The variation in the chemical composition of the terpenes in the black pepper EO can be attributed to the origin, climate, type of culture and type of extraction of the identified samples (García-Díez et al., 2016).

### 3.1.2 NMR analysis

The main five terpenes identified by CG were confirmed by  $^1\text{H}$  and  $^{13}\text{C}$  NMR, as shown in Table 2 and Figure S2. Some signals of the major compounds of black pepper EO were identified mostly due to the presence of the  $\text{sp}^2$  protons at  $\delta_{\text{H}}$  4.51 – 5.41 ppm and the correlations at  $^1J_{\text{H-C}}$  with respective  $\text{sp}^2$  carbons at  $\delta_{\text{C}}$  101 – 125, in the HMQC spectrum. The presence of several methyl group signals was also very informative for assigning some major compounds, mostly due to their long-range correlation signals ( $^{2,3}J_{\text{H-C}}$ ) observed in the HMBC spectrum.

The main components identified in black pepper EO are known and its NMR data were compared to the literature data. For instance, the monoterpene sabinene was detected especially by the signal at  $\delta_{\text{H}}$  0.67 and  $\delta_{\text{C}}$  16.0 ppm of the methylene carbon of the cyclopropyl ring ( $\text{CH}_2$ -6) (Guerrini et al., 2006). Some characteristic signals of the methyl groups were also detected and compared to the literature data, for instance, the methyl groups at  $\delta_{\text{H}}$  0.86 ( $\alpha$ -pinene), 0.91, 0.97 (sabinene), 0.96 and 0.98 ( $\beta$ -caryophyllene) ppm (Guerrini et al., 2006). Limonene was detected, especially due the presence of some characteristic carbon  $\text{sp}^2$  signals at  $\delta_{\text{C}}$  133.7 (C-1), 120.6 (CH-2), 150.2 (C-8) and 108.4 ( $\text{CH}_2$ -10) ppm and its respective proton signals at  $\delta_{\text{H}}$  5.40 (brs, CH-2) and 4.70 (brs,  $\text{CH}_2$ -10) ppm. Additionally,  $\beta$ -pinene was detected due the presence of  $\text{sp}^2$  carbons signals at  $\delta_{\text{C}}$  152.3 (C-2), 105.9 ( $\text{CH}_2$ -10) ppm and the methyl groups at  $\delta_{\text{C}}$  26.1 ( $\text{CH}_3$ -8) and 21.8 ( $\text{CH}_3$ -9) ppm (Skakovskii et al., 2006). In the DEPTQ spectrum (Figure S2) was possible to detect the presence of the quaternary  $\text{sp}^2$  carbons at  $\delta_{\text{C}}$  133.7 – 154.7 ppm and methyl groups at  $\delta_{\text{C}}$  16.3 – 30.1 ppm, which had its positions assigned by HMBC experiment and comparison with the literature data (Guerrini et al., 2006) (All 1D and 2D NMR assignments are shown in the Supplementary Material). Limonene, sabinene,  $\beta$ -pinene and  $\alpha$ -pinene have the same

molar weight that can be justified because they are isomers, these were differentiated by their fragments (Table 2).

The same terpenes were identified by NMR in others EOs:  $\beta$ -caryophyllene, was identified in *Rosmarinus officinalis* (Da Silva Bomfim et al., 2015), *Syzigum aromaticum* (Owen et al., 2017) and *Myrtus communis* (Bouzabata et al., 2015).  $\beta$ -pinene and limonene were identified in *Ocoteabofo Kunth* (Guerrini et al., 2006), *Rosmarinus officinalis* (Da Silva Bomfim et al., 2015) and *Myrtus communis* (Bouzabata et al., 2015) EOs. Finally,  $\alpha$ -pinene and  $\beta$ -pinene were found in *Rosmarinus officinalis* (Da Silva Bomfim et al., 2015) EO. Sabinene was identified in *Ocoteabofo Kunth* (Guerrini et al., 2006).

### 3.2 Intrinsic viscosity and molecular weights of the biopolymers

The molecular weight of NaAlg was determined in a previous study (Bastos, De Carvalho & Garcia-Rojas, 2018), with an  $[\eta]= 0.3911 \text{ cm}^3/\text{g}$  and  $138 \text{ kDa} \pm 0.07$  molecular weight. This molecular weight value is similar to those reported in the literature (Pamies et al., 2010) when the molecular weight of NaAlg was determined using the viscosimetric method. NaAlg can vary its molecular weight from 100 to 270 kDa depending on its origin and extraction (Phillips, 2009).

In the present study, GE had an  $[\eta]= 0.006439 \text{ cm}^3/\text{g}$  and  $249 \text{ kDa} \pm 1.5$  of molecular weight. The GE molecules are subdivided into several molecular weight ranges corresponding to the most commonly occurring sizes. The more commonly found ranges correspond to 'δ chains' of molecular weight 230- 340 kDa (Phillips, 2009).

### 3.3 . Effect of the ratio on the formation of the GE/NaAlg complex

The formation of complex coacervates between proteins and polysaccharides typically occurs between the isoelectric point (pI) of the protein and the pKa of the reactive groups of the polysaccharides. GE has a pI= 5.0 and the pKa of NaAlg is in the range of pH 3.4 - 3.7 (Bokkhim et al., 2015). Thus, the ideal pH for the formation of the GE/NaAlg complex is in the range of pH 3.7 to 5.0.

The ratio of polysaccharide to protein in the mixture influences their charge balance and consequently, their complex coacervation behavior (Bokkhim et al., 2015). Figure 1 shows the effect of the ratio on the formation of the GE/NaAlg complex coacervate. Figure 1 (A) shows the turbidity variation at 600nm as a function of the GE/NaAlg ratios (1:1, 1:2, 1:4, 1:6, 2:1, 4:1, 6:1) and of the biopolymers individually at pH 4.0.

The turbidity of the individual biopolymers was very low, for GE ( $0.7 \pm 0.49$ ) and NaAlg ( $3.0 \pm 0.71$ ). In the ratios 1:1 and 1:6 the turbidity was similar,  $9.7 \pm 0.41$  and  $9.4 \pm 0.71$ , respectively. The increase in the concentration of NaAlg presented a slight increase in turbidity in the ratios 1:2 and 1:4, with a turbidity of  $5.4 \pm 0.6$  and  $6.13 \pm 0.9$ , respectively.

The increase in the concentration of GE doubled the turbidity in the ratios of 2:1 and 4:1, with a turbidity of  $4.16 \pm 0.35$  and  $8.3 \pm 0.63$ , respectively. The 6:1 (GE/NaAlg) ratio had a higher turbidity ( $63 \pm 0.84$ ). As the ratio of protein increased, a large number of positively charged GE in molecules were available to neutralize the negative NaAlg an carboxylic groups ( $-\text{CO}_2^-$ ), which gradually increased the interaction strength between the protein and polymer. A similar behavior was described by Souza et al. (2018) in ovalbumin/carrageenan coacervates. For the ratio 10:1 (ovalbumin/carrageenan) the maximum turbidity was obtained, suggesting that this process occurred due to the increased interaction strength.

The variation in the zeta potential as a function of the ratio (GE/ NaAlg) and of the biopolymers individually at pH 4.0 is presented in Figure 1 (B). The GE had an electric charge of  $15.50 \pm 0.45$  and the NaAlg near-  $44.6 \pm 0.43$ . At the ratios of 1:2 to 1:6, as the NaAlg concentration increased the zeta potential of the ratios became more negative, suggesting that more of the polysaccharide was incorporated into the colloidal particles that formed. All the ratios showed a negative charge at pH 4.0, this result can be explained due to the stoichiometric balance of the charges, where the electric charge density present in GE was not sufficient to balance the charge of the GE/NaAlg complexes (Schimitt & Turgeon, 2011; Bastos, De Carvalho & Garcia-Rojas, 2018).

The  $\zeta$ -potentials of the mixtures changed from negative to positive as the concentrations of GE increased. At low GE/NaAlg ratio, the negatively charged NaAlg dominated the value of the  $\zeta$ -potential. Correspondingly, the mixture carried positive charge when GE was in excess. The same was observed by Yuan et al. (2017) in soy protein/chitosan complex. At the ratio 6:1 (GE/NaAlg), the charge approached

neutrality and higher turbidity, indicating that there was a better balance between the charges of the biopolymers.

### 3.4 . Effect of pH on the formation of the GE/NaAlg complex

The effect of pH on the formation of the GE/NaAlg complex coacervate shown in Figure 2. The GE/NaAlg ratio of 6:1 was selected to evaluate the effect of pH (2.0-7.0) on the formation of the complex coacervate, as measured by turbidity at 600 nm (Figure 2A). The complex presented higher turbidity ( $65.2 \pm 0.24$ ) at pH 4.0. At this pH, the biopolymers had opposite charges, where GE was positive and NaAlg was negative (Figure 2B). At pH values 5.0, 6.0 and 7.0, turbidity was  $2.43 \pm 0.23$ ,  $1.9 \pm 0.52$  and  $1.23 \pm 0.21$ , respectively. At these pH values, the protein presented a negative charge after its pI, both biopolymers were negative charged and for this reason, complex formation did not occur (low turbidity). At pH values 2.0 and 3.0 the turbidity was  $16.16 \pm 0.64$  and  $21.26 \pm 0.25$ , respectively. The pH values below the pKa of NaAlg (3.4-3.7) should be avoided by reducing the pH substantially below the pKa of the anionic polysaccharide, a loss of its charge and, consequently, a reduction in the electrostatic attraction of the complex coacervates occurs. The turbidity observed at  $\text{pH} < \text{pKa}$  can be attributed to the protonation of the carboxylic groups ( $-\text{CO}_2^- \rightarrow -\text{CO}_2\text{H}^+$ ) and possible aggregation of these groups (Bokkhim et al., 2015).

The ideal pH for the GE/NaAlg complex in the ratio of 6:1 was determined by performing zeta potential measurements at each pH value (Figure 2B). At pH 2.0 and 3.0 the complex carries a net positive charge of  $1.8 \pm 0.51$  and  $7.2 \pm 0.86$  mV, respectively. At pH 4.0, 5.0, 6.0 and 7.0, the complexes were negatively charged, with the zeta potential values being  $-7.24 \pm 0.36$ ,  $-38.5 \pm 0.81$ ,  $-48.5 \pm 0.89$  mV, respectively. At pH values 2.0 and 3.0, pH values below the pKa of NaAlg and should be avoided (Bokkhim et al., 2015). The greatest electrostatic interaction occurred near pH 4.0 where the charge approached neutrality, which represents a balance between the biopolymer charges. Similarly, Wang et al. (2016), observed that the ideal pH for formation of the complex between GE/NaAlg was 3.5, but this pH is below the NaAlg pKa and should be avoided. According to the Wang et al. (2016), a better ratio for the formation of the complex was 6:1 (GE/NaAlg), as observed by the present study.

### 3.5 . Formation and characterization of microcapsules

In Table 3 shows the composition of the formulations and the EE of the microcapsules produced by complex coacervation. The theoretical oil value, oil content and EE (equation 6) of microcapsules prepared with different samples is presented (Table 3). The theoretical oil values were 20, 30 and 40 %. The loaded oil content varied from 9.83 (S6) to 25.52% (S4). EE varied from 49.13 (S6) to 82.36% (S3). The core material was black pepper EO and the wall material weight was the biopolymers and the emulsifier.

#### 3.5.1 Encapsulation Efficiency (EE)

The samples S2, S3, S5, S8 and S9 had higher EE values and did not present significant differences ( $p < 0.05$ ) in EE. The samples had different percentages of biopolymers, core material and wall material weight. These samples had core/wall ratios of 0.3:1 (S3, S9) and 0.6:1 (S2, S5 and S8). The similarity in the composition of the samples was that the EO concentrations were lower than that of biopolymers. The concentrations of biopolymers were sufficient to cover a greater amount of core, which is extremely important to ensure that the active material is trapped within the capsule and does not lose functionality (Da Cruz et al., 2019).

S3, S6 and S9 were prepared at a ratio of 0.3:1, but S6 differed from the others (S9 and S6) and presented lower efficiency ( $49.13 \pm 3.41$ ). S6 used intermediary concentrations of biopolymers (%), wall material weight and EO concentration compared to S3 and S9, contributing to the significant differences in EE for S6.

The samples S1, S6 and S7 were prepared with different conditions (percentages and concentrations of biopolymers, EO concentrations and core/wall ratios), as presented in Table 3. S1 and S7 were prepared with core/ wall ratio of 1.2:1 and S6 with a ratio of 0.3:1, however, these conditions did not exert a significant difference in the efficiency of the samples. S1, S6 and S7 had lower EEs, perhaps because an insufficient amount of wall materials was available to cover the entire core, resulting in a high free core concentration, and a high amount of core that was not encapsulated and, hence was lost during the encapsulation process (Timilsena et al., 2016; Wang et al., 2016; Da Cruz et al., 2019).

S2, S4, S5 and S7 did not present significant differences in EE, when S2 and S5 had a core/wall ratio of 0.6:1, S4 and S7 had a core/wall ratio of 1.2:1. In the samples with a core / wall ratio of 0.6:1 (S2 and S5), the EO concentrations were lower than that of biopolymers, in samples with core/wall ratios of 1.2:1 (S4 and S7) the EO concentrations were higher than that of biopolymers. The similarity in the composition of the samples was that the EO concentrations were lower than the biopolymers concentrations.

There were no significant differences in the EE between samples using a core/wall ratio of 1.2:1 (S1, S4 and S7). The samples had different percentages for biopolymers, S1 (0.7%), S4 (1.4%), S7 (2.1%). The similarity in the composition of the samples was the EO concentrations were higher than that of biopolymers. The samples (S1, S4 and S7) with core/ wall ratios of (1.2:1) had lower EEs, which did not favored the EO imprisoned inside the capsule and can be explained because there was core material (EO) in excess, as observed by Wang et al. (2016). Wang et al. (2016) observed higher EE at the core/wall ratio of 1:1 for ginger (*Zingiber officinale*) EO microcapsules prepared using GE/NaAlg to form a complex coacervate. According to the authors, the core/wall ratio of 2:1 had a lower EE, perhaps due to the presence of excess ginger EO, which could be observed from scanning electron microscopy.

Although the samples (S2, S3, S5, S8, and S9) did not present significant differences in EE, sample S3 was selected for the next characterization of the microcapsule because it had a ratio of 0.3: 1 with the low amount of EO. Timilsena et al. (2016) demonstrated that the lowest amount of core relative to the wall material was efficient to entrap chia seed oil in CPI-CSG complex coacervates. However, when the core content was increased in proportion (core/wall material), a small amount of the oil (core) was unencapsulated, and as the core amount was increased, the unencapsulated oil (core) was deposited on the surface of the microcapsules.

### 3.5.2 . FT-IR

Figure 3 shows the infrared (FT-IR) spectroscopy of NaAlg, GE, black pepper EO and the microcapsule (S3) at pH 4.0. The selected wavelength region (4000 to 400  $\text{cm}^{-1}$ ) includes the amides bands of the protein: group I (1625-1750  $\text{cm}^{-1}$ ), group II (1475-1575  $\text{cm}^{-1}$ ), group III (1225 - 1425  $\text{cm}^{-1}$ ). Amide band I corresponds to the

stretching of the C=O, amide band II corresponds to the stretching of the N-H, amide band III is attributed to the stretching of the C-N and N-H groups. In the Gelatin, the amide bands I, II and III were observed at 1697, 1536, and 1337 $\text{cm}^{-1}$ , respectively (Figure 3). The free amino acid O-H groups (Wang et al., 2016) can be identified between the bands 3300 and 3170  $\text{cm}^{-1}$ . In the GE, the O-H group of the free amino acid can be identified by the 3260 band.

The bands of NaAlg were determined in a previous study (Bastos, De Carvalho & Garcia-Rojas, 2018), the first band is at 1591 $\text{cm}^{-1}$ , representing the  $\text{CO}_2^-$  present in the carboxylic acid salts ( $\text{RCOO}^-$ ) in the range of 1650-1550  $\text{cm}^{-1}$ . Band 2, presents at 1404  $\text{cm}^{-1}$ , refers to the C-O bond of the acid group ( $\text{RCOOH}$ ) in the range of 1440-1395  $\text{cm}^{-1}$ . Band 3 (1024  $\text{cm}^{-1}$ ) is attributed to the vibration stretch of the C-O and C-C of the pyranose ring (Bokkhim et al., 2015).

The spectrum peak of black pepper EO shows CH stretching vibration at 2922  $\text{cm}^{-1}$ , vibration of the aliphatic C-H in  $\text{CH}_2$  at 2868, C=C stretching at 1643  $\text{cm}^{-1}$ , C-OH absorption bending vibration at 1446  $\text{cm}^{-1}$  and  $\text{CH}_3$  bending at 1381  $\text{cm}^{-1}$ . The peak 886  $\text{cm}^{-1}$  assigned to the bending vibrations (out of the plane) in  $=\text{CH}_2$  (Li et al., 2018), the peak at 786  $\text{cm}^{-1}$  is assigned to benzene rings  $=\text{CH}$  vibration absorption (Raksa et al., 2017).

The spectrum of microcapsules containing black pepper EO is presented in Figure 3, it shows amide bands II of the GE at 1536  $\text{cm}^{-1}$ , and it shows C-OH absorption bending vibration at 1446  $\text{cm}^{-1}$ , the peak 886  $\text{cm}^{-1}$  correspond to bending vibrations in  $=\text{CH}_2$  in black pepper EO. The peak 1024  $\text{cm}^{-1}$  is attributed to the vibration stretch of the C-O and C-C of the pyranose ring in NaAlg. The results show that the black pepper EO is successfully encapsulated in the GE/NaAlg shell.

### 3.5.3. Composition of the EO after microencapsulation

Black pepper EO after microencapsulation was identified by GC-FID and GC-MS analysis and is shown in Table 1. The  $\beta$ -caryophyllene was at 22.9% after the encapsulation, at low levels (18.3%) compared to the relative content in the original (28%) EO. Therefore, the high percentage of this terpene was preserved (81.7%) after encapsulation.

The others terpenes in the original EO were identified after microencapsulation, and at the following percentages: limonene (12.10%), sabinene (9.13%),  $\beta$ -pinene (8.73%),  $\alpha$ -pinene (8.15%). The other compounds were present at low concentrations. The minor compounds present in the original EO were not identified after microencapsulation (2-carene, linalool and 4-terpineol).

There was a decrease in all terpenes percentages after microencapsulation, this can be explained because these components are volatile and sensitive to the adverse factors (oxygen, light and low pH), which may have contributed to its reduction during the fabrication of the microcapsules (Jun-Xia, Hai-Yan & Jian, 2011; Dima et al., 2016). The same was observed in others studies of encapsulated EOs (Jun-Xia, Hai-Yan & Jian, 2011, Peng et al., 2014; Lv et al., 2014).

The results obtained in the present study showed that encapsulated black pepper EO has great retention capacity. The main terpenes identified in the EO were preserved, with 80% of their original content (unencapsulated EO). The great retention of EOs has been reported in others studies: sweet orange (Jun-Xia, Hai-Yan & Jian, 2011), mustard (Peng et al., 2014), jasmine (Lv et al., 2014). Jun-Xia et al., 2011, identified the major compound D-limonene in the sweet orange EO after microencapsulation by complex coacervation with soybean protein isolate/gum arabic. The same method was used for encapsulated mustard (*Sinapis alba*) EO (Peng et al., 2014), for which the authors confirmed the presence of allyl isothiocyanate in EO after microencapsulation. Linalool was identified in jasmine EO after microencapsulation by complex coacervation with gelatin/gum arabic (Lv et al., 2014).

#### 4. Conclusion

In this study, black pepper EO compounds were identified by GC and NMR. GE had a molecular weight characteristic of 'δ chains', and NaAlg had a low molecular weight. The optimal ratio and pH for complex formation were 6:1 GE/NaAlg and 4.0, respectively and the interaction between the biopolymers was confirmed via FT-IR. Black pepper EO microcapsules produced by complex coacervation using GE and NaAlg as wall materials have a good encapsulation efficiency. The presence of terpenes in the encapsulated black pepper EO identified by GC indicated good core protection with the materials used. Therefore, GE and NaAlg have been shown to have potential for use as a wall material in the microencapsulation process of black pepper EO via the



complex coacervation technique and can be used to encapsulate others bioactive ingredients.

#### **Conflict of interest**

The authors declare no conflict of interest.

#### **Acknowledgment**

The authors thank to CNPq, FAPERJ and CAPES (Finance code 001) for financial support.

## 5. References

- Adams, R. P. (2007). Identification of essential oil components by gas chromatography/mass spectrometry (4th.). Illinois USA: Allured Publishing Corporation.
- Bagheri, L., Madadlou, A., Yarmand, M., & Mousavi, M. E. (2014). Spray-dried alginate microparticles carrying caffeine-loaded and potentially bioactive nanoparticles. *Food Research International*, 62, 1113-1119.
- Bastos, L. P. H., De Carvalho, C. W. P., & Garcia-Rojas, E. E. (2018). Formation and characterization of the complex coacervates obtained between lactoferrin and sodium alginate. *International Journal of Biological Macromolecules*, 120, 332-338.
- Bakkali, F., Averbeck, S., Averbeck, D., & Idaomar, M. (2008). Biological effects of essential oils – a review. *Food and Chemical Toxicology*, 46, 446–475.
- Bokkhim, H., Bansal, N., Grøndahl, L., & Bhandari, B. (2015). Interactions between different forms of bovine lactoferrin and sodium alginate affect the properties of their mixtures. *Food Hydrocolloids*, 48, 38-46.
- Bouzabata, A., Cabral, C., Gonçalves, M. J., Cruz, M. T., Bighelli, A., Cavaleiro, C., & Salgueiro, L. (2015). *Myrtus communis* L. as source of a bioactive and safe essential oil. *Food and Chemical Toxicology*, 75, 166-172.
- Chandran, J., Nayana, N., Roshini, N., & Nisha, P. (2017). Oxidative stability, thermal stability and acceptability of coconut oil flavored with essential oils from black pepper and ginger. *Journal of Food Science and Technology*, 54(1), 144-152.
- Da Cruz, M. C. R., Dagostin, J. L. A., Perussello, C. A., & Masson, M. L. (2019). Assessment of physicochemical characteristics, thermal stability and release profile of ascorbic acid microcapsules obtained by complex coacervation. *Food Hydrocolloids*, 87, 71-82.
- Da Silva Bomfim, N., Nakassugi, L. P., Oliveira, J. F. P., Kohiyama, C. Y., Mossini, S. A. G., Grespan, R., & Machinski Jr, M. (2015). Antifungal activity and inhibition of fumonisin production by *Rosmarinus officinalis* L. essential oil in *Fusarium verticillioides* (Sacc.) Nirenberg. *Food Chemistry*, 166, 330-336.
- De Matos, E. F., Scopel, B. S., & Dettmer, A. (2018). Citronella essential oil microencapsulation by complex coacervation with leather waste gelatin and sodium alginate. *Journal of Environmental Chemical Engineering*, 6(2), 1989-1994.
- Diarrassouba, F., Remondetto, G., Garrait, G., Alvarez, P., Beyssac, E., & Subirade, M. (2015). Self-assembly of  $\beta$ -lactoglobulin and egg white lysozyme as a potential carrier for nutraceuticals. *Food Chemistry*, 173, 203-209.
- Dima, C., Pătrașcu, L., Cantaragiu, A., Alexe, P., & Dima, Ș. (2016). The kinetics of the swelling process and the release mechanisms of *Coriandrum sativum* L. essential oil from chitosan/alginate/inulin microcapsules. *Food Chemistry*, 195, 39-48.

García-Díez, J., Alheiro, J., Pinto, A. L., Soares, L., Falco, V., Fraqueza, M. J., & Patarata, L. (2016). Behaviour of food-borne pathogens on dry cured sausage manufactured with herbs and spices essential oils and their sensorial acceptability. *Food Control*, 59, 262-270.

Girardi, N. S., García, D., Passone, M. A., Nesci, A., & Etcheverry, M. (2017). Microencapsulation of *Lippia turbinata* essential oil and its impact on peanut seed quality preservation. *International Biodeterioration & Biodegradation*, 116, 227-233.

Guerrini, A., Sacchetti, G., Muzzoli, M., Rueda, G. M., Medici, A., Besco, E., Bruni, R. (2006). Composition of the volatile fraction of *Ocotea bofo Kunth (Lauraceae)* Calyces by GC-MS and NMR fingerprint and its antimicrobial and antioxidant activity. *Journal of Agricultural and Food Chemistry*, 54, 7778-7788.

Guo, X., Zhao, W., Liao, X., Hu, X., Wu, J., & Wang, X. (2017). Extraction of pectin from the peels of pomelo by high-speed shearing homogenization and its characteristics. *LWT-Food Science and Technology*, 79, 640-646.

Houwink, R. (1940). The interrelationship between viscosimetric and osmotic identified degree of polymerization in high polymers. *Journal Fürpraktische Chemie*, 157, 15-18.

IUPAC.(1997). IUPAC Compendium of Chemical Technology, North Carolina, USA.

Jun-Xia, X., Hai-yan, Y., & Jian, Y. (2011). Microencapsulation of sweet orange oil by complex coacervation with soybean protein isolate/gum Arabic. *Food Chemistry*, 125(4), 1267-1272.

Karaca, A. C., Nickerson, M., & Low, N. H. (2013). Microcapsule production employing chickpea or lentil protein isolates and maltodextrin: Physicochemical properties and oxidative protection of encapsulated flaxseed oil. *Food Chemistry*, 139, 448-457.

Li, N., Zhang, Z. J., Li, X. J., Li, H. Z., Cui, L. X., & He, D. L. (2018). Microcapsules biologically prepared using *Perilla frutescens* (L.) Britt. essential oil and their use for extension of fruit shelf life. *Journal of the Science of Food and Agriculture*, 98(3), 1033-1041.

Lv, Y., Yang, F., Li, X., Zhang, X., & Abbas, S. (2014). Formation of heat-resistant nanocapsules of jasmine essential oil via gelatin/gum arabic based complex coacervation. *Food Hydrocolloids*, 35, 305-314.

Mark, H, in: *Der feste Körper*, Hirzel, Leipzig, 1938, pp. 65-104.

Masuelli, M. A. (2014). Mark-houwink parameters for aqueous-soluble polymers and biopolymers at various temperatures. Science and Education Publishing, 2, 37-43.

Orchard, A., Sandasi, M., Kamatou, G., Viljoen, A., & Van Vuuren, S. (2017). The in vitro antimicrobial activity and chemometric modelling of 59 commercial essential oils against pathogens of dermatological relevance. *Chemistry & Biodiversity*, 14(1), 160-218.

- Owen, L., Grootveld, M., Arroo, R., Ruiz-Rodado, V., Price, P., & Laird, K. (2017). A Multifactorial Comparison of Ternary Combinations of Essential Oils in Topical Preparations to Current Antibiotic Prescription Therapies for the Control of Acne Vulgaris-Associated Bacteria. *Phytotherapy Research*, 31(3), 410-417.
- Pamies, R. Schmidt, R. R. Martínez, M. D. C. L. de la Torre, J. G. (2010). The influence of mono and divalent cations on dilute and non-dilute aqueous solutions of sodium alginates, *Carbohydrate Polymers*, 80, 248-253.
- Peng, C., Zhao, S. Q., Zhang, J., Huang, G. Y., Chen, L. Y., & Zhao, F. Y. (2014). Chemical composition, antimicrobial property and microencapsulation of Mustard (*Sinapis alba*) seed essential oil by complex coacervation. *Food Chemistry*, 165, 560-568.
- Phillips, O. G. Williams, P. A. (2009). Handbook of hydrocolloids, (2th), Florida, Boca Raton, pp. 902.
- Raksa, A., Sawaddee, P., Raksa, P., & Aldred, A. K. (2017). Microencapsulation, chemical characterization, and antibacterial activity of Citrus hystrix DC (*Kaffir Lime*) peel essential oil. *Monatshefte für Chemie-Chemical Monthly*, 148(7), 1229-1234.
- Rojas-Moreno, S., Osorio-Revilla, G., Gallardo-Velázquez, T., Cárdenas-Bailón, F., & Meza-Márquez, G. (2018). Effect of the cross-linking agent and drying method on encapsulation efficiency of orange essential oil by complex coacervation using whey protein isolate with different polysaccharides. *Journal of Microencapsulation*, 35(2), 165-180.
- Schmitt, C. Turgeon, S. L. (2011). Protein/polysaccharide complexes and coacervates in food systems. *Advances in Colloid and Interface Science*, 167, 63-70.
- Skakovskii, E.D., Lamotin, S.A., Shpak, S.I., Tychinskaya, L.Y., Gaidukevich, O. A., Lamotkin, A.I. (2006). Application of NMR spectroscopy for analysis of the composition of pine needle essential oil. *Journal of Applied Spectroscopy*, 73(2), 275-279.
- Souza, C. J., Souza, C. S., Bastos, L. P. H., & Garcia-Rojas, E. E. (2018). Interpolymer complexation of egg white proteins and carrageenan: Phase behavior, thermodynamics and rheological properties. *International Journal of Biological Macromolecules*, 109, 467-475.
- Timilsena, Y. P., Adhikari, R., Barrow, C. J., & Adhikari, B. (2016). Microencapsulation of chia seed oil using chia seed protein isolate chia seed gum complex coacervates. *International Journal of Biological Macromolecules*, 91, 347-357.
- Vicente, J., de Carvalho, M. G., & Garcia-Rojas, E. E. (2015). Fatty acids profile of sacha inchi oil and blends by <sup>1</sup>H NMR and GC-FID. *Food chemistry*, 181, 215-221.

Wang, L., Yang, S., Cao, J., Zhao, S., & Wang, W. (2016). Microencapsulation of Ginger Volatile Oil Based on Gelatin/Sodium Alginate Polyelectrolyte Complex. *Chemical and Pharmaceutical Bulletin*, 64(1), 21-26.

Yuan, Y., Kong, Z. Y., Sun, Y. E., Zeng, Q. Z., & Yang, X. Q. (2017). Complex coacervation of soy protein with chitosan: Constructing antioxidant microcapsule for algal oil delivery. *LWT-Food Science and Technology*, 75, 171-179.

Yuan, Y., Li, M. F., Chen, W. S., Zeng, Q. Z., Su, D. X., Tian, B., & He, S. (2018). Microencapsulation of shiitake (*Lentinula edodes*) essential oil by complex coacervation: formation, rheological property, oxidative stability and odour attenuation effect. *International Journal of Food Science & Technology*, 53(7), 1681-1688.

Zhang, K., Zhang, H., Hu, X., Bao, S., & Huang, H. (2012). Synthesis and release studies of microalgal oil-containing microcapsules prepared by complex coacervation. *Colloids and surfaces B: Biointerfaces*, 89, 61-66.

### Figure Caption

**Fig.1:** Effect of the ratio on the formation of the GE/NaAlg complex. Figure 1 (A) shows the turbidity variation of the biopolymers individually and as a function of the GE/NaAlg ratios at 600 nm. Figure 1 (B) shows the zeta potential variation of the biopolymers individually and as a function of the GE/NaAlg ratios, both at pH 4.0. Data represent the mean  $\pm$  one standard deviation (n = 3).

**Fig.2:** Effect of the pH on the formation of the GE/ NaAlg complex. Figure 2 (A) shows the turbidity at 600 nm. Figure 2 (B) shows the zeta potential. The GE/NaAlg concentration ratio was 6:1 and the pH values were 2.0, 3.0, 4.0, 5.0, 6.0 and 7.0. Data represent the mean  $\pm$  one standard deviation (n = 3).

**Fig.3:** FT-IR spectra of NaAlg, GE, EO and microcapsule (S3) (GE/NaAlg ratio r= 6:1) at pH 4.0.

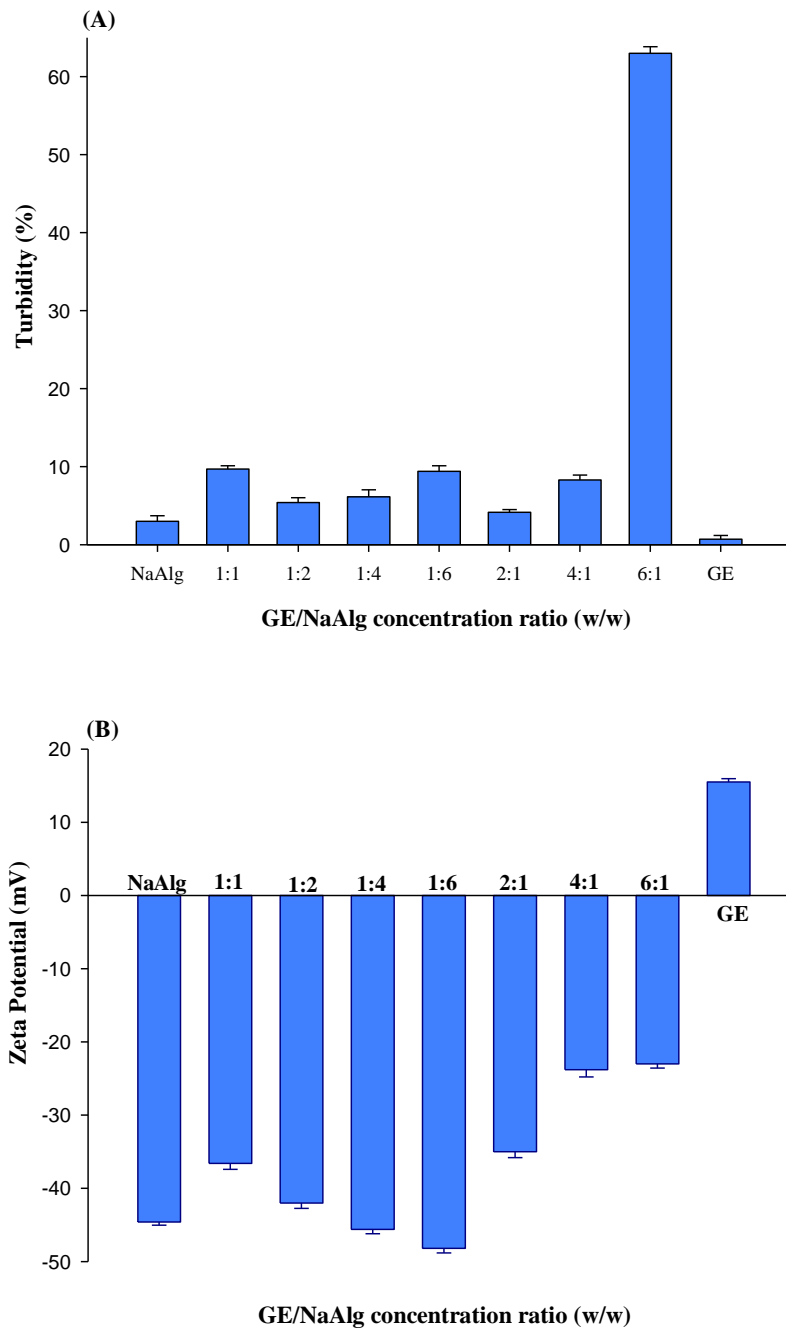


**Fig. 1.**

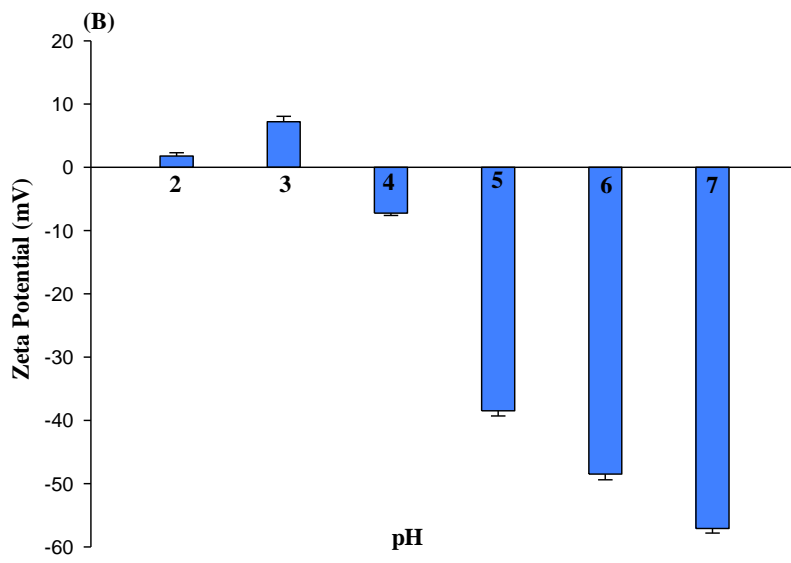
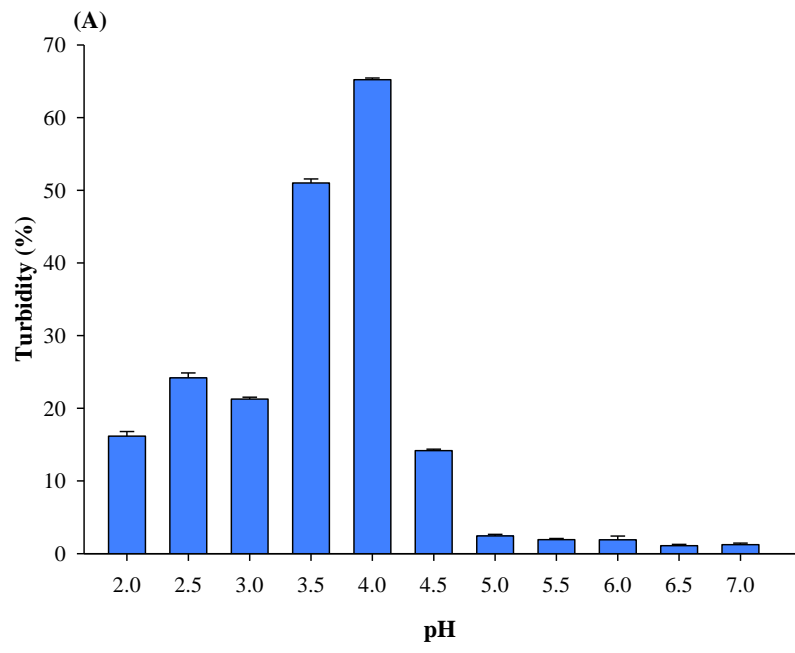


**Fig. 2.**



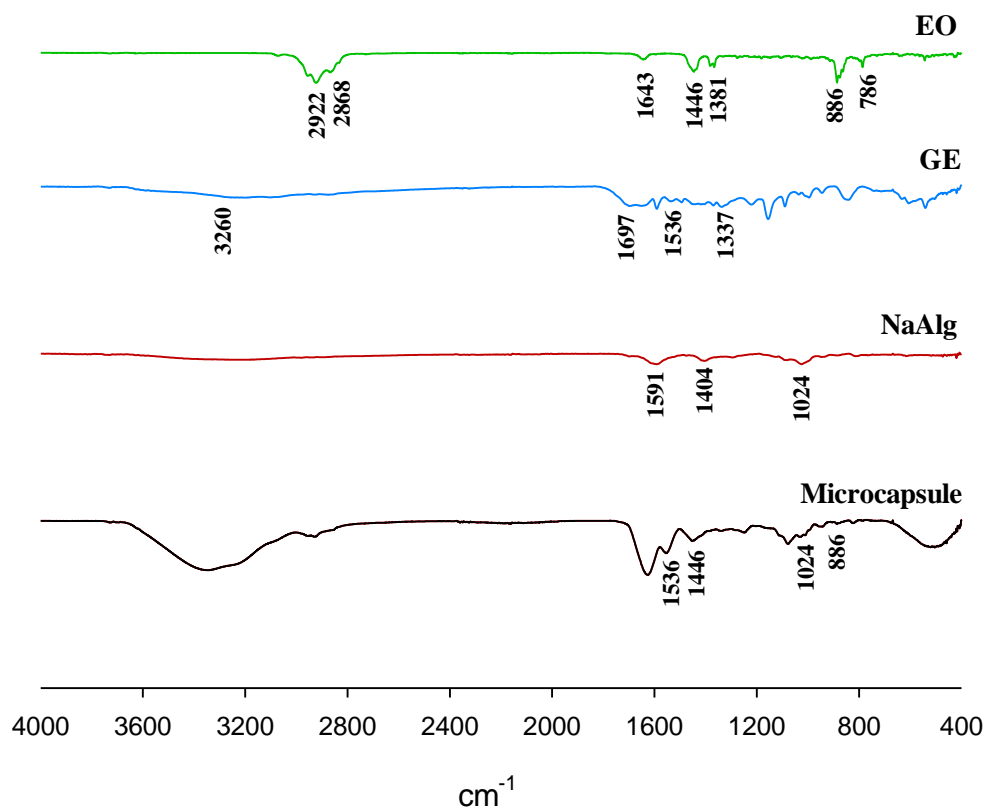
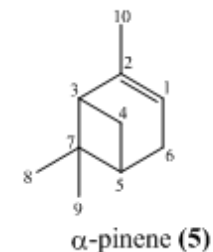
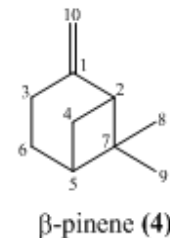
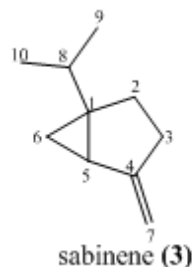
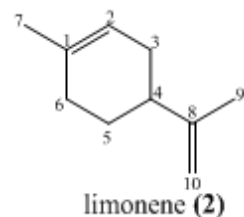
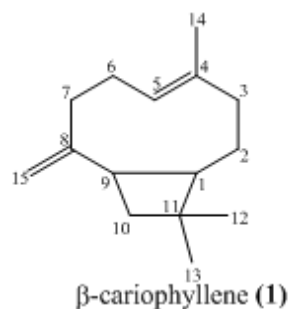


**Fig. 3.**

**Table 1.** Chemical composition of the original black pepper EO and content in microcapsule by GC. <sup>a</sup>KI= Kovats indices to n-alkanes (C<sub>8</sub>–C<sub>20</sub>) on an HP- 5MS column, <sup>b</sup>KI=identification based on comparison of retention index with those of published data (Adams, 2007), <sup>c</sup>RT= Retention time, <sup>d</sup>Relative content obtained by GC-FID.

Component	KI <sup>a</sup>	KI <sup>b</sup>	RT <sup>c</sup> (min)	Relative content in original EO <sup>d</sup> (%)	Relative content EO in microcapsule <sup>d</sup> (%)
β-caryophyllene (1)	1429	1419	26.046	28	22.9
Limonene (2)	1033	1029	9.400	15	12.10
Sabinene (3)	975	975	7.434	11.4	9.13
β-pinene (4)	982	979	7.546	11	8.73
α-pinene (5)	934	939	6.196	10.5	8.15
3-carene (8)	1012	1011	8.672	6	0.81
α-copaene (14)	1379	1376	24.061	3.6	1.83
Elemene (13)	1336	1338	22.428	2	0.18
Mircene (7)	989	990	7.961	1.6	0.98
α-cariophyllene (15)	1457	1454	27.235	1	0.62
α-thujene (6)	924	930	5.967	0.93	0.34
p-cymene (9)	1027	1024	9.168	0.47	0.15
2-carene (10)	1086	1002	11.652	0.4	-
Linalool (11)	1101	1096	12.152	0.3	-
4-terpineol (12)	1117	1177	15.421	0.28	-

**Table 2.**  $^{13}\text{C}$  and  $^1\text{H}$  NMR data of identified major compounds in the black pepper EO ( $\delta_{\text{C}}$  and  $\delta_{\text{H}}$  in ppm).



C	$\delta_{\text{C}}$	$\delta_{\text{H}}$ (J in Hz)	$\delta_{\text{C}}$	$\delta_{\text{H}}$	$\delta_{\text{C}}$	$\delta_{\text{H}}$ (J in Hz)	$\delta_{\text{C}}$	$\delta_{\text{H}}$ (J in Hz)	$\delta_{\text{C}}$	$\delta_{\text{H}}$
1	53.5	1.68(m)	133.7	-	37.6	-	152.3	-	116.0	5.18(br s)
2			120.6	5.40(brs)			51.8	2.45(t, 5.3)	144.5	
3	40.0									
4	135.5		41.1		154.5	-				
5	124.3	5.30 (dd, 5, 10.5)							40.7	
6			30.6	2.10(m)	16.0	0.64(d, 5.5)			37,6	
7	34.8	1.98 (m), 2.20(m)	23.5	1.65(br s)	101.5	4.61(brs) 4.79(brs)				
8	157.4		150.2		32.6	1.52 (m)	26.1	1.23 (s)	26.4	1.26 (s)
9	48.5		20.8	1.72(s)	19.7	0.88(d, 7)	21.8	0.71 (s)	20.8	0.83(s)
10	40.3	1.64(m), 1.93(m)	108.4	4.70(brs)	19.8	0.95(d, 7)	105,9	4.55(brs), 4.61(brs)	23.0	1.65(s)
11	33.9									
12	22.6	0.97(s)								
13	30.1	0.99(s)								
14	16.3	1.60(s)								
15	111.6	4.81(brs), 4.93(brs)								
m/z		204		136		136		136		136

**Table 3.** Composition of the formulations and encapsulation efficiency of the microcapsules produced by complex coacervation.

Samples	Core Material (g)	Wall Material Weight (g)				core/wall ratio (w/w)	CaCl <sub>2</sub> solution(g)	Loaded oil content(%)	Theoretical oil value (%)	EE (%)
		GE (g)	NaAlg (g)	Emulsifiers	Total (g)					
S1	0.42	0.3	0.05	0.28	1.05	1.2:1	10	21.55 ± 1.28	40	52.26 <sup>cd</sup> ± 6.68
S2	0.21	0.3	0.05	0.14	0.7	0.6:1	10	20.95 ± 0.46	30	70.39 <sup>ab</sup> ± 9.57
S3	0.105	0.3	0.05	0.07	0.525	0.3:1	10	16.18 ± 0.7	20	82.36 <sup>a</sup> ± 3.52
S4	0.84	0.6	0.1	0.56	2.1	1.2:1	10	25.52 ± 1.6	40	63.70 <sup>bc</sup> ± 2.90
S5	0.42	0.6	0.1	0.28	1.4	0.6:1	10	21.43 ± 1.36	30	69.51 <sup>ab</sup> ± 4.56
S6	0.21	0.6	0.1	0.14	1.05	0.3:1	10	9.83 ± 0.68	20	49.13 <sup>d</sup> ± 3.41
S7	1.26	0.9	0.15	0.84	3.15	1.2:1	10	24.42 ± 1.67	40	61.03 <sup>bcd</sup> ± 5.50
S8	0.63	0.9	0.15	0.42	2.1	0.6:1	10	24.88 ± 0.57	30	82.20 <sup>a</sup> ± 1.91
S9	0.315	0.9	0.15	0.21	1.575	0.3:1	10	16.34 ± 1.09	20	81.10 <sup>a</sup> ± 8.19

The analyses were performed in three replicates. The same letters in the same column do not differ significantly by the Tukey test with a probability of 5%.

**CAPÍTULO V**  
**INFLUENCE OF THE HEAT TREATMENT OF  $\beta$ -LACTOGLOBULIN ON**  
**THE FORMATION OF INTERPOLYMERIC COMPLEXES WITH SODIUM**  
**ALGINATE**

### **Abstract**

The aim of this study was to evaluate the influence of some parameters (pH, ratio of biopolymers and protein thermal treatment) on the formation of the interpolymeric complexes between  $\beta$ -Lactoglobulin ( $\beta$ -LG) and sodium alginate (NaAlg).  $\beta$ -LG nanoparticle ( $\beta$ -LG<sub>n</sub>) around 6.5nm was obtained by thermal treatment. The  $\zeta$ -potentials showed that the ideal pHs to  $\beta$ -LG/NaAlg and  $\beta$ -LG<sub>n</sub>/NaAlg were 4.5 and 4.0, respectively. Isothermal titration calorimetry further confirmed that per molecule of NaAlg were saturated 131.1 with molecules of  $\beta$ -LG and for 555.1 molecules of  $\beta$ -LG<sub>n</sub>. The thermodynamic parameters demonstrated that the interactions between  $\beta$ -LG and NaAlg were spontaneous with favorable enthalpic and entropic contributions during the interaction. The chemical characteristics of the interpolymeric complexes indicated that occurs electrostatic interaction and the hydrophobic groups were exposed after thermal treatment of the  $\beta$ -LG<sub>n</sub>. The formation of the interpolymeric complexes between  $\beta$ -LG and NaAlg can serve as an alternative to the incorporation of active ingredients in food systems.

**Keywords:** nanoparticle, electrostatic interaction, thermodynamic parameters, thermal characteristic, FT-IR.

## 1. Introduction

Complexes formed between proteins and polysaccharides are of continuing interest due to its great flexibility in the engineering of mechanical and structural properties of foods (Dickinson et al., 2008). The functional properties of the complexes are potentially better than those proteins and polysaccharides alone (Schmitt & Turgeon, 2011; Zeeb et al., 2018). Protein/polysaccharide coacervation commonly results from electrostatic interactions between oppositely charged biopolymers. The electrical charge on protein molecules changes from positive to negative when the pH is altered from below to above their isoelectric point (pI). An anionic polysaccharide has a full negative charge at pH well above the pKa value of its side groups (typically carboxyl or sulfate groups) but progressively loses its charge as the pH is decreased.

This interaction can be affected by several parameters (pH, ionic strength, temperature, biopolymer ratio and concentration, charge density, and molecular weight) (Jones et al., 2009; Schmitt & Turgeon, 2011; Protte et al., 2016). Hydrophobic, hydrogen-bonding and steric interactions may also occur (De Kruif et al., 2001). The thermodynamic parameters of complex formation between proteins and polysaccharides may be studied; where the enthalpy ( $\Delta H$ ) is associated with the energy involved in molecular interactions and reflects the contribution of hydrogen bonds, electrostatic and van der Waals interactions. The entropy ( $T\Delta S$ ) reflects a change in the order of the system and is related to hydrophobic interactions (Pires et al., 2009; Bou-Abdallah et al., 2012).

The study of the complexes is important because they can be used as microencapsulation systems of biomaterials (Dickinson et al., 2008). Therefore,  $\beta$ -LG/NaAlg complex formation has been used as a model system to study the formation of complexes between oppositely charged biopolymers (Hosseini et al., 2013; Qomarudin et al., 2015; Stender et al., 2018).

$\beta$ -LG is the major constituent of whey protein, it is a small globular protein with a well-known structure. It has an isoelectric point of  $\cong 5.1$ , a molecular weight of 18 kDa and a thermal denaturation temperature of  $\cong 70^\circ\text{C}$  at neutral pH (Hoffman et al., 1997; Verheul et al., 1999). At ambient temperature, native  $\beta$ -LG molecules can exist in various quaternary structures (monomers, dimmers, and octamers) depending on solution pH and ionic composition. When  $\beta$ -LG is heated any oligomers tend to dissociate into monomers (Galani & Apenten, 2000; Perez et al., 2014). This is followed

by a partial loss in the secondary structure above 70°C, which exposes the hydrophobic core and internal cysteine residues normally buried in the globular protein interior. The thermal treatment can be controlled to produce biopolymer nanoparticles with well-defined characteristics (Galani & Apenten, 2000; Perez et al., 2014). Nanoparticles refer to functional materials at a length scale of less than 100 nm (Diarrassouba et al., 2017), the particle size of the protein aggregates depends on the heating rate, heating duration, and protein concentration (Bromley et al., 2006; Mehalebi et al., 2008; Jones et al., 2010). Biopolymer nanoparticles and microparticles have useful applications in the food and pharmaceutical industries, as encapsulating agents, delivery systems, texture modifiers (Jones et al., 2011). Studies have shown that  $\beta$ -LG<sub>n</sub> can be formed by thermal treatment (Jones et al., 2010; Perez et al., 2015; Guo et al., 2017).

NaAlg is an anionic biopolymer containing 1,4-linked  $\beta$ -mannuronic and  $\alpha$ -guluronic acid residues. It is one of the most biopolymeric matrices used in delivery systems because of its biodegradability, biocompatibility, structural simplicity (Alipour, Montaseri, & Tafaghodi, 2010; Chan et al., 2011).

The objective of this work was to study the influence of protein thermal treatment, pH and biopolymer ratio on the formation of the interpolymeric complexes from  $\beta$ -LG and NaAlg.

## **2. Material and Methods**

### **2.1. Materials**

Sodium alginate and  $\beta$ -lactoglobulin were obtained from Sigma-Aldrich (St. Louis, USA). Citric acid monohydrate and tribasic sodium citrate were obtained from VETEC® Ltda (Rio de Janeiro, Brazil). The water used was ultrapure with a conductivity of 0.05  $\mu$ S/cm (Master System P&D, Gehaka, Brazil).

### **2.2. Methods**

#### **2.2.1. Preparation of the solutions of $\beta$ -LG and NaAlg**

The biopolymers were weighed in an analytical balance (Shimadzu, AY220, Philippines) for the preparation of a solution containing a fixed concentration of 0.1% (w/w). The biopolymers were homogenized on magnetic stirrer (NT101, Novatecnica,



Brazil),  $\beta$ -LG was homogenized for 30 minutes at 25°C and the  $\beta$ -LG<sub>n</sub> was prepared according to Jones et al. (2010), the protein was homogenized for 15 minutes at 85°C, and the NaAlg was homogenized for 24h.

#### 2.2.2. Determination of the molecular weight of the NaAlg

The NaAlg molecular weight was determined in a previous study (Bastos, De Carvalho & Garcia-Rojas, 2018) using a viscosimetric method. The dynamic viscosity was calculated through the data obtained using Cannon-Fenske viscosimetric capillaries, (Schott-Gerate, Germany). The capillaries were immersed in a thermostatic bath (Schott-Gerate, CT-52, Germany) to control the temperature, maintained around 25°C $\pm$  0.05. The polymer solution was prepared with 0.1M NaCl, with the concentrations 0.1, 0.2, 0.3, 0.4, 0.5, 0.6 and 0.75% (Pamies et al., 2010). The solutions and solvent densities were measured in the densimeter (Anton Paar, DMA 4500M, Austria) with an autoinjector (Anton Paar, Xsample 452, Austria). The NaAlg constants  $a=0.92$  and  $K=7.3 \times 10^{-3} \text{cm}^3/\text{g}$  were used as reported by Pamies et al. (2010) and (Bastos, De Carvalho & Garcia-Rojas, 2018).

#### 2.2.3. Particle size analysis of native $\beta$ -LG and $\beta$ -LG<sub>n</sub>

The hydrodynamic diameter (d.nm) of the  $\beta$ -LG solutions at 0.1% (w/w) was determined by the Dynamic Light Scattering (DLS) technique using a Zetasizer (Malvern Instruments, Nano-ZS, UK) equipped with an He-Ne laser. The measured was performed at 25°C.

#### 2.2.4. Formation of the $\beta$ -LG/NaAlg complexes

##### 2.2.4.1. $\zeta$ -Potential

The  $\zeta$ -potentials of the biopolymers were determined using a Zetasizer Nano ZS90 (Malvern Instruments, UK). The stock solutions were transferred to an MPT-2 autotitrator (Malvern Instruments, UK). The pH was titrated using 0.5M NaOH, 0.25M HCl, and 0.025M HCl solutions. Each experiment was performed three times, and samples readings were made in triplicate at 25°C, as adapted from Bastos et al. (2018).

The strength of the electrostatic interaction (SEI) between oppositely charged polyelectrolytes can be estimated according to Yuan et al. (2017), given by equation (1):

$$\text{SEI (mV}^2\text{)} = |\text{ZP}_1| \times |\text{ZP}_2| \quad (1)$$

where  $\text{ZP}_1$  and  $\text{ZP}_2$  are the measured  $\zeta$ -potential of both proteins at each pHs.

#### 2.2.4.2. Isothermal titration calorimetry (ITC)

To perform a thermodynamic analysis by Nano-ITC equipment (TA Instruments, USA) was used. The solutions were prepared in a 10mM citrate buffer in pHs 4.0 ( $\beta$ -LG<sub>n</sub>) and 4.5 ( $\beta$ -LG) both at 25°C. The pHs were chosen according to SEI (Topic 2.2.4.1). The control was prepared by titration of  $\beta$ -LG in the buffer that was in the sample cell, and the reference cell was filled with ultrapure water. The  $\beta$ -LG solutions were prepared at 0.25mM and NaAlg solutions at  $9.37 \times 10^{-5}$ mM (pH 4.0) and  $3.75 \times 10^{-4}$ mM (pH 4.5). After dissolution of the biopolymers, the solutions were dialyzed using 3.5kDa membranes (Sigma–Aldrich, Midi 3500, USA) to equilibrate ionic strength and pHs ( $4.0$  or  $4.5 \pm 0.05$ ). The solutions were filtered ( $0.45 \mu\text{m}$ ) and degassed under vacuum using a degassing station (TA Instruments, USA). In total, 250  $\mu\text{L}$  of the titration solution ( $\beta$ -LG) was titrated in the sample cell containing the NaAlg solution at 310 rpm, an injection interval of 300 seconds and an injection volume of 10  $\mu\text{L}$ . The dilution energy was subtracted from the raw data, and the thermodynamic parameters were obtained through the program TA Nano Analyze<sup>®</sup>. The results were expressed at the significance level of 0.1.

#### 2.2.5. Characterization of the $\beta$ -LG/NaAlg complexes

The samples were frozen in an ultra-freezer (Terroni, COLD120, Brazil) at  $-40^\circ\text{C}$  for approximately 24 h. Soon after, they were placed in a bench top freeze dryer (Terroni, Enterprise I, Brazil) for drying and stored in a desiccator with silica gel until use.

##### 2.2.5.1. Fourier transform infrared spectroscopy (FT-IR)

FT-IR spectra were obtained from the  $\beta$ -LG, NaAlg and the  $\beta$ -LG/NaAlg and  $\beta$ -LG<sub>n</sub>/NaAlg complexes. The analyses were performed with an FT-IR spectrometer (Bruker, Ver-tex 70, Germany) and read in the range of 4000–400 cm<sup>-1</sup>.

#### 2.2.5.2. Differential Scanning Calorimetry (DSC)

Analysis was performed using a differential scanning calorimeter Q200 (TA Instruments, USA). An indium (In) standard was used to calibrate the energy and temperature of the equipment, and nitrogen was used as the drag gas. The lyophilized samples (~2 mg) in which the moisture content was determined were weighed in hermetic aluminum crucibles with the aid of a precision scale (Mettler Toledo, Mx5, USA). Samples were analyzed over a temperature range of 25 to 300°C at the rate of 5°C/ min, and an empty, sealed crucible was used as a reference (Bastos et al., 2018). The determination of the transition temperature at the maximum peak and the enthalpy variation were analyzed by the Universal V4.5A<sup>®</sup> software (TA Instruments, USA).

### 3. Results and discussion

#### 3.1. Molecular weight of NaAlg

In a previous study (Bastos, De Carvalho & Garcia-Rojas, 2018), the NaAlg presented 138 kDa  $\pm$  0.07 of the molecular weight. This result was in agreement with the literature. Pamies et al. (2010) and Dávila et al. (2017), obtained molecular weight values of NaAlg of 143 and 99.9 kDa, respectively. The molecular weight of the NaAlg can vary from 100 to 270 kDa (Launey et al., 1985), and depending on its origin and extraction (Phillips, 2009).

#### 3.2. Characterization of native $\beta$ -LG and $\beta$ -LG<sub>n</sub>

##### 3.2.1. Particle size

The particle size distributions of  $\beta$ -LG solutions were monitored by DLS. The intensity profiles as a function of the size (d.nm) for solutions of  $\beta$ -LG (0.1%, w/w) at pHs 4.5 ( $\beta$ -LG) and 4.0 ( $\beta$ -LG<sub>n</sub>) was showed in Figure 1. The  $\beta$ -LG and  $\beta$ -LG<sub>n</sub> presented 430nm and 6.5nm, respectively. After heated the  $\beta$ -LG, the protein aggregates

in the range of nanoparticles with sizes  $< 100\text{nm}$  at pH 4.0. The polydispersity indices (PdI) of the  $\beta\text{-LG}$  and  $\beta\text{-LG}_n$  were 0.27 and 0.24, respectively.

Ko & Sundaram Gunasekaran, (2006) produced  $\beta\text{-LG}_n$  of 59 nm by thermal treatment ( $60^\circ\text{C}/30\text{min}$ ). The study observed that small hydrophobic interactions of  $\beta\text{-LG}$  suppressed the aggregation of the molecules and then resulted in small particles. The  $\beta\text{-LG}_n$  presented stable in acidic and neutral environments. Jones et al. (2010) formulated induced the protein aggregates for the  $\beta\text{-LG}$  (0.5%w/w) by heat treatment ( $85^\circ\text{C}/15\text{min}$ ) in pH 5.8. The study demonstrated that native  $\beta\text{-LG}$  presented 400nm and after heated was 177nm. The  $\beta\text{-LG}$  after heated presented PdI was 0.15. The  $\beta\text{-LG}$  produced in present study using 0.1% (w/w) and pH 4.5, this can be contributed for the difference on the PdI when compared with Jones et al. (2010). In present study the  $\beta\text{-LG}$  and  $\beta\text{-LG}_n$  showed  $0.1 < \text{PdI} < 0.4$ , suggesting moderate polydispersity (Bhattacharjee, 2016). The PdI of the  $\beta\text{-LG}$  was decreased after thermal treatment when the pH was adjusted the 4.5 for 4.0. According to Spoton et al. (2017), the polydispersity decreased with heating time over the whole pH studied.

According to  $\zeta$ -potential analysis the pI for the  $\beta\text{-LG}$  and  $\beta\text{-LG}_n$  were 6.2 and 5.3, respectively. The behavior of the heat denatured protein can be explained according to the pH of the solution and the pI of the protein, the  $\text{pH} < \text{pI}$  can favor protein denaturation. When the pH of the protein solution was close to their pI occurs relatively weak electrostatic repulsion between the protein molecules and was formed particulate aggregates with dimensions in the 0.1 to 10  $\mu\text{m}$  range. In pH values far from its pI occurs relatively strong electrostatic repulsion between the protein molecules and was formed filamentous aggregates tend to have widths less than 50 nm (Aymard et al., 1999; Gosalet et al., 2004; Santipanichwong et al., 2008). Aggregation of native  $\beta\text{-LG}$  is completely reversed when the pH is increased or decreased away from pI. The rate of aggregation is maximum at about pH 4.6 (Majhiet et al., 2006) and is negligibly slow for pH 5.5 and higher even at  $50^\circ\text{C}$  (Mehalebi et al., 2008).

### 3.3. Complex between $\beta\text{-LG}$ and NaAlg

#### 3.3.1. Optimal pH for $\beta\text{-LG}/\text{NaAlg}$ complexes

The strength of the electrostatic interaction (SEI) between oppositely charged biopolymers can be estimated by calculating the absolute value of the product of the measured  $\zeta$ -potential of both polymers at each pHs (Espinosa-Andrews et al., 2013;

Yuan et al., 2017). Figure 2 showed the  $\zeta$ -potential and SEI of the biopolymers as function of pH. As shown in  $\zeta$ -potential-pH curves,  $\beta$ -LG and NaAlg carried opposite charges within all tested pHs, indicating that the interpolymeric complexes can be formed between the biopolymers.

In Figure 2A can be observed the  $\zeta$ -potential and SEI of the  $\beta$ -LG -NaAlg and Figure 2B, the  $\zeta$ -potential and SEI of the  $\beta$ -LG<sub>n</sub> -NaAlg was showed. In both, the NaAlg carried more negative charge and the  $\beta$ -LG presented a slight loss of the positive charge when the pH was increased. The  $\beta$ -LG/NaAlg complex can be occurs between pKa (3.4-3.7) of the NaAlg and pI of the  $\beta$ -LG (6.2) (Figure 2A) and  $\beta$ -LG<sub>n</sub>/NaAlg complex between pKa (3.4-3.7) of the NaAlg and pI of the  $\beta$ -LG<sub>n</sub> (5.3) (Figure 2B). The pH < pKa should be avoid due to the protonation of the carboxylic groups ( $-\text{CO}_2^- \rightarrow -\text{CO}_2\text{H}^+$ ) and possible aggregation of these groups (Bokkhim et al., 2015).

The SEI data showed that probability of  $\beta$ -LG/NaAlg interaction was maximum at pH around 4.5 and minimum at pH around 6.0 (Figure 2A) and with  $\beta$ -LG<sub>n</sub> was maximum at pH around 4.0 and minimum at pH around 5.0 (Figure 2B). Based this finding, the pHs of 4.5 ( $\beta$ -LG) and 4.0 ( $\beta$ -LG<sub>n</sub>) was optimized to study the binding between  $\beta$ -LG and NaAlg. Similar pHs was ideal for formation of the whey proteins (WPI) with polysaccharides:  $\beta$ -LG/pectin (Xu et al., 2015),  $\beta$ -LG/persian gum (Hadian et al., 2016),  $\beta$ -LG/gum arabic and carboxymethyl cellulose (CMC) (Hosseini et al., 2016) lactoferrin/NaAlg (Bastos et al., 2018), WPI/quince seed mucilage (Ghadermazi et al., 2019).

### 3.3.2. Isothermal Titration Calorimetry (ITC)

The thermograms of the heat flux over time (obtained from the titration of  $\beta$ -LG in NaAlg in pH 4.5 and  $\beta$ -LG<sub>n</sub> in NaAlg in pH 4.0, both at 25°C) are shown in Figure 3. According to the Figure, the titration profile was exothermic for all injections. Exothermicity is mainly related to the non specific electrostatic neutralization of the opposite charges carried by the two biopolymers demonstrating the enthalpic contribution of complex coacervation (Girard et al., 2003; Schmitt et al., 2005), while its regular decrease is attributed to a reduction in free protein molecules remaining in the reaction chamber after successive injections resulted in a reduction in the released

energy. Hosseini et al. (2013) and Hadian et al. (2016) reported exothermic sequence for  $\beta$ -LG interaction with  $\kappa$ -carrageenan and Persian gum respectively.

The binding isotherms of the  $\beta$ -LG/NaAlg complex, was characterized by one stage. Several studies have reported the same behavior when studying the interaction between proteins and polysaccharides, such as  $\beta$ -LG/Carrageenan (Hosseini et al., 2013),  $\beta$ -LG/Persian gum (Hadian et al., 2016), Lactoferrin/NaAlg (Bastos et al., 2018), Lisozyme/Carrageenan and Ovoalbumin/Carrageenan (Souza et al., 2018).

The “one binding site” model (assuming the existence of one independent binding site for each protein molecule) was used to fit binding isotherms, when study the  $\beta$ -LG and  $\beta$ -LG<sub>n</sub> on the formation of the interpolymeric complexes between NaAlg.

The thermodynamic parameters used included the reaction stoichiometry (N), binding constant (K), enthalpy ( $\Delta H$ ), change for entropy ( $T\Delta S$ ), and Gibbs free energy change ( $\Delta G$ ), which can be calculated from the equation  $\Delta G = \Delta H - T\Delta S$ , where T is the temperature in Kelvin (298.15). The parameters obtained in present study, can be observed in Table 1. The binding stoichiometry (N) with  $\beta$ -LG, was calculated to be 131.1, suggesting that NaAlg became saturated with 131.1 molecules of  $\beta$ -LG bound per molecule of NaAlg. This ratio was equivalent to a  $\beta$ -LG/NaAlg ratio of 17 (w/w), as calculated using 18.000g/mol for a  $\beta$ -LG and 138.000g/mol for NaAlg (Wolf, 1970).

The binding stoichiometry (N) with  $\beta$ -LG<sub>n</sub>, was calculated to be 555.1, suggesting that NaAlg became saturated with 555.1 molecules of  $\beta$ -LG<sub>n</sub> bound per molecule of NaAlg. The  $\beta$ -LG<sub>n</sub>/NaAlg ratio of 72(w/w), as calculated using the same molecular weights for the  $\beta$ -LG and NaAlg. The binding constant was on the order of  $10^7 M^{-1}$ , indicating a strong binding affinity between  $\beta$ -LG and NaAlg.

The  $\Delta G$  value was negative for the  $\beta$ -LG and  $\beta$ -LG<sub>n</sub> on the formation of the interpolymeric complexes between NaAlg, indicating the spontaneous nature of the interaction between  $\beta$ -LG and NaAlg. The  $\Delta H$  were negative and  $T\Delta S$  values were positive, indicating that the complexation process between the biopolymers is favorable enthalpically and favorable entropically. In  $\beta$ -LG<sub>n</sub>, the  $T\Delta S$  was higher than unheated protein, this can be explained because the after heated the hydrophobic groups was exposed indicating increased for the entropy change (Pires et al., 2009; Bou-Abdallah et al., 2012).

The electrostatic interaction is predominant, but others interactions related to hydrophobic interactions occurred. Similar result was described by (Yuan et al., 2017) when study thermodynamic parameters of soy protein and chitosan.

### 3.4. Chemical and thermal characterization of the $\beta$ -LG/NaAlg complexes

The samples were prepared using the pHs obtained by SEI and the ratios obtained by ITC (topic 3.3.2). The  $\beta$ -LG/NaAlg complex was formulated using the ratio 17:1 ( $\beta$ -LG/NaAlg) at pH 4.5 and the  $\beta$ -LG<sub>n</sub>/NaAlg complex using the ratio 72:1 ( $\beta$ -LG<sub>n</sub>/NaAlg) at pH 4.0.

#### 3.4.1. FT-IR

The FT-IR spectra of NaAlg,  $\beta$ -LG,  $\beta$ -LG/NaAlg (pH 4.5) and  $\beta$ -LG<sub>n</sub>/NaAlg (4.0) complexes are shown in Figure 4. The spectrum of the NaAlg was demonstrated in a previous study by Bastos et al, (2018). The band  $1591\text{cm}^{-1}$  representing the  $\text{CO}_2$  present in carboxylic acids salts, the band  $1404\text{cm}^{-1}$  refers to the C-O bond of the acid group, the band at  $1024\text{cm}^{-1}$  is attributed to the vibration stretch of the C-O and C-C of the pyranose ring (Booking et al., 2015).

The free amino acid O-H groups can be identified between the band 3300 and  $3170\text{cm}^{-1}$  (Barth et al., 2002). In the  $\beta$ -LG this group can be identified by the  $3270\text{cm}^{-1}$ . The band  $1634\text{cm}^{-1}$  correspond to amide I ( $1625\text{-}1750\text{cm}^{-1}$ ), and refers to the stretching of the C=O (Huang et al., 2006). The band  $1528\text{cm}^{-1}$  refers to amide II ( $1475\text{-}1575\text{cm}^{-1}$ ) and was related to the secondary structure of the protein, indicating a predominantly,  $\beta$ -sheet structure (Dong et al., 1996; Xu et al., 2019). The bands 1239 and  $1395\text{cm}^{-1}$  refers to amide III ( $1225\text{-}1425\text{cm}^{-1}$ ), and is attributed to the stretching of the C-N and N-H groups (Huang et al., 2006).

The spectrum of the  $\beta$ -LG/NaAlg complexes is a result of the contribution of both biopolymers with the bands 3270, 1634, 1528, 1395, 1239 and  $1024\text{cm}^{-1}$ . These indicated was occurs electrostatic interaction between the carboxylic groups ( $-\text{COO}$ ) of the NaAlg and the amine groups ( $-\text{NH}_3^+$ ) of  $\beta$ -LG (Bokkhing et al., 2015). In  $\beta$ -LG<sub>n</sub>/NaAlg, the bands at 1634 and  $1528\text{cm}^{-1}$  were stretched out when compared with the  $\beta$ -LG/NaAlg (Figure 4). These bands corresponding to stretching of the C=O (hydrophobic group) and  $\beta$ -sheet structure, respectively. The  $\beta$ -sheet formation in protein increases due to an increase in hydrogen bonding (Krimm & Bandekar 1986). The stretched out can be occurs due to the expose the hydrophobic groups after thermal treatment (Bhattacharjee et al., 2005; Ko & Sundaram Gunasekaran, 2006).

Studies demonstrated the formation of complex coacervation between WPI and polysaccharides using the FT-IR analysis: WPI/tamarind seed mucilage (González-Martínez et al., 2017) WPI/pectin (Raei et al., 2018), lactoferrin/NaAlg (Bokkhing et al., 2015; Bastos et al., 2018).

### 3.4.2. DSC

The thermograms of the NaAlg,  $\beta$ -LG and  $\beta$ -LG/NaAlg complex (pH 4.5) were observed in Figure 5. In Figure 5A the main endothermic events corresponding to glass transition ( $T_g$ ) of the NaAlg and the interactions of the  $\beta$ -LG/NaAlg complex and exothermic event in NaAlg at different temperatures. In Figure 5B the endothermic event corresponding to the  $\beta$ -LG denaturation.

In NaAlg was an endothermic peak at 119.8°C (Figure 5 A), similar to that found by Flynn et al. (2012) and Soares et al. (2019). Flynn et al. (2012) observed an endothermic peak at 119 °C and Soares et al. (2019) at 120.27 °C, which was suggested to correspond to the glass transition ( $T_g$ ). The exothermic peak in NaAlg was observed at 241.5°C (Figure 5A), the same was found to El-Houssiny et al. (2016). El-Houssiny et al. (2016) showed an exothermic peak at 240.99°C, which refers to the decomposition of the biopolymer. This decomposition can be resulted from the degradation of polymer due to dehydration and depolymerization reactions most probably to the partial decarboxilation of the protonated carboxylic groups and oxidation reactions of the polymer (El-Houssiny et al., 2016).

The denaturation temperature of  $\beta$ -LG was observed at 70°C (Figure 5 B), which is in agreement with Jones et al. (2010). Jones et al., 2010 found the temperature denaturation of  $\beta$ -LG at 78.3 °C. The  $\beta$ -LG/NaAlg complex was degraded at 106°C (Figure 5A), indicating that the degradation temperature of the complex was between the denaturation temperature of the  $\beta$ -LG and the  $T_g$  of the NaAlg. The higher temperature than those found for the native  $\beta$ -LG demonstrating an increasing thermal stability of the protein in  $\beta$ -LG/NaAlg complex. These can be attributed due to interactions such as hydrogen bonds, steric and electrostatic and water-biopolymer interactions (Joye, Davidov-Pardo, & McClements, 2015). The NaAlg improved the stability of the WPI by affecting in the conformation of the complex coacervates, which agrees with reports by González-Martínez et al. (2017) and Bastos et al. (2018).



González-Martínez et al., (2017), demonstrated that degradation temperature of the complexes WPI/ tamarind seed mucilage (94.95°C) and WPI/ gum arabic (98.2°C) occurs in higher temperatures than native WPI (92.95°C). In a previous study (Bastos et al., 2018), the lactoferrin denaturation was at 53°C, the T<sub>g</sub> of the NaAlg was at 120.27°C and the degradation temperature of the lactoferrin/NaAlg complex at 116.67°C.

The enthalpy of denaturation ( $\Delta H_d$ ) indicates the amount of energy needed to denature the biopolymers (Timilsena et al., 2016). The  $\Delta H_d$  of the  $\beta$ -LG and the  $\beta$ -LG/NaAlg complex were 83.57J/g and 199.6 J/g, respectively. These results indicated that degradation of  $\beta$ -LG in complex coacervate requires a higher thermal energy compared to isolated  $\beta$ -LG (Timilsena et al., 2016). The  $\Delta H_d$  value of the  $\beta$ -LG/NaAlg complex indicates that it can be used as a thermally resistant wall material, and can be used to encapsulate compounds sensitive to high temperatures. The same was observed by Jones et al. (2010) and Bastos et al. (2018).

Jones et al. (2010) showed the  $\Delta H_d$  of the  $\beta$ -LG and the  $\beta$ -LG/carrageen complex were 104.67J/g and 142.35J/g, respectively at pH 4.75. Bastos et al. (2018) showed that  $\Delta H_d$  of the lactoferrin and lactoferrin/NaAlg complex were 1.487J/g and 129.5J/g, respectively at pH 4.0.

#### **4. Conclusion**

In this study, the  $\beta$ -LG/NaAlg and  $\beta$ -LG<sub>n</sub>/NaAlg complexes interpolymeric were formed at the pHs 4.5 and 4.0, respectively. The ITC data indicated a strong binding affinity between  $\beta$ -LG and NaAlg with a favorable enthalpic and entropic contribution during their interaction. The predominance was the electrostatic interactions and the  $\beta$ -LG<sub>n</sub> presented higher hydrophobic interactions. The chemical characteristics of the complex coacervates showed changes produced by the electrostatic interaction between  $\beta$ -LG and NaAlg. The  $\beta$ -LG/NaAlg complex presented a higher thermal resistance, thus presenting its potential to be used as a wall material in the incorporation of functional ingredients sensitive to high temperatures in various food systems.

#### **Conflict of interest**

The authors declare no conflict of interest.

**Acknowledgment**

The authors thank to CNPq, FAPERJ and CAPES (Finance code 001) for financial support.

## 5. References

- Alipour, S., Montaseri, H., & Tafaghodi, M. (2010). Preparation and characterization of biodegradable paclitaxel loaded alginate microparticles for pulmonary delivery. *Colloids and Surfaces B: Biointerfaces*, 81(2), 521-529.
- Aymard, P., Nicolai, T., Durand, D., & Clark, A. (1999). Static and dynamic scattering of  $\beta$ -lactoglobulin aggregates formed after heat-induced denaturation at pH 2. *Macromolecules*, 32(8), 2542-2552.
- Barth, A. Zscherp, C. What vibrations tell about proteins, *Quarterly Reviews of Biophysics* 35 (2002) 369-430.
- Bastos, L. P. H., de Carvalho, C. W. P., & Garcia-Rojas, E. E. (2018). Formation and characterization of the complex coacervates obtained between lactoferrin and sodium alginate. *International Journal of Biological Macromolecules*, 120, 332–338.
- Bhattacharjee, C., Saha, S., Biswas, A., Kundu, M., Ghosh, L., & Das, K. P. (2005). Structural changes of  $\beta$ -lactoglobulin during thermal unfolding and refolding—an FT-IR and circular dichroism study. *The protein journal*, 24(1), 27-35.
- Bhattacharjee, S. (2016). DLS and zeta potential—what they are and what they are not? *Journal of Controlled Release*, 235, 337-351.
- Bokkhim, H., Bansal, N., Grøndahl, L., & Bhandari, B. (2015). Interactions between different forms of bovine lactoferrin and sodium alginate affect the properties of their mixtures. *Food Hydrocolloids*, 48, 38–46.
- Bou-Abdallah, F. Terpstra, T. R. The thermodynamic and binding properties of the transferrins as studied by isothermal titration calorimetry. *Biochimica et Biophysica Acta(BBA)-General Subjects* 1820 (3) (2012) 318-325.
- Bromley, E. H. C., Krebs, M. R. H., & Donald, A. M. (2006). Mechanisms of structure formation in particulate gels of  $\beta$ -lactoglobulin formed near the isoelectric point. *The European Physical Journal E*, 21(2), 145-152.
- Chan, E. S., Lim, T. K., Voo, W. P., Pogaku, R., Tey, B. T., & Zhang, Z. (2011). Effect of formulation of alginate beads on their mechanical behavior and stiffness. *Particuology*, 9(3), 228-234.
- Da Silva Soares, B., Siqueira, R. P., de Carvalho, M. G., Vicente, J., & Garcia-Rojas, E. E. (2019). Microencapsulation of Sacha Inchi Oil (*Plukenetia volubilis L.*) using Complex Coacervation: Formation and Structural Characterization. *Food Chemistry*, 125045.
- De Kruif, C. G., & Tuinier, R. (2001). Polysaccharide protein interactions. *Food hydrocolloids*, 15(4-6), 555-563.
- Dávila, J. L. d'Ávila, M. A. Laponite as a rheology modifier of alginate solutions: Physical gelation and aging evolution, *Carbohydrate polymers* 157 (2017) 1-8.

Diarrassouba, F., Garrait, G., Remondetto, G., & Subirade, M. (2017).  $\beta$ -Lactoglobulin-Based Nano and Microparticulate Systems for the Protection and Delivery of Bioactives. In *Engineering Foods for Bioactives Stability and Delivery* (pp. 199-224). Springer, New York, NY.

Dickinson, E. Interfacial structure and stability of food emulsions as affected by protein–polysaccharide interactions, *Soft Matter* 4 (2008) 932-942.

Dong, A., Matsuura, J., Allison, S. D., Chrisman, E., Manning, M. C., & Carpenter, J. F. (1996). Infrared and circular dichroism spectroscopic characterization of structural differences between  $\beta$ -lactoglobulin A and B. *Biochemistry*, 35(5), 1450-1457.

El-Houssiny, A. S., Ward, A. A., Mostafa, D. M., Abd-El-Messieh, S. L., Abdel-Nour, K. N., Darwish, M. M., & Khalil, W. A. (2016). Drug–polymer interaction between glucosamine sulfate and alginate nanoparticles: FTIR, DSC and dielectric spectroscopy studies. *Advances in Natural Sciences: Nanoscience and Nanotechnology*, 7(2), 025014.

Espinosa-Andrews, H., Enríquez-Ramírez, K. E., García-Márquez, E., Ramírez-Santiago, C., Lobato-Calleros, C., & Vernon-Carter, J. (2013). Interrelationship between the zeta potential and viscoelastic properties in coacervates complexes. *Carbohydrate polymers*, 95(1), 161-166.

Flynn, E. J., Keane, D., Holmes, J. D., & Morris, M. A. (2012). Unusual trend of increasing selectivity and decreasing flux with decreasing thickness in pervaporation separation of ethanol/water mixtures using sodium alginate blend membranes. *Journal of Colloid and Interface Science*, 370(1), 176–182.

Galani, D., & Apenten, R. K. O. (2000). Revised equilibrium thermodynamic parameters for thermal denaturation of  $\beta$ -lactoglobulin at pH 2.6. *Thermochimica Acta*, 363(1-2), 137-142.

Ghadermazi, R., Asl, A. K., & Tamjidi, F. (2019). Optimization of whey protein isolate-quince seed mucilage complex coacervation. *International journal of biological macromolecules*, 131, 368-377.

Girard, M., Turgeon, S. L., & Gauthier, S. F. (2003). Thermodynamic parameters of  $\beta$ -lactoglobulin–pectin complexes assessed by isothermal titration calorimetry. *Journal of Agricultural and Food Chemistry*, 51(15), 4450-4455.

González-Martínez, D. A., Carrillo-Navas, H., Barrera-Díaz, C. E., Martínez-Vargas, S. L., Alvarez-Ramírez, J., & Pérez-Alonso, C. (2017). Characterization of a novel complex coacervate based on whey protein isolate-tamarind seed mucilage. *Food hydrocolloids*, 72, 115-126.

Gosal, W. S., Clark, A. H., & Ross-Murphy, S. B. (2004). Fibrillar  $\beta$ -lactoglobulin gels: Part 2. Dynamic mechanical characterization of heat-set systems. *Biomacromolecules*, 5(6), 2420-2429.

Guo, X. Zhao, W. Liao, X. Hu, X. Wu, J. Wang, X. Extraction of pectin from the peels of pomelo by high-speed shearing homogenization and its characteristics, *LWT-Food Science and Technology* 79 (2017) 640-646.

Hadian, M. Hosseini, S. M. H. Farahnaky, A. Mesbahi, G. R. Yousefi, G. H. Saboury, A. A. Isothermal titration calorimetric and spectroscopic studies of  $\beta$ -lactoglobulin-water-soluble fraction of Persian gum interaction in aqueous solution, *Food Hydrocolloids* 55 (2016) 108-118.

Hoffmann, M. A., & van Mil, P. J. (1997). Heat-induced aggregation of  $\beta$ -lactoglobulin: role of the free thiol group and disulfide bonds. *Journal of Agricultural and Food Chemistry*, 45(8), 2942-2948.

Hosseini, S. M. H. Emam-Djomeh, Z. Razavi, S. H. Moosavi-Movahedi, A. A. Saboury, A. A. Atri, M. S. Van der Meeren, P.  $\beta$ -Lactoglobulin–sodium alginate interaction as affected by polysaccharide depolymerization using high intensity ultrasound, *Food hydrocolloids* 32 (2013) 235-244.

Hosseini, S. M. H., Emam-Djomeh, Z., Negahdarifar, M., Sepeidnameh, M., Razavi, S. H., & Van der Meeren, P. (2016). Polysaccharide type and concentration affect nanocomplex formation in associative mixture with  $\beta$ -lactoglobulin. *International journal of biological macromolecules*, 93, 724-730.

Huang, C.Y. Balakrishnan, G. Spiro, T. G. Protein secondary structure from deep-UV resonance Raman spectroscopy, *Journal of Raman Spectroscopy* 37 (2006) 277-282.

Houwink, R. (1940). The interrelationship between viscosimetric and osmotic identified degree of polymerization in high polymers. *Journal für praktische Chemie*, 157, 15-18.

Jones, O. G., Decker, E. A., & McClements, D. J. (2009). Formation of biopolymer particles by thermal treatment of  $\beta$ -lactoglobulin–pectin complexes. *Food Hydrocolloids*, 23(5), 1312-1321.

Jones, O. G., Decker, E. A., & McClements, D. J. (2010). Comparison of protein–polysaccharide nanoparticle fabrication methods: Impact of biopolymer complexation before or after particle formation. *Journal of Colloid and Interface Science*, 344(1), 21-29.

Jones, O. G., & McClements, D. J. (2011). Recent progress in biopolymer nanoparticle and microparticle formation by heat-treating electrostatic protein–polysaccharide complexes. *Advances in colloid and interface science*, 167(1-2), 49-62.

Davidov-Pardo, G., Joye, I. J., & McClements, D. J. (2015). Food-grade protein-based nanoparticles and microparticles for bioactive delivery: fabrication, characterization, and utilization. In *Advances in protein chemistry and structural biology* (Vol. 98, pp. 293-325).

Ko, S., & Gunasekaran, S. (2006). Preparation of sub-100-nm  $\beta$ -lactoglobulin (BLG) nanoparticles. *Journal of microencapsulation*, 23(8), 887-898.

Launey, B. Doublier, J. L. Cuvelier, G. Flow properties of aqueous solutions and dispersions of polysaccharides, in: J. R. Mitchell, D. A. Ledward, Functional Properties of Food Macromolecules, London, Elsevier, 1985, pp. 1-78.

Mark, H, in: Der feste Körper, Hirzel, Leipzig, 1938, pp. 65-104.

Mehalebi, S., Nicolai, T., & Durand, D. (2008). Light scattering study of heat-denatured globular protein aggregates. *International Journal of Biological Macromolecules*, 43(2), 129-135.

Pamies, R. Schmidt, R. R. Martínez, M. D. C. L. de la Torre, J. G. (2010). The influence of mono and divalent cations on dilute and non-dilute aqueous solutions of sodium alginate, *Carbohydrate Polymers*, 80, 248-253.

Perez, A. A., Andermatten, R. B., Rubiolo, A. C., & Santiago, L. G. (2014).  $\beta$ -Lactoglobulin heat-induced aggregates as carriers of polyunsaturated fatty acids. *Food chemistry*, 158, 66-72.

Perez, A. A., Sponton, O. E., Andermatten, R. B., Rubiolo, A. C., & Santiago, L. G. (2015). Biopolymer nanoparticles designed for polyunsaturated fatty acid vehiculization: Protein-polysaccharide ratio study. *Food chemistry*, 188, 543-550.

Phillips, O. G. Williams, P. A. (2009). Handbook of hydrocolloids, (2th), Florida, Boca Raton, pp. 902.

Pires, A.C.S, Silva, M.C.H, Silva, L.H.M. Microcalorimetry a food science and engineering approach, in: J. Coimbra, J.A. Teixeira (Eds.), Engineering Aspects of Milk and Dairy Products, CRC Press, Boca Raton, 2009, pp. 201-218.

Protte, K., Bollow, C., Sonne, A., Menéndez-Aguirre, O., Weiss, J., & Hinrichs, J. (2016). Impacts on micro- and macro-structure of thermally stabilised whey protein-pectin complexes: A fluorescence approach. *Food Biophysics*, 11(3), 226-234.

Qomarudin, Q., Orbell, J. D., Ramchandran, L., Gray, S. R., Stewart, M. B., & Vasiljevic, T. (2015). Properties of beta-lactoglobulin/alginate mixtures as a function of component ratio, pH and applied shear. *Food Research International*, 71, 23-31.

Raei, M., Rafe, A., & Shahidi, F. (2018). Rheological and structural characteristics of whey protein-pectin complex coacervates. *Journal of Food Engineering*, 228, 25-31.

Santipanichwong, R., Suphantharika, M., Weiss, J., & McClements, D. J. (2008). Core-shell biopolymer nanoparticles produced by electrostatic deposition of beet pectin onto heat-denatured  $\beta$ -lactoglobulin aggregates. *Journal of Food Science*, 73(6), N23-N30.

Schmitt, C., da Silva, T. P., Bovay, C., Rami-Shojaei, S., Frossard, P., Kolodziejczyk, E., et al. (2005). Effect of time on the interfacial and foaming properties of  $\beta$ -lactoglobulin/acacia gum electrostatic complexes and coacervates at pH 4.2. *Langmuir*, 21, 7786-7795.

Schmitt, C. Turgeon, S. L. Protein/polysaccharide complexes and coacervates in food systems. *Advances in Colloid and Interface Science* 167 (2011), 63-70.

Souza, C. J, Souza, C. S, Bastos, L. P. H, Garcia-Rojas, E. E. Interpolymer complexation of egg white proteins and carrageenan: Phase behavior, thermodynamics and rheological properties. *International journal of biological macromolecules* 109 (2018) 467-475.

Stender, E. G., Khan, S., Ipsen, R., Madsen, F., Hägglund, P., Hachem, M. A., ...& Svensson, B. (2018). Effect of alginate size, mannuronic/guluronic acid content and pH on particle size, thermodynamics and composition of complexes with  $\beta$ -lactoglobulin. *Food hydrocolloids*, 75, 157-163.

Timilsena, Y. P. Wang, B. Adhikari, R. Adhikari, B. Preparation and characterization of chia seed protein isolate–chia seed gum complex coacervates, *Food hydrocolloids* 52 (2016) 554-563.

Verheul, M., Roefs, S. P., & de Kruif, K. G. (1998). Kinetics of heat-induced aggregation of  $\beta$ -lactoglobulin. *Journal of Agricultural and Food Chemistry*, 46(3), 896-903.

Xu, A. Y., Melton, L. D., Jameson, G. B., Williams, M. A., & McGillivray, D. J. (2015). Structural mechanism of complex assemblies: characterisation of beta-lactoglobulin and pectin interactions. *Soft matter*, 11(34), 6790-6799.

Xu, H., Lu, Y., Zhang, T., Liu, K., Liu, L., He, Z., ...& Wu, X. (2019). Characterization of binding interactions of anthraquinones and bovine  $\beta$ -lactoglobulin. *Food chemistry*, 281, 28-35.

Yuan, Y., Kong, Z. Y., Sun, Y. E., Zeng, Q. Z., & Yang, X. Q. (2017). Complex coacervation of soy protein with chitosan: Constructing antioxidant microcapsule for algal oil delivery. *LWT*, 75, 171-179.

Zeeb, B., Yavuz-Düzgun, M., Dreher, J., Evert, J., Stressler, T., Fischer, L., ...& Weiss, J. (2018). Modulation of the bitterness of pea and potato proteins by a complex coacervation method. *Food & function*, 9(4), 2261-2269.

## Figure Caption

**Fig.1:** Particle size of the  $\beta$ -LG and  $\beta$ -LG<sub>n</sub> (0.1% w/w) in fixed pHs 4.5 and 4.0, respectively.

**Fig. 2:**  $\zeta$ -Potential and SEI of the  $\beta$ -LG, NaAlg and their  $\beta$ -LG/NaAlg complexes.

**Fig. 3:** (A) Heat flow thermogram ( $\mu\text{cal/s}$ ) as a function of time (s), obtained during the titration of 0.25mM  $\beta$ -LG in  $9.37 \times 10^{-5}$  mM (pH 4.5) at 25°C and graphical representation of the integral of the area under each peak (kcal/mol) as a function of the molar ratio ( $r_m$ ) of  $\beta$ -LG/NaAlg, ( $p < 0.1$ ). (B) Heat flow thermogram ( $\mu\text{cal/s}$ ) as a function of time (s), obtained during the titration of 0.25mM  $\beta$ -LG<sub>n</sub> in  $3.75 \times 10^{-4}$  mM (pH 4.0) and graphical representation of the integral of the area under each peak (kcal/mol) as a function of the molar ratio ( $r_m$ ) of  $\beta$ -LG<sub>n</sub>/NaAlg, ( $p < 0.1$ ).

**Fig. 4:** FT-IR spectra of NaAlg,  $\beta$ -LG,  $\beta$ -LG/NaAlg (pH 4.5) and  $\beta$ -LG<sub>n</sub>/NaAlg (pH 4.0).

**Fig 5:** (A) Thermogram generated by DSC analysis of  $\beta$ -LG, NaAlg and  $\beta$ -LG/NaAlg complex at pH 4.5. (B) Thermogram generated by DSC analysis of  $\beta$ -LG.



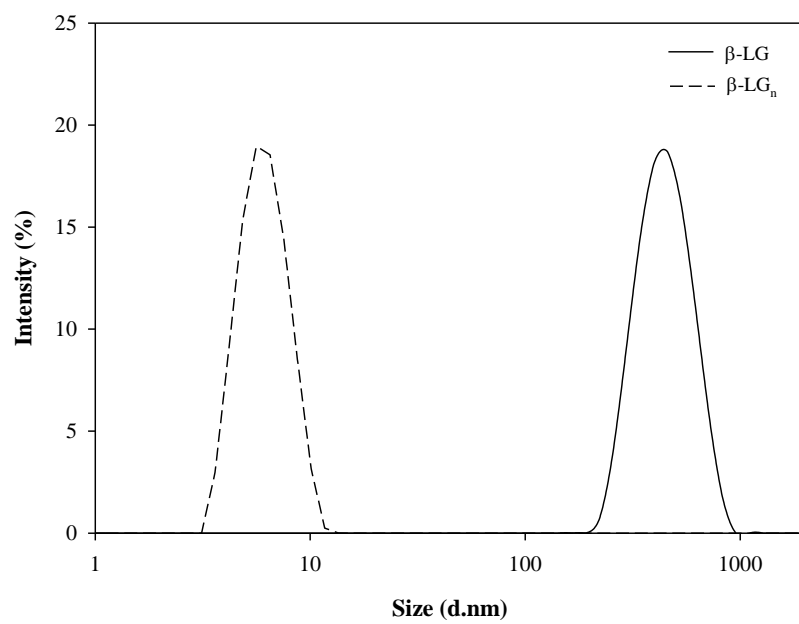


**Fig.1.**

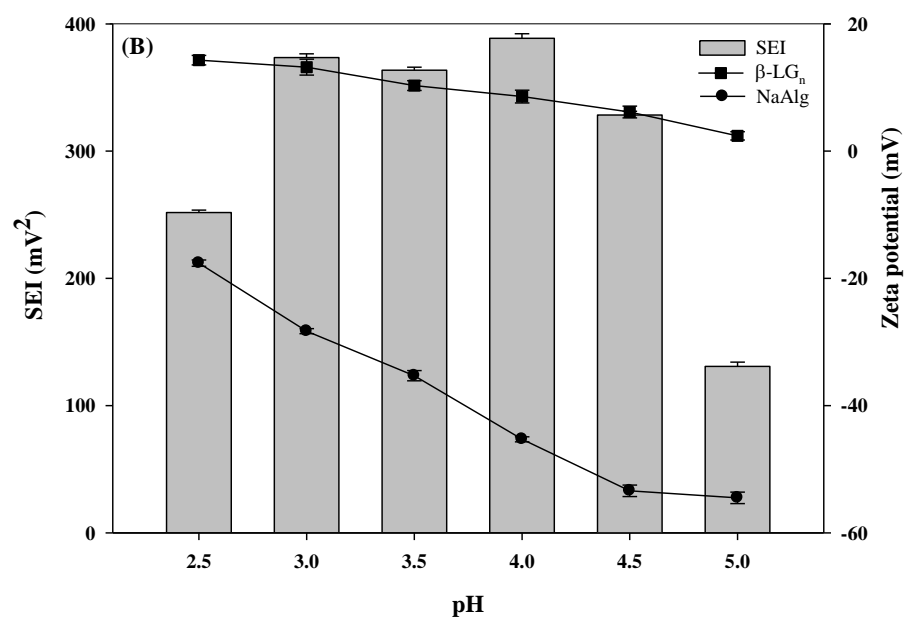
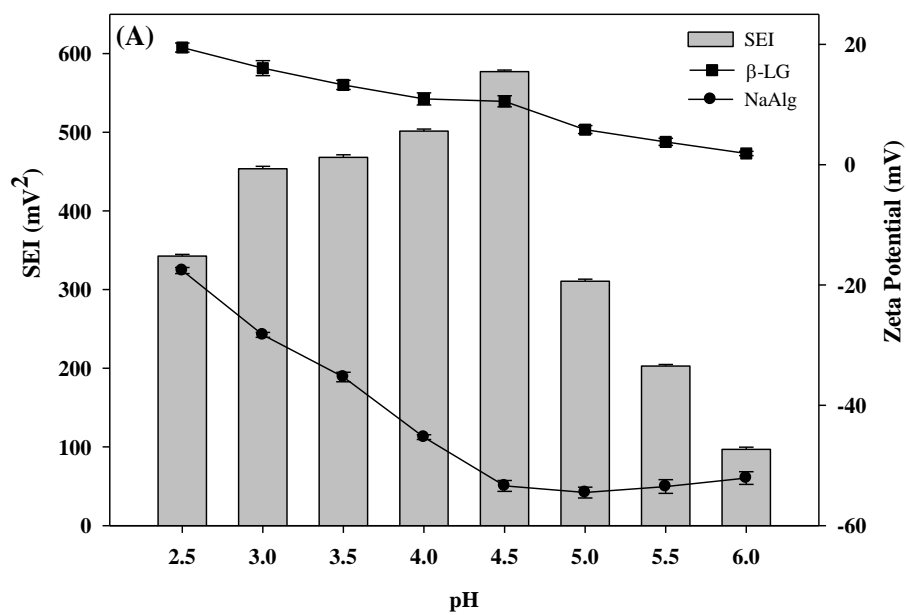
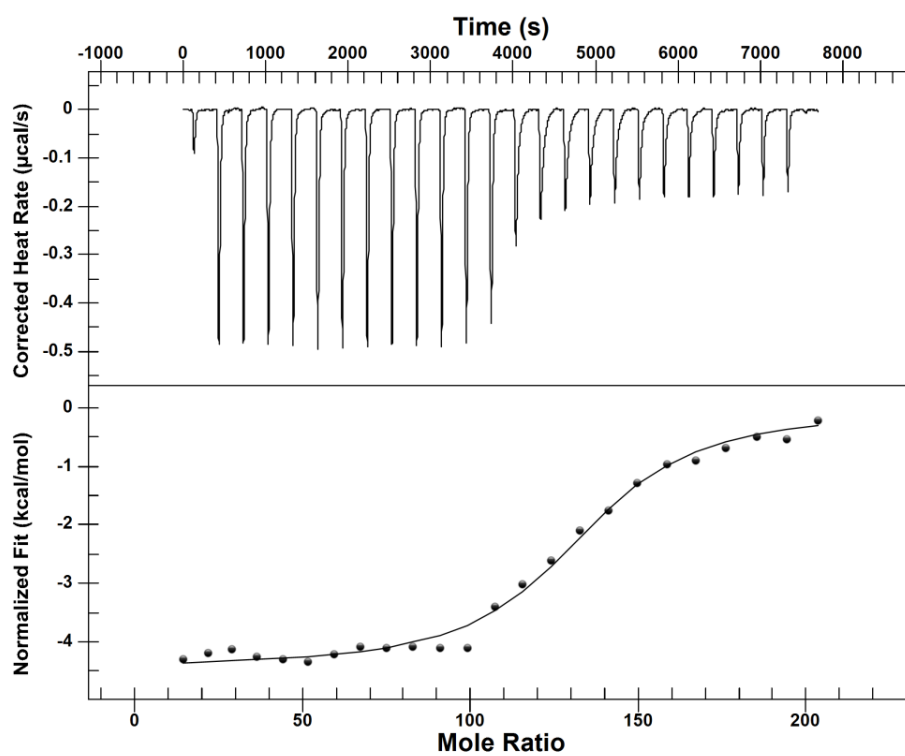


Fig. 2.

(A)



(B)

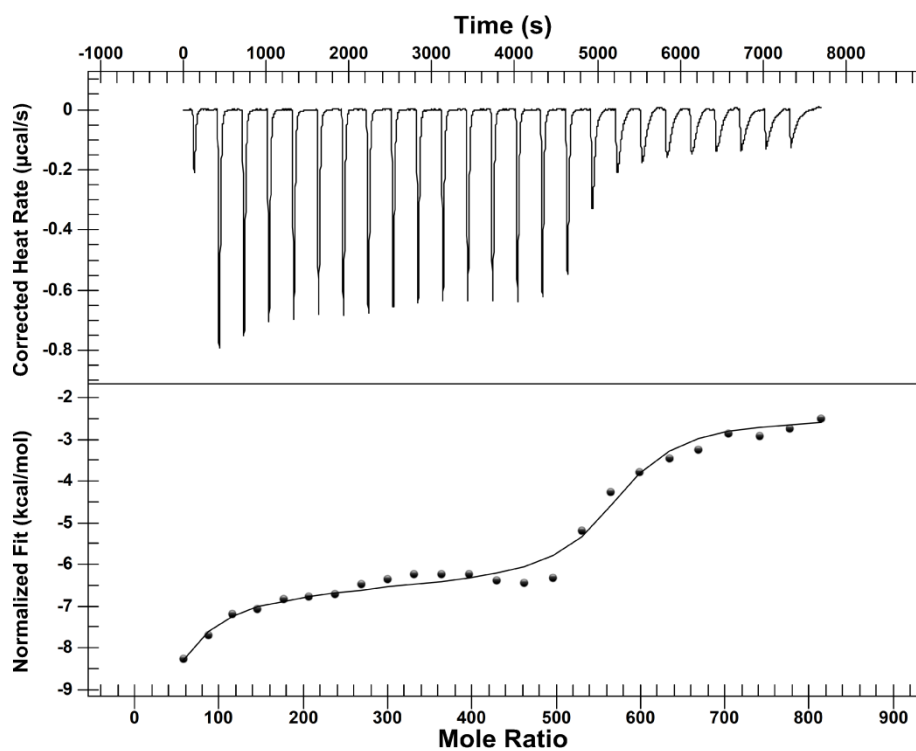


Fig.3.

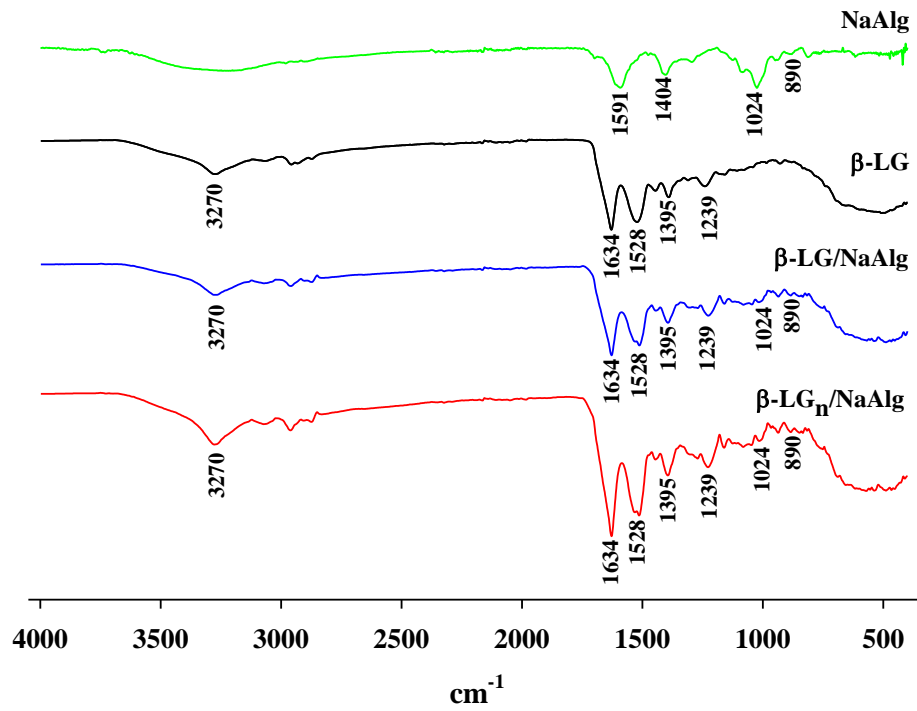


Fig.4.

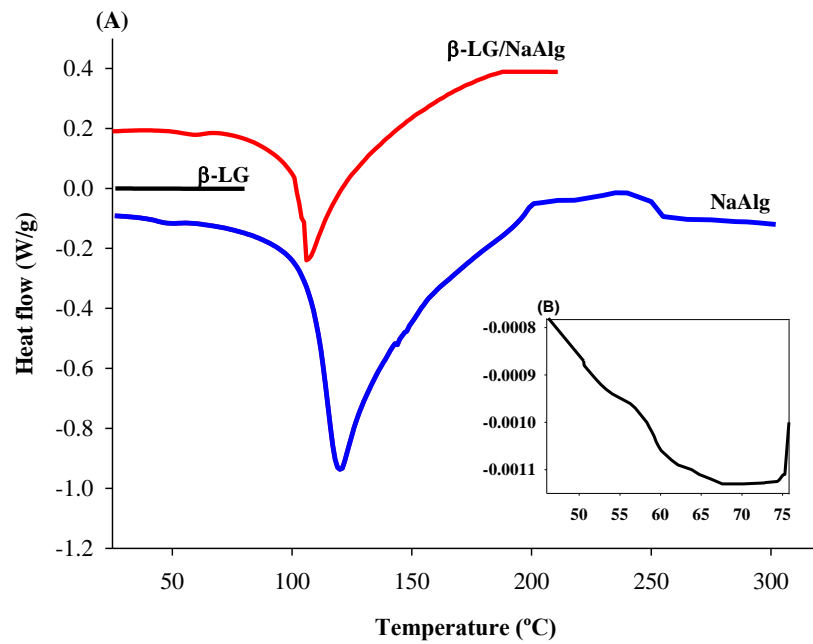


Fig. 5.

**Tabela 1.** Thermodynamic parameters of  $\beta$ -LG/NaAlg complex at pH (4.5) and  $\beta$ -LG<sub>n</sub>/NaAlg complex at pH (4.0), both in 10 mM citrate buffer were determined with the TA NanoAnalyze® software.

$\beta$ -LG /NaAlg complexes		
Thermodynamic Parameters	$\beta$ -LG	$\beta$ -LG <sub>n</sub>
K (M <sup>-1</sup> )	$8.188 \times 10^7 \pm 2.26 \times 10^7$	$2.092 \times 10^7 \pm 2.26 \times 10^7$
N (mol pr/mol ps)	$131.1 \pm 2.32$	$555.1 \pm 1.4$
$\Delta H$ (kcal/mol)	$-4.38 \pm 0.134$	$-3.67 \pm 0.74$
T $\Delta S$ (kcal/mol)	3.92	5.43
$\Delta G$ (kcal/mol)	-8.3	-9.11

**CAPÍTULO VI**  
**MICROENCAPSULATION OF BLACK PEPPER (*PIPER NIGRUM L.*)**  
**ESSENTIAL OIL WITH  $\beta$ -LACTOGLOBULIN AND SODIUM ALGINATE BY**  
**COMPLEX COACERVATION: SIMULATED GASTROINTESTINAL**  
**CONDITIONS AND MODELING THE KINETICS OF RELEASE**

## Abstract

The black pepper essential oil (EO) was encapsulated by complex coacervation with  $\beta$ -Lactoglobulin ( $\beta$ -LG) and sodium alginate (NaAlg) using transglutaminase as a cross-linking. Encapsulation efficiency varied from 20.18 to 85.01%. Chemical and morphological characteristics showed that EO was encapsulated in a  $\beta$ -LG/NaAlg shell. The particle size demonstrated that the capsules produced were in scale micro. The study of the EO release in foods stimulants showed that capsule lost lower release in water, and the Rigger-Peppas model indicated that Fickian diffusion mechanism occurred. In *in vitro* digestion simulate, the capsules demonstrated the low release of the EO during gastric digestion and higher release in intestinal digestion. The EO after digestion presented higher stability ( $84.8\% \pm 0.07$ ), and ( $31.16\% \pm 0.3$ ) of the bioaccessibility. The results obtained in the present study demonstrated that biopolymers used as wall materials shown to protect black pepper EO effectively, and the capsules can be used to transport active ingredients because they are resistant to the human oral and gastric conditions tested *in vitro*.

**Keywords:** Encapsulation efficiency, Fickian diffusion, simulated digestion, SEM, bioaccessibility.

## 1. Introduction

Black pepper (*Piper nigrum L.*) is a plant of *Piperaceae* family, is famous as the spices pungent quality and is used as flavouring agent in foods (Ahmad et al., 2012; Saha et al., 2013). The essential oil (EO) of *Piper nigrum L.* has antioxidant and antimicrobial activity (Ahmad et al., 2012; Chandran et al., 2017). EOs is aromatic volatile oily liquids obtained from plants and is rich sources of biologically active compounds such as terpenes (Bakkali et al., 2008; Dima et al., 2016). EOs are an alternative to natural preservatives in foods, but their biological potential was decrease with environments conditions (oxygen, light, high temperatures, low pH and gastrointestinal fluids). Encapsulation can prevent exposure of EOs and their degradation (Bakkali et al., 2008; Dima et al., 2016).

The microencapsulation is a process which retains an active ingredient inside another (wall material) and creates a physical barrier between the core and wall materials protecting sensitive ingredients from the external environments (Gaonkar et al., 2014). Several studies used complex coacervation for encapsulation EOs (Wang et al., 2016; Girardi et al., 2017; Raksa et al., 2017; De Matos, Scopel & Dettmer, 2018; Rojas-Moreno et al., 2018; Yuan et al., 2018). The complex coacervation process principally consists of three basic steps: emulsification, coacervation, and shell formation and/or hardening (Zhang et al., 2012). The coacervation consist in the electrostatic interaction between two polymers with opposite charges, usually a protein and polysaccharide (Schmitt & Turgeon, 2011; Nesterenko et al., 2014). Many wall material combinations of the protein and polysaccharide are used for encapsulated EOs by complex coacervation: whey protein isolate (WPI)/carboxymethylcellulose (CMC) (Koupantsis et al., 2014; Koupantsis et al., 2016), WPI/pectin (Ghasemi et al., 2017), WPI/ Sodium alginate (Rojas-Moreno et al., 2018).

$\beta$ -Lactoglobulin ( $\beta$ -LG), which represents about 60% of the proteins in bovine whey, it's a globular protein with a molecular weight of 18 kDa, and isoelectric point of  $\cong 5.1$  (Jones et al., 2010; Nicolai et al., 2011). This protein presented high stability at acidic pH and its resistance towards peptic digestion, these of  $\beta$ -LG to formulate a microcapsule wall for encapsulating oral delivery and controlled release active ingredients (Gunasekaran et al. 2007; Bhattacharjee et al., 2014).

Sodium alginate (NaAlg) is a biodegradable hydrophilic polymer, water soluble salt of alginic acid, a certainly happening non-toxic polysaccharide found in all types of



brown algae. It contains two uronic acids, 1–4 connected  $\beta$ -D-mannuronic acid and  $\alpha$ -L-guluronic and consists of homopolymeric blocks M–M or G–G (El-Houssiny et al., 2016). Alginates demonstrated resistance under oral and gastric simulated conditions, they showed to inhibit pepsin activity *in vitro* (Strugala et al., 2005; Chater et al., 2015).

Cross-linkg agents were used to obtain more resistant structures for the microcapsules produced by complex coacervation (Peng et al., 2014). Transglutaminase (TG), is a naturally enzyme, used as cross-linking agent for fabricated EOs microcapsules by complex coacervation (Xiao et al., 2014; Lv et al., 2014; Rojas-Moreno et al., 2018).

The active compounds microcapsules can be added in to food as natural additive to included biological properties (Bakkali et al., 2008). The study of the active ingredients is important for evaluating the industrial application of the encapsulated product. Studies available the encapsulated oils release in different simulated food matrices (Bustos et al., 2015; Atay et al., 2017; Cortés-Camargo et al., 2018; Rezaeinia et al., 2019). In gastrointestinal digestion, the foods are degrading to a molecular scale by the digestive enzymes (Abrahamsson et al., 2005). Studies have been investigating the digestion simulated *in vitro* of the EOs stability microcapsules (Li et al., 2018; Volić et al., 2018).

The objective of this study was encapsulate the black pepper EO by complex coacervation using  $\beta$ -LG and NaAlg as wall materials, to characterize the encapsulation efficiency, chemical and morphology structure, stability of the capsules under human gastrointestinal simulation and kinetics of release in food models.

## **2. Material and Methods**

### **2.1 Materials**

Sodium alginate,  $\beta$ -lactoglobulin,  $\alpha$ -amylase (A3403), porcine pepsin (P6887), pancreatin from porcine pancreas (P7545), porcine bile extract (B3883) was purchased from the company Sigma-Aldrich<sup>®</sup> (St. Louis, USA), Transglutaminase was acquired from the Ajinomoto (São Paulo, Brazil). Black pepper essential oil was obtained from Ferquima (São Paulo, Brazil). The reagents used were of grade P.A. and obtained from the Synth (São Paulo, Brazil) and Proquímios (Rio de Janeiro, Brazil). The water used was ultrapure with a conductivity of 0.05  $\mu$ S/cm (Master System P&D, Gehaka, Brazil).

## 2.2 Methods

### 2.2.1. Preparation of the black pepper EO microcapsules

The biopolymers were weighed in an analytical balance (B-TEC-210, Tecnal, Brazil) for the preparation of a solution containing a fixed concentration of 0.1% (w/w). The NaAlg was homogenized for 24h and the  $\beta$ -LG was homogenized for 30 minutes at 25°C using a magnetic stirrer (NT101, Novatecnica, Brazil). The microcapsules were prepared using the ratio 17:1 ( $\beta$ -LG/NaAlg) at pH 4.5, as previously defined. The  $\beta$ -LG/NaAlg microcapsules were tested using a solution with total concentration of 0.45, 0.9 and 1.8% (w/w) and different core/wall concentrations (1:1, 1:2 and 2:1). Black pepper EO added with  $\beta$ -LG solution and was emulsified with ultra-turrax (T25D, IKA, Germany) at the stirring rate of 10.000 rpm for 3 min (Lv et al., 2014). The NaAlg was added, the mixture was homogenized (NT101, Novatecnica, Brazil) and acidification at pH 4.5 with acetic acid (20%, v/v). The temperature of the suspension of the microcapsule will be reduced to 5 °C in an ice-water bath for 60 minutes (Peng et al., 2014). Transglutaminase solution (0.25% w/w) is added under magnetic stirred at 400 rpm for 3 hours at 25 °C to induce cross-linking (Lv et al., 2014). The microcapsules were kept at 10°C for 48 hours and then the supernatant was removed. Finally, the microcapsules were frozen in liquid nitrogen and freeze-dried (Enterprise I, Terroni, Brazil) for 24 hours.

### 2.2.1 Characterization of the black pepper EO microcapsules

#### 2.2.1.1. Determination of standard curve and encapsulation efficiency (EE)

The black pepper EO was dissolved and diluted with hexane (80%) and ethanol (20%) solution, and then formulated into 0.0 to 1.2 mg/mL standards solutions. The absorption with solutions standard were measured using a spectrophotometer (Biomate 3S, Thermo Fisher Scientific, USA) at 288 nm. A mixture of ethanol and hexane solution was used as a blank. The linear regression of absorption on concentration was made and the regression equation was constructed. In addition, the standard curve was drawn and its equation is  $y = 0.300x$ ,  $R^2=0.986$ .

Ten milligrams of black pepper EO microcapsules powder was weighed (B-TEC-210, Tecnal, Brazil) and 10 mL of the solvent was added (Hexane and Ethanol). The sample was put in 20°C water bath (2510, Soni-tech, Brazil) for 10 min by

ultrasonic (80 W), after the sample was incubated in the shaker (TE-424, Tecnal, Brazil) for 2 hours at 25°C. The sample was homogenized on a Vortex (AP 56, Phoenix, Brazil) and centrifuged (Digicen 21 R, OrtoAlresa, Spain) at 8000 rpm for 15 min, adapted from Li et al. (2018). The supernatant phase was collected, to enable measurement (Biomate 3S, Thermo Fisher Scientific, USA) of its absorption as well as calculating its content. The microcapsule EE is the significant indicator to appraise the quality of the prepared microcapsule products. The oil mass was measured, and theoretical oil value ( $OT\%$ ) was given by equation (1) and the loaded oil content ( $OC\%$ ) was given by equation (2).

$$OT(\%) = \frac{W_{oil}}{W_{ic}} \times 100 \quad (1)$$

$$OC(\%) = \frac{W_{foil}}{W_{fc}} \times 100 \quad (2)$$

where  $W_{oil}$  is the initial mass of oil added in the system,  $W_{ic}$  is the initial mass of the capsule and  $W_{foil}$  is the oil content after encapsulation and  $W_{fc}$  final capsule mass after freeze-dried. The EE is the percentage of loaded oil content divided by the percentage of theoretical oil (Timilsena et al., 2016), given by equation (3).

$$EE(\%) = \frac{OC(\%)}{OT(\%)} \times 100 \quad (3)$$

#### 2.2.1.2. Fourier transform infrared spectroscopy (FT-IR)

The FT-IR spectra of the dried samples ( $\beta$ -LG, NaAlg, EO and the microcapsule) were obtained. The analyses were performed with an FT-IR spectrometer (Ver-tex 70, Bruker, Germany) read in the range of 4000–400  $\text{cm}^{-1}$ .

#### 2.2.1.3. Particle size

The hydrodynamic diameter (d.nm) of the biopolymers and the black pepper EO microcapsule were determined at fixed pH by the Dynamic Light Scattering (DLS) technique using a Zetasizer (Malvern Instruments, Nano-ZS, UK) equipped with an He-Ne laser.

#### 2.2.1.4. Release kinetics of the black pepper EO in food stimulants

Kinetic release was performed according to Atay et al. (2017) and Rezaeinia et al. (2019), 17mg of the samples were weight in an analytical balance (B-TEC-210, Tecnal, Brazil) and added to 10mL for the foods solutions stimulants. Aliquots of the 120 $\mu$ L was collected and were analyzed by spectrophotometer (Biomate 3S, Thermo Fisher Scientific, USA) at 288 nm. To explain the black pepper (*piper nigrum L.*) EO release profile, the release kinetics in food models were fitted to Higuchi, First-Order, Zero-Order, and Rigger-Peppas empirical models (Dash et al., 2010; Rezaeinia et al., 2019). The release kinetics of the EO were simulated in aqueous (distilled water), acidic (3% acetic acid), alcoholic or alkali (10% ethanol) and oily (50% ethanol) food models according to the EU Commission regulation 10/2011 EU (10/2011/EC).

#### 2.2.1.5. Optical microscopy

An aliquot of the microcapsule (sample-S4) was placed between the lamina and cover-slip and taken to the optical microscope (K220, Kasvi, Brazil) coupled to an Moticam camera (5MP, Kasvi, Brazil) that was viewed at 100 $\times$  magnification with immersion oil.

#### 2.2.1.6. Scanning Electron Microscopy (SEM)

Micrograph of the black pepper microcapsule dried and after oral, gastric and intestinal simulated were obtained (500x) with a scanning electron microscope TM3000 (Hitachi, Japan) equipped with a tungsten filament and operated in secondary electron mode at an acceleration voltage of 15 Kv.

### 2.2.2 *In vitro* digestion

*In vitro* digestion was simulated in three stages: oral, gastric and intestinal (Minekus et al., 2014 and Timilsena et al., 2017). Simulated oral, gastric and intestinal digestions were prepared according to Minekus et al., 2014.

#### 2.2.1.7. Simulated oral digestion

Briefly, 0.33g of the microcapsule lyophilized was weighed in an analytical balance (B-TEC-210, Tecnal, Brazil), and then mixed with 0.7mL pre-warmed of simulated salivary fluid (SSF) containing 0.1mL salivary  $\alpha$ -amylase (75 U/mL in final oral solution), the mixture was added followed by 5 $\mu$ L of 0.3 M CaCl<sub>2</sub> and 195 $\mu$ L of water. The pH of the mixture was adjusted to 7.0 with pHmeter (mPA210, Tecnozon, Brazil) and stirred at 95 rpm for 2 minutes at 37°C using the shaking (TE-424, Tecnal, Brazil).

#### 2.2.1.8. Simulated gastric digestion

After mouth digestion, 1.5mL pre-warmed of simulated gastric fluid (SGF) was added to the oral digested mixture with 0.32 mL of the pepsin (2.000U/mL in final gastric solution), the mixture was added followed by 1 $\mu$ L of 0.3 M CaCl<sub>2</sub>, 40 $\mu$ L of 1M HCl and 139 $\mu$ L of water. The pH of the mixture was adjusted to 3.0 with pHmeter (mPA210, Tecnozon, Brazil) and stirred at 95 rpm for 2 h at 37°C using the shaking (TE-424, Tecnal, Brazil).

#### 2.2.1.9. Simulated intestinal digestion

After the completion of gastric digestion, 2.2mL pre-warmed of simulated intestinal fluid (SIF) was added into the mixture with 1mL of the pancreatin (100U/mL in final intestinal volume) and 0.5mL of the bile extract solution (10mM). The mixture was added followed by 8 $\mu$ L of 0.3 M CaCl<sub>2</sub>, 30 $\mu$ L of 1M NaOH and 262 $\mu$ L of water. The pH of the mixture was adjusted to 7.0 with pHmeter (mPA210, Tecnozon, Brazil) and stirred at 95 rpm for 2 h at 37°C using the shaking (TE-424, Tecnal, Brazil).

Aliquots (120µL) of gastric and intestinal juice were taken at 0, 15, 30, 60 and 120 minutes. After withdrawal of each aliquot, 120 µL of gastric or intestinal juice was added to continue the digestion process. The quantity of EO released was calculated from the absorbance according to section (2.2.2.1).

### 2.2.3 Stability and bioaccessibility of the black pepper EO

The stability and bioaccessibility of EO after digestion were measured according to a method described previously (Zhang et al., 2016). The stability ( $S^*$ ) of EO was defined as the fraction that remained in a non-transformed state in the small intestine after *in vitro* digestion model, given by equation (4).

$$S^* = \frac{C_{\text{Digesta}}}{C_{\text{Initial}}} \times 100 \quad (4)$$

where  $C_{\text{Digesta}}$  and  $C_{\text{Initial}}$  are the black pepper EO concentrations in the total digesta collected after the small intestine phase and in the initial samples, respectively. The bioaccessibility ( $B^*$ ) of the black pepper EO, was defined as the fraction that was released from the food matrix and solubilized in the mixed micelle phase after digestion, given by equation (5).

$$B^* = \frac{C_{\text{Micelle}}}{C_{\text{Digesta}}} \times 100 \quad (5)$$

where  $C_{\text{Micelle}}$  is the black pepper EO concentration in the micelle fraction. The effective bioaccessibility (EB), which depends on the values of  $S^*$  and  $B^*$ , given by equation (6).

$$EB = B^* \times S^* = \frac{C_{\text{Micelle}}}{C_{\text{Initial}}} \times 100 \quad (6)$$

#### 2.2.4 Statistical analysis

All experimental measurements were conducted in triplicate, and the data are expressed as the mean  $\pm$  standard deviation. The statistical analyses were performed using Origin<sup>®</sup> Pro 9.0. The Kolmogorov-Smirnov normality test was performed for the populations. After confirming normality for all populations, one-way variance (ANOVA) was performed to determine the existence of significant difference between populations. Significant differences at a level of significance  $\alpha = 0.05$  were identified by Tukey's test.

### 3. Results and Discussion

#### 3.2. Characterization of the microcapsules

##### 3.2.1. Encapsulation Efficiency (EE)

In Table 1 was showed the composition of the formulations and the EE of the microcapsules produced by complex coacervation. The theoretical oil value, oil content and EE (equation 3) of microcapsules prepared with different samples were presented. The theoretical oil values was that 33.33, 50 and 66.66%. Loaded oil content varied from 6.72 (S3) to 56.6 (S4). EE varied from 20.18 (S3) to 85.01 (S4). The core material was black pepper EO and wall material weight was the biopolymers and transglutaminase using as cross-linking agent.

As shown in Table 1, the samples S4 and S7 presented a high (EE %) with no significant difference ( $p < 0.05$ ) between them, with EE  $85.01 \pm 0.26$  and  $83.1 \pm 0.49$ , respectively. These samples presented were formulated with 2:1 (core/wall ratio), the sample S1 was prepared in the same condition but differed significant of EE ( $28.62 \pm 1.9$ ) from the others (S4 and S7) with the same core/wall ratio. This can be explained because the S1 was formulated with the less biopolymers and EO concentration than S4 and S7. The biopolymers percentage between S4 (0.9) and S7 (1.8) not contributed to cause significant difference in EE the samples, but the lower percentage of the biopolymers in S1 (0.45) can be contributed. The hypothesis that in S1 was insufficient amount of wall materials available to cover the entire core, resulting in a high free core concentration, high amount of core that was not encapsulated and hence was lost during the encapsulation process. Regarding samples S4 and S7, they showed high EE, which

can be explained by the higher concentrations of wall material. Thus, these concentrations were sufficient to cover a greater amount of EO and maintained these imprisoned inside the capsule and does not lose functionality. The same results were observed by Wang et al. (2016) and Da cruz et al.(2019).

Wang et al. (2016), observed that higher concentration of ginger EO (core material), reduced the EE of the capsules using the 2:1 core/wall ratio with gelatin and sodium alginate as wall materials. Da Cruz et al. (2019) encapsulated acid ascorbic using gelatin and gum arabic by complex coacervation, the study observed that samples with wall:core ratios of 1:05 and 1:0.75 with 2.5g (w/w) of wall concentration, the increase in core percentage led to a lower encapsulation efficiency.

The samples S3, S6 and S9 were formulated using 1:2 (core/wall ratio) but they presented significant difference in EE. The EE were  $20.18 \pm 0.18$  (S3),  $24.4 \pm 1.21$  (S6) and  $40.42 \pm 1.2$  (S9). The higher EE in S9 compared with the others samples can be attributed to the higher concentration of the biopolymers (1.8%) and the core. The sample S8 and S9 not presented significant difference in EE, and S8 was  $41.91 \pm 2.17$  in this value. The samples with 1.8% of biopolymers concentrations were the best results in EE compared with the others samples. The S3 using the lower core was study, these can be influenced for the lower EE.

The samples S2 and S5, don't presented significant difference in EE ( $p < 0.05$ ) between them, the EE were  $22.85 \pm 0.8$  and  $21.21 \pm 1.02$ , respectively. These samples were formulated using 1:1 (core/wall ratio) and presented lower EE when compared with the S8 using the same ratio. S8 presented higher EE in comparison with the others samples and was formulated with higher biopolymers concentrations and core, these influenced in the difference between the EE.

### 3.2.2. Chemical characteristics

In Figure 1, shows the FT-IR spectra of the NaAlg,  $\beta$ -LG, black pepper EO and the microcapsule (S4) at pH 4.5. The spectrum of the NaAlg was demonstrated in a previous study by Bastos et al, (2018). The band  $1591\text{cm}^{-1}$  representing the  $\text{CO}_2^-$  present in carboxylic acids salts ( $\text{RCOO}^-$ ), the band  $1404\text{cm}^{-1}$  was attributed to the C-O bond of the acid group ( $\text{RCOOH}$ ), the band at  $1024\text{cm}^{-1}$  is attributed to the vibration stretch of the C-O and C-C of the pyranose ring (Booking et al., 2015).



In  $\beta$ -LG spectrum was identified the free amino acid O-H groups in bands  $3270\text{cm}^{-1}$  (Wang et al., 2016), these group can be represented between the bands  $3300$  and  $3170\text{cm}^{-1}$  (Barth et al., 2002). The band  $1634\text{cm}^{-1}$  correspond to amide I ( $1625$ - $1750\text{cm}^{-1}$ ), and refers to the stretching of the C=O (Chanphai et al., 2017). The band  $1528\text{cm}^{-1}$  refers to amide II ( $1475$ - $1575\text{cm}^{-1}$ ) and was related to the secondary structure of the protein, indicating a predominantly,  $\beta$ -sheet structure (Dong et al., 1996; Xu et al., 2019). The bands  $1239$  and  $1395\text{cm}^{-1}$  refers to amide III ( $1225$ - $1425\text{cm}^{-1}$ ), and is attributed to the stretching of the C-N and N-H groups (Huang et al., 2006).

In the spectrum of the black pepper EO the band  $2922\text{cm}^{-1}$  was attributed to CH stretching vibration (Raksa et al., 2017), the band  $2868\text{cm}^{-1}$  refers to vibration of the aliphatic C-H in  $\text{CH}_2$  (Alizadeh-Sani et al., 2018), the band  $1643\text{cm}^{-1}$  was attributed to C=C stretching (Alizadeh-Sani et al., 2018), the band  $1446\text{cm}^{-1}$  correspond to C-OH absorption bending vibration (Volić et al., 2018), the band  $1381\text{cm}^{-1}$  to  $\text{CH}_3$  bending (Alizadeh-Sani et al., 2018), the band  $886\text{cm}^{-1}$  refers to assigned to the bending vibrations in  $=\text{CH}_2$  (Li et al., 2018) and the band  $786\text{cm}^{-1}$  was attributed to assigned to benzene rings  $=\text{CH}$  vibration absorption (Raksa et al., 2017).

The black pepper EO microcapsule is a result of the contribution of both biopolymers and the EO. The bands  $3270$ ,  $1634$  and  $1528\text{cm}^{-1}$  were bands characteristic to the  $\beta$ -LG, the bands  $1404$  and  $1024\text{cm}^{-1}$  were bands presented in NaAlg, and the bands  $2868$  and  $886\text{cm}^{-1}$  were bands identified in black pepper EO.

### 3.2.3. Particle size

The particle size distributions of  $\beta$ -LG, NaAlg solutions (0.1% w/w), and the black pepper EO microcapsule (ME) were monitored by DLS. The intensity profiles as a function of the size (d.nm) for solutions at pHs 4.5 were demonstrated in Figure 2. The  $\beta$ -LG, NaAlg and black pepper EO microcapsule (ME) presented 430, 1.718 and 4.800nm, respectively. The capsule produced was in scale micro, when particles of size ranging from 1 to  $1000\mu\text{m}$  ( $1 \times 10^6$  nm) (Ye et al., 2018). Others studies was prepared EOs microcapsules by complex coacervation (Peng et al., 2014; Rojas-Moreno et al., 2018). Peng et al. (2014) formulated Mustard (*Sinapis alba*) EO microcapsule using gelatin and gum arabic as wall material, and genipin as cross-linkg agent, with  $10\mu\text{m}$ .

Rojas-Moreno et al (2018) produced orange EO microcapsule using WPI and different polysaccharides and cross-linkg agents, with the range of the 10-20 $\mu$ m.

#### 3.2.4. Release of the EO in foods stimulants

Figure 3 showed the release profile of the black pepper microcapsules (sample S4, because it exhibited the best EE) at different foods stimulants. This Figure the results show the lower release of the EO was obtained in water, acid acetic (3%), ethanol (10%) and ethanol (50%) foods stimulants, respectively. In all the foods stimulants the EO release increased until a certain point in which it reduced and remained constant. The microcapsules that remained in contact with water showed the higher EO release (24.75%) at 12 minutes, when observed the sample in contact with acid acetic (3%), the higher EO release was 36.98% at 18 minutes, and with ethanol (10%) the EO release was higher (41.96 %) at 18 minutes and for ethanol (50%) the higher EO release (45.28%) at 12 minutes.

The study of the release profile of an active ingredient is important to understand its behavior and the mechanism by which release occurs. Tests carried out under specific conditions can provide useful information, especially regarding the food matrices this active material can be incorporated (Da cruz et al., 2019). The results of the present study demonstrated that black pepper EO microcapsules were better preserved in aqueous and acidic foods.

To determine the mechanism of release of black pepper EO from  $\beta$ -LG/NaAlg microcapsule, the release profile within various food model systems was fitted with different kinetic equations. Higuchi, First-Order, Zero-Order, and Rigger-Peppas models were used to evaluate the release behavior of the EO. The constants and the coefficient of determination ( $R^2$ ) of each model are shown in Table 2. Concerning the  $R^2$  values, the Rigger-Peppas was appropriate model for explaining the release kinetics of the EO with an  $R^2$  over 0.99.

In Peppas model, the values of n indicate the following release mechanisms: for  $n \leq 0.43$ , the dominant release mechanism is the Fickian diffusion (case I transport);  $0.43 \leq n < 0.85$  indicates the diffusion and the swelling release mechanism (non Fickian or anomalous transport) and  $n \geq 0.85$  corresponds to zero order release kinetics (case II transport) (Ritger; Peppas 1987; Maderuelo et al., 2011; Dima et al., 2016). In the

present study for all foods stimulants the  $n < 0.43$ , this is within what is expected for the controlled release from spherical particles (Ritger; Peppas 1987) that follow predominantly a Fickian diffusion mechanism (Dima et al., 2016). Diffusion is the dominant flavor release mechanism from the capsule, a diffusion-controlled release process caused by the poor swelling degree and by the presence of oil drops at the surface or in the exterior layer of microcapsules (Dima et al., 2016). In diffusion the active ingredient diffuses through the particle matrix and into the surrounding medium. The particle matrix may remain intact throughout this process or its properties may change (erosion, fragmentation, or dissolution). The release rate of an active ingredient from the particles depends on its relative solubility in the particle matrix and surrounding liquid and on its diffusion coefficient through the matrix (McClements et al., 2015). Bustos et al. (2015) and Rezaeinia et al. (2019) observed Fickian diffusion mechanism using Peppas models in lemongrass oil and *Mentha longifolia L.* EO capsules when studies then in foods stimulants.

### 3.3. Gastrointestinal *in vitro* simulated

The extent of oil release from the black pepper EO capsule (S4) at different time intervals in gastric and intestinal environments is shown in Figure 4. The sample was submitted in oral condition simulated for 2 minutes. The hypothesis was, the slight release can be occurred because at pH 7.0 (oral digestion). In this pH the charges of the biopolymers were negative and don't formed complex coacervation, the electrostatic interaction was repulsive and the microcapsule was fragile (Jones et al., 2010; Nicolai et al., 2011; Bastos et al., 2018).

During exposure to gastric conditions (2 hours), the initial black pepper EO loads released about 28.7%, but the higher release of the EO (32.7%) occurs at 15 minutes. After this time the EO release was reducing at 120 minutes. The capsule protects the release of the initial EO load during gastric conditions, and 67.3% of the EO was preserved. Protein digestion is initiated in the stomach by pepsin (Tomé & Debabbi, 1998), but in the microcapsule was not totally ruptured. This can be explained because the  $\beta$ -LG was resistance to peptic digestion (Bhattacharjee et al., 2014), and the NaAlg protect the disintegrated of the  $\beta$ -LG in  $\beta$ -LG/NaAlg complex microcapsule. Alginates have previously been shown to inhibit pepsin activity *in vitro* (Sunderland et

al., 2000; Strugala et al., 2005; Chater et al., 2015). Sunderland et al. (2000) showed alginates could inhibit pepsin activity by 52% *in vitro*. Strugala et al. (2005) showed significant correlations between alginate structure and levels of inhibition, with high frequency of mannuronic acid residues alginates tending to inhibit better than those high in guluronic acid residues. However the mechanism of pepsin inhibition is poorly understood. Wang et al. (2017) observed the protect effect of the NaAlg in Lf on the Lf/NaAlg complex. In pH 3.0 (gastric conditions), electrostatic interaction between  $\beta$ -LG and NaAlg is favorable because in this pH the biopolymers charge were oppositely. However this pH is below the pKa of the NaAlg and is possible aggregation of the carboxylic groups (Bokking et al., 2015).

The release of the EO at intestinal stage was found to be faster compared to that gastric stage. In 2 hours of intestinal digestion the release EO was increased in function of the time, the initial black pepper EO loads released about 86% and the higher release occurs at approximately 150 minutes (90.5%). In this stage occurred the rupture the capsule and only 9.5% of the EO was preserved. In this case the NaAlg not protect the  $\beta$ -LG in  $\beta$ -LG/NaAlg complex microcapsule because this polysaccharide cannot survive from trypsin attack (Chater et al., 2015). The catalytic mechanisms of pepsin and trypsin are distinct, it is therefore possible that alginate is able to interact with and disrupt the catalytic mechanism of pepsin, but not of trypsin (Powers, Harley, & Myers, 1977). Pepsins are preference for cleavage of the hydrophobic amino acids (Powers, Harley, & Myers, 1977), and trypsin preferentially cleaves within the polypeptide chain, and cleaving on the carboxyl side of lysine and arginine (Hedstrom, 2002; Chater et al., 2015). Due to neutral pH (7.0) of intestine, the protective coatings are destroyed and the capsule was degraded that resulted in the sustained release of EO from capsules in stimulated intestinal fluids. The results of this study showed that  $\beta$ -LG and NaAlg effectively prevent the release of EO in oral and gastric conditions which minimizing the chemical degradation of EO in gut environment. These results are in agreement with the others studies with EOs microcapsules (Li et al., 2018; Vólic et al., 2018).

### 3.4. Stability and bioaccessibility of the black pepper EO

The results obtained for stability (S\*), bioaccessibility (B\*) and effective bioaccessibility (EB) of the EO after digestion were 84.8%  $\pm$  0.07, 31.16%  $\pm$  0.3, 26.42%  $\pm$  0.26, respectively.

The EO presented higher stability after digestion, and the *in vitro* bioaccessibility was appreciably higher (31.16%). The bioaccessibility of active ingredients are caused by both environmental conditions (pH, heat, light, oxygen) and physiological conditions in the gastrointestinal tract (pH, enzymes, intestinal mucus barrier). Therefore, delivery systems are needed for protecting these compounds to safely reach the small intestine where they are mostly absorbed (Bao et al., 2019). The similar result was observed by Yao et al. (2017) when study the curcumin-loaded zein nanoparticles, the *in vitro* bioaccessibility of curcumin was 22.4%. Ilyasoglu et al. (2014) found 36.25% of the bioaccessibility for the fish oil with docosahexaenoic (DHA) acid capsules produced by complex coacervation. The lower bioaccessibility was observed by Da Silva Stefani et al. (2018) when found 12.80 % for the linseed oil capsules. Both studies observed the capsules after *in vitro* digestion.

Recent study carried out Papillo et al. (2019), demonstrated that the curcuminoids encapsulated with cellulose derivates and vegetable oil and provided in a carbohydrate-based food (i.e. bread), 6% and 9% of the bioaccessibility, respectively, compared to the non-encapsulated ones (1.3%). Other study, astaxanthin-containing lipid extract from shrimp waste was encapsulated by spray drying, the maltodextrin and gum arabic, separately or mixed, were employed as encapsulating matrices. The capsule formulated using gum arabic demonstrated higher bioaccessibility ( $\cong$ 50%) (Montero et al., 2016).

### 3.5. Morphology

The wet microcapsule as seen by optical microscopy (Figure 5), a spherical and intact shape can be observed. The same result was showed to Manaf et al. (2018) and Yuan et al. (2018) when encapsulated EOs by complex coacervation. Manaf et al. (2018) formulated the citronella EO using gelatin and gum arabic as wall material and Yuan et al. (2018) produced shiitake (*Lentinula edodes*) EO using gelatin and CMC as wall materials.

The dried microcapsules before and after oral, gastric and intestinal phases were seen by SEM (Figure 6). In microcapsule before gastrointestinal simulated, the three-dimensional network and sponge-like structure was observed (Figure 6A), this are particularly of the capsule and the freeze dried process. The same was observed by Rojas-Moreno et al. (2018) when demonstrated orange EO microcapsules using WPI and NaAlg as wall materials. After oral the structure of the microcapsule (Figure 6B) was affected but this not disintegrated, probably because the short exposure to oral enzyme. After gastric digestion, low difference was observed; the structure maintained intact confirming the lower release con concentration off the EO in this stage (Figure 6C). The higher structure modification was observed in microcapsule after intestinal digestion, the enzymatic and shear force erode the shell matrix and disintegrated some particles and release the encapsulated EO (Figure 6D). Timilsena et al. (2017), observed that opposite, in the chia seed oil microcapsule prepared with chia protein isolate and chia seed gum as wall materials. The study observed that microcapsules were disintegrated during gastric digestion. The microcapsules produced by Timilsena et al. (2017) can be used for transport active ingredients were absorption in stomach and the microcapsules produced for the present study were preserved during this stage and was release in higher concentrations in intestinal digestion, suggesting that can be delivery lipophilic actives to absorption in the intestine.

#### **4. Conclusion**

Black pepper EO microcapsules produced by complex coacervation using  $\beta$ -LG and NaAlg as wall materials, and transglutaminase as cross-linking agent have a good encapsulation efficiency. The EO capsule obtained was in scale micro. The encapsulated black pepper EO was confirmed by the chemical and morphological characteristics. The EO release in foods stimulants was lower in aqueous stimulant, and the Rigger-Peppas model demonstrated that Fickian diffusion mechanism was occurs. The black pepper EO capsule demonstrated resistance under oral and gastric conditions and release in the intestine contributing to your absorption. The EO after digestion presented higher stability, and acceptable bioaccessibility. The  $\beta$ -LG and NaAlg showed potential used as wall materials in encapsulated black pepper EO by

complex coacervation, and can be used to transport active ingredients because they are resistant to the human oral and gastric *in vitro* simulate.

**Conflict of interest**

The authors declare no conflict of interest.

**Acknowledgment**

The authors thank to CNPq, FAPERJ and CAPES (Finance code 001) for financial support.

## 5. References

- Abrahamsson, B., Pal, A., Sjöberg, M., Carlsson, M., Laurell, E., Brasseur, J. G. (2005). A novel in vitro and numerical analysis of shear-induced drug release from extended release tablets in the fed stomach. *Pharmaceutical Research*, 22, 1215–1226.
- Ahmad, N., Fazal, H., Abbasi, B. H., Farooq, S., Ali, M., & Khan, M. A. (2012). Biological role of *Piper nigrum* L.(Black pepper): A review. *Asian Pacific Journal of Tropical Biomedicine*, 2(3), 1945-1953.
- Alizadeh-Sani, M., Khezerlou, A., &Ehsani, A. (2018).Fabrication and characterization of the bionanocomposite film based on whey protein biopolymer loaded with TiO<sub>2</sub> nanoparticles, cellulose nanofibers and rosemary essential oil. *Industrial crops and products*, 124, 300-315.
- Atay, E.,Fabra, M. J., Martínez-Sanz, M., Gomez-Mascaraque, L. G., Altan, A., & Lopez-Rubio, A. (2018). Development and characterization of chitosan/gelatin electrosprayedmicroparticles as food grade delivery vehicles for anthocyanin extracts. *Food Hydrocolloids*, 77, 699-710.
- Bakkali, F., Averbeck, S., Averbeck, D., Idaomar, M. (2008).Biological effects of essential oils – a review.*Food and Chemical Toxicology*, 46, 446–475.
- Bao, C., Jiang, P., Chai, J., Jiang, Y., Dan, L., Bao, W.Yuan, L. (2019). The delivery of sensitive food bioactive ingredients: Absorption mechanisms, influencing factors, encapsulation techniques and evaluation models. *Food research international*, 120,130-140.
- Bastos, L. P. H., De Carvalho, C. W. P., & Garcia-Rojas, E. E. (2018). Formation and characterization of the complex coacervates obtained between lactoferrin and sodium alginate. *International journal of biological macromolecules*, 120, p.332-338.
- Bhattacharjee, N., Banerjee, S., &Dutta, S. K. (2014).Cloning, expression and mutational studies of a trypsin inhibitor that retains activity even after cyanogen bromide digestion. *Protein expression and purification*, 96, 26-31.
- Bokkhim, H., Bansal, N., Grøndahl, L., &Bhandari, B. (2015). Interactions between differentforms of bovine lactoferrin and sodium alginate affect the properties of their mixtures. *Food Hydrocolloids*, 48, 38–46.
- Bustos, C., O., R. Alberti, R.,V., S., Matiacevich, B., S. (2016). Edible antimicrobial films based on microencapsulated lemongrass oil.*Journal of food science and technology*, 53, 832-839.
- Chandran, J., Nayana, N., Roshini, N., &Nisha, P. (2017). Oxidative stability, thermal stability and acceptability of coconut oil flavored with essential oils from black pepper and ginger. *Journal of food science and technology*, 54(1), 144-152.
- Chanphai, P., &Tajmir-Riahi, H. A. (2017). Trypsin and trypsin inhibitor bind milk beta-lactoglobulin: Protein–protein interactions and morphology. *International journal of biological macromolecules*, 96, 754-758.



Chater, P. I., Wilcox, M. D., Brownlee, I. A., & Pearson, J. P. (2015). Alginate as a protease inhibitor in vitro and in a model gut system; selective inhibition of pepsin but not trypsin. *Carbohydrate Polymers*, 131, 142–151.

Commission regulation (EU) No 10/2011 of 14 January 2011 on plastic materials and articles intended to come into contact with food. 2011. 10/2011/EC.

Cortés-Camargo, S., Acuña-Avila, P. E., Rodríguez-Huezo, M. E., Román-Guerrero, A., Varela-Guerrero, V. Pérez-Alonso, C. (2019). Effect of chia mucilage addition on oxidation and release kinetics of lemon essential oil microencapsulated using mesquite gum–Chia mucilage mixtures. *Food research international*, 116, 1010-1019.

Da Cruz, M. C. R., Dagostin, J. L. A., Perussello, C. A., & Masson, M. L. (2019). Assessment of physicochemical characteristics, thermal stability and release profile of ascorbic acid microcapsules obtained by complex coacervation. *Food hydrocolloids*, 87, 71-82.

Dash, S., Murthy, P. N., Nath, L. Chowdhury, P. (2010). Kinetic modeling on drug release from controlled drug delivery systems. *Acta PolPharm*, 67(3), 217-23.

Da Silva Stefani, F., de Campo, C., Paese, K., Guterres, S. S., Costa, T. M. H. Flôres, S. H. (2019). Nanoencapsulation of linseed oil with chia mucilage as structuring material: Characterization, stability and enrichment of orange juice. *Food Research International*, 120, 872-879.

De Matos, E. F., Scopel, B. S., & Dettmer, A. (2018). Citronella essential oil microencapsulation by complex coacervation with leather waste gelatin and sodium alginate. *Journal of Environmental Chemical Engineering*, 6(2), 1989-1994.

Dima, C., Pătrașcu, L., Cantaragiu, A., Alexe, P., & Dima, Ș. (2016). The kinetics of the swelling process and the release mechanisms of *Coriandrum sativum L.* essential oil from chitosan/alginate/inulin microcapsules. *Food chemistry*, 195, 39-48.

Dong, A., Matsuura, J., Allison, S. D., Chrisman, E., Manning, M. C., & Carpenter, J. F. (1996). Infrared and circular dichroism spectroscopic characterization of structural differences between  $\beta$ -lactoglobulin A and B. *Biochemistry*, 35(5), 1450-1457.

El-Houssiny, A. S., Ward, A. A., Mostafa, D. M., Abd-El-Messieh, S. L., Abdel-Nour, K. N., Darwish, M. M. Khalil, W. A. (2016). Drug–polymer interaction between glucosamine sulfate and alginate nanoparticles: FTIR, DSC and dielectric spectroscopy studies. *Advances in Natural Sciences: Nanoscience and Nanotechnology*, 7(2), 025014.

Gaonkar, A. G; Vasisht, N; Khare, A. R; Sobel, R. Microencapsulation in the food industry: a practical implementation guide. San Diego: Elsevier, 2014.

Ghasemi, S., Jafari, S. M., Assadpour, E. Khomeiri, M. (2017). Production of pectin-whey protein nano-complexes as carriers of orange peel oil. *Carbohydrate polymers*, 177, 369-377.

- Girardi, N. S., García, D., Passone, M. A., Nesci, A., Etcheverry, M. (2017). Microencapsulation of *Lippia turbinata* essential oil and its impact on peanut seed quality preservation. *International Biodeterioration & Biodegradation*, 116, 227-233.
- Gunasekaran, S., Ko, S., & Xiao, L. (2007). Use of whey proteins for encapsulation and controlled delivery applications. *Journal of Food Engineering*, 83, 31-40.
- Hedstrom, L. (2002). Serine protease mechanism and specificity. *Chemical Reviews*, 102(12), 4501-4524.
- Huang, C. Y., Balakrishnan, G., Spiro, T. G. (2006). Protein secondary structure from deep-UV resonance Raman spectroscopy. *Journal of Raman Spectroscopy* 37, 277-282.
- Ilyasoglu, H., & El, S. N. (2014). Nanoencapsulation of EPA/DHA with sodium caseinate-gum arabic complex and its usage in the enrichment of fruit juice. *LWT-Food Science and Technology*, 56(2), 461-468.
- Jones, O. G., Decker, E. A., & McClements, D. J. (2010). Comparison of protein-polysaccharide nanoparticle fabrication methods: Impact of biopolymer complexation before or after particle formation. *Journal of Colloid and Interface Science*, 344(1), 21-29.
- Koupantsis, T., Pavlidou, E., Paraskevopoulou, A. (2014). Flavour encapsulation in milk proteins-CMC coacervate-type complexes. *Food Hydrocolloids*, 37, 134-142.
- Koupantsis, T., Pavlidou, E., Paraskevopoulou, A. (2016). Glycerol and tannic acid as applied in the preparation of milk proteins-CMC complex coacervates for flavour encapsulation. *Food Hydrocolloids*, 57, 62-71.
- Li, D., Wu, H., Huang, W., Guo, L., Dou, H. (2018). Microcapsule of Sweet Orange Essential Oil Encapsulated in Beta-Cyclodextrin Improves the Release Behaviors In Vitro and In Vivo. *European journal of lipid science and technology*, 120(9), 1-11.
- Lv, Y., Yang, F., Li, X., Zhang, X., Abbas, S. (2014). Formation of heat-resistant nanocapsules of jasmine essential oil via gelatin/gum arabic based complex coacervation. *Food Hydrocolloids*, 35, 305-314.
- Manaf, M. A., Subuki, I., Jai, J., Raslan, R., Mustapa, A. N. (2018). Encapsulation of volatile citronella essential oil by coacervation: efficiency and release study. In *IOP conference series: materials science and engineering*, 358 (1), 1-7.
- Maderuelo, C., Zarzuelo, A., Lanao, J. M. (2011). Critical factors in the release of drugs from sustained release hydrophilic matrices. *Journal of controlled release*, 154(1), 2-19.
- McClements, D. J. (2015). Nanoparticle- and microparticle-based delivery systems (1st ed). Boca Raton: CRC Press.
- Minekus, M., Alminger, M., Alvito, P., Ballance, S., Bohn, T. O. R. S. T. E. N., Bourlieu, C., & Dufour, C. (2014). A standardised static in vitro digestion method suitable for food—an international consensus. *Food & function*, 5(6), 1113-1124.

- Montero, P., Calvo, M. M., Gómez-Guillén, M. C. Gómez-Estaca, J. (2016). Microcapsules containing astaxanthin from shrimp waste as potential food coloring and functional ingredient: Characterization, stability, and bioaccessibility. *LWT-Food Science and Technology*, 70, 229-236.
- Nesterenko, A., Alric, I., Violleau, F., Silvestre, F. Durrieu, V. (2014). The effect of vegetable protein modifications on the microencapsulation process. *Food Hydrocolloids*, 41, 95-102.
- Nicolai, T., Britten, M., & Schmitt, C. (2011).  $\beta$ -Lactoglobulin and WPI aggregates: formation, structure and applications. *Food Hydrocolloids*, 25(8), 1945-1962.
- Papillo, V. A., Arlorio, M., Locatelli, M., Fuso, L., Pellegrini, N. Fogliano, V. (2019). In vitro evaluation of gastro-intestinal digestion and colonic biotransformation of curcuminoids considering different formulations and food matrices. *Journal of Functional Foods*, 59, 156-163.
- Peng, C., Zhao, S. Q., Zhang, J., Huang, G. Y., Chen, L. Y., & Zhao, F. Y. (2014). Chemical composition, antimicrobial property and microencapsulation of Mustard (*Sinapis alba*) seed essential oil by complex coacervation. *Food chemistry*, 165, 560-568.
- Powers, J. C., Harley, A. D., & Myers, D. V. (1977). Subsite specificity of porcine pepsin. *Advances in Experimental Medicine and Biology*, 95, 141-157.
- Raksa, A., Sawaddee, P., Raksa, P. Aldred, A. K. (2017). Microencapsulation, chemical characterization, and antibacterial activity of *Citrus hystrix* DC (*Kaffir Lime*) peel essential oil. *Monatshefte für Chemie-Chemical Monthly*, 148(7), 1229-1234.
- Rezaeinia, H., Ghorani, B., Emadzadeh, B. Tucker, N. (2019). Electrohydrodynamic atomization of Balangu (*Lallemantiaroyleana*) seed gum for the fast-release of *Mentha longifolia* L. essential oil: Characterization of nano-capsules and modeling the kinetics of release. *Food Hydrocolloids*, 93, 374-385.
- Ritger, P. L., & Peppas, N. A. (1987). A simple equation for description of solute release I. Fickian and non-fickian release from non-swellable devices in the form of slabs, spheres, cylinders or discs. *Journal of controlled release*, 5(1), 23-36.
- Rojas-Moreno, S., Osorio-Revilla, G., Gallardo-Velázquez, T., Cárdenas-Bailón, F., & Meza-Márquez, G. (2018). Effect of the cross-linking agent and drying method on encapsulation efficiency of orange essential oil by complex coacervation using whey protein isolate with different polysaccharides. *Journal of microencapsulation*, 35(2), 165-180.
- Saha, K. C., Seal, H. P., & Noor, M. A. (2013). Isolation and characterization of piperine from the fruits of black pepper (*Piper nigrum*). *Journal of the Bangladesh Agricultural University*, 11, 11-16.
- Schmitt, C. Turgeon, S. L. (2011). Protein/polysaccharide complexes and coacervates in food systems. *Advances in Colloid and Interface Science* 167, 63-70.

Strugala, V., Kennington, E. J., Campbell, R. J., Skjak-Braek, G., Dettmar, P. W. (2005). Inhibition of pepsin activity by alginates in vitro and the effect of pepsin. *International Journal of Pharmaceutics*, 304(1–2), 40–50.

Sunderland, A. M., Dettmar, P. W., Pearson, J. P. (2000). Alginates inhibit pepsin activity in vitro; a justification for their use in gastro-oesophageal reflux disease (GORD). *Gastroenterology*, 118(4), A21.

Timilsena, Y. P., Wang, B., Adhikari, R., Adhikari, B. (2016). Preparation and characterization of chia seed protein isolate–chia seed gum complex coacervates, *Food hydrocolloids*, 52, 554-563.

Timilsena, Y. P., Adhikari, R., Barrow, C. J., Adhikari, B. (2017). Digestion behaviour of chia seed oil encapsulated in chia seed protein-gum complex coacervates. *Food hydrocolloids*, 66, 71-81.

Tomé, D., Debabbi, H. (1998). Physiological effects of milk protein components. *International Dairy Journal*, 8, 383–392.

Wang, L., Yang, S., Cao, J., Zhao, S., & Wang, W. (2016). Microencapsulation of Ginger Volatile Oil Based on Gelatin/Sodium Alginate Polyelectrolyte Complex. *Chemical and Pharmaceutical Bulletin*, 64(1), 21-26.

Wang, B., Blanch, E., Barrow, C. J., & Adhikari, B. (2017). Preparation and study of digestion behavior of lactoferrin-sodium alginate complex coacervates. *Journal of functional foods*, 37, 97-106.

Volić, M., Pajić-Lijaković, I., Djordjević, V., Knežević-Jugović, Z., Pećinar, I., Stevanović-Dajić, Z., Bugarski, B. (2018). Alginate/soy protein system for essential oil encapsulation with intestinal delivery. *Carbohydrate polymers*, 200, 15-24.

Xiao, Z., Liu, W., Zhu, G., Zhou, R., Niu, Y. (2014). Production and characterization of multinuclear microcapsules encapsulating lavender oil by complex coacervation. *Flavour and fragrance journal*, 29 (3), 166-172.

Xu, H., Lu, Y., Zhang, T., Liu, K., Liu, L., He, Z., Wu, X. (2019). Characterization of binding interactions of anthraquinones and bovine  $\beta$ -lactoglobulin. *Food chemistry*, 281, 28-35.

Yao, K., Chen, W., Song, F., McClements, D. J., Hu, K. (2018). Tailoring zein nanoparticle functionality using biopolymer coatings: Impact on curcumin bioaccessibility and antioxidant capacity under simulated gastrointestinal conditions. *Food hydrocolloids*, 79, 262-272.

Ye, Q., Georges, N., Selomulya, C. (2018). Microencapsulation of active ingredients in functional foods: From research stage to commercial food products. *Trends in food science & technology*, 78, 167-179.

Yuan, Y., Li, M. F., Chen, W. S., Zeng, Q. Z., Su, D. X., Tian, B., & He, S. (2018). Microencapsulation of shiitake (*Lentinula edodes*) essential oil by complex

coacervation: formation, rheological property, oxidative stability and odour attenuation effect. *International Journal of Food Science & Technology*, 53(7), 1681-1688.

Zhang, K., Zhang, H., Hu, X., Bao, S. Huang, H. (2012). Synthesis and release studies of microalgal oil-containing microcapsules prepared by complex coacervation. *Colloids and surfaces B: Biointerfaces*, 89, 61-66.

Zhang, Z., Zhang, R. McClements, D. J. (2016). Encapsulation of  $\beta$ -carotene in alginate-based hydrogel beads: Impact on physicochemical stability and bioaccessibility. *Food Hydrocolloids*, 61, 1-10.

## Figure Caption

**Fig.1:** FT-IR spectra of NaAlg,  $\beta$ -LG, black pepper EO and black pepper microcapsule (pH 4.5).

**Fig. 2:** Particle size of the  $\beta$ -LG, NaAlg and black pepper microcapsule (ME) at pH 4.5.

**Fig. 3:** The cumulative release profile of the black pepper EO in different food stimulants.

**Fig. 4:** Release of the black pepper EO from the capsule during *in vitro* digestion.

**Fig .5:** Optical microscopy image at 100 x of black pepper EO microcapsules.

**Fig. 6:** (A)SEM of the black pepper EO microcapsule, (B) after oral digestion, (C) after gastric digestion, (D) after intestinal digestion. All the micrographs were obtained at 500x.

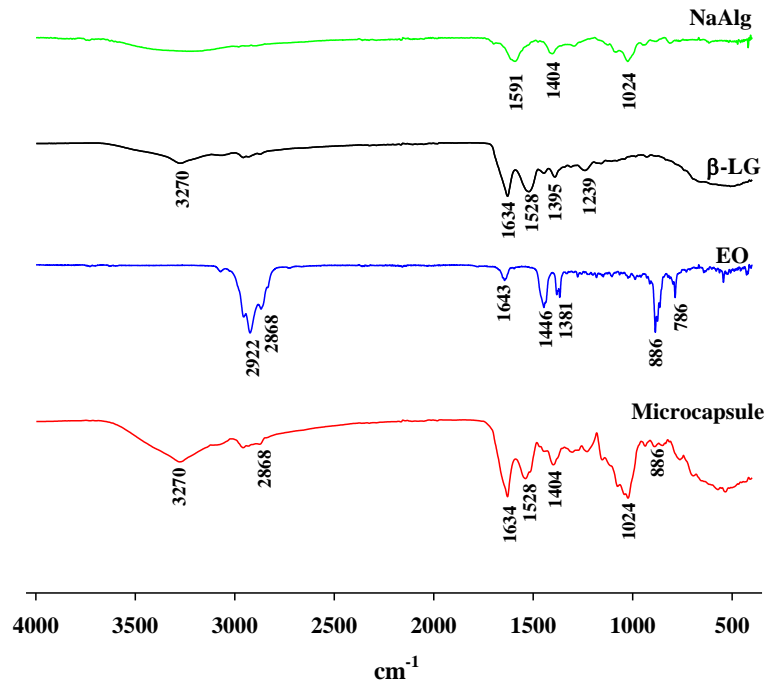


**Fig.1.**

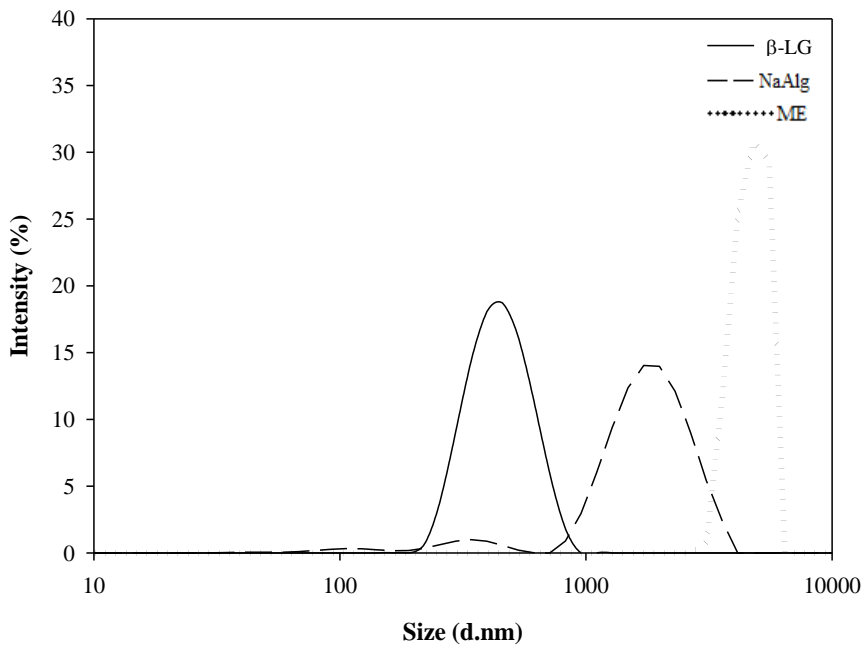


**Fig. 2.**

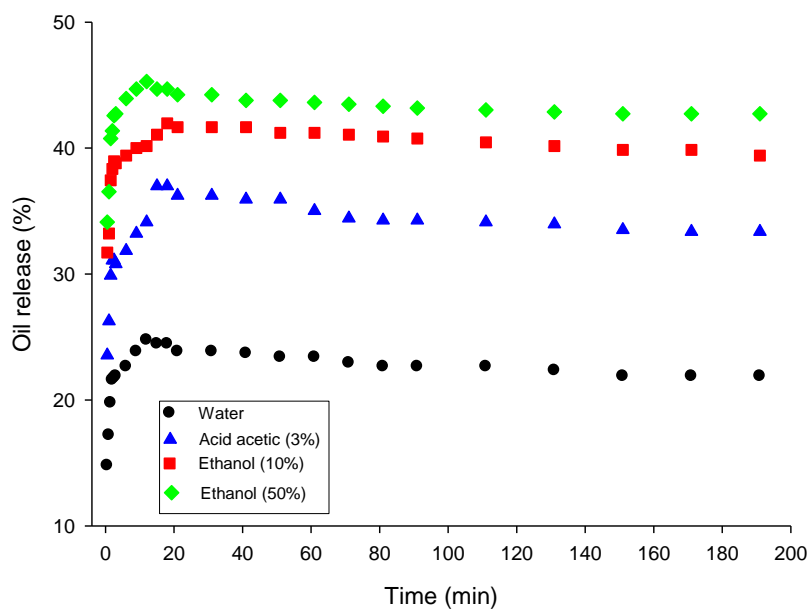


Fig. 3.

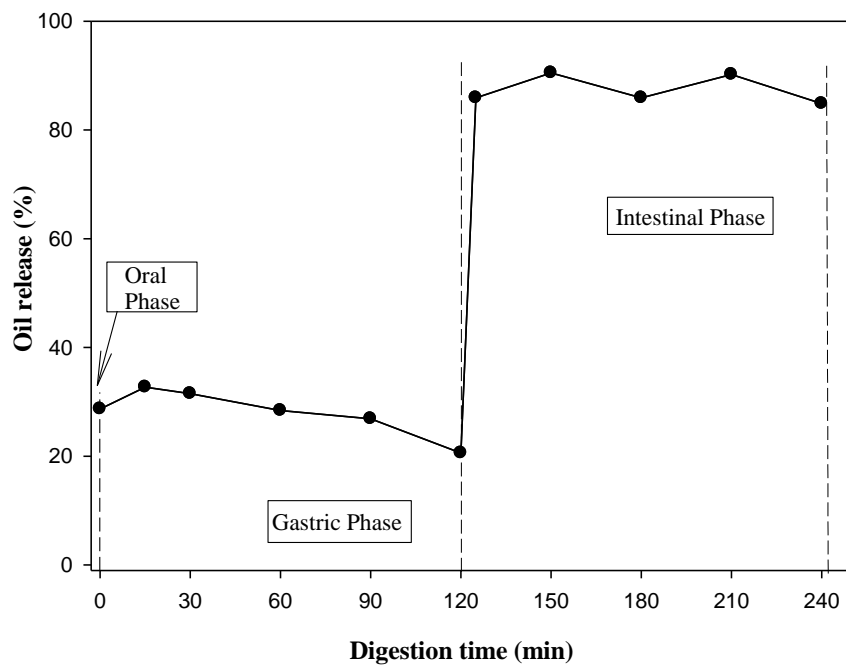
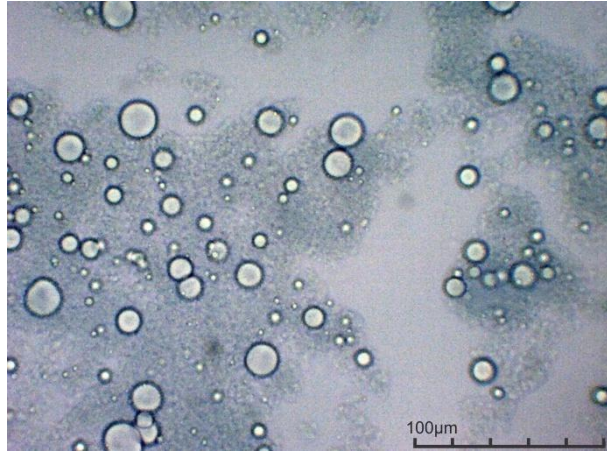
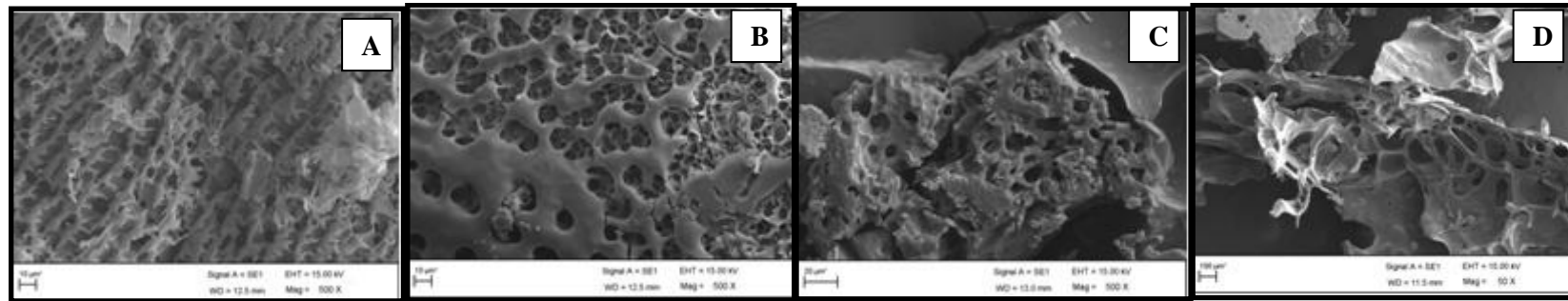


Fig.4.





**Fig.5.**



**Fig.6.**

**Table 1.** Composition of the formulations and EE of the microcapsules produced by complex coacervation.

Samples	Core Material (g)	Wall Material Weight (g)			core/wall (w/w)	Transglutaminase solution (g)	Loaded oil content(%)	Theoretical oil value (%)	EE (%)
		$\beta$ -LG (g)	NaAlg (g)	Total (g)					
S1	0.18	0.085	0.005	0.26	2:1	10	19.08 $\pm$ 1.29	66.66	28.62 <sup>c</sup> $\pm$ 1.9
S2	0.09	0.085	0.005	0.18	1:1	10	11.41 $\pm$ 0.4	50	22.85 <sup>de</sup> $\pm$ 0.8
S3	0.045	0.085	0.005	0.135	1:2	10	6.72 $\pm$ 0.6	33.33	20.18 <sup>c</sup> $\pm$ 0.18
S4	0.36	0.17	0.01	0.54	2:1	10	56.6 $\pm$ 0.17	66.66	85.01 <sup>a</sup> $\pm$ 0.26
S5	0.18	0.17	0.01	0.36	1:1	10	10.6 $\pm$ 0.51	50	21.21 <sup>de</sup> $\pm$ 1.02
S6	0.09	0.17	0.01	0.27	1:2	10	8.1 $\pm$ 0.4	33.33	24.4 <sup>d</sup> $\pm$ 1.21
S7	0.72	0.34	0.02	1.08	2:1	10	55.38 $\pm$ 0.33	66.66	83.1 <sup>a</sup> $\pm$ 0.49
S8	0.36	0.34	0.02	0.72	1:1	10	20.95 $\pm$ 1.58	50	41.91 <sup>b</sup> $\pm$ 2.17
S9	0.18	0.34	0.02	0.54	1:2	10	13.47 $\pm$ 0.4	33.33	40.42 <sup>b</sup> $\pm$ 1.2

The analyses were performed in three replicates. The same letters in the same column do not differ significantly by the Tukey test with a probability of 5%

**Table 2:** Kinetics constant of the black pepper EO release profile in different food simulants.

<b>Food Model</b>	<b>Higuchi</b>		<b>First order</b>		<b>Zero order</b>		<b>Rigger-Peppas</b>		
	K	R <sup>2</sup>	K	R <sup>2</sup>	K	R <sup>2</sup>	K	R <sup>2</sup>	n
Water	10.7	0.998	0.05	0.998	5.19	0.998	22	0.999	0.01
Acid acetic 3%	1	0.72	0.09	0.85	1	0.76	32.34	0.999	0.015
Ethanol 10%	1	0.78	0.11	0.996	1	0.63	36.84	0.998	0.02
Ethanol 50%	1	0.64	0.12	0.81	1	0.55	42.49	0.999	0.005

## CONCLUSÃO GERAL

Diante do trabalho realizado foi possível determinar a massa molar do alginato de sódio pelo método viscosimétrico, sendo este de baixa massa molar. Foi formado complexo coacervado entre a lactoferrina (Lf) e o alginato de sódio (NaAlg) e as melhores condições para sua formação foram o pH 4.0 e a razão de 8:1 (Lf/NaAlg) em baixa concentração salina. Os parâmetros termodinâmicos indicaram forte afinidade de ligação entre esses biopolímeros com favorável contribuição entalpia e desfavorável contribuição entrópica durante a interação entre eles. As características químicas e morfológicas observadas no complexo coacervado Lf/NaAlg indicaram mudanças decorrentes da interação eletrostática entre esses biopolímeros e o complexo Lf/NaAlg apresentou elevada resistência térmica.

Após formação e caracterização do complexo Lf/NaAlg, foi possível encapsular o óleo essencial de pimenta preta (*Piper nigrum L.*) utilizando a Lf e o NaAlg como materiais de parede e a transglutaminase como agente reticulante. Os terpenos presentes no óleo essencial de pimenta preta foram identificados pelas técnicas de cromatografia gasosa (CG) e ressonância magnética nuclear (RMN), sendo o  $\beta$ -cariofileno o principal terpeno (28%). As cápsulas produzidas apresentaram elevada eficiência de encapsulação e os principais terpenos foram preservados após encapsulação (97.5%), sendo estes identificados pelas técnicas de CG e RMN. As características químicas e morfológicas indicaram a formação das cápsulas de óleo essencial de pimenta preta. Após simulação da digestão *in vitro*, as cápsulas apresentaram resistência oral e gástrica (24.3%) e maior liberação do óleo essencial durante a simulação intestinal (52%).

Assim como realizado anteriormente com NaAlg, foi possível determinar a massa molar da gelatina (GE) pelo método viscosimétrico, a proteína apresentou características próprias correspondentes as suas cadeias  $\delta$ . O complexo GE/NaAlg foi formado, sendo as melhores condições para sua formação o pH 4.0 e a razão de 6:1 (GE/NaAlg). As características químicas do complexo GE/NaAlg indicaram que ocorreram mudanças decorrentes da interação eletrostática entre esses biopolímeros. Em seguida o óleo essencial de pimenta preta foi encapsulado utilizando a GE e o NaAlg como materiais de parede e o cloreto de cálcio como agente de reticulação. As cápsulas apresentaram elevada eficiência de encapsulação e os principais terpenos presentes no óleo essencial de pimenta preta foram preservados após encapsulação (81.7%), sendo estes identificados pela técnica de CG.

Após tratamento térmico da proteína  $\beta$ -lactoglobulina ( $\beta$ -LG), foi possível reduzir seu tamanho de partícula para uma escala nano ( $\beta$ -LG<sub>n</sub>). Foi possível formar complexos interpoliméricos entre a  $\beta$ -LG nativa e após tratamento térmico ( $\beta$ -LG<sub>n</sub>) e o NaAlg, os melhores pHs para formação dos complexos interpoliméricos entre  $\beta$ -LG/NaAlg e  $\beta$ -LG<sub>n</sub>/NaAlg foram pHs 4.5 e 4.0, respectivamente. As razões ideais para formação dos complexos interpoliméricos foram: 17:1 ( $\beta$ -LG/NaAlg) e 72:1 ( $\beta$ -LG<sub>n</sub>/NaAlg). Os parâmetros termodinâmicos indicaram forte afinidade entre a  $\beta$ -LG e NaAlg com a proteína nativa e após tratamento térmico. Em ambos foi observada contribuição entálpica e entrópica, ao avaliar a interação entre  $\beta$ -LG<sub>n</sub> e NaAlg houve maior contribuição entrópica, devido a exposição dos grupos hidrofóbicos  $\beta$ -LG após tratamento térmico. As características químicas demonstraram mudanças decorrentes das interações eletrostáticas entre os complexos interpoliméricos e devido a exposição dos grupos hidrofóbicos no complexo interpolimérico  $\beta$ -LG<sub>n</sub>/NaAlg. O complexo interpolimérico  $\beta$ -LG/NaAlg apresentou elevada resistência térmica.

Após formação e caracterização do complexo  $\beta$ -LG/NaAlg, foi possível encapsular o óleo essencial de pimenta preta (*Piper nigrum L.*) utilizando a  $\beta$ -LG e o NaAlg como materiais de parede e a transglutaminase como agente reticulante. As cápsulas foram produzidas em escala micro e apresentaram elevada eficiência de encapsulação. As características químicas e morfológicas indicaram que ocorreu a formação da microcápsula. Após realizar simulação das microcápsulas em diferentes matrizes alimentares, foi possível observar que a liberação do óleo essencial de pimenta preta foi menor em matrizes alimentares aquosas. A liberação do óleo essencial de pimenta preta ocorreu por difusão *Fickian* de acordo com modelo de *Rigger-Peppas* em todas as matrizes alimentícias simuladas. Após simulação da digestão *in vitro* das microcápsulas, foi observada que esta apresentou resistência oral e gástrica (28.7%) e que a maior parte do óleo essencial foi liberado durante simulação intestinal (90.5%). Após simulação da digestão o óleo essencial apresentou elevada estabilidade e aceitável bioacessibilidade.

Em conclusão, foram formados complexos coacervados entre as proteínas estudadas e o alginato de sódio. O complexo Lf/NaAlg e o complexo interpolimérico  $\beta$ -LG/NaAlg apresentaram elevada resistência térmica. Os biopolímeros e agentes reticulantes utilizados foram eficazes na proteção do óleo essencial de pimenta preta apresentando cápsulas com alta eficiência de encapsulação (>80%) e preservando os principais terpenos em sua composição. As cápsulas produzidas utilizando a Lf e NaAlg

como matérias de parede protegeram melhor os terpenos quando comparado as cápsulas produzidas utilizando a GE e o NaAlg. As microcápsulas formadas com  $\beta$ -LG/NaAlg foram as que apresentaram maior eficiência de encapsulação (85.01%). As cápsulas produzidas por Lf/NaAlg e  $\beta$ -LG/NaAlg apresentaram resistência durante simulação oral e gástrica.

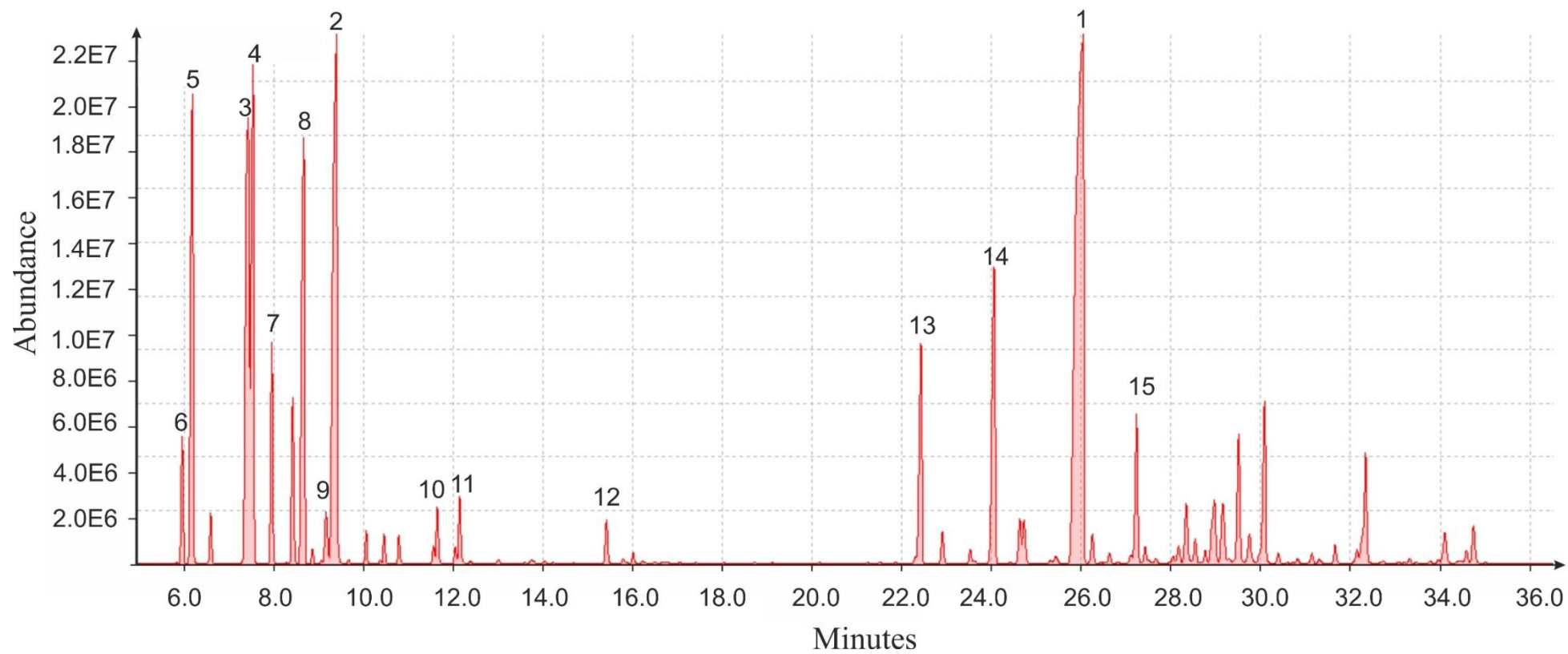
Por fim, as cápsulas produzidas apresentaram-se potencialmente úteis para o transporte de ingredientes ativos, como o óleo essencial de pimenta preta (*Piper nigrum L.*). Futuros estudos sobre a aplicação do óleo essencial de pimenta preta encapsulado em produtos alimentícios podem ser avaliados, assim como sua atividade antimicrobiana e antioxidante após encapsulação.

## ANEXOS



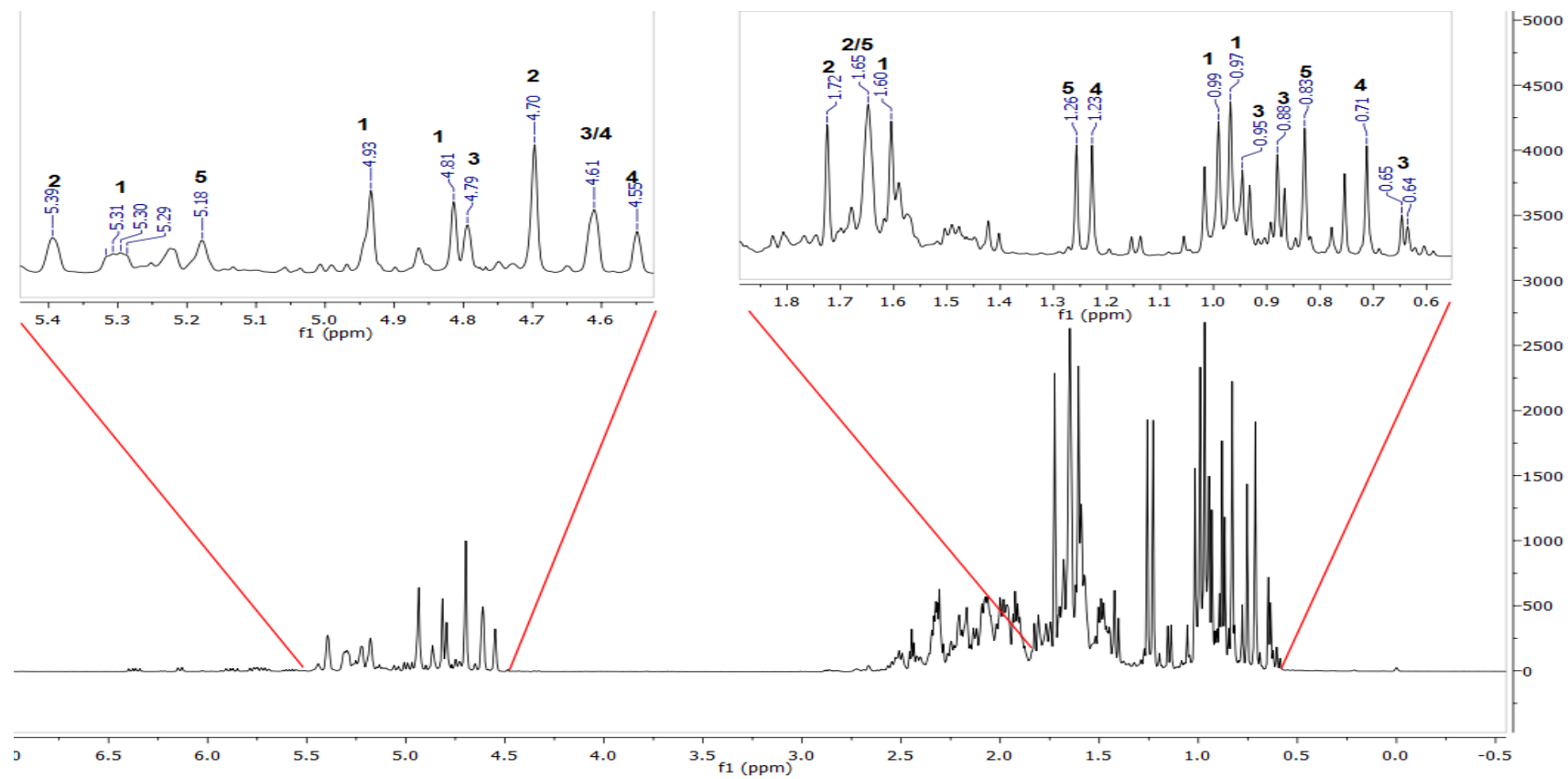
**ANEXO A:**

**A1:** Chromatogram of volatile compounds from black pepper EO identified by GC-MS. Peak numbers correspond to that in Table 1



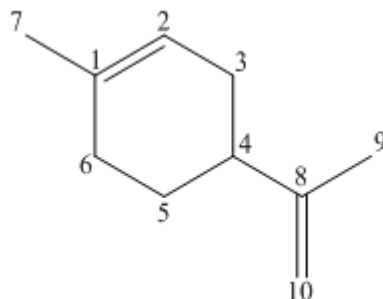
## ANEXO B:

**B1:**  $^1\text{H}$  NMR spectrum of Black pepper EO at 500.13MHz. Peak numbers correspond to that in Table 2.



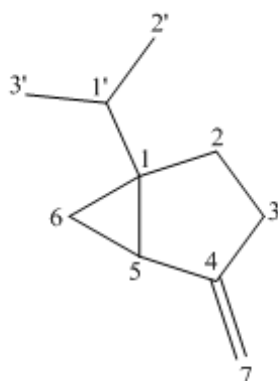
## ANEXOS C:

C1: NMR data of Limonene (CDCl<sub>3</sub>, 500MHz)



C	HMQC		HMBC
	$\delta_C$	$\delta_H$	$^{2,3}J_{H-C}$
1	133,7	-	
2	120,6	5,43 ( <i>sl</i> )	
3	*	*	
4	41,1 <sup>1</sup>	*	
5	*	*	
6	30,6	2,12 ( <i>m</i> )	
7	23,5	1,64 ( <i>sl</i> )	
8	150,2	-	
9	108,4	4,69 ( <i>sl</i> )	
10	20,8	1,71 ( <i>s</i> )	8, 9, 4

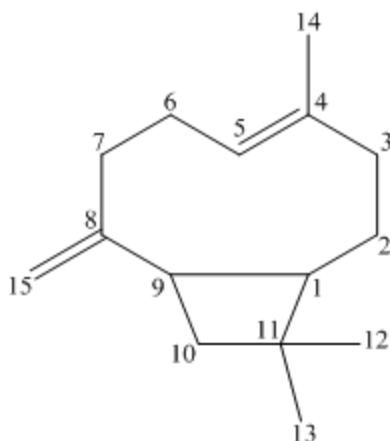
**C2:** NMR data of Sabinene (CDCl<sub>3</sub>, 500MHz)



C	HMQC		HMBC
	$\delta_C$	$\delta_H$	$^{2,3}J_{H-C}$
<b>1</b>	37,6 <sup>1</sup>	-	
<b>2</b>	*	*	
<b>3</b>	*	*	
<b>4</b>	154,5	-	
<b>5</b>	48,5	2,30 (m) <sup>1</sup>	
<b>6</b>	16,0	0,63 (d, 5,5)	
<b>7</b>	101,5	4,60 (sl), 4,78 (sl)	4
<b>1'</b>	32,6	1,48 <sup>1</sup>	
<b>2'</b>	19,7	0,86 (d, 7)	1'
<b>3'</b>	19,8	0,92 (d, 7)	1'

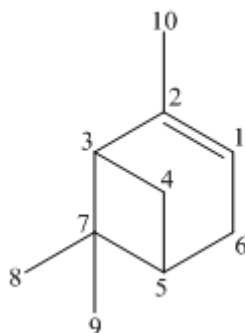
\*it was not possible to determine; <sup>1</sup> determined by two-dimensional experiments

**C3:** NMR data of  $\beta$ -cariophyllene ( $\text{CDCl}_3$ , 500MHz)



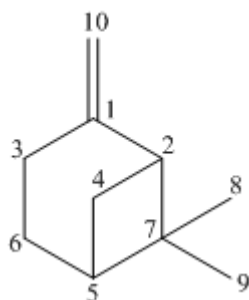
<b>C</b>		<b>HMQC</b>		<b>HMBC</b>
-	$\delta_{\text{C}}$	$\delta_{\text{H}}$		$^{2,3}J_{\text{H-C}}$
<b>1</b>	53,5	1,71 ( <i>m</i> )		
<b>2</b>	*	*		
<b>3</b>	40,0	*		
<b>4</b>	135,5	-		
<b>5</b>	124,3	5,29 ( <i>dd</i> , 5 e 10,5 Hz)		
<b>6</b>	*	*		
<b>7</b>	34,8	2,02 ( <i>m</i> ), 2,24 ( <i>m</i> )		
<b>8</b>	154,7	-		
<b>9</b>	48,5	*		
<b>10</b>	40,3	1,67 ( <i>m</i> ), 1,97 ( <i>m</i> )		
<b>11</b>	33,9	-		
<b>12</b>	22,6	0,96 ( <i>s</i> )		1, 10, 11
<b>13</b>	30,1	0,98 ( <i>s</i> )		1, 10, 11
<b>14</b>	16,3	1,59 ( <i>s</i> )		3, 4, 5
<b>15</b>	111,6	4,80 ( <i>sl</i> ), 4,92 ( <i>sl</i> )		7, 8, 9

**C4:** NMR data of  $\alpha$ -pinene ( $\text{CDCl}_3$ , 500MHz)



<b>C</b>	<b>HMQC</b>		<b>HMBC</b>
	$\delta_C$	$\delta_H$	$^{2,3}J_{H-C}$
<b>1</b>	116,0	5,20 ( <i>sl</i> )	
<b>2</b>	144,5	-	
<b>3</b>			
<b>4</b>			
<b>5</b>	41,1		
<b>6</b>			
<b>7</b>			
<b>8</b>			
<b>9</b>			
<b>10</b>	23,5	1,68 ( <i>s</i> )	2

**C5:** NMR data of  $\beta$ -pinene (CDCl<sub>3</sub>, 500MHz)



<b>C</b>	<b>HMQC</b>		<b>HMBC</b>
	$\delta_C$	$\delta_H$	$^{2,3}J_{H-C}$
<b>1</b>	152,3	-	
<b>2</b>	51,8	2,48 ( <i>t</i> , 5,3 Hz)	
<b>3</b>			
<b>4</b>			
<b>5</b>	40,4	1,66 ( <i>m</i> )	
<b>6</b>			
<b>7</b>			
<b>8</b>			
<b>9</b>			
<b>10</b>	105,9	4,57 ( <i>sl</i> ), 4,63 ( <i>sl</i> )	2